Abstracts 9151-9452

SOLID STATE ABSTRACTS

an abstract journal devoted to the theory, production and use of solid state materials and devices

VOLUME 1 NUMBER 12

PHYSICS

METALLURGY

ELECTRONICS

SEMICONDUCTORS

PHOSPHORS

MAGNETICS

DIELECTRICS

SUPERCONDUCTORS

METALS

SOLID STATE ABSTRACTS

VOLUME 1, NUMBER 12

September 1961

Abstracts 9151–9452

TABLE OF CONTENTS

Abstracts of the Solid State Literature

Metallurgy and Chemistry of Solids

Thermodynamic Properties . . . 535
Crystal Structure . . . 535
Crystal Growth . . . 540
Crystal Surfaces . . . 541
Environmental Effects . . . 541

Solid State Physics

General . . . 542
Crystal Physics . . . 542
- Binding Properties . . . 542
- Energy Band Structure . . . 543
- Lattice Potentials and Vibrations . . . 544
- Other Properties . . . 545

Electrical Properties . . . 545
- General . . . 545
- Dielectric Properties . . . 545
- Carrier Properties . . . 548
- Conductivity (Resistivity) . . . 551
- Superconductivity . . . 554
- Magnetoelectric (Galvanomagnetic) Properties . . . 555
- Noise . . . 557
- Electrical Properties of Surfaces . . . 557

Magnetic Properties . . . 559
- Ferro- and Ferrimagnetism . . . 559
- Paramagnetism . . . 566
- Diamagnetism . . . 568

Optical Properties . . . 569
- General . . . 569
- Absorption (Transmission) . . . 569
- Radiation and Luminescence . . . 571
- Photoelectronic Properties . . . 573

Thermal Properties . . . 575
Mechanical Properties . . . 577

Annual Cumulative Subject Index . . . 579

Annual Cumulative Author Index . . . 629

Editor: GEOFFREY KNIGHT, JR., Ph.D.

Managing Editor: JOHN A. MURPHY

PUBLISHED MONTHLY BY

Cambridge Communications Corporation, 238 Main Street, Cambridge 42, Massachusetts, Tel. 491-0710

Subscription Rate: $25.00 per year. Back Copies: Single Issues $2.50; Double Issues $5.00. Advertising Rates on Request.

Cambridge Communications Corp. is not prepared to furnish copies of the articles abstracted. However, there are many libraries throughout the country which maintain photocopying services.

SYMBOLS USED IN THE ABSTRACTS

L: Letter to the Editor. A: Only an abstract is given in the reference. R: Only a review is given in the reference. E: Erratum.

The reference numbers in the indices are the abstract numbers, not the page numbers.

Copyright 1962 by Cambridge Communications Corp. Printed in the U.S.A. by the University Press, Inc.

ABSTRACTS OF THE SOLID STATE LITERATURE

METALLURGY AND CHEMISTRY OF SOLIDS

THERMODYNAMIC PROPERTIES

9151 THEORETICAL MODEL FOR CUBIC-TO-TETRAGONAL PHASE TRANSFORMATIONS IN TRANSITION METAL SPINELS by P. J. Wojtowicz (RCA Labs.); J. Appl. Phys., Suppl. Vol. 30, pp. 30S-31S, Apr. 1959

The detailed properties of the transformations from tetragonal to cubic phases which are observed at elevated temperatures in transition metal spinels are investigated. An approximate model has been constructed which explicitly takes into account the interactions between local Jahn-Teller distortions about neighboring site transition metal cations. By the use of the usual method of statistical mechanics it has proved possible to derive the thermodynamic behavior of this model, and hence to contribute to an understanding of the cooperative nature of these transformations. The principle result of importance is the demonstration that the transformations from tetragonal to cubic spinel phases are thermodynamically of the first order. That is, a latent heat, a volume discontinuity, lattice parameter discontinuities, and a lambda anomaly in the heat capacity are to be expected at the transformation temperature. The available evidence seems to support the conclusions drawn from the model.

9152 BEHAVIOR OF POLYTETROFLUOROETHYLENE (TEFLON) UNDER HIGH PRESSURE by R. I. Beecroft and C. A. Swenson (Iowa State U.); J. Appl. Phys., Vol. 30, pp. 1793-1798, Nov. 1959

The presence of polymorphic phase transitions, apparently unique among high polymers, enhances interest in polytetrofluoroethylene, while its potentialities for cryogenic applications make low temperature data particularly valuable. Compression measurements have been made on samples of Teflon at various temperatures between 75° and 380°K and at pressures up to 21,000 atm. The phase diagram found for the region above the ice point is in qualitative agreement with previously published results, with a possible additional transition appearing above room temperature at pressures of over 11,000 atm. Time effects and a large pressure hysteresis make the transition parameters quite ambiguous, and the hysteresis becomes so broad at low temperatures that the phase diagram cannot be extended below the ice point. An apparent negative thermal expansion indicated by the isothermal compression measurements is shown to result from an incomplete high pressure transition. From an engineering standpoint, the measurements indicate that a Teflon gasket loaded to 300 atm at room temperature should maintain a seal at any lower temperature.

CRYSTAL STRUCTURE

9153 DISTRIBUTION OF CATIONS IN SPINELS by A. Miller (RCA Labs.); J. Appl. Phys., Suppl. Vol. 30, pp. 24S-25S, Apr. 1959

The concept of octahedral site preference energy in spinels is extended to include Madelung and short-range as well as crystal field terms. A set of site preference energies is formulated which can be used to predict the ionic distribution of spinels involving the nontransition as well as the transition ions. The agreement between predicted and experimentally determined ionic distributions is surprisingly good, and a number of heretofore puzzling distributions are explained.

9154 ABSORPTION CORRECTION IN PRECISION DETERMINATION OF LATTICE PARAMETERS by M.E. Straumanis (U. Missouri); J. Appl. Phys., Vol. 30, pp. 1965-1969, Dec. 1959

X-ray powder and rotation patterns of six cubic substances (W, Si, Cr, TiO, Al and V) taken with specimens of different thickness are reported and the lattice constants are calculated and plotted against the angle or against the Nelson and Riley function. Such curves for thin mounts, semitransparent to X-rays (below 0.2 in diam), consist of two parts: a region of high slope (due to absorption) and one approaching a zero slope at high Bragg angles. The latter, varying in extent with the size and nature of the mount, indicates that due to the rapid decrease in absorption, the lines in this region are shifted little, if any, from their correct positions. Hence, the lattice constants calculated from the reflections of the high θ angles lying on the horizontal portion of the curve need not be corrected for absorption. The constant, with negligible error, can be calculated from a single last strong α_1 or β reflection. If an extrapolation is applied, the curve must be traced through points in the high back reflection region. Otherwise any extrapolation, disregarding the horizontal part, would lead to lattice constants too high in value. The amount of line displacement due to absorption in thin samples (below 0.2 mm in diam) agrees with the geometrical concept of Hadding and Buerger.

9155 NUCLEAR MAGNETIC RESONANCE AND THERMAL EXPANSION IN PARTIALLY CRYSTALLINE POLYPROPYLENE,

POLY (BUTENE-1), AND POLY (PENTENE-1) by J. A. Sauer, A. E. Woodward and N. Fuschillo (U. Pennsylvania); J. Appl. Phys., Vol. 30, pp. 1488-1491, Oct. 1959

A study of the specific volume of partially crystalline specimens of polypropylene, poly (butene-1), and poly (pentene-1) from about 160°K to about the melting point is reported. In addition, proton spin magnetic resonance of a partially crystalline poly (butene-1) specimen has been observed from 77° – 320°K. Per cent crystallinities as functions of temperature for polypropylene and poly (butene-1) calculated from the specific volume data are compared. The poly (butene-1) specimens show higher densities than the polypropylene samples at 170° - 180°K although the crystallinities of the former are 25-40 per cent lower than the latter. In addition, the temperature dependence of the specific volume from 160° - 280°K is greater for poly (butene-1) than for polypropylene. Somewhat similar trends are noted in a comparison of the NMR second moment versus temperature curves for these two materials.

9156 DENSITY MEASUREMENTS OF SOME THIN COPPER FILMS by N. Wainfan, N. J. Scott and L. G. Parratt (Cornell U.); J. Appl. Phys., Vol. 30, pp. 1604-1609, Oct. 1959

Density measurements made on vacuum-deposited Cu films in the thickness ranges 50 to 150 A and 500 to 1000 A are given. To obtain the density, an analysis was made of the relation between the reflection coefficient and the glancing angle of incidence for 1.54 A X-rays. For films in the range 500-1000 A, this analysis was augmented by a chemical determination of the average mass per unit area. Although there is evidence of nonuniform density with depth in the film, especially for very thin films, the average density of a film thicker than about 300 A was found within the limits of the experimental accuracy to be equal to the bulk density. This conclusion is in disagreement with some previously published work; the discrepancy seems to lie in differences between the X-ray method of measuring film thickness and the conventional optical interference method.

9157 SMALL-ANGLE SCATTERING OF X-RAYS FROM NEUTRON IRRADIATED COPPER by H. H. Atkinson (Cavendish Lab.) and R. E. Smallman and K. H. Westmacott (Atomic Energy Res. Estab.); J. Appl. Phys., Vol. 30, pp. 646-649, May 1959

The increase in scattering of X-rays at small angles from polycrystalline copper when the recrystallized metal is bombarded with fast neutrons is discussed. The observed effects above 2 are due to double Bragg reflections; below about 1-1/2 they can be explained in terms both of double reflections and "true" small-angle scattering. The results indicate that either small coherent regions (of diameter about 100 A) or severe strains are present in the irradiated metal. The results are consistent with other measurements (particularly of mechanical properties) on irradiated metals.

9158 TEMPERATURE DIFFUSE SCATTERING OF X-RAYS IN CUBIC POWDERS. Part I. COMPARISON OF THEORY WITH EXPERIMENT by D. R. Chipman and A. Paskin (Mat. Res. Lab.); J. Appl. Phys., Vol. 30, pp. 1992-1997, Dec. 1959

Experimental data on temperature diffuse scattering of X-rays (TDS) in cubic powders is used to validate current TDS theory. Measurements of the diffuse scattering of Cu and Pb are reported along with the Bragg reflections of these metals at room and liquid nitrogen temperatures. These measurements were made using a scintillation counter diffractometer and crystal monochromated CuK a radiation. The TDS so obtained is compared with TDS calculations based on the one- and two-phonon calculation as well as on the Warren (modified one-phonon) calculation. Both formulas are found to fit the magnitude of TDS by choosing appropriate Debye characteristic temperatures. The Debye Θ's which fit the copper and lead TDS data at room temperature are: 324° and 96° (one- and two-phonon) and 269° and 64° (Warren formula) as compared to values of 307° and 79° taken from the temperature dependence of the Bragg reflections and 315° and 88° from specific heat values for Cu and Pb, respectively. Evidence is also found for extra diffuse scattering in the low-angle region. This extra scattering is tentatively ascribed to a multiple scattering process.

9159 TEMPERATURE DIFFUSE SCATTERING OF X-RAYS IN CUBIC POWDERS. Part II. CORRECTIONS TO INTEGRATED INTENSITY MEASUREMENTS by D. R. Chipman and A. Paskin (Mat. Res. Lab.); J. Appl. Phys., Vol. 30, pp. 1998-2001, Dec. 1959

In order to obtain accurate values for the integrated Bragg intensities, it is necessary to correct for the fact that temperature diffuse scattering (TDS) peaks occur in the same regions of reciprocal space as the Bragg peaks. On the basis of recent calculations of TDS in cubic powders it is possible to calculate the contribution of TDS to apparent measured Bragg intensities. Measurements have been made on a counter spectrometer using crystal-monochromated CuK a radiation. The contribution of TDS to the measured Bragg intensities is demonstrated on several peaks of Pb. A simple relationship is derived for the correction and compared with a graphical solution by plotting TDS under the Bragg peak. The agreement between the two methods of correcting for TDS is good. The magnitude of the correction varies with the material, the wavelength of the X-rays and the region of reciprocal space studied. For a typical material such as Cu using Cu radiation, the correction is about 3 per cent of the integrated intensity. For Pb, again using Cu radiation, it is about 15 per cent.

9160 EFFECT OF THERMAL MOTION ON THE X-RAY REFLECTIVITY OF QUARTZ by D.W. Berreman and T.T. Chang (U. Oregon); J. Appl. Phys., Vol. 30, pp. 963-969, July 1959

Two characteristic temperatures for quartz have been determined which, when substituted into the Debye-Waller formula and then used to compute the ratios of temperature corrected integrated reflection coefficients of various pairs of sets of Bragg planes, give results in best agreement with experimentally determined ratios. These temperatures are 508° ± 16°K in the direction of the trigonal axis and 452° ± 15°K in any particular direction. Corresponding values obtained from an approximate formula relating characteristic temperatures with elastic constants were 448° and 398°K, respectively. The fairly good agreement between the characteristic temperatures obtained by the two methods seems to support the conjecture that the modification of the Debye theory used gives a fairly good approximate description of the effect of thermal motion on the X-ray reflectivity of quartz. Calculations based upon the experimentally determined characteristic temperatures indicate that when Bragg spacings are less than about 0.7 A, the reflectivity of quartz at room temperature is reduced to less than half the value that would be obtained if the atoms were rigidly fixed.

9161 INTERNAL DOUBLE REFLECTION IN A PERFECT CRYSTAL by A. Guinier and E. Guyon (Cons. Arts-Metiers, Paris); J. Appl. Phys., Vol. 30, pp. 622-628, May 1959

The theory of double Bragg reflections in single crystals is derived. Both a kinematical and dynamical basis are employed. Experiments using single crystals of LiF, diamond, aluminum-copper, pentaerithritol, and stilbene are described and comparisons are made with the theory.

9162 DIFFUSE X-RAY SCATTERING IN POWDER PATTERNS ARISING FROM STATIC DISPLACEMENTS IN CUBIC SOLID SOLUTIONS by C. R. Houska and B. L. Averbach (MIT); J. Appl. Phys., Vol. 30, pp. 1532-1534, Oct. 1959

An evaluation of the diffuse scattering arising from static atomic displacements from the average lattice sites for cubic powder patterns is presented. This excess scattering results from elastic interactions between atoms of different size in binary solid solutions, and is compatible with the conservative intensity loss of the main reflections. The resultant scattering was found to take the form $I_s f^2 H(x) 1-\exp -2M'(x)$, where $H(x)$ is a weak modulation which varies by approximately 10 per cent about unity.

9163 STUDY OF X-RAY SCATTERING FROM FATIGUED METALS by K. Thomas and A. Franks (Natl. Phys. Lab., England); J. Appl. Phys., Vol. 30, pp. 649-655, May 1959

A new explanation for the low-angle X-ray scattering from cold worked metals is presented. The experimental results obtained by an examination of individual grains of polycrystalline fatigue specimens indicate that double Bragg reflection plays an important role in this phenomenon. The fatigue process results in the formation of subgrains, the misorientations within a grain amounting to 15.

9164 SMALL ANGLE X-RAY SCATTERING FROM COPPER AND ALUMINUM UNDER CYCLIC STRESS by J. C. Grosskreutz and F. R. Rollins (Midwest Res. Inst.); J. Appl. Phys., Vol. 30, pp. 668-674, May 1959

Small angle scattering intensities of Cu and Al samples subjected to cyclic stress and run to fatigue while being held in an X-ray beam are reported. These intensities were found to increase with the number of elapsed stress cycles. The observed angular dependence and intensity of the scattered radiation agree most nearly with a double Bragg scattering mechanism. The relation of the fatigue mechanism to the formation of small angle subgrain boundaries responsible for the double Bragg scattering is not clear-cut. However, the evidence favors the view that the formation of subgrains, while probably necessary to the propagation of the fatigue crack, is not sufficient either for its formation or propagation. Complete annealing of the scattering was not possible, indicating that recrystallization does not take place following cyclic stress of the order of one-fourth the yield stress. No evidence exists for a widespread formation of voids in the fatigued specimen.

9165 SMALL ANGLE SCATTERING OF X-RAYS BY PLASTICALLY DEFORMED SINGLE CRYSTALS by W. H. Robinson and R. Smoluchowski (Carnegie Inst. Tech.); J. Appl. Phys., Vol. 30, pp. 617-621, May 1959

Measurements of the small angle scattering of X-rays from single crystals of Mg plastically deformed in simple shear in the angular range of 4 to 5 are reported. The crystals were subjected to both unidirectional and cyclic shear stresses applied along the [1120] direction. Thin slices of the deformed single crystals were prepared using strain-free cutting and polishing techniques. The thin slices have orientations such that the slip direction was either parallel or perpendicular to the incident X-ray beam in order to observe any anisotropy in the scattering that might be due to dislocations. It was found that those samples which contained deformation twins within the irradiated volume produced rather large scattered intensity. This scattered intensity is interpreted as being due to double Bragg scattering. The scattered intensity from other specimens was attributed to surface scattering. No evidence for small angle scattering by dislocations was found.

9166 QUENCHED-IN DEFECTS IN TIN AND THE SUPERCONDUCTING TRANSITION TEMPERATURE by W. Desorbo (GE Res. Lab.); J. Phys. Chem. Solids, Vol. 15, pp. 7-12, Aug. 1960

Wire specimens of tin quenched from a temperature T_Q ($370°K < T_Q < T_{m.p.}$), exhibit a resistivity component, $\Delta\rho_0$, which disappears on annealing at lower temperatures. It is inferred that this increase in resistivity is the result of quenched-in defects. The activation energy of motion of the defects, $E_m = 0.68 \pm 0.06$ ev; while the activation energy of formation, $E_f = 0.51 \pm 0.05$ ev. The sum of these values, $E_f + E_m = Q$, is in fair agreement with the measured value of Q, the activation energy of diffusion, suggesting that the imperfections are vacancies. These defects depress the resistive superconducting transition temperature by a measurable amount which depends on the chemical purity of the specimen.

9167 ON THE KINETICS OF QUENCHED-IN LATTICE VACANCIES IN PLATINUM by G. L. Bacchella, E. Germagnoli and S. Granata (Cent. Info. Studio Esperienze, Milan); J. Appl. Phys., Vol. 30, pp. 748-752, May 1959

An activation energy of 1.20 ± 0.04 ev for vacancy formation in high purity Pt has been determined. Quenching experiments are described, and annealing behavior after quenching is studied. First-order annealing is found when the concentration of quenched-in defects is low; the migration energy turns out to be 1.48 ± 0.08 ev. The annealing kinetics are not simple if the quenching temperature is high and the concentration of defects at least 10^{-4}.

9168 THERMAL BLEACHING OF COLOR CENTERS IN KCl CRYSTALS CONTAINING U CENTERS by M. Hirai (Tohoku U.); J. Phys. Soc. Japan, Vol. 15, pp. 1308-1315, July 1960

From the study of thermal bleaching of the F, M and R_2 bands in KCl crystals containing U centers, the behavior of the hydrogen molecules produced from U centers is examined. The hydrogen molecules do not react with F centers but with M centers by bimolecular reaction and make M centers convert to U centers. Furthermore, thermal bleaching of the Z_1 and Z_2 bands in KCl crystals containing divalent cations has also been investigated. The Z_1 and Z_2 bands are thermally unstable at temperature above 80°C, while they are stable up to 110°C and 250°C, respectively, in the crystal containing no U centers. From these results, in KCl:Sr crystals it is supposed that Z_1 centers do not return to U centers but form unknown centers by combining with the hydrogen molecules.

9169 COLLOIDS IN ADDITIVELY COLORED SODIUM CHLORIDE by H. W. Etzel (U.S. Naval Res. Lab.); Phys.

Rev., Vol. 118, pp. 1150-1153, June 1, 1960

A study of the formation of colloids in additively colored sodium chloride is discussed. Both natural and synthetic single crystals were additively colored by heating in a vapor of sodium and by injecting electrons from a point cathode. Subsequent irradiation with ultraviolet light and heating of the synthetic crystals produced an absorbing type colloid throughout the crystal. The same treatment applied to the natural crystals produced F centers throughout the bulk of the crystal and absorbing type colloid specks at localized points in the crystal. In the synthetic crystals the formation of these colloids is shown to be related to the presence of hydroxyl ions in the crystals prior to coloration. In the natural crystal the formation of such colloids is dependent upon the presence of small occlusions of water distributed randomly in the crystal prior to coloration.

9170 NUCLEAR MAGNETIC RESONANCE STUDIES OF DISLOCATIONS IN NaI and KI by J. F. Hon and P. J. Bray (Brown U.); J. Appl. Phys., Vol. 30, pp. 1425-1428, Sept. 1959

Intensity anomalies which have been observed in the nuclear magnetic resonance of I^{127} in NaI and KI single crystals when the magnetic field is along a [100] type direction are described. The intensity enhancement in these cases indicates a collapse of the satellite transitions ($m \rightarrow m-1$, $m \neq 1/2$) into the central transition ($m = 1/2 \rightarrow m = -1/2$). It is concluded that the crystals contain edge and/or screw dislocations which are preferentially oriented along [110] and [100] type directions, respectively. The degree of orientation is greater in NaI than in KI. These studies afford an explanation of anomalous resonance line widths reported for NaI by other observers.

9171 OBSERVATIONS OF DISLOCATION NETWORKS IN AN ALLOY OF BODY-CENTERED CUBIC LATTICE BY ELECTRON MICROSCOPY by S. Nenno, T. Saburi, M. Tagaya and Z. Nishiyama (Osaka U.); J. Phys. Soc. Japan, Vol. 15, pp. 1409-1412, Aug. 1960

Electron microscopic observations made on dislocation networks in thin foils of 55 per cent Cr-Fe alloy annealed at 720°C after cold working are reported. Dislocation cross-grids, hexagonal networks and networks of irregular shape have been observed. From the presence of three-fold nodes, it is suggested that Burgers vectors of type [100] may be stable as well as those of type 1/2[111].

9172 GRAPHITIZATION STRESS IN POLYCRYSTALLINE CARBON AS AN ORIGIN OF DISLOCATIONS by T. Tsuzuku (Nihon U.); J. Phys. Soc. Japan, Vol. 15, pp. 1373-1379, Aug. 1960

When a polycrystalline carbon is heat-treated for graphitization, large thermal stress is produced owing to the interference of the extremely anisotropic expansion of each crystallite. This stress is expected to promote the rearrangement of the crystallites, directly or indirectly, from the so-called turbostratic structure to the tri-dimensional graphite lattice, and so it may be adequately called "graphitization stress". A stress analysis has been made on each of the spherical and the cylindrical (filamentarily textured) polycrystals in which the carbon crystallites are aligned with the basal planes parallel to the external surface. These two models accommodate to the structure of a pyrolytic carbon particle and to that of fibrous soft coke respectively. It is shown that in either of these two cases about 3×10^{10} dynes/cm^2 tension in the a-direction and about 0.9×10^{10} dynes/cm^2 compression in the c-direction can be produced by heat treatment at 2500°C, which are enough to buckle the crystal lattice at the stress concentrations of $5 \sim 20$ times and may lead to the generation of dislocations. From the corresponding strain distribution curves, the criterion for stress relaxation by these dislocations has been determined in connection with the crystallite size, which may give a measure of distinction between the so-called soft and hard carbons.

9173 DISLOCATION SOURCES IN CRYSTALS by J. J. Gilman (GE); J. Appl. Phys., Vol. 30, pp. 1584-1594, Oct. 1959

Dislocation nucleation in LiF crystals subjected to short stress pulses (1–10 sec in length) is discussed. It was found that several heterogeneities can lead to dislocation nucleations: (a) cleavage steps, (b) dislocation loops, (c) glide bands, (d) incisions or "dirt" particles, (e) precipitates (as grown), and (f) radiation-induced precipitates. Annealing treatments at moderate temperatures (200°-600°C) followed by "rapid" cooling (5°C/hr made segments of previously pinned dislocations become mobile. These mobile segments multiplied as they moved through the crystals. Several treatments which were ineffective in producing dislocation nucleation are also described. It is concluded that small foreign heterogeneities cause most of the dislocation nucleation in real crystals. Homogeneous nucleation occurs only at high stresses. Relatively little dislocation multiplication results from classical Frank-Read sources (almost none in LiF). Most dislocation multiplication occurs as a prior dislocation moves through a crystal.

Dislocations in Quenched and Irradiated Metals - See 9197

9174 STRESS-ASSISTED PRECIPITATION ON DISLOCATIONS by F. S. Ham (GE); J. Appl. Phys., Vol. 30, pp. 915-926, June 1959

The kinetic theory for the rate of stress-assisted precipitation on dislocations is re-examined. Two approximate expressions are used for the elastic interaction between a solute atom and edge and screw dislocations: $V = -A \sin\theta/r$ and $V = B/r$ respectively. The resulting partial differential diffusion equations are integrated numerically to get the time-dependent rate of precipitation on an isolated dislocation. These results are used to calculate the short-time part of the precipitation curve for an array of dislocations. Exact steady-state solutions to the diffusion equations are derived for both interactions and are used with a variational procedure to establish the long-time part of the curve for a regular array. For very short times the precipitated fraction W is proportional to t as derived by Cottrell and Bilby, but this result is not accurate over the range of t during which most of the precipitation occurs. The long-time part of the curve is given accurately by $W = 1 - \exp(-t/\tau)$, where τ can be calculated by replacing each dislocation and its stress field by a cylinder with an "effective capture radius," the value of which is calculated for each form of interaction. Complete precipitation curves are obtained for a regular array by combining the short- and long-time results, and it is shown that these are changed but slightly if the array is random. These results differ significantly from a formula suggested by Harper to extend Cottrell and Bilby's work, and they thereby indicate that the interpretation of the precipitation process for C in an a-Fe is not yet entirely established.

9175 DISLOCATION DAMPING EFFECTS IN ROCK SALT by C. L. Bauer and R. B. Gordon (Yale U.); J. Appl. Phys.,

Vol. 31, pp. 945-949, June 1960

Internal friction measurements made as a function of strain amplitude on deformed sodium chloride single crystals followed by elastic modulus measurements made during X-irradiation of the same crystals are reported. Etch pit densities were also determined. These data were used to evaluate the constants in a theory proposed by Granato and Lücke which permits the calculation of the average length of the dislocation segments, L, which vibrate under an applied alternating stress. An independent determination of the magnitude of L was made from the elastic modulus data using a method developed by Gordon and Nowick. It is concluded that the theories tested in this paper give a useful representation of dislocation damping phenomena in sodium chloride and permit use of internal friction measurements for the continuous observation of dislocations.

9176 ON THE CRYSTAL PERFECTION OF IRON WHISKERS by P. D. Gorsuch (GE); J. Appl. Phys., Vol. 30, pp. 837-842, June 1959

X-ray rocking curve measurements of the density and distribution of dislocations in tip grown iron whiskers produced by reduction of liquid iron halide slats show that the more perfect whiskers have dislocation densities below 10^6 dislocation lines per cm^2. Thus, many of these whiskers which are less than 10μ in diameter would contain, at most, only a small number of dislocations and should behave as perfect crystals. No evidence of a large elastic twist was found in any of the whiskers as would be expected for a whisker grown by a screw dislocation mechanism. This did not completely prove that iron whiskers must grow, therefore, by a mechanism based on two-dimensional nucleation as there are combinations of specific types of screw dislocations which will not produce elastic twists in the whiskers.

9177 X-RAY MEASUREMENT OF TWIN FAULTING IN FACE-CENTERED CUBIC METALS by B. E. Warren (MIT); Austl. J. Phys., Vol. 13, pp. 384-390, July 1960

A method of evaluating the twin fault probability in cold-worked fcc metals is presented. These twin faults produce a peak asymmetry, which is expressed by sine terms when the peak shape (produced by deformations) is represented by a Fourier series. The overlapping of the tails of neighboring reflections and uncertainty in the peak origin make the evaluation of the sine coefficients difficult. The method presented combines the tails of the (111) and (200) reflections; the result achieved is more nearly independent of overlapping of the tails and choice of peak origin.

9178 STUDY ON THE TWIN FORMATION IN EVAPORATED SILVER FILMS by A. Nagasawa and S. Ogawa (Tohoku U.); J. Phys. Soc. Japan, Vol. 15, pp. 1421-1425, Aug. 1960

Well oriented silver films have been formed by evaporation onto heated cleavage (001) surfaces of rock-salt in vacuum, the evaporation period having been changed in a wide range in case of the thickness kept at about 400 A, and the influence of the formation speed on the twinning in the films has been examined by electron diffraction and electron microscopy. The diffraction patterns have shown that the frequency of the twin formation is not seriously decreased by the lowest formation speed, but that imperfections such as bending or twisting of films are largely decreased. The interference fringes caused by the dynamical effect have been observed on the electron micrographs of slowly formed films. This fact means that the slow formation of films also decreases imperfections such as dislocations and vacancies and makes the lattice more perfect. The fringes are believed to be so-called equal thickness fringes originated from wedges due to the twin formation.

9179 CAPACITANCE AND BARRIER HEIGHT IN GRAIN BOUNDARIES by R. K. Mueller (Genl. Mills); J. Appl. Phys., Vol. 30, pp. 546-550, Apr. 1959

The dependence of the capacitance of a grain boundary on the height of the potential barrier ϕ is discussed. The capacitance depends on ϕ only if $\phi < 2kT \ln (N_d/n_i)$ (ev). For higher barrier potentials the capacitance is in good approximation a function of the bulk properties only. The capacitance as a function of applied bias and temperature (100°-250°K) has been measured on tilt boundaries of 4°, 6°, and 25°, with donor concentrations ranging from 10^{14} to $10^{16}/cm^3$. In all cases the barrier height was larger than $2kT \ln (N_d/n_i)$. This gives for the highest doped samples at 100°K a lower limit for the barrier height of 0.66 (ev).

9180 GRAIN-BOUNDARY DIFFUSION OF ZINC IN COPPER MEASURED BY THE ELECTRON-PROBE MICROANALYZER by M. R. Achter, L. S. Birks and E. J. Brooks (U.S. Naval Res. Lab.); J. Appl. Phys., Vol. 30, pp. 1825-1827, Nov. 1959

Grain-boundary and lattice diffusion of Zn vapor into Cu at 550°C have been measured with the electron-probe microanalyzer; a calculation of the diffusion coefficients from these results is presented. The lattice diffusion coefficient D_1 increases from 5×10^{-13} to 3×10^{-11} over the concentration range from 2 to 27.5 atomic per cent Zn. Over the same concentration range, the grain boundary diffusion coefficient D_B changes from 1×10^{-7} to 7×10^{-6}. The ratio of grain boundary diffusion coefficient to lattice diffusion D_B/D_L remains approximately 10^6.

9181 DIFFUSION OF ALUMINUM, MAGNESIUM, SILICON, AND ZIRCONIUM IN NICKEL by H. W. Allison and H. Samelson (Bell Labs.); J. Appl. Phys., Vol. 30, pp. 1419-1424, Sept. 1959

Measurements of the diffusion rates of Al, Mg, Si, and Zr alloyed as single additives in Ni in the temperature range from 800° to 970°C are reported. The method consisted of measuring the weight gain caused by surface oxidation of the additive in a wet hydrogen ambient; the surface oxides were identified by electron diffraction. Grain size was about 0.05 mm in Al-Ni, Si-Ni, and Mg-Ni, but less than 10^{-3} mm in Zr-Ni. The composite volume and grain boundary diffusion coefficients are given by $D_{Al \rightarrow Ni} = 1.1 \exp(-59{,}500/RT)$; $D_{Mg \rightarrow Ni} = 2.3 \times 10^{-5} \exp(-31{,}300/RT)$; $D_{Zi \rightarrow Ni} = 10.6 \exp(-64{,}800/RT)$; $D_{Zr \rightarrow Ni} = 10^{-5} \exp(-26{,}700/RT)$. Stereo and photomicrographs indicate considerable grain boundary diffusion, particularly in Mg-Ni and Zr-Ni.

9182 DIFFUSION OF TIN IN TIN-INDIUM ALLOYS by E. Klokholm (Temple U.); Diss. Abstr., Vol. 21, p. 1606 (A), Dec. 1960

An investigation of the diffusion rates in Sn-In alloys (1.83-2.66 per cent In) is reported. No increase was observed in diffusion rates for the compositions in the excess vacancy regions. An abrupt increase in the diffusion ratio D_a/D_c was observed in the alloys of 1.96 and 2.10 per cent In which are

in the excess vacancy composition region. A model for diffusion in the β-Sn structure is derived and extended to describe the diffusion in the Sn-In alloys. The model, when applied to the experimental diffusion data, indicates that the presence of excess vacancies causes a change in diffusion mechanism. Diffusion of Sn and In in β-Sn is shown by application of the model to the available data to proceed by slightly different mechanisms.

9183 TEXTURE OF EVAPORATED NiFe THIN FILMS by R.R. Verderber (Burroughs); J. Appl. Phys., Vol. 30, pp. 1359-1363, Sept. 1959

The texture of 28 evaporated NiFe thin films of various compositions has been investigated by the Geiger counter X-ray reflection technique. The grain orientation of the thin films is described by one of the following three textures; random, [111] fiber axis, or a [311] fiber axis. The development of a texture was influenced by the temperature of the substrate during deposition. The coercive force and the selectivity (which is a measure of the slope of the sides of the hysteresis loop) of the films were measured on a 60-cycle hysteresis loop tracer. Only the selectivity was found to be related to the texture of the films.

9184 SOME CRYSTALLOGRAPHIC AND MAGNETIC PROPERTIES OF SQUARE-LOOP MATERIALS IN FERRITE SYSTEMS CONTAINING COPPER by A. P. Greifer and W. J. Croft (RCA); J. Appl. Phys., Suppl. Vol. 30, pp. 34S-36S, Apr. 1959

Rectangular hysteresis loops have been found in ferrite systems containing Cu during an investigation based on the proposal by Baltzer that a zero or near-zero value of the effective magnetocrystalline domain anisotropy is a necessary condition for loop squareness. Data on hysteresis loop squareness of polycrystalline bodies as a function of composition, firing conditions and magnetostrictive effects are presented for the system: copper ferrite-magnesium ferrite. This system is characterized in general by large grains and long switching times. Abrupt flux changes occur in the hysteresis loop at low temperatures. Simultaneously a decrease in the coercive force with decreasing temperature and squareness values approaching unity are observed. No crystalline transitions were detected at low temperatures. Magnetostrictive measurements do not unequivocally show whether anisotropy goes through zero at compositional region of maximum squareness. The saturation magnetostriction and probably the λ_{111} go through a minimum in this region.

9185 STRUCTURAL AND MAGNETIC PROPERTIES OF Mn-Co-C ALLOYS by A. H. Holtzman and G. P. Conrad, II (duPont and Lehigh U.); J. Appl. Phys., Suppl. Vol. 30, pp. 103S-104S, Apr. 1959

A study of the magnetic properties, crystal structure, and metallographic appearance of $Mn_xCo_{(80-x)}C_{20}$ alloys is reported. A superlattice having the stoichiometric composition Mn_2Co_2C was found to be markedly magnetic. The structure of this alloy is pseudo-fcc with the C atom in the central 1/21/21/2 position, the Mn atoms in the 000 and 1/21/20 sites, and the Co atoms in the 01/21/2 and 1/201/2 sites. A magnetic structure is deduced from a consideration of the effect of atomic separation on magnetic vector alignment and an indication that electrons transfer from the central C atom to its nearest neighbors, the face atoms.

9186 SHAPE DISTRIBUTION OF MAGNETITE POWDERS by C. E. Johnson, Jr. (MMM) and W. F. Brown, Jr. (U. Minnesota); J. Appl. Phys., Suppl. Vol. 30, pp. 136S-139S, Apr. 1959

An investigation of why the shape distribution curves of single-domain magnetite powders calculated from magnetic data do not agree with those observed in the electron microscope is presented. The Stoner-Wohlfarth theory, from which the magnetic unaveraging process was derived, ignores magnetocrystalline anisotropy. This may be one of the contributory causes to the lack of agreement. To establish this, the shape curves were measured magnetically on both acicular and equant magnetic powders at various temperatures. The magnetocrystalline anisotropy of magnetite is temperature dependent, changing from about -1×10^5 ergs/cc at room temperature to $+1 \times 10^5$ ergs/cc at −165°C. The magnetically calculated shape curves show some change with temperature; this indicates a contribution from the magnetocrystalline anisotropy.

9187 STUDY OF ORIENTED POLYCRYSTALLINE FERRITES WITH CUBIC ANISOTROPY by C. F. Kooi, R. W. Moss and D. C. Stinson (Lockheed); J. Appl. Phys., Vol. 30, pp. 895-898, June 1959

A study of crystalline orientation in cubic ferrites when pressed in a magnetic field is reported. One easy axis orients in the field direction, the other easy axes lying at random in or near a perpendicular plane. Experimental torque curves have the theoretically predicted shape. The magnetic field required for microwave resonance is lower than in the same nonoriented ferrite if the axis of alignment and the field are parallel. This occurs because the anisotropy field H_a is no longer randomly oriented but helps to supply part of the resonant field requirement. Values of saturation magnetization (M_s), anisotropy energy (K), and resonant field (H_r) at 14,775 mc/sec were measured on a series of oriented polycrystalline Ni-Co ferrites. Values of the measured resonant field are compared with values obtained from Kittel's resonance relation using the independently measured values of M_s and K.

CRYSTAL GROWTH

9188 SOLUTION GROWN CRYSTALS OF AN ACETAL RESIN by P.H. Geil, Jr., N. K. J. Symons and R. G. Scott (duPont); J. Appl. Phys., Vol. 30, pp. 1516-1517, Oct. 1959

The growth of single crystals of polyoxymethylene from dilute solution is described. The crystals consist of hexagonal lamellae, often thickened by growth from screw dislocations. The chain molecules are normal to the lamellae which are 100 A thick. Thus, it is suggested that the molecules have a folded conformation. In many of the crystals double Bragg reflections were found in the electron diffraction patterns, resulting from rotations of the lamellae during growth. Dark field electron microscope photographs of these crystals exhibit moiré patterns.

9189 MAGNETIC PROPERTIES AND GRAIN STRUCTURE OF Mn-Zn FERRITES by W. Heister (Fried. Krupp Widia-Fabrik, Germany); J. Appl. Phys., Suppl. Vol. 30, pp. 22S-24S, Apr. 1959

The relations between sintering temperature, grain size, and magnetic properties of a Mn-Zn ferrite of composition MnO: ZnO:Fe_2O_3 = 28:19:53 are reported. With proper preparation, very low loss materials can be obtained.

CRYSTAL SURFACES

9190 SURFACE PHENOMENA DURING THE INTERACTION BETWEEN MgO(s) AND VARIOUS GASES AT ELEVATED TEMPERATURES by D.M. Speros and L.J. Schupp (GE); J. Phys. Chem. Solids, Vol. 15, pp. 157-166, Aug. 1960

The interaction between MgO(s) and various gases at elevated temperatures causes the appearance of pronounced etch patterns on the surface of the crystal. These patterns are of two distinct types with respect to their orientation relative to the crystallographic axes. In some atmospheres the etch lines are parallel to the edges of the naturally cleaved cubic MgO(s) while in other atmospheres the etch lines form a 45° angle with the edges of the crystal. In all the cases etch patterns consist of multi-atomic layer surface discontinuities that render them clearly visible to the unaided eye. Experimental and theoretical evidence is offered supporting the following postulates: (1) The pronounced surface discontinuities (i.e., multi-layer steps, kinks, pyramids, etc.) caused by etching are fundamentally due to the dependence of protective chemisorption on surface structure. (2) The orientation of the etch patterns is dependent on whether the etching agent attacks one surface ion (Mg^{++} of O=) preferentially over the other.

9191 HIGH-TEMPERATURE OXIDATION OF IRON WHISKERS by J.V. Laukonis and R.V. Coleman (Genl. Motors); J. Appl. Phys., Vol. 30, pp. 1364-1368, Sept. 1959

The early stages in the oxidation of single crystal Fe whiskers at high temperatures are discussed. Well defined oxide patterns were observed on clean Fe surfaces, with characteristic differences between the patterns on {100} and {110} faces. These differences tend to be eliminated if a natural oxide film is present before the high temperature oxidation is performed. Unusual mosaic oxide patterns which form on clean {100} Fe surfaces are shown.

9192 CALORIMETRIC DETERMINATION OF THE HEAT OF ADSORPTION OF OXYGEN ON EVAPORATED FILMS OF GERMANIUM AND SILICON by D. Brennan, D.O. Hayward and B.M.W. Trapnell (U. Liverpool); J. Phys. Chem. Solids, Vol. 14, pp. 117-123, July 1960

The heats of adsorption of oxygen on evaporated films of germanium and silicon have been determined to an absolute accuracy of ± 5 per cent by means of a Beeck type calorimeter. The variation of the heat of adsorption with surface coverage has been studied, together with the simultaneous change in film resistance. The significance of the results is discussed.

9193 APPLICATION OF MAGNETIC RESONANCE TECHNIQUES TO THE STUDY OF SEMICONDUCTOR SURFACES by G. K. Walters (Texas Instr.); J. Phys. Chem. Solids, Vol. 14, pp. 43-50, July 1960

After a brief discussion of the magnetic resonance phenomenon experimental methods and sensitivity considerations, there follow sections on the application of electron and nuclear paramagnetic resonance techniques respectively to the study of solid surfaces. Attention is given to the pioneering work done in these fields. The various types of surface information, such as absorption and mechanical damage, which one might hope to obtain by resonance investigations are outlined, and some preliminary new experimental results are presented.

9194 REDUCTION OF STATIC FRICTION BY SONIC VIBRATIONS by H. D. Friedman and P. Levesque (Raytheon); J. Appl. Phys., Vol. 30, pp. 1572-1575, Oct. 1959

Measurements of the effect of sonic vibrations on the coefficient of static friction for highly polished, ground, and sand-pitted steel surfaces are discussed. The coefficient of static friction can virtually be reduced to zero as a result of increased vibrations at frequencies between 6 and 42 kc.

9195 LOW FRICTION OF METALS IN RECIPROCATING SLIDING by Y. Tamai (Aeronaut. Res. Inst., Japan); J. Appl. Phys., Vol. 30, pp. 1874-1875, Dec. 1959

The observation of a very low friction in reciprocating sliding with Au, Ag, Cu, and Pt, about 10^{-2}, is reported. It was found that the characteristics common to those metals were soft metal substrate and no surface oxide or soft oxide. Some discussion is given on this phenomenon.

9196 NOTE ON THE SCRATCHING OF DIAMOND by R.H. Wentore, Jr. (GE); J. Appl. Phys., Vol. 30, pp. 1765-1768, Nov. 1959

The resistance of diamond to wear is a strong function of its orientation. The observed facts can be explained by assuming that a scratched diamond surface fails in tension behind the scratching particle. The octahedral cleavage planes are most easily pulled apart and give rise to the strong dependence of wear on crystal orientation.

ENVIRONMENTAL EFFECTS

9197 STRUCTURE OF QUENCHED AND IRRADIATED METALS by R. E. Smallman and K. H. Westmacott (Atomic Energy Res. Estab.); J. Appl. Phys., Vol. 30, pp. 603-616, May 1959

The effect of introducing point defects into pure metals by quenching and irradiation has been studied using the small-angle X-ray technique. Scattering was obtained from both quenched Cu and Al after appropriate aging treatments, from irradiated Cu after annealing, and from neutron-irradiated Cu. The source of scattering has been considered in each case. Direct observation of the scattering defects has been obtained for the quenched and irradiated metals using thin film electron transmission microscopy. The quenched Cu and Al contain dislocation loops of the order of a few hundred A diameter formed by the condensation of vacancies, while the irradiated metal contains small cavities. Some additional electron microscopic studies of quenched Ag and Au are also mentioned, and the results are discussed in relation to the mechanical and physical properties of quenched metals. No direct evidence has yet been found in neutron-irradiated Cu (because of the difficulties in electropolishing) but the small-angle scattering when considered with mechanical property measurements strongly suggests the existence of small "regions" ~ 100 A in diameter. Direct observation of "damage" in neutron-irradiated Al is observed, however, and shows the existence of dislocation loops, "jogged" dislocations, and "spiral" dislocations in agreement with theoretical predictions.

Quenched-In Defects in Sn - See 9166

9198 NEUTRON IRRADIATION EFFECTS IN A COPPER-ALUMINUM ALLOY by C. R. Houska and B. L. Averbach (MIT); J. Appl. Phys., Vol. 30, pp. 1525-1531, Oct. 1959

Diffuse X-ray scattering and peak intensities for a polycrystal-

line alloy of Cu-14.5 atomic per cent Al before and after irradiation are reported. It was shown that the average short-range order configuration in the first five neighboring shells was somewhat enhanced as a result of the irradiation. In addition, a temperature independent rise was observed in the diffuse scattering. This was interpreted in terms of static atomic displacements arising from the localized volume changes associated with neutron damage. The absence of line broadening or significant line shifts after irradiation is further confirmation of the localized nature of the damage. Defect models of radiation damage involving short range effects which average out over larger distances in the lattice are discussed.

9199 EFFECT OF NEUTRON IRRADIATION ON THERMALLY AND MECHANICALLY INDUCED NONEQUILIBRIUM STATES IN AuCu by R. L. McCollum and G. Allen (NASA); J. Appl. Phys., Vol. 30, pp. 1105-1108, July 1959

Studies of the effect of neutron irradiation on the resistivity and magnetoresistivity of the alloy AuCu when subjected to various pre-irradiation thermal and mechanical treatments are reported. The specimens were exposed to estimated fast neutron fluxes up to 7.3×10^{18} neutrons/cm^2 in the Brookhaven pile. In the case of thermally disordered specimens, the effect of the irradiation was to decrease the resistivity in completely disordered states and to increase the resistivity in completely ordered states; viz., there was some tendency for specimens to reach intermediate degrees of order. The effect on mechanically disordered specimens was to increase the resistivity in all cases. The irradiation effected a larger percentage change in the coefficient of magnetoresistivity than in the resistivity.

Small-Angle Scattering of X-Rays from Neutron Irradiated Cu - See 9157

9200 NEW METHOD FOR RANGE MEASUREMENTS OF LOW-ENERGY ELECTRONS IN SOLIDS by J.E. Holliday and E. J. Sternglass (Westinghouse); J. Appl. Phys., Vol. 30, pp. 1428-1431, Sept. 1959

A new method for determining the range of low-energy electrons in solids is described and compared with older techniques. In the new method, the material under study is deposited on a thick layer of greatly different electron backscattering characteristics. When the incident electrons have just sufficient energy to penetrate to the support and return to the surface, a marked change in the backscattered fractions occurs. In this manner, the need for very thin organic supporting films of unknown stopping power is avoided. Range-energy data from 1 to 15 kev for films of Al on a Au substrate obtained by this technique are found to agree with the data obtained by the use of cathode luminescence to detect electron penetration. The technique was applied to thin films of Au in the energy region from 2 to 15 kev. It was found that the practical ranges in mg/cm^2 for Au and Al were the same below 10 kev, unlike the situation in the mev region where the effective penetration into Al is about twice that for Au due to the importance of nuclear scattering in a high Z element. Good agreement is found with the Bohr-Bethe theory for Al at all energies and for Au below 10 kev.

9201 EFFECT OF ATMOSPHERE CONDITIONS ON THE BRITTLENESS OF NaCl by E.S. Machlin (Columbia U.) and G. T. Murray (Mats. Res. Corp.); J. Appl. Phys., Vol. 30, pp. 1731-1732, Nov. 1959

Contrary to the results of previous investigators, it has been found that molecular O_2 and N_2 have no effect on the ductility of rock salt single crystals. Also, it has been found that air-aged crystals are brittle in summer and ductile during a major fraction of the time in winter. Ductile rock salt crystals have been made brittle by subjecting them to ozone, NO, and atomic oxygen atmospheres. It is believed the ozone content of the atmosphere is responsible for the repeated effect on brittleness. Other embrittling agents have been found.

SOLID STATE PHYSICS

GENERAL

9202 RULES FOR THE PREDICTION OF SEMICONDUCTIVITY IN THE INORGANIC CRYSTALLINE LATTICE [in French] by J. P. Suchet (Serv. Rech. Fondam., Saint-Gobain); J. Phys. Chem. Solids, Vol. 12, pp. 74-88, Dec. 1959

The exact significance of the "8-N" rule for predicting semiconductivity with respect to the rule proposed by Mooser and Pearson for compound semiconductors is discussed. Mooser and Pearson's rule must be supplemented by two analogous rules for 3- and 2-coordinated nets. Purely covalent formulae are preferable to ionic ones for visualizing such electronic rules, and bonding schemes using them are capable of including defect lattices by treating the vacant sites as atoms of zero valency. A new concept of a "compensated lattice" based upon knowledge of interactions between substitutional and interstitial impurities in germanium and silicon is introduced and is applied to the study of compounds such as Li_3Bi which do not satisfy the bonding schemes mentioned above. The Bi_2Te_3-type structure is discussed in detail and a classification of all known inorganic semiconductors into a few fundamental lattice types is proposed.

9203 APPROXIMATE WAVE FUNCTIONS FOR VALENCE ELECTRONS OF CERTAIN ATOMS by A.I. Gubanov (Phys.-Tech. Inst., Leningrad); Soviet Phys.-Solid State, Vol. 1, pp. 182-186, Feb. 1959

Approximate wave functions for the s and p electrons in atoms which form sp^3 type covalent bands are derived. The parameters of the wave functions for eleven elements are derived using the covalent radius and the ionic radius of each atom. The approximate wave function cannot give quantitative information but can indicate changes which take place from one element to another. Suggestions for improving the agreement between the approximate and the Hartree functions are given.

CRYSTAL PHYSICS

BINDING PROPERTIES

9204 THE BINDING ENERGY OF THE σ BOND. Part II. APPLICATION TO THE DIAMOND CRYSTAL by K. O-Ohata (Tokyo Inst. Tech.); J. Phys. Soc. Japan, Vol. 15, pp. 1258-1263, July 1960

The cohesive energy of the diamond crystal is calculated using a general scheme derived by the Heitler-London approximation. It is found that the value of the binding energy is about 3.26 ev per a bond, in good agreement with the observed value.

9205 GENERAL FORMULATION AND THE CASE OF ZERO DEFORMATION OF THE POTENTIAL ON THE GOODWIN-ARTMANN MODEL by J. Koutecký and M. Tomásek (Czech. Acad. Sci.); J. Phys. Chem. Solids, Vol. 14, pp. 241-247, July 1960

Within the framework of the tight-binding method, general equations are set up for the calculation of orbital energies and wave functions of the electron in a crystal model in which an interaction between atomic s orbitals and p orbitals is assumed. Simple explicit expressions are derived for the case of zero deformation of the potential of the crystal surface. From a discussion of the hybridization of the wave functions of the volume and surface states the connection with the concept of free valence localized in the crystal surface follows.

9206 THE NATURE OF BINDING IN CADMIUM TELLURIDE by G. F. J. Garlick, J. M. Hough and R. A. Fatehally (U. Hull); Proc. Phys. Soc., Vol. 72, pp. 925-926, Nov. 1958

Measurements of the refractive index of a single crystal of CdTe at wavelengths beyond the absorption edge of the crystal (880 mμ at 290°K) employing interference filters to provide 903 mμ and 1100 mμ monochromatic radiation are reported. The refractive indexes are 3.47 ± 0.05 and 3.13 ± 0.04 respectively. There is reasonable agreement between the dielectric constant at low frequencies and the square of the optical refractive index. It is concluded that in CdTe the lattice binding is predominantly homopolar in character.

ENERGY BAND STRUCTURE

9207 ELECTRON ENERGY BANDS IN SOLIDS by J. Callaway (U. Miami); Solid State Phys.-Adv. Res. and Appl., Vol. 7, Academic Press, 1958, pp. 99-212

The general theory of electronic structure of solids is introduced. It is pointed out that there is no method of calculation which is really practical for a general point in the Brillouin zone. The OPW method, cellular method, and tight binding method are described briefly. Energy band calculation and the band structures of metals and semiconductors are also discussed. For Si and Ge many detailed features have been determined. Agreement between theory and experiment is a valid test of the crystal potential used and the one-electron approximation. So far, the theory is adequate to describe a large number of phenomena in semiconductors and metals, but quantitatively the results tend to be somewhat disappointing. More information on electron-electron interaction is needed.

9208 BAND STRUCTURE OF ALUMINUM by W. A. Harrison (GE Res. Labs.); Phys. Rev., Vol. 118, pp. 1182-1189, June 1, 1960

Calculations of the band energies at symmetry points in Al by Heine are extended into the zone using the pseudopotential interpolation scheme in order to obtain constant-energy curves in the neighborhood of the Fermi surface. In conjunction with this calculation, the lines of contact between various bands are found in detail. The de Haas-van Alphen effect, cyclotron-resonance effect, anomalous skin effect, and low-temperature specific heat are discussed in terms of these constant-energy curves and the results are compared with experiment. It appears from this comparison that the geometry of the Fermi surface is given quite well by the band calculations, but that there is a discrepancy of a factor of order two between the derived and measured effective masses. A "single orthogonalized-plane-wave approximation" is compared with the more exact treatment and found to be a good starting approximation, suitable for semiquantitative treatment of the electronic structure.

9209 ELECTRONIC STRUCTURE OF POLYVALENT METALS by W. A. Harrison (GE Res. Labs.); Phys. Rev., Vol. 118, pp. 1190-1208, June 1, 1960

A single-orthogonalized-plane-wave approximation is defined and used to construct the Fermi surface for face-centered-cubic and body-centered-cubic metals of valence one through four and for hexagonal-close-packed metals of valence one through three. The de Haas-van Alphen effect, cyclotron-resonance effect, and anomalous skin effect are discussed in detail in terms of these surfaces and the deduced properties are compared with experiment where suitable experiments exist. In particular, earlier and equivalent comparisons for lead and for aluminum are reviewed, and detailed comparisons with existing experimental data on zinc and cadmium are made. It is found that the single-OPW approximation is in semiquantitative agreement with experiment in all of these cases, both as to the form of the Fermi surface and its associated effective masses. In conjunction with these studies, detailed descriptions of the apparent Fermi surfaces in zinc and cadmium are given. An extension of the method to allow experimental determination of a more precise description of the band structure is discussed, and the generalization of the method to studies of alloys is outlined.

9210 FERMI SURFACE AND SOME SIMPLE EQUILIBRIUM PROPERTIES OF A SYSTEM OF INTERACTING FERMIONS by J. M. Luttinger (U. Pennsylvania); Phys. Rev., Vol. 119, pp. 1153-1163, Aug. 15, 1960

Certain analytical properties of the propagators of many-fermion systems that lead rigorously to the existence of sharp discontinuities of the momentum distribution and their use to define a Fermi surface for a system of interacting fermions are discussed. It is shown that the volume of this surface in momentum space is unaffected by the interaction. The same analytic properties are shown to lead, by direct statistical mechanical arguments to simple expressions for the low-temperature heat capacity, the spin paramagnetism, and the compressibility of the system. These expressions are analogous to the corresponding expressions for noninteracting particles. The whole formalism may be generalized when an external periodic potential is present (band case).

9211 SURFACE STATES ASSOCIATED WITH ADSORBED ATOMS by T. B. Grimley (U. Liverpool); J. Phys. Chem. Solids, Vol. 14, pp. 227-232, July 1960

The effects of adsorption upon surface levels are discussed. When a foreign atom is in interaction with a crystal surface, discrete electron levels may exist. These levels lie outside the normal crystal bands (including any surface bands) and the corresponding wave functions are large on the foreign atom and on the crystal atoms near it in the surface but fall to zero at points in the crystal remote from the foreign atom. Such levels allow for the formation of localized bonds between the foreign atom and the crystal. For semiconducting crystals they can provide surface traps for either electrons or positive holes. When the surface is completely covered by foreign atoms, bands of surface states may exist although no surface states exist when the surface is clean and no discrete levels are formed when only one foreign atom is present.

9212 CROSS SECTIONS OF MIDGAP SURFACE STATES IN SILICON BY PULSED FIELD EFFECT EXPERIMENT by G. Ruprecht (Raytheon); J. Phys. Chem. Solids, Vol. 14, pp. 208-213, July 1960

The cross sections and energy levels of surface states in silicon around midgap have been investigated by a pulsed field effect technique. Two energy levels have been found, one acceptor-like (A), the other one donor-like (D). The results are: $(E_C - E_A) = 0.52$ ev, $\sigma_n^A = 3 \times 10^{-16} cm^2$, $(E_A - E_V) = 0.72$ ev, $\sigma_p^A = 4 \times 10^{-12} cm^2$, $(E_D - E_V) = 0.54$ ev, $\sigma_p^D = 2 \times 10^{-15} cm^2$, $(E_C - E_D) = 0.63$ ev, $\sigma_n^D = 1 \times 10^{-13} cm^2$.

9213 FAST SURFACE STATES IN GERMANIUM AT LOW TEMPERATURES by E. Harnik, Y. Goldstein, N. B. Grover and A. Many (Hebrew U.); J. Phys. Chem. Solids, Vol. 14, pp. 193-199, July 1960

The characteristics of fast states on real germanium surfaces at low temperatures are discussed. Measurements of the time-constant of relaxation processes involving the interaction between the fast states and the majority-carrier band have been carried out on n-type samples as a function of temperature and surface potential using a pulsed field-effect technique. These have been complemented with measurements of trapped charge density as a function of barrier height at various low temperatures. It is shown that the experimental results at such temperatures can be reconciled with room temperature data only by the assumption that both the energy of the recombination center, with respect to the conduction-band edge, and its capture cross-section for electrons are temperature dependent. The recombination level is found to move closer to the conduction band as the temperature is reduced while its capture cross-section for electrons decreases as $\exp(-E_r/kT)$, where the activation energy E_r is about 0.2 ev. There are also indications of surface traps within 0.06 ev from the conduction band which have very small capture cross-sections for electrons. It has been observed that for values of the surface potential corresponding to strong depletion layers the relaxation phenomena are dominated by a process of enhanced generation of minority carriers, the mechanism of which is not understood.

9214 ANALYSIS OF THE SEMICONDUCTING PROPERTIES OF COBALT FERRITE by G.H. Jonker (Philips); J. Phys. Chem. Solids, Vol. 9, No. 2, pp. 165-175, 1959

An energy level scheme which describes the semiconducting properties of $CoFe_2O_4$ is derived from measurements of resistivity, activation energy, and Seebeck effect. These properties differ considerably from those of normal semiconductors since the charge carriers are not free to move through the crystal lattice but jump from ion to ion.

Energy Levels of Ag Luminescent Centers in Sulfides - See 9418

9215 ON THE DIAMAGNETISM OF GRAPHITE. Part I. ENERGY LEVELS OF π-ELECTRONS by H. Sato (Nagoya U.); J. Phys. Soc. Japan, Vol. 14, pp. 609-617, May 1959

The energy levels of the conduction electrons in graphite in the presence of a magnetic field are calculated by the tight binding approximation method. The effect of band-to-band transitions, which is not included in the Landau-Peierls treatment, is taken into account. The theory is a natural extension of the Luttinger-Kohn and McClure theories for the band structure of graphite. The relation to the diamagnetic susceptibility is discussed.

Energy Band Structure of CdS - See 9250

LATTICE POTENTIALS AND VIBRATIONS

9216 CRYSTAL POTENTIAL AND ENERGY BANDS OF SEMICONDUCTORS. Part III. SELF-CONSISTENT CALCULATIONS FOR SILICON by L. Kleinman and J. C. Phillips (U. California); Phys. Rev., Vol. 118, pp. 1153-1167, June 1, 1960

An approximately self-consistent crystal potential for Si is constructed from a superposition of free-atom core and a sampling of crystal valence band charge densities. Valence-core exchange is calculated directly from core wave functions while valence-valence exchange is included using momentum-independent and momentum-dependent approximations taken from the results for a free-electron gas. The resulting crystal potential is surprisingly similar to one previously obtained by Woodruff from a superposition of free-atom charge densities. The calculated valence wave functions in the core region differ substantially from those of Woodruff because of the variational method used by him to calculate wave functions in that region. As a result the calculated energy gap is changed from Woodruff's value of 4 ev to about 1.5 ev, in substantially better agreement with the experimental value (1.1 ev). The various uncertainties in the calculation are listed; it is concluded that the relative position of levels near the band gap should be correct to within about 1 ev. Effective masses are also calculated and compared with experiment; the agreement is quite good.

9217 LATTICE DYNAMICS OF ALKALI HALIDE CRYSTALS by A.D.B. Woods, W. Cochran and B.N. Brockhouse (Atomic Energy of Canada); Phys. Rev., Vol. 119, pp. 980-999, Aug. 1, 1960

Theoretical and experimental studies of the lattice dynamics of alkali halides are reported. A theory of the lattice dynamics of ionic crystals is given based on replacement of a polarizable ion by a model in which a rigid shell of electrons (taken to have zero mass) can move with respect to the massive ionic core. The dipolar approximation then makes the model exactly equivalent to a Born-von Kármán crystal in which there are two "atoms" of differing charge at each lattice point, one of the "atoms" having zero mass. The model has been specialized to the case of an alkali halide in which only one atom is polarizable, and computations of dispersion curves have been carried out for sodium iodide. The dispersion $\nu(q)$ relation of the lattice vibrations in the symmetric [001], [110], and [111] directions of sodium iodide at 110°K was determined using neutron spectrometry. The transverse acoustic, longitudinal acoustic, and transverse optic branches were determined completely with a probable error of about 3 per cent. The dispersion relation for the longitudinal optic (LO) branch was determined for the [001] directions with less accuracy. Frequencies of some important phonons with their errors (units 10^{12} cps) are: TA [0,0,1] 1.22 ± 0.04, LA [0,0,1] 1.82 ± 0.06, TA $[\frac{1}{2},\frac{1}{2},\frac{1}{2}]$ 1.52 ± 0.05, LA $[\frac{1}{2},\frac{1}{2},\frac{1}{2}]$ 2.32 ± 0.06, TO [0,0,0] $3.6_0 \pm 0.1$, TO [0,0,1] $3.8_0 \pm 0.1$, TO $[\frac{1}{2},\frac{1}{2},\frac{1}{2}]$ $3.5_0 \pm 0.1$. The agreement between the experimental results and the calculations based on the shell model, while not complete, is quite satisfactory. The neutron groups corresponding to phonons of the LO branch were anomalously energy broadened, especially for phonons of long wavelength, suggesting a remarkably short lifetime for the phonons of this branch.

9218 LATTICE VIBRATIONS IN ALKALI HALIDE CRYSTALS. Part II. POTASSIUM AND RUBIDIUM HALIDES; CESIUM FLUORIDE by A. M. Karo (U. California); J. Chem. Phys., Vol. 33, pp. 7-20, July 1960

Vibrational frequency distributions for the potassium and rubidium halides and for cesium fluoride are evaluated on the basis of the Born lattice theory by the use of Blackman's numerical sampling method. Both room-temperature and extrapolated 0°K parameters have been used in the calculation. Specific heats, the corresponding Debye characteristic temperatures, and the moments of the distributions have been obtained directly from the frequencies. Comparison is made with experimental data and with other theoretical work.

9219 ELECTRICAL, OPTICAL AND ELASTIC PROPERTIES OF DIAMOND TYPE CRYSTALS. Part IV. INTERACTION BETWEEN CONDUCTION ELECTRONS AND LATTICE VIBRATIONS by V. S. Mashkevich (Kiev Polytech. Inst.); Soviet Phys.-JETP, Vol. 9, pp. 1237-1241, Dec. 1959

The interaction produced between conduction electrons and lattice vibrations in diamond type crystals by the polarization due to these vibrations is discussed. The possible existence of polaron states is investigated and the electron mobility is evaluated.

Lattice Vibrations in CdS - See 9231

9220 PHONON BROADENING OF IMPURITY LINES by E. O. Kane (Hughes Prod.); Phys. Rev., Vol. 119, pp. 40-42, July 1, 1960

The theory of line broadening given by Lax is found not to apply to shallow impurities in Ge and Si. Observed broadening may be instrumental at low temperatures and may be due to lifetime broadening through phonon interaction at nitrogen temperature. Calculations suggest that p-type spin resonance in Ge and Si may be observable.

9221 MEASUREMENT OF TRANSMITTED PHONON DRAG IN SILICON by K. Hubner and W. Shockley (Shockley); Bull. Am. Phys. Soc., Ser. II, Vol. 5, p. 376(A), June 15, 1960

The transmitted phonon drag effect has been used to observe the direct passage of phonons over distances of up to 200μ and to measure their mean free path at liquid nitrogen temperature. An electric ac field E_{n1} is applied parallel to the p-n junctions in one n-layer of a diffused n-p-n-structure. A field E_{n2} of opposite polarity in the other n-layer indicates the transmitted phonon drag across the p-layer. The measurements are taken at 77°K for various widths W_p of the separating p-layer of 10-ohm-cm resistivity. E_{n2}/E_{n1} decreases exponentially with increasing W_p with a characteristic length $L = 90\mu$. For the low hole concentration used in the base layer, phonon-phonon scattering is dominant over phonon-hole scattering, and L is therefore the mean free path of those phonons which interact with the carriers due to scattering by the high-frequency phonons. The experiments and the prospects for further investigations were described.

9222 ELASTIC WAVES IN TRIGONAL CRYSTALS by G. W. Farnell (McGill U.); Bull. Am. Phys. Soc., Ser. II, Vol. 5, p. 372(A), June 15, 1960

In nonisotropic single crystals the normals to the wavefronts of elastic waves are not colinear with the vectors representing either the energy flow or the particle displacement. Some calculations of the propagation characteristics of sound waves in two particular trigonal crystals, quartz and ruby (Al_2O_3), were illustrated. The solution of the equations of motion for the crystal was assumed to be a plane wave with wavefront perpendicular to a given direction. The three velocities obtained from the eigenvalue equation were plotted for many different directions in the crystal. The displacement and energy flow vectors corresponding to each direction were determined for the quasi-longitudinal and the quasi-transverse waves. For both the displacement and the energy flow the results were presented by the points of intersection of the various vectors with a unit sphere.

OTHER PROPERTIES

9223 SOME APPLICATIONS OF THE DISCRETE FOURIER TRANSFORM TO PROBLEMS OF CRYSTAL LATTICE by I. Babuska, E. Vitasek and F. Kroupa (Czech. Acad. Sci.); Czech. J. Phys., Vol. 10B, No. 6, pp. 419-427, 1960

The theory of the discrete Fourier transform is applied in solving a system of difference equations describing the positions of atoms in a deformed crystal lattice. The crystal lattice is approximated by the Born-Kármán model modified to include the internal energy of the undeformed crystal.

ELECTRICAL PROPERTIES

GENERAL

9224 PROPERTIES AND STRUCTURE OF TERNARY SEMICONDUCTOR SYSTEMS. Part VI. ELECTRIC AND PHOTOELECTRIC PROPERTIES OF FILMS OF THE Sb_2S_3-Bi_2S_3 SYSTEM by B. T. Kolomiets and V. M. Lyubin; Soviet Phys.-Solid State, Vol. 1, pp. 674-680, Nov. 1959

The electric and photoelectric properties of Sb_2S_3-Bi_2S_3 films are compared with those of bulk material and the effect of thermal treatment on the films is described.

DIELECTRIC PROPERTIES

9225 CONTRIBUTION TO THE THEORY OF THE DIELECTRIC PROPERTIES OF THE ALKALI HALIDES by E. E. Havinga (Phillips Res. Labs.); Phys. Rev., Vol. 119, pp. 1193-1198, Aug. 15, 1960

Some relations between dielectric properties of diagonal cubic ionic crystals are derived on the basis of the shell model for ions of Dick and Overhauser. The relations, which contain no model constants, are in a good agreement with experimental data. Also it is shown that Dick and Overhauser overestimated the number of electrons in the shells of the ions, which accounts for the failure of their quantitative treatment. In an appendix the paper of Hanlon and Lawson on the same subject is also discussed.

9226 THEORY OF DIELECTRIC CONSTANTS OF LiF by E.R. Levin (Pitman-Dunn Labs.) and E. L. Offenbacher (Temple U.); Phys. Rev., Vol. 118, pp. 1142-1149, June 1, 1960

The static and high-frequency dielectric constants and the effective charge of LiF are calculated using a simplified model in which the polarizability of the positive ion is neglected and

that of the negative ion is attributed entirely to perturbations in the outermost subshell (2p) of electrons. The present calculation differs from the variational treatment of Yamashita mainly in the inclusion of perturbed wave functions for the 2p electrons which are orthogonal to the core-electron wave functions. Also, different methods are employed in evaluating portions of the energy of the crystal in a field and in deducing the effective charge ratio e^*/e from the calculated energy. It is found that the use of trial wave functions which preserve the orthogonality within individual ions is of prime importance, and leads to results in generally better agreement with observation than the previously used nonorthogonal functions.

9227 DIELECTRIC PROPERTIES OF YTTRIUM GARNET CONTAINING GALLIUM by E. E. Anderson (U.S. Naval Ord. Lab.); Bull. Am. Phys. Soc., Ser. II, Vol. 5, p. 357(A), June 15, 1960

Measurements of dc and ac resistivities and k' made on a single crystal of YIG and on polycrystalline samples of YIG with gallium as substituent were reported. The room temperature values of ρ_{dc} are $\sim 10^{12}$ and $\sim 10^{10}$ ohm-cm, respectively, for the YIG single crystal and YIG polycrystals. Plots of $\ln \rho_{dc}$ vs $1/T$ are linear and have slopes corresponding to activation energies of 0.90 ev for the single crystal and 0.77 ev for the polycrystals. The partial replacement of iron by gallium results in significant decreases in ρ_{dc} and reduces the activation energy of the current carriers to 0.65 ev for a wide range of gallium substitutions. For all samples ρ_{ac} falls off rapidly with frequency to values of 10^3-10^5 ohm-cm at ~ 10 Mc/sec.

Dielectric Properties of YIG - See 9368

9228 DIELECTRIC BREAKDOWN OF POROUS CERAMICS by R. Gerson and T. C. Marshall (Clevite); J. Appl. Phys., Vol. 30, pp. 1650-1653, Nov. 1959

The effect of porosity in ceramic materials on dielectric breakdown strength is calculated using a statistical approach. The drop in dielectric strength obtained in this way is in good agreement with the experimental data for $PbZrO_3$-$PbTiO_3$ ceramics. The theory shows that the measured dielectric strength in porous materials is a function of the porosity, the void size, and the dimensions of the sample.

9229 HIGH TEMPERATURE DIELECTRIC BREAKDOWN OF ALKALI HALIDES by J. J. O'Dwyer (U. New South Wales); Austl. J. Phys., Vol. 13, pp. 270-277, July 1960

In the high temperature region much of the experimental work on the dielectric breakdown of the alkali halides is apparently conflicting. If, however, it is assumed that breakdown is thermal in nature instead of intrinsic, reasons can be given which reduce the difference between various sets of existing experimental results. A calculation of the thermal breakdown strength is given based on the assumption that the electrical conductivity is principally ionic. The magnitude and temperature variation of the breakdown strength is given correctly without disposable constants. Some suggestions are made for experimental work which may clear up outstanding difficulties.

9230 BETA PARTICLE TRANSMISSION CURRENTS IN SOLID DIELECTRICS by B. Gross (Inst. Nacional de Tecnologia, Brasil), A. Bradley and A. P. Pinkerton (Radiation Res.); J. Appl. Phys., Vol. 31, pp. 1035-1037, June 1960

The current from a beta particle source measured through a thin dielectric cannot be predicted simply from the absorption curve. A model is considered in which the space charge formation in the medium results in a component of current in addition to that of the betas transmitted. Calculations developed from this model give a close approximation to experimental results.

Conductivity of KCl-KBr Solid Solutions - See 9270

9231 DIELECTRIC SUSCEPTIBILITY TENSOR OF CADMIUM SULFIDE by T. Masumi (U. Tokyo); J. Phys. Soc. Japan, Vol. 14, pp. 1140-1142, Sept. 1959

Measurements of the components of the static dielectric tensor $|(\kappa_{s_{ij}})|$ of wurtzite structure cadmium sulfide are reported. An anisotropy of κ_s was found between the two orientations $[2\bar{1}\bar{1}0]$ and [0001]. This provides some information about the lattice vibration spectra of cadmium sulfide and on the scattering mechanisms of electrons in several semiconductors.

9232 TEMPERATURE DEPENDENCE OF ϵ' AND ϵ'' OF STRONTIUM-BISMUTH TITANATE AND OF BARIUM TITANATE AT FREQUENCIES OF 9400 MC by G.L. Lipaeva and G.I. Shanavi (Lebedev Phys. Inst., Moscow); Soviet Phys.-Solid State, Vol. 2, pp. 472-474, Sept. 1960

Measurements of the complex dielectric permeability of strontium-bismuth titanate (80.3 $SrTiO_3$–19.7 $Bi_2O_3 \cdot TiO_2$), known as SBT, and of $BaTiO_3$, made at temperatures from -180° to 250°C at 10 kMc, are reported. Data confirming the relaxation nature of the SBT polarization are presented. As the frequency is increased from 10^6 to 10^{10} cps, the relaxation maximum of the dielectric losses occurs at increasingly higher temperatures.

9233 ON THE ISOTOPIC EFFECTS IN THE FERROELECTRIC BEHAVIOUR OF CRYSTALS WITH SHORT HYDROGEN BONDS by R. Blinc (J. Stefan Inst., Yugoslavia); J. Phys. Chem. Solids, Vol. 13, pp. 204-211, June 1960

An attempt to correlate the isotopic effects in the ferroelectric properties of hydrogen-bonded crystals with the observed anomalies in their IR and NMR spectra has led to the conclusion that the protons in the hydrogen bonds are tunneling in double-minimum potential fields. The ferroelectric transition is assumed to be the result of a deformation of the protonic distribution due to electrostatic interactions. It has been found that a quantum-mechanical extension of Mason's and Devonshire's long-range-forces model is able to explain, by the same mechanism, the results of IR and NMR spectroscopy as well as the dependence of the Curie point on the mass of the hydrogen isotope, the sharper increase of the spontaneous polarization with falling temperature and the larger value of the spontaneous polarization at absolute zero for deuterated rather than for hydrogen compounds. The proposed model predicts that a ferroelectric transition occurs only if the dipole-dipole interactions, expressed as frequencies, are greater than the tunnelling frequency on the lowest vibrational level.

9234 DOMAIN EFFECTS IN THE DEUTERON MAGNETIC RESONANCE SPECTRUM OF KD_2PO_4.Z by E. A. Uehling and J. L. Bjorkstam (U. Washington); Bull. Am. Phys. Soc., Ser. II, Vol. 5, p. 345(A), June 15, 1960

An additional splitting which occurs in the NMR spectrum of the deuteron in the ferroelectric KD_2PO_4 when the crystal is

ooled below the Curie temperature was discussed. Since the rystal had not been poled into a single domain, the addition- l splitting was previously attributed to alternately polarized omains. The magnitude of this additional domain splitting as reasonably consistent with the shear known to occur when he crystal polarizes spontaneously. The possible effects of lternately positioned deuterons in the double minimum hydro- en bond potential and the different frequencies of shuttling etween these positions above and below the Curie temperature ave now been investigated by studying the resonance in the resence of an electric field. These experiments show that olarization of the crystal causes one set of the split lines to isappear. Reversing the direction of polarization brings out he second set of lines in place of the first. These results eem to confirm the belief that the splitting in question is a omain effect.

9235 DEUTERON MAGNETIC RESONANCE SPECTRUM IN DEUTERATED ROCHELLE SALT by J. L. Bjorkstam and E. A. Uehling (U. Washington); Bull. Am. Phys. Soc., Ser. II, Vol. 5, p. 345(A), June 15, 1960

Although the dielectric anomalies associated with ferroelectric materials were first discovered in Rochelle salt [NaK(tartrate) $\cdot 4H_2O$], the complexity of the crystal structure has precluded, o date, a complete analysis. To complement the available eutron diffraction, infrared, and NMR data an investigation f the NMR spectrum of the deuterated crystal has been under- aken. Upon deuteration, all but 2 of the 12 protons in the S molecule are replaced. As a result of the quadrupolar plitting, this large number of nonequivalent deuterons leads o a very complex spectrum. The over-all splitting is of the rder of 200 kc/s. The relaxation time T_1 is less than 1 sec nd depends on factors which have to be studied in detail. The ature of the spectrum and its dependence on temperature were escribed.

9236 FORMATION OF POLARONS IN CRYSTALS WITH THE ABSORPTION OF LIGHT by E. F. Gross and I. Pastrnyak Phys.-Tech.Inst.,Leningrad); Soviet Phys.-Solid State, Vol. , pp. 466-468, Mar. 1959

A new mechanism for polaron formation in ionic crystals which xplains the double step at the short wave absorption limit of Cu_2O is discussed. Thermal motion of the ions can cause, at me instant, a local ion grouping characteristic of a polaron ell. If at this time optical excitation of electrons from the alence band is occurring, an electron can land in a polaron ell, resulting in a stable complex. Since the effective asses of holes and electrons are equal for Cu_2O, the absorp- on frequencies for both these transitions to the polaron levels ill be equal. The theory is in good agreement with the ex- erimental results.

9237 DYNAMIC PROPERTIES OF THE POLARIZABILITY IN $BaTiO_3$ CRYSTAL by K. Husumi (Elect. Commun. Labs.); . Appl. Phys., Vol. 30, pp. 978-981, July 1959

study of the second harmonic distortion by a $BaTiO_3$ crystal f a small high-frequency sinusoidal electric field, superim- osed on a low-frequency switching field, is reported. From he phase relationship of the second harmonic distortion with espect to the measuring signal, together with the increase of he fundamental component of the capacitive current, it is oncluded that the polarizability increases markedly for the ackward direction during switching.

9238 MODEL FOR POLARIZATION REVERSAL IN ROCHELLE SALT by H.H. Wieder (U.S. Naval Ord. Lab.); Bull. Am. Phys. Soc., Ser. II. Vol. 5, p. 357(A), June 15, 1960

Nucleation and wall motion of ferroelectric domains have been studied by means of the electro-optic Kerr effect and the displacement currents observed during polarization reversal. A theoretical model for the reversal mechanism similar to that proposed for colemanite was shown to be applicable to Rochelle salt. Large internal stresses localized at crystal imperfections inhibit growth of a nucleus except along the ferroelectric axis, and the reversal process is then controlled mainly by the nucleation rate of domains.

9239 POLARIZATION REVERSAL BY SIDEWAYS EXPANSION OF DOMAINS IN FERROELECTRIC TRIGLYCINE SULFATE by A. G. Chynoweth and J. L. Abel (Bell Labs.); J. Appl. Phys., Vol. 30, pp. 1073-1080, July, 1959

At fields in the range 30-35 v cm^{-1}, polarization reversal in liquid-electroded triglycine sulfate crystals is accomplished by the formulation and sideways expansion of a relatively few domains. While small, the domains are elliptical or lenticular in shape, but as they grow, they tend to become irregular before amalgamating with each other. In some cases, at least, the elliptical domains have approximately equilibrium shapes as determined by the wall energy. Some general results are given concerning the sites at which the domains form and the way in which domains contract when the field is reversed.

9240 THE MOVEMENT OF SINGLE 90° DOMAIN WALLS OF $BaTiO_3$ IN AN ALTERNATING ELECTRIC FIELD by J. Fousek and B. Brezina (Czech. Acad. Sci.); Czech. J. Phys., Vol. 10B, No. 7, pp. 511-528, 1960

The origin and characteristics of 90° domain wall movements in $BaTiO_3$ crystals in an alternating 50 cps electric field are discussed.

9241 AGING PROCESS IN TRIGLYCINE SULPHATE by J. Stankowska and J. Stankowski (A. Mickiewicz U.); Proc. Phys. Soc., Vol. 75, pp. 455-456, Mar. 1960

The rejuvenation and aging of ferroelectric triglycine sulphate are discussed. An "old" sample, which exhibits a double hysteresis loop, can be converted to a "young" sample, which exhibits a normal hysteresis loop, by heating the sample above its Curie point or by applying an ac field. Oscillographs showing the rejuvination process in both pure triglycine sulphate and in triglycine sulphate doped with $CuSO_4$ are presented. High concentrations of $CuSO_4$ were found to decrease ϵ and P_s and increase the coercive field E_c. By considering the processes involved in aging it is pointed out that for practical purposes pure ferroelectrics, in which ϵ, P_s and E_c undergo small changes with time, should be used.

9242 BIAS IN FERROELECTRIC COLEMANITE by E. Fatuzzo (RCA Labs., Ltd., Zurich); J. Appl. Phys., Vol. 31, pp. 1029-1034, June 1960

The question of the existence of an intrinsic bias in colemanite above the Curie point is studied and compared with experimental results. It is concluded that a bias does exist above the Curie point and that it is completely responsible for the pyroeffect experimentally observed there. Some formulas connecting the pyroeffect and the intrinsic bias are derived and compared with data available in the literature.

9243 FERROELECTRIC PROPERTIES OF COLEMANITE by H. H. Wieder (U.S. Naval Ord. Lab.); J. Appl. Phys., Vol. 30, pp. 1010-1018, July 1959

The ferroelectric properties of the calcium borate mineral, colemanite, in the ferroelectric and paraelectric temperature regions are discussed. It is shown that Devonshire's phenomenological theory may be applied successfully to account for the experimental measurements of spontaneous polarization and electrical susceptibility over a wide temperature range. The thermodynamic transition is confirmed to be of second order, occurring for unbiased crystals at −7°C. It is shown, in general, that the temperature T_o at which such a transition takes place depends upon the effective electric field E as $T_o - kE^{2/3}$ where k is a constant evaluated from Devonshire's expansion. The effect of space charge fields is evaluated and the ferroelectric properties of colemanite are compared with those of KDP.

9244 FERROELECTRICITY IN POTASSIUM FERROCYANIDE TRIHYDRATE AND ITS ISOMORPHOUS SUBSTANCES by S. Waku, K. Masuno, T. Tanaka and H. Iwasaki (Nippon Tel. and Tel.); J. Phys. Soc. Japan, Vol. 15, pp. 1185-1189, July 1960

Measurements of ferroelectricity in several $A_4[M(CN)_6] 3H_2O$ type cyano-complexes belonging to the crystal class C_{2h} are reported. Isomorphous substances obtained through replacing the Fe^{2+} ion by Ru^{2+}, Os^{2+} and Mn^{2+} ions show ferroelectric behavior below −14°, −2.4° and −40°C respectively. The ferroelectric behavior of these compounds is very similar to that of potassium ferrocyanide trihydrate. The potassium ferrocyanide group ferroelectrics have a ferroelectric axis parallel to the [10$\bar{1}$] direction. The ferroelectric transition of these substances is probably of second order.

9245 $BaTiO_3$-BASED SOLID SOLUTION OF NIOBATES AND TANTALATES OF TRANSITION METALS by E.V. Sinyakov and E.A. Stafiichuk (Dnepropetrovsk State U.); Soviet Phys.-Solid State, Vol. 2, pp. 66-71, July 1960

The preparation and properties of metaniobates, pyroniobates, and tantalates of manganese, cobalt, and nickel are described. It was found that these compounds are nonferroelectric. A study of $BaTiO_3$-based solid solutions of metaniobates, pyroniobates, and tantalates of Mn, Ni, and Co showed that the solid solutions of pyroniobates and tantalates possess ferroelectric properties. These properties disappear on addition of more than 1 mol per cent of metaniobates and tantalates to $BaTiO_3$.

9246 ELECTROCHEMICAL BEHAVIOR OF SINGLE CRYSTALS OF BARIUM TITANATE FROM 25 TO 100°C by E.J. Huibregtse, W. H. Bessey and M. E. Drougard (IBM); J. Appl. Phys., Vol. 30, pp. 899-905, June 1959

Dynamic piezoelectric resonance measurements made on single crystals of $BaTiO_3$ in the temperature range from room temperature to 160°C are reported. In the ferroelectric region (room temperature to 120°C) the material is spontaneously polarized and hence naturally piezoelectric. For this range of temperature results are presented for the elastic compliance coefficients s_{11}^E and s_{11}^P, the combination $(2s_{12} + s_{66})$ at constant field and constant polarization, and the piezoelectric coefficient d_{31} as functions of temperature. Above the Curie temperature (120°C) the piezoelectric resonances can be observed only by polarizing the crystal with an external field. From measurements of the resonant frequencies in crystals having their longitudinal axes along the (100) and the (110) direction, and the assumption of the validity of the Cauchy relation ($c_{12} = C_{44}$) the elastic coefficients at constant polarization have been determined as functions of temperature and polarization from the Curie point to 160°C. The strains induced by the polarization in a stress-free crystal are shown to be proportional to the square of the polarization, for values of polarization up to one-third of the spontaneous polarization at room temperature.

Piezoelectric Constants of Anisotropic Media - See 9443

CARRIER PROPERTIES

9247 SLOW ELECTRONS IN POLAR CRYSTALS: SELF-ENERGY, MASS, AND MOBILITY by T. D. Schultz (U. Birmingham); Phys. Rev., Vol. 116, pp. 526-543, Nov. 1, 1959

The parameters for the Feynman model of a polaron are evaluated numerically for various values of the electron lattice interaction α in the usual idealization of the problem of a slow electron in a polar crystal. The self-energy and effective mass thus obtained are compared with earlier polaron theories, indicating the superiority of the Feynman model for a wide range of α. The polaron size and the effect of the continuum approximation are estimated, and it is concluded that the alkali halides, at least, may be in the border region for the validity of this approximation. The problem of calculating polaron mobility as determined by scattering with longitudinal optical mode phonons is analyzed and previous theories are critically reviewed. A new theory based on the Feynman model in which the Boltzmann equation is used and in which resonance scattering is considered as the fundamental scattering process is developed.

9248 LCAO TREATMENT OF EXCITON STRUCTURE IN ALKALI HALIDE CRYSTALS by R. A. Pappert (Cornell U.); Phys. Rev., Vol. 119, pp. 525-532, July 15, 1960

A Heitler-London treatment is applied to the transfer mechanism which has been traditionally associated with the fundamental absorption of alkali halide crystals. In particular, detailed calculations are made for NaCl using the free atom Na 3_s Hartree-Fock solution for the one-electron transfer function and the free ion Hartree-Fock solutions for the remaining one-electron functions. The energy and oscillator strength so determined are irreconcilable with experiment, showing that the free atom Na 3_s function cannot be used in conjunction with the transfer model if the model is to yield sensible results. In a very semiquantitative way it is shown that an electron-hole overlap integral of about 0.1 coupled with Overhauser's exciton model leads to a doublet structure which is in agreement with experimental results for many of the chlorides, bromides, and iodides. These findings do not distinguish the transfer model from the "excitation model."

9249 OPTICAL SPECTRUM AND MAGNETO-OPTICAL PROPERTIES OF EXCITONS by E. F. Gross (Phys.-Tech. Inst., Leningrad); J. Phys. Chem. Solids, Vol. 8, pp. 172-176, Jan. 1959

Experimental evidence that the complex structure of distinct strong lines observed at the edge of fundamental absorption in a number of crystals at low temperatures is due to the creation of excitons is presented. A hydrogen-like series of narrow lines in Cu_2O indicates the existence of Mott electrons in the crystal. The quadratic diamagnetic Zeeman effect detected in Cu_2O and CdS is a proof of the large dimensions of excitons

and their enormous diamagnetism. The linear paramagnetic Zeeman effect of the members of the Cu_2O series was not observed. This proves the existence of positronium-like excitons with equal effective masses of electron and hole. On the other hand some of the Cu_2O and CdS absorption lines show the linear Zeeman splitting only. This can be explained by excitation of localized excitons whose radii do not exceed the size of the crystal cell. In such a case the spectra of ortho- and para-excitons may be different. A group of almost equidistant absorption maxima beyond the exciton series limit with a fine structure has been detected in Cu_2O in a magnetic field. These maxima are due to the Landau diamagnetic levels and the spacing between successive maxima is determined by the exciton cyclotron frequency. In luminescence in a number of crystals, narrow emission lines are observed at the very edge of the fundamental absorption nearly coinciding with the absorption lines. Some of these may be due to the annihilation of excitons with the emission of light. Some of the crystals show a fine structure of the spectral dependence of photoconductivity which is closely related to the line structure of the absorption edge. This reveals the role of excitons in photoconductivity.

9250 EXCITON SPECTRUM OF CADMIUM SULFIDE by D.G. Thomas and J.J. Hopfield (Bell Labs.); Phys. Rev., Vol. 116, pp. 573-582, Nov. 1, 1959

Measurements of the reflectance and fluorescent spectra of hexagonal CdS crystals carried out at 77° and 4.2°K using polarized light in the region of 5000 A are given. Structure not previously reported has been found in the reflectivity curves, which leads to the identification of three exciton series. These can be understood in terms of the splitting of the valence band into three levels at k = 0. The observation of excited exciton states and the polarization properties of the excitons make possible: 1) determination of two of the three exciton binding energies; 2) determination of the energy splittings of the three valence bands; 3) verification of the symmetry assignments of the valence and conduction bands; and 4) correlation of the present work with that of others. The fluorescent experiments strongly suggest that the radiative decay of excitons occurs not directly but from localized impurity exciton states, in agreement with theory.

9251 INTERACTION OF CONDUCTION ELECTRONS WITH ACOUSTIC WAVES IN MANY-VALLEY SEMICONDUCTORS by N. Mikoshiba (Electrotech. Lab.); J. Phys. Soc. Japan, Vol. 15, pp. 1189-1199, July 1960

A semiclassical theory for explaining the characteristics of the interaction of conduction electrons with acoustic waves in many-valley semiconductors such as n-Ge is developed. In general, the ultrasonic absorption coefficient can be written as $\Lambda = \Lambda_p + \Lambda_k$, where Λ_p is due to the change of the deformation potential energy of electrons caused by net intervalley transitions and Λ_k is due to the change of the kinetic energy caused by intravalley transitions. The acousto-electro-motive force can be also written as $F = F_p + F_k$. In the low frequency range the dominant terms are Λ_p and F_p, but Λ_k and F_k predominate at sufficiently high frequencies. For longitudinal waves propagating in the <010> direction, F is identical with the formula of Weinreich-Sanders-White in the low frequency range. But in contrast to their formula, F does not decrease in the high frequency range owing to the increase of F_k and has the same order of magnitude as that for longitudinal waves in simple semiconductors. In special cases such as for longitudinal waves propagating in the <100> direction and transverse waves propagating in the <110> direction and polarized in the $<1\bar{1}0>$ direction, $\Lambda_p = F_p = 0$ and then the interaction becomes essentially identical with that in simple semiconductors.

9252 INFLUENCE OF TRAPPING, DIFFUSION AND RECOMBINATION ON CARRIER CONCENTRATION FLUCTUATIONS by M. Lax and P. Mengert (Bell Labs.); J. Phys. Chem. Solids, Vol. 14, pp. 248-267, July 1960

The dependence of carrier concentration on traps, diffusion and recombination properties is discussed. Carrier concentration fluctuations are found to be relatively large in regions of low concentration. Diffusion is shown to add a $(1/\omega)^{3/2}$ boundary term (important at high frequencies) to the usual volume recombination spectrum. This result is found to be valid independent of the geometry or the number of dimensions. But for the case of surface recombination it is multiplied by a frequency dependent probability that an electron having left the region will not return. Traps of large cross section are characterized by a fast trapping rate and an exceedingly slow effective recombination rate caused by multiple trapping. The fast rate is unaffected by diffusion. The slow rate is shown by a method of low mode isolation to be approximately describable in terms of an effective diffusion constant reduced in about the same ratio as the recombination. The resulting $(1/\omega)^{3/2}$ spectrum is thus shifted to a low frequency region and increased enormously in strength.

9253 MICROWAVE INDUCED CARRIER MULTIPLICATION IN GERMANIUM by K. Seeger (U. Illinois); J. Appl. Phys., Vol. 30, pp. 443-444(L), Mar. 1959

Microwave power transmission measurements performed in n-type Ge at ~4.5°K and 34.67 kMc are discussed. The measurements were made on a 2.5 ohm-cm single crystal which filled the waveguide for a length of 7.74 mm. When the field intensity was below breakdown intensity, the sample in the first order was transparent to microwaves. A breakdown field of 13.3 v/cm was found. In the low power range the increase in transmitted power was proportional to the increase in incident power. A peak transmitted power of 80 mw was observed between the low and high power regions and for incident powers above 100 w the transmitted power was 25 mw, independent of the incident power. The device can be used as a TR switch and for frequency multiplication.

9254 AUGER EFFECT IN SEMICONDUCTORS by A. R. Beattie and P.T. Landsberg (U. Aberdeen); Proc. Roy. Soc., Vol. 249, Ser. A, pp. 16-29, Jan. 1, 1959

The lifetimes (τ) of excess electrons and holes in a semiconductor are calculated assuming the Auger effect between bands (electron-electron and hole-hole collisions) to be the only recombination mechanism. By counting pair annihilation and pair creation separately, there are four classes of processes to be counted separately. The suitably weighted algebraic sum of the rates of these processes yields a net recombination rate R. If n be the non-equilibrium number of pairs, then $\tau = n/R$. Details of the calculations which employ quasi-Fermi levels and Bloch functions of the form $\psi_{\vec{k}} = \mu(\vec{k},\vec{r})\exp(i\vec{k}\cdot\vec{r})$ are given. Most of the terms of the Coulomb interaction matrix element correspond to Umklapp-type processes whose probability of occurrence is small. The dominant term, after integration over all states, yields the dependence of lifetime on temperature, carrier concentration, energy gap and other parameters. The theory is compared with measured lifetimes in InSb

and shows fair agreement in the temperature range 240°-330°K.

9255 MICROWAVE MEASUREMENT OF SEMICONDUCTOR CARRIER LIFETIMES by H. A. Atwater (Pennsylvania State U.); J. Appl. Phys., Vol. 31, pp. 938-939(L), May 1960

The experimental conditions under which the lifetime of minority carriers injected into a semiconductor placed transversely across a waveguide can be determined from the variation of microwave attenuation in the semiconductor are found from an analysis of the wave propagation. It is assumed that the carrier lifetime has an exponential time decay. It is shown that the lifetime can be determined when the sample thickness is small and when the carrier injection level is low. The logarithm of the transmitted power decay curve should be used when the ratio of attenuation constant to propagation constant is small.

9256 CARRIER DENSITY FLUCTUATIONS IN SEMICONDUCTORS AND PHOTOCONDUCTORS WITH ONE KIND OF TRAPPING CENTERS by F. M. Klaassen, K. M. Van Vliet and J. Blok (U. Amsterdam); Physica, Vol. 26, pp. 605-617, Aug. 1960

Applying the general theory of carrier density fluctuations in semiconductors (Van Vliet), based on the formalism of irreversible thermodynamics, expressions for the matrix elements of carrier density fluctuations and for the relaxation times are given in the case of semiconductors with one kind of trapping- or recombination centers. These expressions have been approximated in some cases by formulae that can be verified experimentally, for instance trapping of minority carriers in deep lying centers (occurring in PbS photoconductors) and trapping of carriers at shallow traps in nearly intrinsic semiconductors. With the aid of the extended g-r theorem, the derived expressions for the noise in semiconductors are shown to hold for photoconductors only if the centers act as traps.

9257 PHOTOELECTRONIC ANALYSIS OF HIGH RESISTIVITY CRYSTALS: (a) GaAs, (b) Sb_2S_3 by R. H. Bube (RCA Labs.); J. Appl. Phys., Vol. 31, pp. 315-322, Feb. 1960

Photoelectronic measurements on some basic properties of high resistivity crystals, i.e., majority carrier lifetime, band gap, activation energy for dark conductivity, and activation energies and densities of trapping centers for carriers, are reported. These measurements have been made on representative n-type crystals of GaAs and Sb_2S_3. The results are reported together because both crystals show evidence for trapping of photoexcited carriers by compensated donor centers of the same type as those which uncompensated give rise to the normal dark conductivity. Additional data on Sb_2S_3, together with other results on similar crystals, suggest that these same uncompensated donor centers may play an important role in the recombination process.

Photovoltaic Measurement of Lifetime in Si - See 9426

9258 ON THE DETERMINATION OF THE POSITION OF THE ENERGY LEVEL OF SURFACE RECOMBINATION CENTRES by S. Koc (Czech. Acad. Sci.); Czech. J. Phys., Vol. 10B, No. 8, pp. 579-583, 1960

A detailed analysis of the dependence of the surface recombination velocity s on the surface potential Φ_s leads to the conclusion that the position of the surface recombination level with respect to the center of the energy gap $E_t - E_i$ does not coincide with the value $q\Phi_s^*$, while the surface recombination velocity s decreases to half its maximum value. The difference between the two quantities is negligible only when the width of the curve $s(\Phi_s)$ between the points corresponding to the values $s = 1/2 s_{max}$ is greater than 8kT.

9259 INFLUENCE OF THE AMBIENT ATMOSPHERE ON THE SURFACE RECOMBINATION OF SILICON by H. U. Harten (Valvo); Philips Res. Rep., Vol. 14, pp. 207-210, June 1959

The effect of the ambient atmosphere on the surface recombination of Si is discussed. Surface photovoltage measurements show that the surface potential of Si can be altered, as in Ge, in a wide range by chemical surface treatments and in a smaller range by the ambient atmosphere. Simultaneous investigation of the surface recombination shows that this process is determined chiefly by Hall-Shockley-Read type recombination centers

9260 THE SURFACE RECOMBINATION ON SILICON CONTACTING AN ELECTROLYTE by H. U. Harten (Philips Labs.); J. Phys. Chem. Solids, Vol. 14, pp. 220-225, July 1960

Excess carriers recombine at the Si-electrolyte interface in a way not very different from that at dry surfaces, with a recombination velocity which depends on the surface potential in a bell-shaped manner similar to the "Stevenson-Keyes curve". The surface potential can be varied in a relatively wide range by applying only some tenths of a volt between silicon and electrolyte. A part of the applied voltage drops across the oxide layer present at the Si surface. This part is larger the thicker the oxide layer in relation to the space charge layer inside the silicon.

9261 TRAPPING AND DIFFUSION IN THE SURFACE REGION OF CADMIUM SULFIDE by J. J. Brophy (Armour Res. Found.); Phys. Rev., Vol. 119, pp. 591-596, July 15, 1960

In lightly doped single crystal CdS illuminated with 4400 A radiation hole-electron pairs generated at the surface diffuse into the crystal until the hole is trapped. The electrons experience multiple retrapping until they disappear through recombination. Current noise and photoconductivity measurements used to study these processes are reported. The noise data establish the ambipolar diffusion length as 30 microns, confirm that diffusion is important though the appearance of a $f^{-3/2}$ trend in the noise spectra, and show that discrete traps are located the same distance below the conduction band in the surface regions as in the bulk. Discrete trap levels at 0.35, 0.40, and 0.43 volt below the conduction band are observed in the surface region. Trap densities of 10^{16} traps/cm^3 volt, an order of magnitude greater than that in the bulk, are determined. The trap frequency factors are of the order 10^{10} sec^{-1}.

9262 ON RECOMBINATION PROCESSES IN NEUTRON-IRRADIATED n-TYPE GERMANIUM by M. Bertolotti (Ist. Sup. delle Poste e Telecom., Roma) and D. Sette (U. Messina); Nuovo Cim., Vol. 20, pp. 438-442, May 1, 1961

Minority charge carrier lifetime in neutron irradiated n-type Ge is calculated taking into account the presence of damage regions produced by fast secondaries. The results are compared with experimental data.

9263 VOLUME RECOMBINATION IN P-TYPE SILICON SUBJECTED TO HEAT-TREATMENT AT HIGH TEMPERATURES by G.N. Galkin (Lebedev Phys. Inst., Moscow); Soviet Phys.--

Solid State, Vol. 2, pp. 5-10, July 1960

P-type silicon was subjected to heat-treatment above 1200°C. It was found that the resultant recombination level lay in the lower half of the energy gap, 0.13 ± 0.01 ev from the valence band. The temperature dependence of the capture cross sections for electrons and holes was obtained.

9264 ON THE SPIN MECHANISM OF RECOMBINATION OF CURRENT CARRIERS IN FERROMAGNETIC SEMICONDUCTORS by V. L. Bonch-Bruevich (Lomonosov Moscow State U.); Soviet Phys.-Solid State, Vol. 1, pp. 166-170, Feb. 1959

A current carrier recombination process in which the liberated energy is transferred to spin waves is discussed. The dependence of the recombination coefficients on temperature, saturation magnetization, and properties of the material is obtained and the order of magnitude of the capture cross-section is estimated.

9265 THEORY AND APPLICATION OF A MINORITY CARRIER SWEEP-OUT EFFECT by R. D. Larrabee (RCA); J. Appl. Phys., Vol. 30, pp. 1535-1538, Oct. 1959

The phenomenon whereby minority carriers (and their compensating majority carriers) can be removed from a semiconductor by application of an electric field through ohmic contacts is discussed. A simplified analytical description of this phenomenon is derived and is illustrated by simple experiments. It is demonstrated that by utilizing this effect, along with Hall data, one can determine the density and drift mobility of both the majority and minority carriers. Consequently, it is possible to measure many parameters that depend on these qualities (e.g., intrinsic density, estimate of surface space charge and carrier mobility in inversion surfaces, etc.).

9266 THE THEORY OF THE MOBILITY OF ELECTRONS IN SEMICONDUCTORS by I.I. Boiko (Moscow State U.); Soviet Phys.-Solid State, Vol. 1, pp. 518-522, Apr. 1959

The scattering of electrons by charged impurities is analyzed by means of the Born approximation and an expression for the dependence of the theoretical mobility on the concentration of charged impurities is derived. Elliptical isoenergetic surfaces are assumed. The expression does not utilize the indeterminate parameter m_{eff} but utilizes values of $m_{\parallel}$ and $m_{\perp}$ determined experimentally by means of cyclotron resonance. The calculated mobilities are compared with those obtained by the Conwell-Weisskopf and Brooks-Herring formulae. The calculated mobilities are twice as high as the experimental values.

9267 TECHNIQUE FOR MEASURING PARTICLE DRIFT MOBILITIES IN NEAR INTRINSIC AND NARROW BAND GAP SEMICONDUCTORS by N. J. Harrick (Philips Res. Labs.); J. Appl. Phys., Vol. 30, pp. 451-452(L), Mar. 1959

A modification of the drift mobility technique which permits direct measurement of the particle drift mobility in near intrinsic and narrow band gap semiconductors is described. The modification consists in completely extracting the free carriers, minority carriers and an equal number of majority carriers, without affecting the requirement of space charge neutrality. A mobility of 4000 cm^2/v-sec was measured in a 48 ohm-cm P-type sample. The corresponding ambipolar mobility at 300°K is 1800 cm^2/v-sec. The type and resistivity of near intrinsic materials can be determined by means of drift mobility measurements.

9268 DIFFUSION AND RECOMBINATION DURING MEASUREMENTS OF THE DRIFT MOBILITY by V. N. Dobrovol'skii (Shevchenko Kiev State U.); Soviet Phys.-Solid State, Vol. 1, pp. 655-660, Nov. 1959

The processes of diffusion and recombination which take place during measurements of drift mobility are discussed. Criteria for the applicability of the simplified formula for calculating the mobility in the case of one-, two-, and three-dimensional propagation of injected carriers are derived and verified experimentally.

9269 NOTE ON THE FIELD DEPENDENCE OF THE MOBILITY IN SEMICONDUCTORS by M. Hattori (U. Nagoya); J. Phys. Soc. Japan, Vol. 15, pp. 1237-1242, July 1960

By assuming that the mobility μ can be expanded in powers of the field strength F as $\mu = \mu_0 (1 - \nu F^2)$, ν is calculated for nonpolar and polar semiconductors. The electron-electron interactions are neglected completely and the Boltzman equation is solved by means of the variation method. It is shown that ν calculated in this way differs significantly from other previously calculated values, particularly at low temperatures. The electric-field dependence of the Hall coefficient is also estimated.

9270 PHONON SCATTERING IN KCl-KBr SOLID SOLUTIONS AT LOW TEMPERATURES by W. S. Williams (Cornell U.); Phys. Rev., Vol. 119, pp. 1021-1024, Aug. 1, 1960

Measurements of the scattering of phonons by point defects at liquid helium temperatures are reported. Single crystals of KCl-KBr solid solutions were employed, since it is known that the Cl^- and Br^- ions are randomly distributed in the anion lattice sites. A 1 mole per cent addition of KBr reduced the conductivity of KCl by a factor of three. For all the crystals measured, including pure KCl and pure KBr, the thermal conductivity showed a maximum at the same temperature (5°K). Hence, point defects reduce the conductivity on both the high- and low-temperature sides of the maximum. For the mixed crystals the thermal conductivity was found to be related to the absolute temperature by the empirical formula $K = K_{0e}^{0.099T}$ for the temperature interval 6° to 16°K.

9271 THE ELECTRICAL CONDUCTIVITY AND THE HALL EFFECT IN A POLAR SEMICONDUCTOR, TAKING INTO ACCOUNT THE SCATTERING OF CURRENT CARRIERS ON THE OPTICAL AND ACOUSTICAL LATTICE VIBRATIONS AND ON IMPURITY IONS by N. N. Porfir'eva (Leningrad Shipbuilding Inst.); Soviet Phys.-Solid State, Vol. 1, pp. 794-798, Dec. 1959

The electrical conductivity and the Hall constant of an ionic crystal are calculated taking into account simultaneous scattering of current carriers on the optical and acoustical lattice vibrations and on impurity ions. It is found that in a certain range of temperatures all three scattering mechanisms are present. The results of the calculations are shown graphically.

CONDUCTIVITY (RESISTIVITY)

9272 HEITLER-LONDON APPROACH TO ELECTRICAL CONDUCTIVITY. Part II. A PROOF OF THE HOPPING MOTION by T. Kurosawa (Tokyo U.); J. Phys. Soc. Japan, Vol. 15, pp. 1211-1216, July 1960

The Heitler-London approach to electrical conductivity is proved using Van Hove's method. The hopping motion of

electron is realized under the conditions of large effective mass, strong interaction with the lattice and the presence of a potential fluctuation through the lattice.

9273 A CONTINUOUS-READING FOUR-POINT RESISTIVITY PROBE by J. C. Brice and A. A. Stride (Mullard); Solid State Electronics, Vol. 1, p. 245, July 1960

The continuous measurement of resistivity by means of four probes consisting of balls ~0.5 mm in diam held in metal tubes 2 mm in diam is described. The probes are placed in holes in a 1/4 inch perspex block, with 2.5 mm between centers, and are held in place by means of wire leaf springs which also serve as electrical connections. The assembly is fastened to an arm which is moved at a constant speed by a lead screw and motor system. A weight is placed on the arm to provide the necessary contact pressure. A constant current is supplied to the two outer probes and the EMF between the inner probes is displayed on a 10 mv full scale potentiometric recorder. Resistivity can be calculated from

$$\rho = \frac{V}{I} \frac{2\pi}{1/S_1 + 1/S_3 - 1/(S_1+S_2) - 1/(S_1+S_3)}$$

where ρ is the resistivity, V the EMF between the outer probes, I the current between the outer probes, and S_1, S_2, and S_3 are the probe spacings.

9274 MEASUREMENT OF THE SHEET RESISTIVITY OF A SQUARE WAFER WITH A SQUARE FOUR-POINT PROBE by F. Keywell (Semicon. Devices) and G. Dorosheski (Hughes Prod.); Rev. Sci. Instr., Vol. 31, pp. 833-837, Aug. 1960

Correction factors for converting to sheet resistivity the current and potential difference values measured on the surface of a square semiconductor wafer with a square four-point probe are calculated. The correction factors are given for square dimensions, in units of probe spacing, over the range 1 to 50. The data include the special case d/s = 1 in which the probe points are on the corners of the square.

9275 EDDY-CURRENT METHOD FOR MEASURING THE RESISTIVITY OF METALS by C. P. Bean, R. W. DeBlois and L. B. Nesbitt (GE); J. Appl. Phys., Vol. 30, pp. 1976-1980, Dec. 1959

A method for measuring the resistivity of metallic specimens which is based on the rate of decay of flux from a bar situated in an external magnetic field that has been rapidly reduced to zero is described. The method is suitable for specimens greater than 5×10^{-3} cm in diameter. For a specimen 1 cm in diameter, resistivities from 10^{-11} to 10^{-3} ohm-cm may be measured with an error of less than 3 per cent. The method requires no contact to the specimen, and local values of resistivity may be measured.

9276 MEASUREMENT OF THE RESISTIVITY CONSTANTS OF ANISOTROPIC CONDUCTORS BY MEANS OF PLANE-PARALLEL DISCS OF ARBITRARY SHAPE by J. Hornstra and L. J. van der Pauw (Philips); J. Electronics Control, Vol. 7, pp. 169-171, Aug. 1959

A method for determining the resistivity constants of anisotropic conductors of arbitrary shape is presented. It is an extension of a previously derived method for determining the resistivity of isotropic conductors of arbitrary shape.

9277 MEASUREMENT OF THE HALL COEFFICIENT AND ELECTRICAL CONDUCTIVITY IN SEMICONDUCTORS BY THE METHOD OF AN ALTERNATING MAGNETIC FIELD AND ALTERNATING CURRENT by J. Dusek (Inst. Tech. Phys., Prague); Czech. J. Phys., Vol. 9, No. 2, pp. 250-255, 1959

An instrument in which the Hall coefficient and electrical conductivity can be measured simultaneously by using an alternating magnetic field and alternating current is described. The instrument can measure a minimum Hall coefficient of 3×10^{-11} vcm/AG and electrical resistance from 10^{-5} to 10^{+3} ohms. The smallest measurable Hall voltage is 1 μv. Deviations from results obtained by the ordinary dc method do not exceed 5 per cent.

9278 REACTIONS OF GROUP III ACCEPTORS WITH OXYGEN IN SILICON CRYSTALS by C. S. Fuller, F. H. Doleiden and K. Wolfstirn (Bell Labs.); J. Phys. Chem. Solids, Vol. 13, pp. 187-203, June 1960

Measurements of the Hall effect and conductivity of Si crystals containing from 5×10^{17} to 1.6×10^{18} cm^{-3} of oxygen and various dopings of B, Al and Ga before and after reaction at various temperatures (410°-1350°C) are reported. Evidence in support of the tetrahedral SiO_4 model for the donor formed from oxygen suggested by Kaiser is presented. A large hole-electron effect is noted in the presence of excess acceptor concentration. In addition, specific interactions with the acceptor atoms occur. Although the reactions are complex and are not understood, three kinds are postulated in order to account for the results: (1) The formation of isolated SiO_4 donors such as occurs in undoped Si crystals containing oxygen. (2) The reaction of oxygen at an acceptor atom to form a neutral compound or a "molecular pair". (3) The formation of a donor involving eight oxygen atoms and an acceptor atom. The latter reaction is believed to occur most readily in the case of Al-doped crystals and, in an excess of oxygen, leads to the formation of one donor per Al atom.

9279 SOME EFFECTS OF OXYGEN ON RESISTIVITY IN SILICON by D. H. Roberts and B. L. H. Wilson (Plessy); J. Appl. Phys., Vol. 30, pp. 447-448(L), Mar. 1959

The axial variation of oxygen concentration in a p-type vacuum grown single crystal of Si has been determined by absorption coefficient measurements at 9 μ. Resistivity measurements have also been made before and after annealing for 100 hr at 450°C. These measurements indicate that the oxygen lowers the resistivity before annealing and raises it after annealing.

Effect of Neutron Irradiation on the Resistivity of AuCu - See 9199

9280 THE MOBILITY OF ELECTRONS HEATED BY MICROWAVE FIELDS IN N-TYPE GERMANIUM by T. N. Morgan (IBM); J. Phys. Chem. Solids, Vol. 8, pp. 245-249, Jan. 1959

The perturbed distribution function and the resulting electron conductivity changes in Ge when the current flow is modified by a microwave field with frequencies above 50 kMc at room temperature and 5 kMc at liquid nitrogen temperature are calculated. It is found that the changes in current flow arise from two terms differing in their dependence on frequency. One represents the current produced by a change in the average dc conductivity. The other represents an average value of the microwave current produced by an ac conductivity variation in phase with the microwave field. The results of these

calculations are compared with measurements performed at frequencies from 8 kMc to 35 kMc between 77° and 300°K.

9281 INFLUENCE OF ATOMIC HYDROGEN ON THE CONDUCTIVITY OF CLEANED GERMANIUM SURFACES by G. Heiland and P. Haudler (U. Illinois); J. Appl. Phys., Vol. 30, pp. 446-447(L), Mar. 1959

An experimental investigation of the effect of atomic hydrogen on the surface conductivity and field effect mobility of Ge surfaces cleaned by argon bombardment and annealing is reported. It was found that atomic hydrogen increases the p-type conductivity of cleaned surfaces and decreases the p-type conductivity of unclean surfaces. It is suggested that hydrogen acts as a donor on oxide-covered surfaces because the hydrogen forms a bond with the oxygen of the Ge oxide and donates its electron to the crystal. Acceptor action of atomic hydrogen on cleaned surfaces is discussed but no definite explanation for the effect is given. The changes were not caused by photoconductive, temperature, gas generation, or water vapor effects. A larger field effect mobility than previously reported was measured on the clean surface. Atomic hydrogen on a cleaned surface increased the field effect mobility. This is caused by a change in the distribution of holes between the valence band and the surface states.

9282 IMPURITY CONDUCTION OF CLEANED GERMANIUM SURFACES AT LOW TEMPERATURES by A. Kobayashi, Z. Oda, S. Kawaji, H. Arata and K. Sugiyama (Elect. Commun. Lab.); J. Phys. Chem. Solids, Vol. 14, pp. 37-42, July 1960

Measurements of the conductivity and Hall effect of cleaned Ge surfaces from 1.7° to 300°K are reported. The surface was cleaned by Joule heating at 800° - 850°C in ultra-high vacuum for 20-30 hr and was then annealed at 650°C for several hours. Results obtained with 20-40 ohm-cm p-type samples show that the Hall coefficient has a steep maximum at 10°-20°K and the resistivity becomes almost flat below this temperature range. This character is similar to that of bulk impurity conduction found by Hung et al, but disappears on exposure to air, which causes marked increases in both the Hall coefficient and resistivity at low temperatures. This impurity conduction is attributed to the surface imperfections introduced by the cleaning treatment of the surface. The mobility and concentration of carriers in this surface conduction are estimated.

9283 CHEMICAL CONFIGURATION OF GERMANIUM SURFACES IN AQUEOUS MEDIA by W. W. Harvey (Lincoln Lab.); J. Phys. Chem. Solids, Vol. 14, pp. 82-86, July 1960

Variations in the surface recombination velocity (v_s) for an n-type Ge electrode, measured by an essentially electrochemical technique, are discussed. Displacement of dissolved oxygen from the solution leads to an increase in v_s. During cathodic polarization v_s is large, but is small subsequently. The results indicate that v_s varies in a regular way with the surface potential ϕ_s of the Ge, but that chemisorption of hydrogen results in a decrease in the density of surface recombination centers.

9284 SURFACE CONDUCTIVITY OF SEMICONDUCTORS AND ITS VARIATION BY ADSORPTION, TRANSVERSE ELECTRIC FIELDS AND IRRADIATION by G. Heiland (U. Erlangen); Disc. Faraday Soc., No. 28, pp. 168-182, 1959

The surface conductivity of semiconductors is discussed. The surfaces of semiconductors are covered with a space-charge layer whose conductivity differs greatly from the bulk value. Examples are given for ZnO and Ge with oxygen and hydrogen. Information on the energy levels for electrons at the surface can be gathered from systematic variations of the surface conductivity. With ZnO three such experiments have been carried out: field effect (change of carrier density at the surface due to transverse electric fields), adsorption of oxygen, and irradiation with light or electrons. The results are given as drift mobilities of electrons. A consistent explanation is possible with a surface model containing a set of continuously distributed surface states just below the conduction band. Closely connected with the surface photoconductivity are photodesorption and photolysis. Not only electron transitions but also ion migrations are involved in these cases. Examples are given for ZnO and the sulphides of zinc and cadmium.

9285 IMPURITY CONDUCTION IN TRANSMUTATION-DOPED p-TYPE GERMANIUM by H. Fritsche and M. Cuevas (U. Chicago); Phys. Rev., Vol. 119, pp. 1238-1245, Aug. 15, 1960

Measurements of the Hall coefficient and resistivity of Ge single crystals bombarded with slow neutrons made between 1.2° and 300°K are reported. Slow neutron capture and subsequent nuclear transmutation produce majority impurities, Ga atoms, and compensating impurities, As and Se atoms. P-type samples with a Ga concentration ranging from 8×10^{14} to 5×10^{17} per cc with a fixed compensation ratio of 0.40 were thus prepared and the impurity conduction was studied as a function of the average distance between the majority impurities. The effective radius a of the acceptor ground-state wave function is 90.1 A according to Miller's theory of impurity conduction, whereas a = 40 A according to Twose's theory. The latter value agrees well with the effective radius of the Kohn-Schechter acceptor wave function. The activation energy of impurity conduction changes slowly with impurity concentration from 3.5×10^{-4} to 5.9×10^{-4} ev and agrees well with the predictions of Miller's theory for gallium concentration below 5×10^{15} per cc. Measurements on samples which contain different dislocation densities but identical impurity concentrations show that up to 10^4 dislocations per cm^2 do not affect impurity conduction.

9286 MEASUREMENT OF THE HALL EFFECT AND CONDUCTIVITY OF SUPER-PURE SILICON by A. Hoffmann, K. Reuschel and H. Rupprecht (Siemens AG); J. Phys. Chem. Solids, Vol. 11, pp. 284-287, Oct. 1959

Measurements on super-pure, uncompensated p-type silicon with a resistivity above 100,000 ohm-cm obtained by the floating zone technique are given. Intrinsic conduction takes place in these samples at temperatures as low as 40°C. The intrinsic density n_i obtained over a range from 50° to 100°C agrees well with the n_i values determined by other investigators. The distribution coefficient k of boron is found to be slightly below 0.9.

9287 THEORY OF THE RESISTANCE MINIMUM IN DILUTE PARAMAGNETIC ALLOYS by A. D. Brailsford and A.W. Overhauser (Ford); J. Phys. Chem. Solids, Vol. 15, pp. 140-145, Aug. 1960

The observed anomalous temperature dependence of the resistivity of dilute paramagnetic alloys is attributed to s-d exchange scattering of conduction electrons by nearest neighbor pairs of ferromagnetically coupled solute ions. Occurrence of a resistance minimum can be explained quantitatively only if the effective range of the s-d exchange potential is not too short; and only if the periodic structure of energy bands is taken into

account. The size of the minimum is proportional to the square of the solute concentration in the limit of extreme dilution (less than 1 per cent). Deviations from this law at higher concentrations are explained satisfactorily.

9288 ELECTRICAL RESISTANCE MAXIMUM FOR FERROMAGNETS AT THEIR CURIE POINTS AT LOW TEMPERATURES by E. I. Kondorskii, O. S. Galkina and L. A. Chernikova (Moscow State U.); Soviet Phys.-JETP, Vol. 2, pp. 464-466(L), Aug. 1960

Measurements of the temperature dependence of the resistivity of copper-nickel alloys containing 58 and 59.25 per cent copper in the vicinity of their Curie points (below 20°K) are reported. Maxima in the resistance were observed in the region of the magnetic transition, with that of the 59.25 per cent Cu specimen being particularly prominent. The maxima are smoothed out when a magnetic field is applied. At the maximum of the 49.25 per cent Cu sample the value of $\rho - \rho_0$, where ρ_0 is the residual resistivity, is 0.7 per cent of the residual resistivity and agrees with the calculation of Krivoglaz and Rybak. The existence of the resistance maximum confirms previous theoretical considerations of the effect of disorder of the magnetic moment of the lattice on the electrical resistivity of ferromagnetics at low temperatures.

9289 ELECTRICAL PROPERTIES OF TYPE A ZEOLITE POWDER COMPACTS by W. Peria (Honeywell Res. Ctr.); Bull. Am. Phys. Soc., Ser. II, Vol. 5, p. 376(A), June 15, 1960

Conductivity and charge storage measurements on pressed pellets of Linde Type A zeolite were reported. Such compacts behave as ionic conductors, and the observed results suggest that they are two-phase systems. This supposition has been further supported by measurements of the frequency dependence of the complex impedance and by conductivity measurements on single polycrystalline particles and on single crystals.

9290 TWO-CARRIER SPACE-LIMITED CURRENT IN A TRAP-FREE INSULATOR by R. H. Parmenter and W. Ruppel (RCA Labs., Switzerland); J. Appl. Phys., Vol. 30, pp. 1548-1558, Oct. 1959

The space-charge-limited electrical behavior of a trap-free insulator containing both mobile electrons and holes is investigated under the approximation of neglecting diffusion current. When both contacts are ohmic, the dependence of two-carrier space-charge-limited current on voltage and interelectrode spacing remains the same as in the one-carrier case; i.e., the current varies as the square of the voltage and as the inverse cube of the spacing. For given voltage and spacing, however, the two-carrier current is usually orders of magnitude larger than the one-carrier current. This is in striking contrast to the case of space-charge-limited flow of electrons and positive ions in a vacuum. The two-carrier current in an insulator can be reduced to the size of the one-carrier current either by making one contact highly blocking or by reducing the mobility of one of the carriers to zero. While the first approach yields in detail the well-known one-carrier case, the second approach differs from the one-carrier case in that no net excess space charge can be injected into the insulator. The intermediate case of a slightly blocking contact shows that, while the current may be carried mainly by one sign of carrier, the net space charge of the insulator can have the opposite sign. When both contacts are blocking, the current saturates for sufficiently high voltages. The current is smaller than the saturation value by an amount proportional to the cube of the interelectrode spacing and the inverse square of the voltage. Near such saturation, the space charge is negligible and the electric field is uniform across the insulator. It is plausible that many of the above results will also be true for an insulator with traps.

SUPERCONDUCTIVITY

9291 THEORY OF SUPERCONDUCTING CONTACTS by R.H. Parmenter (RCA); Phys. Rev., Vol. 118, pp. 1173-1182, June 1, 1960

The BCS theory of superconductivity is generalized to include the case of a position-dependent energy gap (at the absolute zero of temperature and in the absence of magnetic fields). The BCS integral equation for the energy gap goes over into an integro-differential equation. The latter has nontrivial solutions (i.e., finite energy gap) even for the case of normal material ($V = 0$). Expressions are obtained for the energy gap, for the volume energy density, and for the surface energy density at an interface, for both normal and superconducting material. These results are applied to a number of problems involving superconducting contacts. When a thin slice of normal material is sandwiched between bulk normal material, the slice acts like normal material for thicknesses less than about 10^{-5} cm. The energy gap at the free surface of a bulk superconductor may differ by as much as thirty per cent from its constant value deep inside the material, the former being either larger or smaller than the latter depending on the value of $N(O)V$, where $N(O)$ is the density of one-electron states of a given spin at the Fermi level in the normal metal.

9292 IRREVERSIBILITY IN THE SUPERCONDUCTING TRANSITION OF LEAD by R. W. Shaw and D. E. Mapother (U. Illinois); Phys. Rev., Vol. 118, pp. 1474-1484, June 15, 1960

The nature and origins of the hysteresis in the magnetic transition of pure superconducting Pb are discussed. The effect can be introduced in nonhysteretic specimens by plastic deformation at liquid He temperatures. The hysteresis becomes apparent somewhat below T_c and its width increases monotonically with decreasing temperature. Similar effects can be caused by dilute additions of Ca to Pb. Strain induced hysteresis anneals out near 300°K but temperatures approaching the melting point appear necessary to remove impurity induced effects. Isothermal resistive measurements show a small fraction of the superconducting phase persisting to fields several hundred gauss above H_c. The residual superconductivity at high fields is increased by plastic deformation, and in general seems closely related to the hysteresis effect. The observations suggest the existence of a connected network which pervades the entire specimen volume and consists of very small filaments having a critical field exceeding the reversible critical field of bulk Pb. The filaments are believed to be associated with defects in the crystalline lattice.

Effect of Quenched-In Defects on the Superconducting Transition Temperature in Sn - See 9166

9293 DESTRUCTION OF SUPERCONDUCTIVITY BY A CURRENT by E. Troinar (Moscow State U.); Soviet Phys.-JETP, Vol. 2, pp. 470-471(L), Aug. 1960

The dependence on wire diameter of the resistance jump caused by the passage of a critical current through a wire in the superconducting state is discussed. Measurements were made on

wires of different diameter prepared from tin of different purity. The measurements show that the resistance jump depends primarily on q, the heat flow from the specimen per unit area. The limiting value of the resistance jump is found to be 0.5. The dependence of the magnitude of the resistance jump on the sample diameter and on the ratio of the diameter to the mean free path can be determined only if the specimen is not overheated.

9294 ON FLUX TRAPPING IN A SUPERCONDUCTING RING by W. H. Mieklejohn (GE Res. Labs.); Bull. Am. Phys. Soc., Ser. II, Vol. 5, p. 358 (A), June 15, 1960

It is well known that a magnetic field may be trapped in a doubly connected body such as a ring or hollow cylinder. It was shown that the flux trapped upon application and removal of a magnetic field is consistent with calculations. A hollow cylinder of proper geometry will trap a flux proportional to $(H_a - H_O)$ where H_O may be made vanishingly small and H_a is the applied field.

9295 COOLING BY ADIABATIC MAGNETIZATION OF SUPERCONDUCTORS by M. Yaqub (Clarendon Lab.); Cryogenics, Vol. 1, pp. 101-107, Dec. 1960

The fall in temperature on magnetizing superconductors has been investigated. It was found that by magnetizing a cylindrical specimen of pure tin from an intitial temperature of 0.9°K, the lowest temperature which can be reached is 0.35°K. This is substantially higher than the expected value of 0.02°K for ideal cooling. In magnetizations of tin-indium alloys, the lowest temperatures obtained with 0.5, 1.0, and 2.0 per cent alloys were 0.19°, 0.18°, and 0.345°K, respectively. It was found that the time required by pure tin in a steady magnetic field of 305 oe to warm up to 0.75°K from 0.35°K after magnetization is more than 6 hrs. The causes of irreversibility are discussed.

MAGNETOELECTRIC (GALVANOMAGNETIC) PROPERTIES

9296 GALVANOMAGNETIC AND THERMOMAGNETIC POTENTIALS IN ZINC AT LIQUID HELIUM TEMPERATURES by C. J. Bergeron, C. G. Grenier and J. M. Reynolds (Louisiana State U.); Phys. Rev., Vol. 119, pp. 925-934, Aug. 1, 1960

Measurements of the Hall effect, magnetoresistance, thermoelectric voltage, and transverse Ettingshausen-Nernst potential in a single crystal of Zn at liquid He temperatures are reported. Oscillations as a function of magnetic field strength were observed in all of these potentials. The measured period in 1/H for the transverse oscillations was 6.2×10^{-5} gauss^{-1} ± 0.5 per cent, with the magnetic field parallel to the hexagonal axis. Both transverse effects possessed strong second harmonic oscillations. The oscillations in the longitudinal effects both exhibited a phase inversion in the neighborhood of 4.2 kgauss, the same field region for which the gross Hall field changed sign. In this same field region the period of the oscillations for the longitudinal effects was that of the second harmonic. Empirical correlations between the reversal of sign of the Hall effect and: (1) the phase reversal of the magnetoresistance oscillations, (2) the strong second harmonic content of these oscillations in the region of the phase reversal, and (3) the quadratic shape of the envelope of the magnetoresistance oscillations in this region can be achieved by assuming the oscillatory component of σ_{21} to be much more significant than that of σ_{11}, where σ_{ik} is the conductivity tensor. A further correlation between the oscillatory thermal effects can be achieved by assuming that the difference of the absolute thermoelectric power and the temperature derivative of the chemical potential is negligible.

9297 MAGNETORESISTANCE EFFECT IN INDIUM ANTIMONIDE by C. H. Champness (McGill U.); Bull. Am. Phys. Soc., Ser. II, Vol. 5, p. 374 (A), June 15, 1960

Measurements of weak field magnetoresistance carried out on oriented single crystals of indium antimonide at 300° and 77°K were reported. The results appear to throw doubt on the simple picture for the conduction band of spherical energy surfaces in k space. Preliminary measurements also have been made using pulsed techniques with fields up to 500 kgauss at room temperature in an attempt to observe oscillatory effects.

9298 WEAK-FIELD MAGNETORESISTANCE IN P-TYPE LEAD TELLURIDE AT ROOM TEMPERATURE AND 77°K by R. S. Allgaier (U.S. Naval Ord. Lab.); Phys. Rev., Vol. 119, pp. 554-561, July 15, 1960

Measurements of the weak-field magnetoresistance of six single crystals of p-type PbTe at room temperature and 77°K are reported. The general predictions of weak-field theory were precisely obeyed in the range of magnetic-field intensities for which the theory should apply. In stronger fields at 77°K, deviations from weak-field behavior of three types were observed which agree with the Gold-Roth theory of magnetoresistance at arbitrary magnetic-field strengths. The weak-field data at both temperatures conformed very closely to the (111) ellipsoid-of-revolution multivalley model with values of the mass and scattering-time anisotropy parameter K of 4.7 (room temperature) and 4.2 (77°K), and with values of the statistical-scattering factor G of 1.17 (room temperature) and 1.016 (77°K). The dependence of the magnetoresistance at 77°K on the Fermi level was used to make a rough calculation of the effective-mass components of the carriers in p-type PbTe which led to a total density-of-states effective mass of 0.16 times the free electron mass. Some preliminary room-temperature magnetoresistance data on n-type PbTe and on PbS and PbSe were also obtained which revealed that the longitudinal magnetoresistance in both n- and p-type PbS and PbSe was an order-of-magnitude smaller than in p-type PbTe.

9299 NEW GALVANOMAGNETIC EFFECTS IN N-TYPE GERMANIUM BELOW 4.2°K by R. W. Keyes and R. J. Sladek (Westinghouse Res. Labs.); Bull. Am. Phys. Soc., Ser. II, Vol. 5, p. 358 (A), June 15, 1960

Two new galvanomagnetic effects have been found in n-type germanium below 4.2°K by employing magnetic field strengths up to 28,000 gauss: (1) magnetoresistance having a different crystalline anisotropy than conduction band magnetoresistance, and (2) a large decrease in the Hall coefficient with increasing field strength. The electrical conductivity at these temperatures is dominated by impurity conduction. The order of magnitude and the crystalline anisotropy of the magnetoresistance has been interpreted as a consequence of changes in the impurity wave functions which are produced by the magnetic field; the field dependence of the Hall coefficient has been interpreted as a magnetoresistance effect of the conduction band. This effect occurs because the current due to the Lor-

entz force is carried by conduction band electrons. Consequently, the effect can be used to determine the conduction band mobility at very low temperatures.

9300 TRANSVERSE MAGNETORESISTANCE AND HALL EFFECT IN N-TYPE InSb by R. T. Bate, R. K. Willardson and A. C. Beer (Battelle); J. Phys. Chem. Solids, Vol. 9, No. 2, pp. 119-128, 1959

Transverse magnetoresistance and Hall effect data for InSb at fixed temperatures between 50° and 200°K are given. The data cover the range from the weak magnetic field region to the strong field quantum limit in InSb samples of high mobility and sufficient purity for which classical statistics apply. At weak fields the results are in semiquantitative agreement with theoretical predictions based on a simple mixed-scattering mechanism and a spherical conduction band. At the highest fields the transverse magnetoresistance data approach the H/T behavior expected on the basis of the quantum treatment of Argyres and Adams and the result in the quantum limit for the purest specimen shows good agreement with the theory for reasonable values of the electron effective mass.

Effect of Neutron Irradiation on the Magnetoresistance of AuCu - See 9199

Measurement of the Hall Constant - See 9277

Electric Field Dependence of Hall Constant - See 9269

Hall:
Effect in Ge - See 9282
Constant of Polar Semiconductors - See 9271

9301 CYCLOTRON RESONANCE OF NEGATIVE MASS CARRIERS UNDER NONEQUILIBRIUM CONDITIONS by R. C. Williams (RCA Labs.); Bull. Am. Phys. Soc., Ser. II, Vol. 5, p. 374 (A), June 15, 1960

The cyclotron resonance spectrum of optically excited carriers in a re-entrant, axially symmetric energy band has been calculated on the basis of classical transport theory. The conditions which the distribution function must satisfy in order that power be emissive at the negative-mass resonance are obtained along with a description of the way in which the power emission varies throughout the negative mass cone. The use of contour integration methods yields an exact evaluation of the power absorption spectrum as a function of the magnetic field and the anisotropy in the distribution function. The poles of the integrand of the power absorption or emission integral give information on the orbits, masses, and frequencies of the carriers undergoing resonance while the residues correspond to the contribution of each carrier to the power absorption or emission. The conditions for emission have been demonstrated by calculating the power spectrum for various distribution functions for an energy band model which approximates the heavy hole band of germanium. The results of these calculations were compared with recent experimental data.

9302 INFRARED CYCLOTRON RESONANCE IN SEMICONDUCTORS by J. Sosniak (McGill U.); Bull. Am. Phys. Soc., Ser. II, Vol. 5, p. 374 (A), June 15, 1960

Cyclotron resonance experiments using monochromatic infrared radiation and pulsed magnetic fields were described. Radiation reflected from the sample surface produces at resonance a signal which is observed by means of a zinc-doped germanium photoconductive detector. The object is to study the band structure of GaSb and InSb by investigating the theoretically predicted shift of the resonance frequency as a function of the magnetic field.

Cyclotron Resonance in Polyvalent Metals - See 9209

9303 MAGNETOPLASMA RESONANCE IN GERMANIUM by R. E. Michel and R. Rosenblum (RCA Labs.); Bull. Am. Phys. Soc., Ser. II, Vol. 5, p. 375 (A), June 15, 1960

Microwave plasma resonance has been observed previously in InSb at a fixed carrier concentration. In the present experiments the carrier concentration could be controlled by adjusting the temperature of an n-germanium sample in the 4° to 15°K region. The observations were made at a frequency of 25,000 Mc/sec and with a modulation of the carrier concentration by chopped light. With the magnetic field in a [100] direction a single electron cyclotron resonance line was observed to move to lower magnetic field, through zero field, and back to high field as expected. The heavy hole cyclotron resonance line remained in a fixed position as the electron line shifted toward zero field. The effect of the sample depolarization factor (as determined by sample shape) also has been investigated. The results so far obtained are in qualitative agreement with the theory. With the magnetic field in directions other than the [100], the electron line is not single and the effects of this anisotropy on the plasma effects have been studied.

9304 SPIN-LATTICE RELAXATION OF SHALLOW DONOR STATES IN Ge AND Si THROUGH A DIRECT PHONON PROCESS by H. Hasegawa (Carnegie Inst. Tech.); Phys. Rev., Vol. 118, pp. 1523-1534, June 15, 1960

It is pointed out that the many-valley character of the conduction band edge of Ge and Si causes an anisotropy of the g shift and of the deformation potential for the conduction electrons. It is shown that the combination of these two effects provides a mechanism for spin-lattice relaxation of the donor spins in Ge and Si that yields $1/T_s$ proportional to the temperature T and to the fourth power of the static magnetic field H. Using known data about the deformation potential constant, the g shift, the energy of the inter-valley splitting, and the elastic constants, the magnitude of T_s is found to be approximately 2×10^{-3} sec for phosphorus donors in Ge, and 1×10^{4} sec for phosphorus donors in Si. These values refer to T = 1.25°K, H = 3000 gauss, with the field applied along the [111] axis. The mechanism fails to give a finite T_s for donors in Si, when the field is applied along the [100] axis.

9305 G FACTOR AND DONOR SPIN-LATTICE RELAXATION FOR ELECTRONS IN GERMANIUM AND SILICON by L. M. Roth (Lincoln Lab.); Phys. Rev., Vol. 118, pp. 1534-1540, June 15, 1960

The g factors of electrons in Ge and Si are calculated on the basis of the effective mass approximation. The results are consistent with experimental spin resonance data. The effect is predicted to be anisotropic, with $g_{\parallel}$ less than $g_{\perp}$. This anisotropy introduces a strong interaction between the electron spin and shear waves for the singlet donor ground state. This interaction can account in order of magnitude for the observed spin-lattice time τ_s for donor electrons in Si at low temperatures, including both a one-phonon process and a two-phonon Raman-type process. The temperature and magnetic-field dependence for the two processes are predicted to be $\tau_s^{-1} \propto TH^4$

and $\tau_s^{-1} \propto T^7 H^2$, respectively. The temperature dependence agrees with experiment; however, there are discrepancies in the magnetic-field dependence. τ_s is predicted to be anisotropic.

9306 ELECTRON SPIN RESONANCE OF Mn^{++} ION IN IONIC CRYSTALS by J. Kondo (Nihon U.); Prog. Theoret. Phys., Vol. 23, pp. 106-114, Jan. 1960

The fine structure constants of the ESR spectrum of Mn^{2+} in ionic crystals are calculated using overlap and covalent models and the results are compared with the experiments of Watkins and of Tinkham. From the sign of the experimentally determined constants D and E, it can be shown that for Mn^{2+} in the alkaline chlorides covalency is dominant and that for Mn^{2+} in ZnF_2 the overlap effect is dominant. It is shown in each case that the model gives the correct order of magnitude of the fine structure constants. The model also accounts for the fact that the magnitude of D increases from LiCl to KCl.

Use of Magnetic Resonance to Study Semiconductor Surfaces - See 9193

NOISE

9307 INTERVALLEY NOISE by P. J. Price (Columbia U.); J. Appl. Phys., Vol. 31, pp. 949-953, June 19, 1960

A theory for the spectrum of electrical noise due to electron transitions between several quasi-isolated groups of states is developed for the general case in which each group may carry part of an electric current and is applied to the noise due to transitions between valleys of the conduction band of Ge. The possibility of observing this noise is discussed using the data of Weinreich, Sanders, and White on the frequency of intervalley transitions.

9308 SURFACE-DEPENDENT 1/f NOISE IN GERMANIUM by A. U. MacRae and H. Levinstein (Syracuse U.); Phys. Rev., Vol. 119, pp. 62-69, July 1, 1960

The surface characteristics of 1/f noise have been investigated by using field effect techniques on 100 micron thick single crystal Ge filaments. The 1/f noise is independent of the surface potential when an accumulation layer is on the surface but increases rapidly as the surface conductivity gradually becomes inverted with respect to the bulk. No 1/f noise is observed due to charge transfer between the bulk and the slow surface states. An increase in the 1/f noise associated with the inversion layer occurs when the temperature of the Ge is decreased. The magnitude of the 1/f noise depends on the ambient, increasing as the slow state relaxation time decreases. An investigation of the relaxation processes associated with the charge transfer between the bulk and the slow surface states after the application of a dc electric field to the field effect electrode reveals a 1/f noise relaxation which is independent of the mode of the conductivity relaxation. The noise relaxes back to its original value with a logarithmic time dependence which is characteristic of a $1/\tau$ distribution in time constants and the conductance decays with a combination of exponential and logarithmic terms, depending on the surface conditions.

9309 CURRENT NOISE DUE TO OHMIC CONTACTS ON CADMIUM SULFIDE by J. J. Brophy and R. J. Robinson (Armour Res. Found.); J. Appl. Phys., Vol. 31, pp. 1343-1344, Aug. 1960

Measurements of current noise in lightly doped CdS crystals having indium soldered contacts of different quality are used to demonstrate the strong influence of contacts on the observed noise spectra. The results suggest the presence of shallow trapping states distributed in energy and located near the electrodes. The concentration of these states depends on the quality of the contact. These effects are not contact noise in the usual sense since the shape of the noise spectra is only moderately affected; however, the noise level may change by orders of magnitude.

ELECTRICAL PROPERTIES OF SURFACES

9310 SEMICONDUCTOR SURFACE PROPERTIES DEDUCED FROM FREE CARRIER ABSORPTION AND REFLECTION OF INFRARED RADIATION by N. J. Harrick (Philips Res. Labs.); J. Phys. Chem. Solids, Vol. 14, pp. 60-71, July 1960

The use of infrared radiation to study semiconductor bulk properties through the absorption by the free carriers is reviewed. Numerous applications of this technique and variations thereof, whereby properties of semiconductor surfaces may be determined, are discussed. It is shown that in many instances the techniques described here have distinct advantages over other techniques presently in use.

9311 THE EVALUATION OF GERMANIUM SURFACE TREATMENTS by S. R. Morrison (Honeywell Res. Ctr.); J. Phys. Chem. Solids, Vol. 14, pp. 214-219, July 1960

The variation of electrical surface properties with surface treatment is discussed. The variables measured are the field effect mobility and surface recombination velocity. Various etch systems, the influence of contamination in the etch or rinse water (some contaminants are found seriously to alter the characteristics with as low as 0.5 ppm) and the variation of surface properties during heat treatment are described. A method has been developed for rapid estimation of surface barrier, density of fast states and reproducibility of the surface. (With the large number of variables associated with surface treatments, rapidity in accumulation and interpretation of data is essential.) These parameters (surface barrier, etc.) are obtained from the measurements discussed above and a set of calibration curves developed for the purpose. The method requires the energy levels of the fast states to be independent of surface treatment (or another set of calibration curves must be developed for the new set of energies) but is self-checking with respect to this energy level parameter. Of those treatments used to date, the only one which has not been comparable in energy levels produced is the electrolytically etched surface, and a more exact analysis by Wallis and Wang has indicated also that here the energy levels are at considerably different values. The experimental results are interpreted in terms of fast state density and surface barrier using this method. Evidence was presented to show that under certain treatments water vapor can change the density of recombination centers.

9312 ELECTRICAL PROPERTIES OF CLEAVED GERMANIUM SURFACES by D. R. Palmer, S. R. Morrison and C. E. Dauenbaugh (Honeywell Res. Ctr.); J. Phys. Chem. Solids,

Vol. 14, pp. 27-32, July 1960

The effects of oxygen on the electrical properties of a cleaved Ge surface have been studied by measuring the field effect, conductance, and photoconductance. Upon cleavage, the surface is more p-type than the bulk and remains unchanged in a vacuum of about 10^{-9} mm Hg or less. When initially exposed to oxygen, the conductance tends toward a more p-type surface; then the surface changes towards n-type continuously at a constant oxygen pressure. When the system is evacuated, the surface reversibly becomes more p-type, indicating that oxygen tends to make the surface more n-type. In addition, the slow relaxation of the field effect in oxygen almost disappears in vacuum. The surface eventually becomes n-type in oxygen at 15 mm Hg for all of the samples measured, an effect which has apparently not been observed on surfaces cleaned by argon bombardment. The results are interpreted in terms of acceptor states at the surface and donor states which depend on sorbed oxygen and produce a slow relaxation of the field effect.

9313 CHARACTERISTICS OF UC, ZrC, AND (ZrC) (UC) AS THERMIONIC EMITTERS by R. W. Pidd (U. Michigan); G. M Grover, D. H. Roehling, E. W. Salmi, J. D. Farr, N. H. Kirkorian and W. G. Witteman (Los Alamos Sci. Lab.); J. Appl. Phys., Vol. 30, pp. 1575-1578, Oct. 1959

Uranium carbide has been found to have high thermionic emission in the temperature range 1400°-1800°K. The parameters of the Richardson equation which can be used to fit the data are $A = 7.3 \times 10^5$ amp/cm^2 (K)^2 and +4.57 v. While these parameters accurately predict the observed saturated currents, it is doubtful that such anomalous values are of theoretical significance within the framework of the Richardson-Dushman derivation. A solid solution form of UC and ZrC gives substantially the same thermionic emission as UC, and for other reasons appears to be the more useful emitter. The carbides require no surface preparation or activation schedule for use as emitters.

9314 STUDIES OF AUGER ELECTRONS EJECTED FROM GERMANIUM BY SLOWLY MOVING POSITIVE IONS by H. D. Hagstrum (Bell Labs.); J. Phys. Chem. Solids, Vol. 14, pp. 33-36, July 1960

Measurements of total yield and kinetic energy distribution of Auger electrons ejected from a Ge surface by singly charged noble gas ions are reported. The surface changes have been monitored during procedures designed to clean the surface. Ion bombardment yielded a reproducible surface which showed the Auger characteristics to be expected for the clean surface. Heating at lower temperatures for days and for a total of about 3 hr at 1170°K (40°below the melting point) prior to any sputtering only partially cleaned the surface. From the kinetic energy distribution of the Auger electrons some of the principal characteristics of the state density function in the valence band of Ge have been determined.

9315 SECONDARY ELECTRON EMISSION by A. T. Dekker (U. Minnesota); Solid State Phys.-Adv. Res. and Appl., Vol. 6, Academic Press, 1958, pp. 251-311

Experimental information that is pertinent to the understanding of the secondary emission process is discussed and a semi-empirical theory of secondary emission is given. Because of oversimplifying assumptions, the theory cannot predict the magnitude of the yield of any material and it provides no basis for a discussion of the energy distribution of the emitted electrons, but it can give some information regarding the reduced yield curves. Various approaches to the theory of secondary emission of metals are outlined. They are all based on the assumption that there are two distinct steps in the secondary emission process: one corresponding to the production of secondaries, the other corresponding to the diffusion towards and escape from the surface. Elastically reflected primaries and inelastically backscattered primaries by a bombarded material are discussed in detail. The results show that this study provides information regarding the electronic structure of the target material.

9316 SECONDARY ELECTRON EMISSION OF ALKALI HALIDE SINGLE CRYSTALS CLEAVED IN HIGH VACUUM by N. R. Whetten (GE Res. Labs.); Bull. Am. Phys. Soc., Ser. II Vol. 5, p. 347 (A), June 15, 1960

Measurements of the secondary electron emission yield of several alkali halide single crystals made immediately after cleaving the crystals in a high vacuum of 10^{-10} mm Hg were reported. Only a small fraction of a monolayer of gas could be adsorbed on the surface of the freshly cleaved crystal before the measurements were completed. Single pulse measurement techniques were employed to minimize charging of the surface and damage to the crystals. Some of the crystals examined and their corresponding yield after cleaving in a high vacuum are NaBr-23; KBr-14; KI-10; KCl-13; NaCl-14.

9317 TRANSFER OF ELECTRIC CHARGES THROUGH RUTILE SINGLE CRYSTALS by K. G. Srivastava (MIT); Phys. Rev., Vol. 119, pp. 520-524, July 15, 1960

Electron transfer and onset of field emission have been investigated in TiO_2 single crystals with dc current-time characteristics parallel and perpendicular to the optic axis as function of voltage, temperature, electrode material, and light absorption. The currents are much larger and field emission sets in at lower voltage when the field is parallel to the optic axis. Higher temperature favors the current transfer by increasing the carrier mobility. The effect of different electrode materials proved minor, except in the case of Ti, which as cathode raised the current by about one order of magnitude. Photoelectric measurements showed that, in the critical voltage region of incipient field emission, light absorption can apparently force the current reversibly into the field-emitting stage.

9318 MECHANISM OF THE INCREASING LONGTIME CHANGES OF THE FIELD EFFECT by V. I. Lyashenko and N. S. Chernaya (Inst. Phys., Ukrainian SSR); Soviet Phys.-Solid State, Vol. 1, pp. 799-805, Dec. 1959

Longtime changes of the field effect in Ge are discussed. Under given conditions a decrease of the screening of the field with time is observed. The conditions under which this phenomenon occurs are investigated and it is shown that it is caused by the desorption of ions from the surface of the semiconductor.

9319 SURFACE RELAXATION EFFECTS IN GERMANIUM AT REDUCED TEMPERATURES by D. H. Lindley and P. C. Banbury (U. Reading); J. Phys. Chem. Solids, Vol. 14, pp. 200-207, July 1960

Measurements of small signal field effect mobility on germanium as a function of frequency of the applied ac field and under-pulsed fields extended in temperature down to 100°K are reported. The measurements have been made for various values of a superimposed dc field giving a range of barrier

heights as deduced from the dc conductance. Relaxation processes have been observed with characteristic times in the range 1 - 10^{-6} sec depending on the temperature and the barrier height. In inversion layers the relaxation can be represented by a single time constant, while in other types of barrier the relaxations are not exponential. The effects are sensitive to illumination. The results are discussed in terms of surface trapping and recombination, and a comparison is made with predictions from Garrett's analysis.

9320 SURFACE PROPERTIES OF VACUUM CLEANED SILICON by J. T. Law (Bell Labs.); J. Phys. Chem. Solids, Vol. 14, pp. 9-21, July 1960

Measurements of conductivity, photoconductivity, and change in contact potential with light are reported. Single crystal Si produced by floating zone techniques, cleaned by positive ion bombardment and annealed was used. The absence of a conducting p-film after such treatment has been demonstrated. The annealing after bombardment has been measured as a function of time at various temperatures. Changes in the bulk carrier concentration have been studied after various heating treatments. Changes in conductivity produced by argon ions indicate that in the clean condition the Fermi level is about 0.1 to 0.2 ev above the valence band edge. Adsorption of atomic hydrogen decreases the conductivity of both heated and bombarded and annealed samples. At the same time ΔCP becomes more negative, indicating a downward movement of the energy bands at the surface.

MAGNETIC PROPERTIES

FERRO- AND FERRIMAGNETISM

9321 SOME PROBLEMS OF PHENOMENOLOGICAL THEORY OF FERRO- AND ANTIFERROMAGNETISM by S. V. Vonsovsky and E. A. Turov (Inst. Metal. Phys., USSR); J. Appl. Phys., Suppl. Vol. 30, pp. 9S-19S, Apr. 1959

A general review of the modern state of phenomenological theory of ferro- and antiferromagneticism is presented and the results of some investigations of the authors in this field are given.

9322 GENERAL SPIN-WAVE DISPERSION RELATIONS by R. F. Soohoo (Lincoln Lab.); Bull. Am. Phys. Soc., Ser. II, Vol. 5, pp. 356-357 (A), June 15, 1960

The general spin-wave dispersion relations obtained by a simultaneous solution of Maxwell's equations and the equation of motion of the magnetization were given. In this calculation, the effects of conductivity, propagation, and exchange were properly taken into account. The special conditions under which the general result will lead to the Kittel-Herring dispersion relation were discussed. The question of the compatability of the requirement of Maxwell's equations and the equation of motion of the magnetization were examined. It has been found that, whereas the requirements of these two equations are always compatible for spin-waves, they are compatible for the spatial non-varying mode only under very special conditions. It appears that only when the permeability of one of the normal modes in a gyromagnetic medium is equal to zero or perhaps in the static limit can the uniform mode simultaneously satisfy both Maxwell's equations and the equation of motion of the magnetization.

9323 SURFACE MAGNETOSTATIC MODES AND SURFACE SPIN WAVES by J. R. Eshbach and R. W. Damon (GE Res. Labs.); Phys. Rev., Vol. 118, pp. 1208-1209, June 1, 1960

An examination of the spatial configuration of the magnetostatic modes of a ferromagnetic body is reported. The modes whose frequencies lie between $\omega = \gamma(B_i H_i)^{1/2}$ and $\omega = \gamma(H_i + 2\pi M)$ are found to be surface modes. It is also found that the complete spin-wave spectrum consists of a set of surface spin waves in addition to the spin-wave band usually considered. The magnetostatic mode spectrum thus merges smoothly into the spin-wave spectrum. The characteristic equation for the surface modes on a plane surface at an arbitrary angle to the applied dc field is given. The properties of the surface modes on plane surfaces and on spheroidal bodies are discussed.

9324 HIGH FIELD MAGNETIZATION STUDY OF FERRI-MAGNETIC ARRANGEMENTS IN CHROMITE SPINELS by I. S. Jacobs (GE Res. Labs.); J. Phys. Chem. Solids, Vol. 15, pp. 54-65, Aug. 1960

A differential susceptibility observed at high magnetic fields and low temperatures in spinel-type compounds that has been shown to be useful for detecting non-collinear ferrimagnetic arrangements is discussed. Such an increase in net magnetization with field is not expected for the Néel model of tetrahedral A-site moments antiparallel to octahedral B-site moments. It is, however, expected for the triangular arrangements proposed by Yafet and Kittel in which the moments on one kind of site subdivide into two groups making angles with each other. The latter arrangements have frequently been suggested for chromium-containing spinels, usually on the basis of the observed anomalously low spontaneous magnetizations. Measurements of magnetization curves at 4.2°K in pulsed fields up to 140 koe reveal high field susceptibilities in $MnFe_{2-t}Cr_tO_4$, $t > 0$; $CuCr_2O_4$; $FeCr_2O_4$; and $NiFe_{2-t}Cr_tO_4$, $t > 1$. These are interpreted as triangular ferrimagnetic arrangements and choices are made between alternative triangular models. In some cases the sign of the dominant anisotropy is suggested. Néel antiparallel ferrimagnetic arrays are confirmed for $MnFe_2O_4$ and for $NiFe_{2-t}Cr_tO_4$, $t < 1$. The present evidence for these conclusions is of a new and occasionally more direct type.

9325 ON THE ORIGIN OF LOW MOMENTS IN CHROMIUM-CONTAINING SPINELS by P. K. Baltzer and P. J. Wojtowicz (RCA Labs.); J. Appl. Phys., Suppl. Vol. 30, pp. 27S-29S, Apr. 1959

It is suggested that the origin of the low moments in the chromites is the spin-quenching effect imposed on the Cr^{3+} ions by the appropriate Jahn-Teller distortions of their neighbors. A macroscopically distorted phase is not required for this effect; it is only necessary that a distribution of distorting neighbors be present, sufficient in number to alter the symmetry about (and hence spin quench) at least a fraction of the Cr^{3+} ions. With the aid of these hypotheses it has proved possible to explain the moment data for many chromites in a consistent way. Of particular interest are the recently studied systems, $(CuFe_2O_4)_{1-x} + (CuCr_2O_4)_x$ and $(NiFe_2O_4)_{1-x} + (NiCr_2O_4)_x$.

9326 MAGNETIC CONTRIBUTION TO THE ANOMALOUS γ-LOOP SHEAR OF Fe-Al ALLOYS by R. Kikuchi (Wayne State U.) and H. Sato (Ford); J. Appl. Phys., Suppl. Vol. 30, pp. 92S-94S, Apr. 1959

The free energy of the Fe-Al system is calculated using the cluster variation method of cooperative phenomena on the Ising-type scalar spin model under the assumption that there

are a direct positive (ferromagnetic) interaction between nearest neighboring Fe atoms and an indirect negative (antiferromagnetic) superexchange interaction between a pair of Fe atoms which are separated by an Al atom. These assumptions have proved to be quite successful in explaining the magnetic properties over the entire range of Fe-Al system. It is found that the magnetic free energy of the system can be lowered by adding Al atoms while the Curie point is also lowered. This kind of situation is required for explaining the anomalous upward shear of γ loop in Fe-Al system, but this type of conclusion cannot be obtained from the nearest neighbor interaction model or from the concept of the corresponding state.

9327 MAGNETIC PROPERTIES OF SOME FERRITE MICROPOWDERS by A. E. Berkowitz and W. J. Schuele (Franklin Inst.); J. Appl. Phys., Suppl. Vol. 30, pp. 134S-135S, Apr. 1959

An investigation of the magnetic properties of micropowders of stoichiometric Cu, Ni, and Co ferrites prepared by low temperature (< 800°C) treatment of the co-precipitated metal oxalates is reviewed. The magnetic properties of each ferrite were determined as functions of particle or crystalline size in the range from 70 to > 2000 A. Particle sizes were determined from X-ray line broadening and from electron micrographs. The micropowders exhibited superparamagnetic, single domain, or multidomain behavior depending on the particle size. The critical size for single domain behavior, depending on composition, was between 300 and 700 A. In this size range, high coercive force and remanence were observed in spite of appreciable sintering of the particle in some cases. The remanence values and the magnitude and temperature dependence of the coercive force indicated that magnetocrystalline anisotropy determined the properties of the single domain particles.

9328 PROPERTIES OF MULTIDOMAIN PARTICLES by H. Amar (Franklin Inst.); J. Appl. Phys., Suppl. Vol. 30, pp. 139S-141S, Apr. 1959

The theoretical interpretation of the size-dependence of the coercive force $H_c(x)$ of fine ferromagnetic powders and thin films is discussed. Kittel and Néel's treatments are reviewed, and some recent work of the author along similar lines is presented. An alternative heuristic approach is suggested, leading to an expression $H_c = \text{const} \times (x^2 + b^2)^{-1}$, and is compared to some of the recent experimental data.

Shape Distribution of Magnetite Powders - See 9186

9329 ON THE FERROMAGNETISM OF THIN FILMS by A. Corciovei (Inst. Atomic Phys., Bucharest); Czech. J. Phys., Vol. 10B, No. 8, pp. 568-578, 1960

The magnetic properties of ferromagnetic thin layers are studied by calculating the partition function for the magnetic system in Kirkwood's approximation of the second order. The results obtained for the Curie temperature and the magnetization are in somewhat better agreement with the experiment than those obtained by Valenta.

9330 FARADAY ROTATION AND SOME MAGNETIC PROPERTIES OF EVAPORATED THIN FILMS OF IRON, NICKEL, AND GADOLINUM by J. R. Holmes and F. J. McClung, Jr. (U. Southern California); Bull. Am. Phys. Soc., Ser. II, Vol. 5, p. 356 (A), June 15, 1960

Thin films of iron, nickel, cobalt, and gadolinium have been evaporated, and measurements have been made in the same vacuum system without exposing the films to air. The rotation measurements for iron, nickel, and cobalt were reported. The films were deposited on glass for the rotation measurements and on carbon for the diffraction studies which also were made. Thickness measurements were made using the Tolansky method. The gadolinium films which were prepared did not show any rotation at temperatures as low as 77°K. These films usually were unstable in the vacuum system unless the film was very thick. Resistance measurements show a large and rapid increase in resistance while still at a pressure of 10^{-6} mm Hg.

Texture of Evaporated Ni-Fe Thin Films - See 9183

9331 ELECTRON MIRROR MICROSCOPY OF MAGNETIC STRAY FIELDS ON GRAIN BOUNDARIES by L. Mayer (Genl. Mills); J. Appl. Phys., Vol. 30, pp. 1101-1104, July 1959

The application of electron mirror microscopy to direct visual observation of magnetic stray fields at grain boundaries in magnetic materials is described. Si-Fe disks were used as specimens. By mounting these specimens on a special magnetic stage of axial symmetry, the appearance and the growth of magnetic stray fields with increasing external applied magnetic fields could be observed directly, and motion picture recordings were taken from the viewing screen of the microscope. A series of electron mirror micrographs shown demonstrates that grain boundaries behave quite differently stray-field-wise. The fact that magnetic stray fields on grain boundaries are now accessible to direct visual observation is considered valuable for many magnetic investigations. The still controversial subject of grain size effects on the magnetic properties of such important magnetic materials as Si-Fe is one subject which might profit from the potentialities inherent in electron mirror microscopy. This electronic observation method might also be helpful in grain boundary studies concerned with the basic physics of magnetics in such narrow regions of distorted order.

9332 RECENT DEVELOPMENTS IN THE FIELD OF ELONGATED SINGLE-DOMAIN IRON AND IRON-COBALT PERMANENT MAGNETS by R. B. Falk, G. D. Hooper and R.J. Studders (GE); J. Appl. Phys., Suppl. Vol. 30, pp. 132S-133S, Apr. 1959

The experimental physical and magnetic properties of elongated single-domain permanent magnets are briefly reviewed with respect to their means of preparation. A successful process is described for making ESD magnets available commercially at a limited initial rate. The material produced contains elongated single-domain particles of Fe or Fe-Co embedded in a metallic matrix to protect them from environmental attack. Maximum magnetic energies of 2.2 megagauss-oersteds for Fe and 3.6 megagauss-oersteds for Fe-Co are available.

9333 GYROMAGNETIC RATIOS OF Fe AND Ni by G. G. Scott (Genl. Motors); Phys. Rev., Vol. 119, pp. 84-85, July 1, 1960

Decreases in the values of g' for weakly magnetized specimens of Fe and Ni are discussed. The decreases were caused by a systematic error in the measurement of magnetic moment. Recent experiments on these two metals indicate g' values of 1.919 ± 0.002 for Fe and 1.835 ± 0.002 for Ni.

9334 SYNTHESIS OF A (101) 001 TYPE TORQUE CURVE IN SILICON IRON by C. G. Dunn and J. L. Walter (GE);

J. Appl. Phys., Vol. 30, pp. 1067-1072, July 1959

The orientations and sizes of all the grains in a polycrystalline disk specimen of high-purity 3.25 per cent Si iron have been measured in order to determine a calculated magnetic torque curve and the texture of the specimen. The torque results agree with the experimentally determined values. The curves approximate a (110) 001 single crystal torque curve, which is reduced about 75 per cent, and thus indicate a possible texture consisting of about 25 per cent (110) 001 and 75 per cent random. The true texture obtained from the orientation data is found to have more than ten components, none of which is (110) 001. Illustrations showing how a (110) 001 type torque curve may be synthesized from non-(110) 001 type components in the texture are given.

9335 SATURATION MAGNETIZATION AND FERROMAGNETIC INTERACTION IN TERBIUM METAL by W. E. Henry (U.S. Naval Res. Lab.); J. Appl. Phys., Suppl. Vol. 30, pp. 99S-100S, Apr. 1959

Direct measurements of the magnetic moment of Tb metal at 295°K, 100°K, 4.2°K, and 1.25°K in applied magnetic fields up to 70,000 gauss are reported. In the liquid He range, $(\partial M/\partial T)_H = 0$. Between 35,000 gauss and 70,000 gauss, $(\partial M/\partial H)_t = (\alpha\beta^2/\Delta E) = 1.04 \times 10^{-5}$ Bohr magneton per atom per gauss for 100°K and for the liquid He range. At 1.25°K and 70,000 gauss, the magnetization is 7.5 Bohr magnetons per atom of Tb. This is perhaps near saturation. At 295°K the magnetization is linear up to about 45,000 gauss and shows a slight beginning saturation at higher fields. At 60,000 gauss the magnetization is 1.53 Bohr magnetons per atom of Tb. From the magnetization curve at 295°K (in the paramagnetic range) and a Brillouin function for the Tb atom in the $^7F_6$ ground state, a molecular exchange field of 700,000 gauss is calculated. A sample motion ballistic technique is used to measure magnetic moments.

9336 SATURATION MAGNETIZATION AND CURIE POINTS IN DILUTE ALLOYS OF IRON by A. Arrott and J. E. Noakes (Ford); J. Appl. Phys., Suppl. Vol. 30, pp. 97S-98S, Apr. 1959

A report of the initial stages of an investigation of the intrinsic properties of dilute alloys of Fe is given. Methods of determining spontaneous magnetization and Curie temperatures with precision of one part in 30,000 are discussed. The results for Fe-Ti alloys are singled out for attention. The decrease of spontaneous magnetization at a rate of more than 1.6 times that of simple dilution implies either a negative moment on the Ti atoms or more probably that the occupation of states contributing to the moment of the Fe is decreased by the addition of Ti. The increase in the Curie temperature at a rate of 3.7°C per atomic per cent Ti is discussed on the basis of the Bethe-Slater curve of exchange interaction as a function of atomic separation.

9337 EFFECT OF CHEMISORBED HYDROGEN ON THE MAGNETIZATION OF NICKEL AT LOW TEMPERATURES by R. E. Dietz and P. W. Selwood (Northwestern U.); J. Appl. Phys., Suppl. Vol. 30, pp. 101S-102S, Apr. 1959

The saturation magnetization of Ni particles in the range 10-100 A has been determined by extrapolating from magnetization measured at 4.2°K in fields up to 10^4 oe. Measurements have been made prior to, and after, the admission of hydrogen to the Ni at room temperature. The Ni is supported on silica in the manner familiar in heterogeneous catalysis. The number of d electrons paired per hydrogen atom absorbed has been calculated from the fractional change in saturation magnetization assuming the magnetic moment per atom of Ni to be 0.606 Bohr magneton. The ratio of d electrons paired to hydrogen atoms adsorbed is shown to be less than one. On sintered samples in which the average Ni particle diameter is 40-80 A the ratio is about 0.7. On smaller Ni particles the ratio may be less. This ratio does not appear to be sensitive to surface coverage. The fact that the ratio of d electrons paired to hydrogen atoms adsorbed is less than one is considered evidence for a localization of the electronic interaction between adsorbent and adsorbate.

9338 THEORETICAL APPROACH TO THE ASYMMETRICAL MAGNETIZATION CURVE by A. Aharoni, E. H. Frei and S. Shtrikman (Weizmann Inst. Sci.); J. Appl. Phys., Vol. 30, pp. 1956-1961, Dec. 1959

A method previously used to calculate the magnetization curve of an infinite cylinder is applied to the new Meiklejohn and Bean material which is made of Co particles in a CoO shell. It is assumed that the interface of the ferromagnetic and antiferromagnetic materials is held parallel to the cylindrical axis and does not change its direction for any value of the applied field. The crystal anisotropy is neglected. The easiest nucleation modes are buckling for small radii and curling for large radii. The transition from buckling to curling is about $RI_s A^{-1/2} = 2$, where R is the radius of the cylinder, I_s is the saturation magnetization and A is the exchange constant. Numerical solution of the nonlinear equations involved yields two branches in the magnetization curve which are both stable with respect to curling perturbations. The general stability is not tested. A similar calculation is carried out for an infinite slab with the spins on the surface held at a fixed direction and with the crystal anisotropy neglected.

9339 INDUCTION APPARATUS FOR THE CONTINUOUS MEASUREMENT OF MAGNETIC SUSCEPTIBILITY by W. A. Norder (Tufts U.); Rev. Sci. Instr., Vol. 31, pp. 849-851, Aug. 1960

An induction apparatus for measuring the paramagnetic susceptibility of metals during exposure to gases (specifically hydrogen) is described. Provision is made for heating to 500°C and for removal or addition of gas during measurement. The device may be adapted for use at low temperatures.

9340 THE RECOVERY OF INITIAL MAGNETIC SUSCEPTIBILITY IN PURE NICKEL by M. Asanuma (Hokkaido U.); J. Phys. Soc. Japan, Vol. 15, pp. 1469-1474, Aug. 1960

An investigation of the process of recovery in cold-worked pure nickel by means of initial magnetic susceptibility and electrical resistance measurements is described. In the specimens studied, which were elongated by about 5 per cent, the recovery of the initial magnetic susceptibility was observed above 450°C, and could not be observed below that temperature. The recovery in the temperature range of the investigation was expressed by logarithmic law and analyzed by Kuhlmann's formulation, its activation energy being 3.0 ev. This value is in good agreement with the activation energy of self-diffusion in pure nickel. Therefore, it is considered that the recovery of the initial magnetic susceptibility is due to the disappearance of dislocation in the stage of recrystallization. On the other hand, the recovery below 450°C in which the change of initial magnetic susceptibility could not be observed was investigated by measuring the electrical resistance and the activation energy

0.91 ev was obtained. This value is in good agreement with the activation energy of vacancy migration. Therefore, it is assumed that the disappearance of vacancies does not affect the initial magnetic susceptibility.

9341 EFFECTS OF HIGH TEMPERATURE ON MAGNETIC PROPERTIES OF CORE MATERIALS by M. Pasnak and R. H. Lundsten (U.S. Naval Ord. Lab.); J. Appl. Phys., Suppl. Vol. 30, pp. 107S-108S, Apr. 1959

Results are reported for an experimental study of the effects of temperature on the dc and 60 cps magnetic properties of the following alloys: Orthonol, 4-79 Mo Permalloy, AEM 4750, L- and Z-Silectron, Transformer A, Audio Transformer A, 11.7 Alfenol, 15.5 Alfenol, Thermenol, 7-70 Perminvar, and Supermendur. The results indicate that, in general, an increase in temperature decreases the coercive force and the maximum and residual inductions. Maximum and initial permeabilities increase with increasing temperature until the Curie temperature is approached, then they decrease. The initial permeability generally reaches a maximum at a lower temperature than does the maximum permeability.

9342 TEMPERATURE DEPENDENCE OF THE MAGNETIC PROPERTIES OF NICKEL-IRON ALLOYS by J. J. Clark and J. F. Fritz (Westinghouse); J. Appl. Phys., Suppl. Vol. 30, pp. 105S-107S, Apr. 1959

The effect of temperature on the magnetic properties of six commercially available Ni-Fe alloys is reported for the temperature range 60°-250°C. The trade names of the alloys are: Hypernik, Deltamax, Hipernik V, Supermalloy, 4-79 Mo-Permalloy, and Hymu 80. The temperature dependence of both ac and dc magnetic properties was determined experimentally over the temperature range. Dc properties were measured by the standard ballistic testing method. At each test temperature sufficient data was taken to plot a normal magnetization curve. Remnant induction and coercive force were also determined at each temperature, these properties being measured relative to magnetization forces in excess of 100 oe. Ac properties were measured by means of a modified Hay bridge, the tests being conducted at frequencies of 60,400 and 1000 cps. At each test temperature, and for each frequency, total core loss was measured at various inductions in the range characteristic of the alloy being tested. The data presented are the average of the results of tests on six samples of each alloy.

9343 MAGNETIC ANNEALING IN PERMIVAR. Part II. MAGNETIC PROPERTIES by E. A. Nesbitt and R. D. Heidenreich (Bell Labs.); J. Appl. Phys., Vol. 30, pp. 1000-1003, July 1959

Previous work on Alnico single crystals (permanent magnet alloys) showed that magnetic torque reversals are associated with an inhomogeneous structure. More recently it has been found that alloys of Ni, Fe, and Co in the perminvar region also exhibit these torque reversals although the alloys are considered to be solid solutions. An inhomogeneous structure occurs simultaneously with the torque reversals in some of these alloys. The inhomogeneous structure has been observed by means of electron diffraction, and the observations have been interpreted to mean that there are faults in the lattice normal (111) directions. The faults form in the temperature region where the magnetic field heat treatment is effective and their density is roughly proportional to the response of the magnetic field treatment. When the crystals are not treated in a field, the faults are arranged to have cubic symmetry and their magnetic anisotropy has cubic symmetry. When the crystals are heat treated in a magnetic field, electron diffraction indicates that the faults are usually affected also. Evidence has been obtained that small amounts of oxygen as an impurity in Perminvar cause both the faulting and the heat treatment in a magnetic field. An extremely small amount of oxygen (0.0014 per cent) is sufficient to cause such effects. The magnetic anisotropy introduced by heat treatment in a magnetic field probably arises either from short range order within the faults or from the arrangements of the faults each of which is parallel to a (111) into regions whose shape anisotropy is along the direction of the magnetic field.

9344 EFFECT OF MAGNETIC ANNEALING ON THE PROPERTIES OF (100) [001] ORIENTED 3-1/4% SILICON-IRON STRIP by H. C. Fiedler and R. H. Pry (GE); J. Appl. Phys., Suppl. Vol. 30, pp. 109S-110S, Apr. 1959

Measurements of the ac and dc properties of a Si-Fe strip, before and after magnetic annealing with the field parallel to the <100>, <110>, and <111> directions, are discussed. Distinct improvement in properties was obtained, particularly in the <110> and <111> directions. This improvement is the result of the realignment of domain boundaries to <100> directions that more nearly coincide with the direction of the applied field. The anisotropy energy that arises from the magnetic annealing is about 900 ergs/cm^3, which is but a small fraction of the magnetocrystalline anisotropy energy of this material.

9345 ON THE EFFECT OF HEAT TREATMENT IN A MAGNETIC FIELD ON MAGNETIC PROPERTIES OF IRON-ALUMINUM ALLOYS by M. Sugihara (Nippon Tel. and Tel.); J. Phys. Soc. Japan, Vol. 15, pp. 1456-1460, Aug. 1960

The effect of heat treatment in a magnetic field upon the permeability of Fe-Al alloys is discussed. When specimens of Fe-Al alloys are cooled in a magnetic field from high temperatures, the per cent increase of initial permeability is generally not large; however, the per cent increase in maximum permeability is considerable and has a maximum at a concentration of 10.20 per cent Al. The effect of heat treatment in a magnetic field is small when the Al concentration is more than 11.5 per cent. When a quenched specimen containing 10.20 per cent Al is annealed again at various temperatures and cooled in a magnetic field, the lowest effective temperature of heat treatment in a field becomes about 225 ~ 250°C. This temperature is 100°C lower than the usual lowest effective temperature for the specimen without quenching. Maximum permeability of the specimen which was quenched at first and heat treated at about 250°C in a magnetic field reached a value of about 30,000.

9346 INFLUENCE OF VARIOUS HEAT EXPOSURES ON ALNICO V MAGNETS by R. K. Tenzer (Indiana Steel Prod.); J. Appl. Phys., Suppl. Vol. 30, pp. 115S-116S, Apr. 1959

Measurements on Alnico V magnets exposed to temperatures between 350° and 550°C for as long as 1000 hours are reported. Remanence was determined at room temperature intermittently during the exposures. The changes in remanence appeared to be caused by metallurgical as well as magnetic processes. The two effects were separated and it was found that the Alnico V material responds to temperatures as low as 350°C.

9347 FLUX REVERSAL IN SOFT FERROMAGNETICS by F. B.

umphrey and E. M. Gyorgy (Bell Labs.); J. Appl. Phys., l. 30, pp. 935-939, June 1959

he flux reversal process in soft ferromagnetics is described, ing three different mechanisms. A domain wall motion proc- s is satisfactory only when the drive field is slightly larger an the coercive force. In the immediate drive region, a nuniform rotation model is necessary to be consistent with e experimental observations. In particular such a model edicts the observed linear relationship between drive and e inverse of the reversal time, the observed shape of the ux reversal transient, and the observed value of the switch- g coefficient. In the high drive region with a transverse eld applied, a coherent rotation model provides the best planation of the experimental observations. The three gions can be demonstrated with a single sample in the case the thin film.

348 UNIFORM ROTATIONAL FLUX REVERSAL OF FERRITE OROIDS by E. M. Gyorgy and F. B. Hagedorn (Bell Labs.); . Appl. Phys., Vol. 30, pp. 1368-1375, Sept. 1959

model is presented for the high speed uniform rotational flux eversal of ferrite toroids. The magnetization is uniform in the nse that the components of magnetization in a cylindrical oordinate system are independent of position. Analysis of the odel, to a very good approximation, leads to results identical ith those obtained from uniform rotation in isotropic thin lms. The minimum switching coefficient predicted by this odel is 0.005 oe μsec. Experimental confirmation of a high eed switching mode in ferrite toroids is given. A toroid with wire loop imbedded in it was used to induce the proposed ux configuration. The switching coefficient and the extrapo- ted threshold field associated with the high speed mode have een found to decrease with increasing temperature.

349 ISOLATION OF ROTATIONAL REVERSAL IN FERRO- AGNETIC FILMS by A. L. Hanzel and R. L. Conger (U.S. aval Ord. Lab.); J. Appl. Phys., Vol. 30, pp. 1932-1936, ec. 1959

uantitative data which show the relative contributions of all motion and domain rotation to the magnetization reversal ocess in thin ferromagnetic films for driving fields ranging om the coercivity to many times the anisotropy field are pre- nted. An equation for the total magnetization reversal time developed. This expression consists of two distinct compo- nts: one represents wall motion reversal time and the other versal time due to domain rotation. The equation is similar one published previously but contains a more realistic and ore suitable wall nucleation distribution function.

350 MILLIMICROSECOND SWITCHING PROPERTIES OF ERRITE COMPUTER ELEMENTS by W. L. Shevel, Jr. (IBM); . Appl. Phys., Suppl. Vol. 30, pp. 47S-48S, Apr. 1959

he switching properties of square loop ferrites are examined. witching times have been studied over the range 5μsec to 10 μsec. The switching parameters, threshold field and switch- g constant, have been studied as a function of temperature d of ceramic processing. The plot of inverse switching time ersus applied field displays three nearly linear portions for hich the slopes vary by a factor of from two to ten. The in- erse slope, known as the switching constant of the material, s therefore three values; this is interpreted as indicating ree mechanisms to be responsible for the process of flux re- versal, each mechanism being dominant over a certain region of the switching curve. These mechanisms are believed to be wall motion, incoherent rotation, and coherent rotation. A model allowing a coherent rotation process is proposed. Data are presented for several ferrites which have widely varying properties.

9351 EVALUATION OF NEW HIGH-SPEED MAGNETIC FERRITE SYSTEM FOR USE IN COMPUTER COMPONENTS by B. R. Eichbaum (IBM); J. Appl. Phys., Suppl. Vol. 30, pp. 49S-53S, Apr. 1959

A study of a new ferrite system, namely, the $CdO \cdot MnO \cdot Fe_2O_3$ system, which has proved to be feasible for many new high-speed applications, is presented. Some of the compositions of this new system exhibiting square hysteresis loops have switching constants as low as 0.200 oe μsec. Such materials in comparison with those of the $MgO \cdot MnO \cdot Fe_2O_3$ system have a much lower coercive force, require lower driving currents, and have a flux reversal or switching time which is five times as fast. These materials have been used in fast switching multipath elements and matrix switch cores. The operation of such elements is described.

9352 SINGLE CRYSTAL ANISOTROPY AND MAGNETOSTRICTION CONSTANTS OF SEVERAL FERROMAGNETIC MATERIALS INCLUDING ALLOYS OF NiFe, SiFe, AlFe, CoNi, AND CoFe by R. C. Hall (Westinghouse); J. Appl. Phys., Vol. 30, pp. 816-819, June 1959

Experimental determinations of the anisotropy and magnetostriction of single crystals of several ferromagnetic materials are reported. The materials include the metals Fe and Ni, binary alloys of Ni-Fe, Si-Fe, Al-Fe, Co-Ni, and Co-Fe, ternary alloys of Mo-Ni-Fe, Ni-Co-Fe, and Mo-Al-Fe, and magnetite. The effect of the order-disorder reaction on these properties has been measured for several of the alloys. The present data for the nickel iron and silicon iron systems agree well with recently published values. Ordering generally raises the magnetostriction and lowers the anisotropy of the aluminum iron alloys near the Fe_3Al composition. The first anisotropy constant, K_1, for the cobalt nickel system as derived from torque curves is similar to old data derived from magnetization curves. However, K_1 for cobalt iron (30, 35, and 45 per cent cobalt) appears to be considerably larger than previously reported. In general, the addition of cobalt to nickel and to iron changes the magnetostriction constants (λ_{100} and λ_{111}) toward large positive values. Thus, λ_{100} increases to 100×10^{-6} for 50 per cent cobalt nickel and to 130×10^{-6} for 45 per cent cobalt iron; λ_{111} increases to 30×10^{-6} for 45 per cent cobalt iron but remains approximately constant for the cobalt nickel alloys.

9353 TRIGONAL MAGNETOCRYSTALLINE ANISOTROPY IN HEXAGONAL OXIDES by L. R. Bickford, Jr. (IBM Res. Ctr.); Phys. Rev., Vol. 119, pp. 1000-1009, Aug. 1, 1960

Torque measurements of the magnetocrystalline anisotropy between 77° and 300°K for single crystals of two different ferrimagnetic oxides having structures related to that of the mineral magnetoplumbite are reported. The compounds, with chemical compositions $Co_2Ba_2Fe_{12}O_{22}$ and $Co_2Ba_3Fe_{24}O_{41}$, are known as Co_2Y and Co_2Z, respectively. Both compounds, after suitable magnetic field cooling treatment, display trigonal anisotropy in the basal plane at 77°K. The field cooling is shown to have the effect of placing the magnetization into one of two energetically equivalent orientations, each of which leads to a trigonal term of different sign. Examination of the crystal

structures shows that in the case of Co_2Y an additional term $K_2' \sin^3\theta \times \cos\theta \cdot \cos 3\phi$ (where θ and ϕ are the polar coordinates of the magnetization) should be added to the generally accepted phenomenological hexagonal anisotropy expression. The anisotropy constant K_2' is evaluated as 6×10^5 erg/cm^3 at 117°K. In the case of Co_2Z this trigonal anisotropy term is not consistent with the crystal symmetry, although it is appropriate for structural subgroups of the unit cell. Its trigonal anisotropy is explained in terms of a "puckered" magnetization pattern whereby the sign of the c-axis component of magnetization is different for adjacent subgroups. The existence of this puckered pattern implies that the exchange coupling across the boundaries between subgroups is relatively weak. A new rotational hysteresis effect in Co_2Y is described and explained phenomenologically. An atomic theory assigning the origin of the trigonal anisotropy of both compounds to the cobalt ions is presented.

9354 MAGNETIC ANISOTROPY OF IRON-COBALT FERRITE MEASURED BY FERROMAGNETIC RESONANCE by Y. Sugiura (Nagata-cho); J. Phys. Soc. Japan, Vol. 15, pp. 1561-1568, Aug. 1960

A study of the magnetic anisotropy of iron-cobalt ferrite by means of ferromagnetic resonance is discussed. The cubic magnetic anisotropy K_1/M and the uniaxial magnetic anisotropy K_T/M induced by heat treatment in magnetic field have been measured in the temperature range between 70° and 250°C. The secondary peaks observed in the ferromagnetic resonance of iron-cobalt ferrite are explained by the domains having different orientation of uniaxial magnetic axis. From the experimental results the g-factor of iron-cobalt ferrite is determined to be 2.86. The temperature dependence of g-factor has not been observed within limits of experimental errors.

9355 OBLIQUE-INCIDENCE ANISOTROPY IN EVAPORATED PERMALLOY FILMS by D. O. Smith, M. S. Cohen and G.P. Weiss (Lincoln Lab.); Bull. Am. Phys. Soc., Ser. II, Vol. 5, p. 357 (A), June 15, 1960

Observations of magnetic anisotropy in evaporated Permalloy films deposited at oblique incidence of the vapor were reported. Electron micrographs reveal chains of crystallites whose long axes are oriented perpendicular to the vapor beam. A difference in the absorption of light polarized parallel and perpendicular to these chains gives rise to optical dichroism. Chain growth cannot be basically a magnetic effect since dichroism has been observed in oblique-incidence films of Ag, Pt, W, and Mg. A "self-shadowing" model was proposed to explain chain growth, i.e., the area behind a crystallite is left vacant because it is in this crystallite's shadow. Experiments involving the stripping of oblique-incidence Permalloy films from their substrates indicate the presence of an anisotropic stress which, when acting through magnetostriction, gives another contribution to the magnetic anisotropy; this contribution explains the observed compositional dependence of the magnetic anisotropy. Surface tension acting on the crystallite chains was postulated as the motivation leading to the anisotropic stress.

9356 DIRECTIONAL ORDER AND DIFFUSION AFTEREFFECT by L. Néel (U. Grenoble, France); J. Appl. Phys., Suppl. Vol. 30, pp. 3S-8S, Apr. 1959

If an anisotropic local atomic configuration is produced in some way or other, the magnetization is stabilized in a direction related to this anisotropy, causing an additional uniaxial magnetic anisotropy. This kind of anisotropy in the configuration is called a directional ordering. This may be an anisotropic distribution of constituent atoms in substitutional ferromagnetic alloys, of interstitial atoms in a body centered cubic lattice, or of different atoms or ions on the sites of mixed ferrite etc. A brief explanation of the phenomena is given in each case. Also because of the coupling between the atomic arrangement and the direction of the magnetization, a relaxation phenomenon may be observed in the magnetization process which depends on the diffusion of atoms. The magnetic aftereffect arising from a small amount of carbon in α-iron is explained in detail.

9357 MAGNETIC PROPERTIES OF NICKEL-IRON FERRITE by N. Menyuk and K. Dwight (Lincoln Lab.); J. Appl. Phys., Suppl. Vol. 30, pp. 36S-37S, Apr. 1959

The magnetic anisotropy of a single crystal of Ni-Fe ferrite with composition $Fe^{3+}_{1.00}[Ni^{2+}_{0.79}Fe^{3+}_{0.36}-Fe^{3+}_{0.90}]O_4$ is given between 450° and 4.2°K. At high temperatures the anisotropy energy has cubic symmetry, and the absolute value of the first order anisotropy constant is a maximum at about 200°K. Below 200°K, $|K_1|$ decreases until 10°K, at which temperature there is an abrupt transition in the anisotropy characteristics. Below 10°K the anisotropy energy contains a uniaxial term of the form $\Sigma_i a_i^2 \beta_i^2$ where a_i and β_i are the direction cosines of the magnetization at the measuring temperature and at the annealing temperature (10°K), respectively.

Oriented Polycrystalline Ferrites with Cubic Anisotropy - See 9187

9358 CORRELATION OF ENERGY LOSSES WITH PERFECTION OF CRYSTAL ORIENTATION AND DOMAIN STRUCTURE by H. Hu and G. Wiener (Westinghouse Res. Labs.); J. Appl. Phys., Suppl. Vol. 30, pp. 86S-89S, Apr. 1959

Hysteresis and core loss measurements, made on single crystal strips of the (110) [001] orientation, the commercial single oriented material with a (110) [001] texture, and the doubly oriented material with a fair amount of (100) [001] cube texture, are discussed. All these specimens were 3 per cent Si-Fe had a thickness of 0.012 in and were measured using an Epstein frame. The energy losses calculated on a domain model are compared with the experimental data. Results indicate that there is little correlation of the observed eddy-current losses with the proposed domain model, and that the energy losses may be strongly dependent on the perfection of crystal orientation.

9359 INTERNAL STRUCTURE OF CROSS-TIE WALLS IN THIN PERMALLOY FILMS THROUGH HIGH-RESOLUTION BITTER TECHNIQUES by R. M. Moon (Lincoln Lab.); J. Appl. Phys., Suppl. Vol. 30, pp. 82S-83S, Apr. 1959

The use of a water immersion objective with the optical microscope for Bitter pattern studies has resulted in a significant improvement in resolution. Applied to the study of cross-tie domain walls in thin Permalloy films, this technique has revealed details of internal wall structure. In the proposed model for such walls the magnetization within the walls is thought to be predominantly in the plane of the film. This configuration reduces the large magnetostatic energy which would be associated with a conventional 180° wall. Areas of low particle density are observed at the intersection of the main wall and cross-ties and in the main wall midway between cross-ties. From conventional ideas of colloid-pattern forma-

ion, these areas might be expected to have a high particle ensity because they are the transition regions in which the nagnetization is normal to the film. The apparent conflict is esolved by assuming that these regions are large compared to he colloid particle size so that the fringing field at the edge f the region governs the particle distribution. In support of he model, convincing evidence is presented of the reported hift of colloid particles when an external field is applied ormal to the film.

9360 SOME OBSERVATIONS OF BITTER PATTERNS ON POLYCRYSTALLINE "SQUARE LOOP" FERRITES, AND A THEORETICAL EXPLANATION OF THE LOOP SHAPE AND PULSE CHARACTERISTICS OF THE MATERIAL by J. E. Knowles (Mullard Res. Labs., England); Proc. Phys. Soc., Vol. 75, pp. 885-897, June 1960

Observations of Bitter patterns on polycrystalline Mg-Mn ferrite, conducted in an attempt to obtain an experimental knowledge of the domain configuration of a "square loop" ferrite, are reported. A technique was developed which enabled the progress of a magnetization reversal to be followed in a single grain of the material. As a result of these observations it was postulated that the magnetization in each grain of the polycrystalline material lay along a [111] direction, and that the magnetization reversed by the motion of 180° domain walls. Hysteresis loops and pulse shapes calculated on the basis of this model show a close resemblance to the experimental curves.

9361 DOMAIN TUBE STRUCTURES IN SILICON IRON by L. F. Bates and R. Carey (U. Nottingham); Proc. Phys. Soc., Vol. 75, pp. 880-884, June 1960

A theoretical discussion and a quantitative study of Neil spike formation by the extension and subsequent collapse of a domain tube which joins an inclusion to a domain wall are presented. The results are discussed in terms of a formula given by Brenner, and an attempt is made to assess the importance of the phenomena in the explanation of coercivity.

9362 MAGNETIC VISCOSITY IN IRON DUE TO CARBON ATOMS ANCHORED IN DISLOCATIONS by G. Biorci, A. Ferro and G. Montalenti (Inst. Elletrotec. Naz.); J. Appl. Phys., Vol. 30, pp. 1732-1735, Nov. 1959

A specimen of Fe containing 0.01 per cent of C in solid solution has been cold worked by 7 per cent and aged at room temperature. After this treatment the Fe shows a new peak of magnetic viscosity at 180°C. The diffusion process giving rise to the peak is controlled by an activation energy of about 12,000 cal/g atom and a time constant at infinite temperature of about 10^{-14} sec. These figures agree with those of a peak of internal friction observed in similar specimens by Kê and by Köster, and interpreted as due to diffusion of C atoms in the surroundings of the dislocations. Hence the peak of magnetic viscosity can be related to the same mechanism.

9363 FERRIMAGNETIC RESONANCE MODES IN SPHERES by R. C. Fletcher and R. O. Bell (Hughes Aircraft); J. Appl. Phys., Vol. 30, pp. 687-698, May 1959

The magnetostatic solutions of ferrimagnetic resonance equations for ferrite spheres are derived. General and specific solutions are given for values of n up to five for the magnetostatic potentials, RF distributions of magnetization, and fields for resonance. Some experimental results are given and compared with the theory.

9364 MICROWAVE PROPERTIES OF YTTRIUM IRON GARNET by E. G. Spencer, R. C. LeCraw and C. S. Porter (Diamond Ord. Fuze Labs.); U.S. Gov. Res. Rep., Vol. 33, p. 562 (A), May 13, 1960 PB 145 010

Single crystal yttrium iron garnets grown from PbO solution have the narrowest ferromagnetic resonance line widths of any material yet reported. Measurements, on spheres, of line width, threshold field, and relaxation times are reported. These properties are shown to be strongly dependent on the degree of polish of the specimen surface.

9365 ANTIFERROMAGNETIC ORDERING IN $FeCo_3$ by S. J. Pickhart (U.S. Naval Ord. Lab. and Brookhaven Natl. Lab.); Bull. Am. Phys. Soc., Ser.II, Vol. 5, p. 357 (A), June 15, 1960

Neutron diffraction data taken on a powder sample of synthetic siderite ($FeCo_3$) have confirmed the antiferromagnetism suggested by the susceptibility measurements of Bizette and Tsai. The crystal structure of this compound is isomorphous with calcite and may be visualized as a NaCl type lattice contracted along a body diagonal. The resulting structure has rhombohedral symmetry (space group $R\bar{3}C$) and consists of layers of cations and layers of complex $(Co_3)^{2-}$ ions stacked in sequence along the [111] direction. The nuclear intensities are in good agreement with the reported oxygen parameter of 0.27, corresponding to a C-O bond distance of 1.26 A. Below the transition temperature (about 20°K on this sample) additional coherent reflections appear that are characteristic of an antiferromagnetic ordering. The Fe^{2+} moments on a given cation layer are parallel and point along the trigonal axis, while neighboring layers are antiparallel. The magnetic structure is thus reminiscent of that found in FeO, although the super-exchange interactions in this case are dissimilar. A g factor of 2.5 ± 0.15, derived from the observed magnetic scattering amplitude, suggests that the orbital angular momentum of the Fe^{2+} ion is incompletely quenched.

9366 ANTIFERROMAGNETIC STRUCTURE OF CrN by L. M. Corliss, N. Elliott and J. M. Hastings (Brookhaven Natl. Lab.); Phys. Rev., Vol. 117, pp. 929-935, Feb. 15, 1960

Measurements which show that CrN, crystallizing with the rock salt structure, is antiferromagnetic with a Néel point of 0°C are reported. The magnetic ordering scheme, as determined by neutron diffraction, is that of the fourth kind, with moments arranged in double ferromagnetic sheets which alternate along a line parallel to a face-diagonal. The structure is orthorhombic below the transition and the space ground P_{nma} has been tentatively assigned. The atomic displacements accompanying the distortion have been partially determined from the diffraction data and are discussed in relation to the magnetic structure. A value of $2.4 \mu_B$ has been assigned to the Cr moment; the moment direction is parallel to the b-axis of the orthorhombic cell (face-diagonal of the cube).

9367 MEASUREMENT OF THE LINEAR MAGNETOSTRICTION OF HARD-WORKED NICKEL by H. E. Stauss (U.S. Naval Res. Lab.); J. Appl. Phys., Vol. 30, pp. 1648-1650, Nov. 1959

The influence of plastic deformation upon the linear magnetostriction of hard-worked Ni has been determined by use of direct measurements of strain in three normal directions and

then by measurement of magnetostriction in the same three directions. The specimen was rotated 90° for each measurement. The combination of measurements appears to have advantages for the interpretation of magnetostriction in non-isotropic bodies. The value of magnetostriction at saturation for grade A Ni plastically deformed with an 84 per cent reduction of cross-sectional area was found to be $-33.5 \pm 1 \times 10^{-6}$. This compares with $-35 \pm 1 \times 10^{-6}$ for annealed Ni of the same quality. The hard-worked Ni was free of volume magnetostriction of determinable magnitude. It showed inappreciable preferred domain orientation, but it did appear to have a small amount of preferred crystalline orientation.

9368 MICROWAVE PROPERTIES OF NONSTOICHIOMETRIC POLYCRYSTALLINE YTTRIUM IRON GARNET by P.E. Seiden (Lockheed and Stanford U.), C. F. Kooi and J. M. Katz (Lockheed); J. Appl. Phys., Vol. 31, pp. 1291-1296, July 1960

The microwave properties of nonstoichiometric YIG ranging from 31 per cent iron excess through stoichiometric to 12 per cent yttrium excess are discussed. No ion substitution in the garnet lattice has been observed. All material in excess of stoichiometric proportions goes into ceramic second phases. The phases observed are perovskite ($YFeO^3$) for yttrium excess, hematite (Fe_2O_2) for iron-excess samples fired in oxidizing atmospheres, and magnetite (Fe_3O_4) for iron-excess samples fired in neutral atmospheres. On the basis of the assumption that all excess material goes into the appropriate ceramic second phase, the behavior of the saturation magnetization, spectroscopic splitting factor, and line width can be explained as a function of composition. It is found that the line width is strongly narrowed by the large magnetization as predicted by Geschwind and Clogston. The behavior of the dielectric constant can be explained, at least qualitatively, by a theory of Wagner and Sillars which considers particles of one dielectric material imbedded in a matrix of another. The behavior of the dielectric loss tangent is not understood and cannot be accounted for by this theory.

9369 MAGNETISM OF EUROPIUM GARNET by W. P. Wolf (Clarendon Labs.) and J. H. Van Vleck (Harvard U.); Phys. Rev., Vol. 118, pp. 1490-1492, June 15, 1960

The theoretical expressions for the magnetic moment of a trivalent Eu ion in a molecular field arising from exchange are applied to Pauthenet's measurements on Eu iron garnet. It is a good approximation to assume that the exchange interaction stems entirely from the coupling with the Fe atoms, which greatly simplifies the theory since the molecular field on the Eu is then an impressed one and does not have to be determined self-consistently. The calculated variation of the magnetization with temperature is in excellent accord with experiment. The magnitude of the exchange interaction is compared with that in the other rare earth iron garnets; it is almost exactly the same as in Gd iron garnet.

Crystallographic and Magnetic Properties of Square Loop Materials in Ferrite Systems Containing Cu - See 9184

Structural and Magnetic Properties of Mn-Co-C Alloys - See 9185

Magnetic Properties and Grain Structure of Mn-Zn - See 9189

9370 SUPERPARAMAGNETISM by C. P. Bean and J. D. Livingston (GE); J. Appl. Phys., Suppl. Vol. 30, pp. 120S-129S, Apr. 1959

The experimental and theoretical foundations of the effect whereby single domain ferromagnetic particles at elevated temperatures can behave magnetically in a manner analogous to the Langevin paramagnetism of moment-bearing atoms are reviewed. The main distinction is that the moment of the particle may be 10^5 times the atomic moment. Applications of this phenomenon are mentioned and attention is drawn to some current problems in this area.

Spin Paramagnetism Expressions - See 9210

9371 SUSCEPTIBILITY OF PHOTOGENERATED CARRIERS IN SOLIDS by C. Weissfloch and R. Stevenson (McGill U.); Bull. Am. Phys. Soc., Ser. II, Vol. 5, p. 374 (A), June 15, 1960

A vibrating sample magnetometer of the Foner type has been used for a series of room-temperature measurements on the change of magnetic susceptibility when samples of Ge and InSb were irradiated with infrared radiation. The wavelength dependence of apparent susceptibility changes and the dependence on sample carrier concentration have been studied. The results were compared with the earlier experiments of Kessler and Moore in order to determine the contribution of excitons to the observed magnetic moment.

9372 MAGNETIC SUSCEPTIBILITY OF METALLIC EUROPIUM by R. M. Bozorth (Bell Labs.) and J. H. Van Vleck (Harvard U.); Phys. Rev., Vol. 118, pp. 1493-1498, June 15, 1960

Measurements of the susceptibility of Eu from 1.3° to 300°K in fields up to 12,000 oersteds are reported. This metal is not ferromagnetic, but has at low temperatures a very high paramagnetic susceptibility, about forty times higher than for the free ion or hydrated salts. Variation of susceptibility with field strength is observed below 100°K. The saturation curvature at low temperatures is very large, and practically independent of temperature. The susceptibility at high temperatures is consistent with a divalent model. The magnetic behavior at low temperatures is hard to interpret on the basis of a divalent ion and can be more readily explained with a trivalent one for which the theory is developed. Metallurgical evidence, however, indicates that metallic Eu is divalent even at low temperatures. On the other hand, it is generally believed that Eu is trivalent in $EuIr_2$, but if the conventional molecular field theory is used the reported ferromagnetism of $EuIr_2$ cannot be ascribed to Eu^{3+} with a value of the exchange field consistent with that in $GdIr_2$.

9373 MAGNETIC PROPERTIES OF THE Pd AND Pt GROUP TRANSITION METAL COMPLEXES by H. Kamimura, S. Koide, S. Sugano (U. Tokyo), and H. Sekiyama (Kanagawa U.); J. Phys. Soc. Japan, Vol. 15, pp. 1264-1272, July 1960

The magnetic susceptibilities and the g-values of the Pd and Pt group transition metal complexes are calculated by means of the intermediate coupling scheme. Crystalline field with cubic symmetry is assumed to be strong, so that the effect of $d\gamma$ orbitals is neglected. The effect of Coulomb repulsion is considered to be comparable with that of the spin-orbit interaction. The results are expressed by functions of parameters $\eta = \zeta_d/(3B + C)$ and kT/ζ_d, where B and C are Racah's parameters and ζ_d the

coefficient of spin-orbit coupling of a d-electron. Comparison with available experimental data is also made.

9374 MAGNETIC SUSCEPTIBILITY, HEAT CAPACITY AND THIRD-LAW ENTROPY OF $MgNi_2$ by J. S. Wollam and W.E. Wallace (U. Pittsburgh); J. Phys. Chem. Solids, Vol. 13, pp. 212-220, June 1960

A study of the heat capacity and magnetic susceptibility of $MgNi_2$, undertaken to evaluate the report by Voss that this compound is ferromagnetic at temperatures below 235°C, is described. The results of the investigation reveal no evidence of ferromagnetism in this Laves phase. $MgNi_2$ is found to be a moderately strong paramagnetic material with a susceptibility which is practically constant between 25° and 450°C. Thermomagnetic analysis shows a very slight but abrupt drop in the susceptibility at 194°C, and heat-capacity measurements reveal a very small thermal anomaly at the same temperature. The effects are thought to be associated with some type of irregularity in the lattice, such as the defect structure which occurs when a nickel atom replaces a magnesium atom in the $MgNi_2$ lattice. Third-Law entropies of $MgNi_2$ at temperatures up to 555°K are also presented.

9375 PARAMAGNETIC SUSCEPTIBILITIES OF Fe AND Fe-Si ALLOYS by S. Arajs and D. S. Miller (U.S. Steel Res. Ctr.); J. Appl. Phys., Vol. 31, pp. 986-991, June 1960

Measurements of the paramagnetic susceptibilities of Fe and Fe-Si alloys (5.75, 6.82, 9.45, 12.65, 14.70, 18.11, 20.85 and 24.38 at. per cent Si) at temperatures up to 1200°C are reported. At high temperatures the paramagnetic susceptibilities of bcc Fe-Si alloys obey the Curie-Weiss law, possibly indicating that the contribution due to s-d exchange interactions is small in comparison with the temperature dependent paramagnetism. The effective Bohr-magneton number of Fe from the high-temperature region is independent of Si content up to about 14 at. per cent Si. At higher Si concentrations, gradual decrease in the effective Bohr-magneton number occurs. According to the paramagnetic susceptibility measurements, the α-γ transition in iron takes place at 910 ± 3°C. Assuming that the critical temperatures for chemical ordering as given by Glaser and Ivanick are correct, these measurements indicate that the paramagnetic susceptibility, within the experimental error, is not influenced by the destruction of the superlattice above 13 at. per cent of Si.

9376 PARAMAGNETIC RESONANCE AND OPTICAL SPECTRA OF DIVALENT IRON IN CUBIC FIELDS. Part I. THEORY by W. Low and M. Weger (Hebrew U.); Phys. Rev., Vol. 118, pp. 1119-1130, June 1, 1960

The energy level splittings of the ground state of the d^6 configuration in cubic and axial fields are given. The Zeeman splittings of the various levels are calculated for weak and strong magnetic fields. In the case of tetrahedral symmetry the effect of the perturbations of the odd parity configurations d^5p and d^5f on the ground state is estimated.

9377 SPIN-PHONON INTERACTION FOR Mn^{2+}, Fe^{3+}, AND Cr^{3+} IN MgO by N. S. Shiren (GE Res. Labs.); Bull. Am. Phys. Soc., Ser. II, Vol. 5, p. 343 (A), June 15, 1960

By utilizing ultrasonic spin resonance techniques previously reported the relative phonon induced electron spin transition probabilities at 9.2 kMc for Mn^{2+}, Fe^{3+}, and Cr^{3+} in MgO crystals bonded to quartz rods have been measured. The relative product of transition matrix element and ultrasonic coupling has been extracted from a comparison of the resonance saturation by ultrasonics, with the saturation by microwaves. In these preliminary experiments only longitudinal acoustic waves on the 100 axis have been used, and H_0 was rotated in the 001 plane. In all cases the interaction bandwidth is approximately the same as the observed microwave resonance line width.

9378 QUADRUPOLE COUPLING CONSTANT AND LINE WIDTHS OF Al IN RUBY AS A FUNCTION OF T AND Cr^{3+} CONCENTRATION by W. J. Veigele, W. H. Tanttila and C. M. Verber (U. Colorado); Bull. Am. Phys. Soc., Ser. II, Vol. 5, p. 344 (A), June 15, 1960

Measurements of the quadrupole coupling constant $\Delta\nu$ and the line widths of Al in ruby at 300°, 77° and 4.2°K and Cr^{3+} impurity concentrations of 0.1%, 1.5%, and 4% were given. The value of $\Delta\nu$ at 300°K agreed with that obtained by Pound. It was found that $\Delta\nu$ decreased 3 kc with a decrease in T from 300° to 4.2°K and was independent of the Cr^{3+} concentration. Broadening of the lines with a decrease in T was observed as shown below, where $\Delta\nu 3$ is the average value of the central line width over a number of crystal orientations in the magnetic field.

$\Delta\nu 3$ (kc)	0.1%	1.5%	4.0%
300.0°K	7.41	6.99	7.18
77.0°K	8.46	8.64	7.93
4.2°K	10.5	10.3	15.5

The satellite line widths were observed to be equal to the values of $\Delta\nu 3$.

9379 MEASUREMENT BROADENING IN MAGNETIC RESONANCE by O. E. Myers and E. J. Putzer (Convair); J. Appl. Phys., Vol. 30, pp. 1987-1991, Dec. 1959

Phase-detection techniques used in recording magnetic resonances as the source of a measurement broadening are discussed. Results of a general mathematical treatment for arbitrary line shape and of machine computation for a Lorentz line shape lead to a series of curves which may be used to correct observed widths under circumstances where the Lorentz shape may be verified and effects of finite modulation frequency may be ignored.

9380 CROSS RELAXATION IN RUBY by W. B. Mims and J.D. McGee (Bell Labs.); Phys. Rev., Vol. 119, pp. 1233-1237, Aug. 15, 1960

A pulsed microwave method used to study paramagnetic relaxation in synthetic ruby at Cr/Al concentrations from 0.02 per cent to 0.3 per cent, and over a wide range of fields and angles with respect to the crystal axis is described. The experimental frequency was 7.17 kmc. At settings for which one interval between energy levels was twice as large as another, decay traces with two characteristic periods were observed. The more rapid decay was independent of temperature, and is attributed to a cross-relaxation process involving three spins. Similar behavior became apparent at all concentrations whenever two intervals approached the same value. At 0.3 per cent, two period decay traces were observed for any arbitrary field and angle setting, indicating at this concentration, a general cross relaxation between the Zeeman levels in times of 0.3 millisecond and less.

9381 THEORY OF NUCLEAR RESONANCE INTENSITY IN DILUTE ALLOYS by W. Kohn and S. H. Vosko (Carnegie Inst. Tech.); Phys. Rev., Vol. 119, pp. 912-918, Aug. 1, 1960

Experiments of Bloembergen and Rowland have shown that the intensity of the nuclear resonance signal in metallic Cu decreases rapidly when small quantities of other elements are alloyed with it. These results require that each solute atom produces significant electric field gradients in its vicinity, sometimes affecting as many as 85 neighboring Cu nuclei. It is shown in this paper that field gradients of approximately the required magnitude arise from the redistribution of the conduction electron charge density near the solute atoms. A crucial feature of the theory presented is that at large distances r from a solute atom the electron density behaves as $\cos(2k^0r + \phi)/r^3$ where k^0 is the Fermi wave number and ϕ is a phase. The observed agreement with experiment is a confirmation of this behavior. Such an oscillatory behavior is a consequence of a discontinuous drop at the Fermi surface of n(K), the occupation probability of the conduction band function with wave vector K.

9382 NUCLEAR SPIN-LATTICE RELAXATION CAUSED BY PARAMAGNETIC IMPURITIES by W. E. Blumberg (U. California); Phys. Rev., Vol. 119, pp. 79-84, July 1, 1960

The behavior of the nuclear magnetization has been examined for the transient region immediately following saturation of the nuclear spin system in the case in which the nuclear relaxation is limited by spin diffusion to paramagnetic impurities. Relaxation effects in the absence of diffusion and the presence of rapid diffusion are described. An experiment is reported which substantiates the calculations for the case of diffusion-limited relaxation and, in addition, allows a determination of the correlation time of the magnetic moment of the paramagnetic ion and the coefficient of nuclear spin diffusion.

9383 NUCLEAR MAGNETIC RESONANCE IN COPPER ALLOYS. ELECTRON DISTRIBUTION AROUND SOLUTE ATOMS by T. J. Rowland (Union Car. Met.); Phys. Rev., Vol. 119, pp. 900-912, Aug. 1, 1960

The effects of the addition to copper of a wide variety of B sub-group elements on the NMR absorption of copper are described. The resonance amplitude, which undergoes a sharp reduction upon alloying, is of special interest; its dependence upon solute valence and size argues decisively in favor of conduction electron charge redistribution (valence effects) as the dominant source of the electric field gradients surrounding these solutes. Furthermore, these gradients are shown to decrease only about as $1/r^3$ rather than exponentially as had been supposed. Using the proportional change in the lattice parameter of the solid solution as a measure of the local strains surrounding a solute atom, only slight correlations between local strains and resonance amplitude were found. It is concluded that the origin of electric gradients around multivalent solutes in copper is almost purely an effect of conduction electron distribution and that this distribution is not of the exponentially screened Coulomb charge type. The spatially oscillating charge distribution derived and recognized by Friedel and recently elaborated by Kohn and Vosko and Friedel and co-workers satisfactorily explains the observations.

9384 NUCLEAR MAGNETIC RESONANCE IN $KMnF_3$ by R.G. Shulman and K. Knox (Bell Labs.); Phys. Rev., Vol. 119, pp. 94-101, July 1, 1960

The nuclear magnetic resonance of fluorine in $KMnF_3$ has been studied and hyperfine interactions between the fluorine nucleus and the magnetic electrons measured. The values are $A_s = (16.26 \pm 0.4) \times 10^{-4}$ cm^{-1} and $(A_\sigma - A_\pi) = (0.17 \pm 0.1) \times 10^{-4}$ cm^{-1}. These values correspond to $(0.52 \pm 0.02)\%$ 2s and $(0.18 \pm 0.1)\%$ 2p character for the unpaired electron. The implications of these results in terms of the σ and π bonding in this compound are discussed. By a comparison with hyperfine interactions measured in recent paramagnetic resonance studies of $KMgF_3:Mn^{2+}$ the amount of distortion in the mixed crystal is estimated. An antiferromagnetic transition is observed at 88.5°K.

9385 NUCLEAR MAGNETIC RESONANCE IN PARAMAGNETIC FeF_2 by J. W. Stout (U. Chicago) and R. G. Shulman (Bell Labs.); Phys. Rev., Vol. 118, pp. 1136-1141, June 1, 1960

Nuclear magnetic resonance of F^{19} in paramagnetic FeF_2 is discussed. The hyperfine interactions with the magnetic electrons have been measured and are shown to be important in determining the resonance properties. The isotropic hyperfine interaction indicates the presence of $(0.46 \pm 0.03)\%$ unpaired 2s spins in F^- orbitals from each Fe^{2+} ion neighbor.

NMR Studies of Dislocations in NaI and KI - See 9170

9386 PARAMAGNETIC RESONANCE AND OPTICAL SPECTRA OF DIVALENT IRON IN CUBIC FIELDS. Part II. EXPERIMENTAL RESULTS by W. Low and M. Weger (Hebrew U.); Phys. Rev., Vol. 118, pp. 1130-1136, June 1, 1960

Observations of the paramagnetic resonance absorption of Fe^{2+} in MgO at g = 3.428 and 6.86 are reported. The optical absorption line is found at 10,000 cm^{-1}. The paramagnetic resonance spectrum indicates considerable covalent bonding. The origin of the line at 6.86 is discussed. In tetrahedral ZnS a paramagnetic line is found at g = 2.25 and optical absorption at 3μ and 0.7μ. Possible explanations of this spectrum are discussed. A short discussion of the optical absorption spectra of trivalent iron in MgO is presented.

9387 THE ELECTRON PARAMAGNETIC RESONANCE OF Mn^{2+} IONS SURROUNDED BY AN OCTAHEDRON OF FLUORINE IONS by S. Ogawa (Hokkaido U.); J. Phys. Soc. Japan, Vol. 15, pp. 1475-1481, Aug. 1960

Measurements of the EPR of Mn^{2+} ions as dilute, substitutional impurities in the single crystals of $KMgF_3$, $KCdF_3$, K_2MgF_4 and $NaMgF_3$ are reported. An X-ray examination revealed that divalent metal ions in these crystals were surrounded by an octahedron of six fluorine ions. The F^{19} "super-hfs" superimposed on the usual hfs of Mn^{55} has been observed. The dependence of the F^{19} hf interaction constant (A_s) upon the Mn^{2+}-F^- distance has been noticed and discussed. The A_s in $KMnF_3$ has been estimated to be somewhat smaller than 16.7×10^{-4} cm^{-1}.

DIAMAGNETISM

Diamagnetic Susceptibility of Graphite - See 9215

GENERAL

88 OPTICAL PROPERTIES OF METALS by M. P. Givens . Rochester); Solid State Phys.-Adv. Res. and Appl., Vol. Academic Press, 1958, pp. 313-352

e two optical constants — index of refraction and absorption efficient — are defined and their relations to electrical nstants are derived. It is shown that the energy absorbed m the light wave is converted into heat and that classical lean heating accounts for the entire energy conversion. variety of attempts to predict the optical constants are dis- sed. Studies of the internal photoelectric effect and the molous skin effects are presented. Various experimental thods such as Drude's method and Schultz' method for asuring the optical constants are presented. Experimental ults for a few typical metals are given. Discrepancies ap- ared among the results obtained by various experimenters d it was determined that these were the result of differences sample preparation.

89 THEORY OF THE OPTICAL PROPERTIES OF IMPERFEC- ONS IN NONMETALS by D. L. Dexter (U. Rochester); lid State Phys.-Adv. Res. and Appl., Vol. 6, Academic ess, 1958, pp. 353-411

theoretical account of the current knowledge of optical operties in nonmetals is presented. Interaction of radiation th atomic systems embedded in a dielectric medium is dis- ssed. The oscillator strength, decay time, and integrated sorption coefficient are obtained with (1) one-electron ap- oximation, (2) Born-Oppenheimer approximation, (3) Con- n approximation, and (4) the narrow band approximation by ing phenomenological parameters of the crystal, the index refraction and the "effected field." Two extreme cases are ated in detail with considerable simplification. One is the tremely diffuse, spread-out center, the other is the extreme- well-localized center. Several special topics regarding the tical properties, such as the anisotropy effects, effects of locations, colloidal particles, reflection and excitation ectra, and nonradiative transitions are discussed.

90 ELECTRONIC SPECTRA OF MOLECULES AND IONS IN YSTALS. Part I. MOLECULAR CRYSTALS by D. S. McClure CA Labs.); Solid State Phys.-Adv. Res. and Appl., Vol. 8, ademic Press, 1959, pp. 1-47

eoretical and experimental studies of the electronic spectra molecules are given. The theory has been developed to a hit necessary for the interpretation of spectra and for the rivation of useful empirical constants from the spectra. The in emphasis is on the group theoretical considerations and the approximate magnitudes of the numbers to be expected. ough experimental data are included for the purpose of il- trating the kinds of results that can be obtained. A fairly mplete survey of the literature has been made. A simplest del, namely a lattice of fixed molecules, is used to ex- ain the principal observation. The energy levels, polariza- n properties, and transition probabilities in the crystal are nd. The effects of molecular vibrations and lattice vibra- ns are examined. Some data suggest that "trapped" or eforming" excitons may exist in molecular crystals. Fluores- nce spectra of molecules are also discussed. It is pointed that attempts to interpret the factor group splitting as well other features of the spectra have led to a detailed under- standing of the energy transfer mechanism and have revealed several unsuspected problems.

9391 ELECTRONIC SPECTRA OF MOLECULES AND IONS IN CRYSTALS. Part II. SPECTRA OF IONS IN CRYSTALS by D. S. McClure (RCA Labs.); Solid State Phys.-Adv. Res. and Appl., Vol. 9, Academic Press, 1959, pp. 399-525

The theory of crystal field spectra is discussed. Calculations of charge distribution and energy levels are presented. Energy levels for many electron systems are also considered. Weak, strong, and intermediate crystal fields are discussed. The effect of spin-orbit coupling is investigated. The selection rules for transitions of various multiple orders between the component states are determined. The distinction between electric and magnetic transition processes is discussed and a semiempirical and descriptive method for the interpretation of the spectra of ions in crystals is described.

9392 THE ELECTRONIC SPECTRA OF AROMATIC MOLECULAR CRYSTALS by H. C. Wolf (Phys. Inst. Tech. Hoch., Stuttgart); Solid State Phys.-Adv. Res. and Appl., Vol. 9, Academic Press, 1959, pp. 1-81

A brief survey of the spectra of organic molecules, particularly those of the aromatic type, is given. The II electrons of the rings are responsible for the essential form of the spectra. In the region where the electron excitation spectra are observed, their intensities can be described in terms of two selection rules: (1) In the allowed transitions the totally symmetrical molecular vibrations are excited most intensely. (2) Forbidden transitions can be made "allowed" as a result of the presence of vibrations which are not totally symmetric. Experimental investigation of the spectra of aromatic molecular crystals is presented. The methods developed to undertake the quantitative measurements of absorption, fluorescence, and reflection spectra are described and the results are discussed for several types of organic molecular crystals. The theory of spectra of molecular crystals is presented and a comparison with experiments is made.

ABSORPTION (TRANSMISSION)

9393 THE EFFECT OF PRESSURE ON THE ABSORPTION SPECTRA OF ALKALI HALIDE PHOSPHORS by R. A. Eppler and H. G. Drickamer (U. Illinois); J. Phys. Chem. Solids, Vol. 15, pp. 112-118, Aug. 1960

Measurements of the effect of pressure (over 150,000 atm) on the spectra of twenty-six alkali halide phosphors, including nine doped with Tl^+, two doped with In^+, twelve doped with Pb^{2+}, two doped with Cu^{2+} andone doped with Bi^{3+} are reported. ν_{max} for the Tl^+ doped phosphors depends very strongly on the crystal structure and very little, if any, on the halide ion involved, which is consistent with the Seitz model. The In^+ doped phosphors behave like the Tl^+ analogs. For the Pb^{2+} phosphors, the shift of ν_{max} depends very strongly on the halide ion, and only incidentally on the lattice structure. This is consistent with the complex model.

9394 EFFECT OF PRESSURE ON THE SPECTRA OF OLIVINE AND GARNET by A. S. Balchan and H. G. Drickamer (U. Illinois); J. Appl. Phys., Vol. 30, pp. 1446-1447, Sept. 1959

Measurements of the effect of pressure on the absorption of olivine and on the Fe^{++} peak of garnet to over 150,000 atm

are reported. The absorption edge of olivine shifts red by about 9 per cent of the gap in this pressure range. The Fe^{++} peak in garnet shifts to higher energies by 700 cm^{-1} in 170,000 atm, due to increased splitting of the d levels by the ligand field. This is consistent with previous experimental work on transition metals, and with available theory. The temperature coefficient of the absorption edge of olivine was also measured at atmospheric pressure to 327°C. It exhibited a linear red shift of 4.21×10^{-4} ev/°C over this range.

Effect of a Magnetic Field on the Absorption of CdS - See 9413

9395 TEMPERATURE DEPENDENCE OF OPTICAL BLEACHING OF KCl CRYSTALS NEAR 0°C by W. E. Bron and A.S. Nowick (IBM); Phys. Rev., Vol. 119, pp. 114-121, July 1, 1960

Further insight has been sought into the mechanism of optical bleaching in the vicinity of room temperature by studying the temperature dependence of the bleaching curves for KCl crystals which had been initially irradiated by hard (filtered) X-rays. The absorption at the maxima of the F, M, R_1 and R_2 bands were observed to change during illumination with F-light and to be strongly temperature dependent in the range of -30° to +10°C, whereas the absorption at the V_3 band was essentially unchanged. For comparison an analysis was made of the data of Petroff on the early growth of the M band during bleaching with F-light in additively colored KCl crystals. In this case a unique activation energy, ϵ, of 0.35 ± 0.05 ev and a number of defect jumps $N_j \approx 10^{10}$ are indicated by the data. It appears that the bleaching curves of the X-irradiated samples are composed of a temperature independent and a temperature dependent part. The temperature dependent part probably is the same as that responsible for bleaching in additively colored crystals. The above results for ϵ and N_j suggest that the temperature dependent bleaching process results from the trapping of photoelectrons at vacancy clusters which are formed during bleaching through the migration of mobile defects, possibly vacancy pairs. This conclusion is supported by the observations by others that the a band is not observed during bleaching at room temperature.

9396 BREADTH OF THE F BAND IN NaCl by A. M. Karo (Lawrence Radiation Lab.), C. W. McCombie (U. Aberdeen) and A. M. Murray (The University, Sheffield); Phys. Rev., Vol. 119, pp. 504-507, July 15, 1960

The breadth of the F band in NaCl is calculated for various temperatures, primarily in order to investigate the status of the semiempirical configuration coordinate treatment of such problems. The main new feature of the calculation, which involves no adjustable parameters, is the use of the realistic normal modes employed in the Born-Blackman theory of specific heats. The eigenvectors as well as the eigenfrequencies of these modes are used. Modifications of the modes due to the missing ion at the F center are ignored. The coupling to the F center is determined from electrostatic forces on individual ions. Simpson's F center wave functions are used and the calculated breadths are all about 85 per cent of the experimental values. It is found that the main contributions to the breadth come from modes in a fairly small range of frequencies (much lower than the frequencies of the longitudinal optical modes considered in previous calculations) which includes the empirical configuration coordinate frequency. This last result helps to clarify the relation of the hypothetical configuration coordinate mode to the actual modes of lattice vibration.

9397 DICHROISM OF Z BANDS by M. Ishiguro, E. Sugioka, and N. Takeuchi (Osaka U.); J. Phys. Soc. Japan, Vol. 15, pp. 1302-1307, July 1960

The dichroic properties of Z bands and their correlation to that of the F band in NaCl:Sr and KCl:Sr single crystals are discussed. From an experiment on anisotropic bleaching, the Z_1 center was found to be a center of high symmetry in agreement with the result of paramagnetic resonance experiment. The Z_2 band showed dichroism when irradiated with [010] polarized light in the Z_2 or F band at room temperature, accompanying the dichrosim of opposite sign in the F band. This is another example of the correlation in dichrosim between two absorption bands as shown in the F-M system which has been found by Van Doorn and Haven. It is, however, questionable to simply decide the symmetry of the Z_2 center from the dichroism mentioned above, because in the case of KCl:Sr its peak position is shifted to shorter wavelength than the normal Z_2 band.

9398 FINE STRUCTURE IN THE OPTICAL ABSORPTION EDGE OF ANISOTROPIC CRYSTALS by J. J. Hopfield (Bell Labs.); J. Phys. Chem. Solids, Vol. 15, pp. 97-107, Aug. 1960

The group theory of weakly bound direct excitons is developed without explicit use of effective mass theory. For the usual case in which the direct band gap occurs at a point of high symmetry, direct exciton wave functions can be expanded in one-electron wave functions which have the symmetry of this point. The expansion is the k-space analog to the expansion of a tightly bound exciton envelope wave function in real space. A quasi-cubic model of the valence band structure for hexagonal ZnO, CdS and ZnS is developed. The model, in conjunction with the group theory of weakly bound excitons, explains on a semi-quantitative basis most of the observed exciton fine structure in ZnO and CdS. A theorem which aids in constructing higher order "Kubic Harmonics" (for any point group) is given in an appendix.

9399 EXCITONS AND THE ABSORPTION EDGE OF CADMIUM SULFIDE by D. G. Thomas, J. J. Hopfield and M. Powell (Bell Labs.); Phys. Rev., Vol. 119, pp. 570-574, July 15, 1960

Measurements of the absorption coefficient between 10 and 300 cm^{-1} of CdS crystals in polarized light between 20° and 300°K, at wavelengths near 5000 Z are reported. Analysis of the results at various temperatures near 70°K shows that the absorption is in agreement with that calculated for a process involving the simultaneous creation of an exciton and the absorption of a phonon, both particles having a small wave vector. This agreement is strong evidence that the conduction band minimum and the valence band maximum in CdS both occur at the center of the Brillouin zone.

9400 INFRARED ABSORPTION AND VALENCE BAND IN INDIUM ANTIMONIDE by G. W. Gobeli and H. Y. Fan (Purdue U.); Phys. Rev., Vol. 119, pp. 613-620, July 15, 1960

Infrared absorption measurements made at near liquid helium temperature in n- and p-type degenerate samples of InSb with various carrier concentrations are reported. The absorption in p-type samples, at photon energies larger than the energy gap, depends on the hole concentration. The results show that the valence band is warped and that the energy at k = 0 is very close to the maximum energy of the band. A step in the absorption of n-type samples which gives an estimate of ~0.012m for the effective mass of light holes is observed. The long wavelength absorption in p-type samples is characteristic of intervalence band transitions.

401 INFRARED ABSORPTION BY ONE-DIMENSIONAL ONIC LATTICES by H.B. Rosenstock (U.S. Naval Res. Lab.); . Phys. Chem. Solids, Vol. 15, pp. 50-53, Aug. 1960

he absorption spectrum due to the atomic motion in a one-imensional ionic lattice, considered to consist of point parti-es of equal mass and alternating charge with coulomb inter-ction and nearest-neighbor repulsion, is found to consist of a ine of shape $[-\ln(\omega_{max} - \omega)]^{1/2}/(\omega_{max} - \omega)^{3/2}$.

402 INFRARED ABSORPTION OF DEFECTS IN QUARTZ by . L. Wood (Bell Labs.); J. Phys. Chem. Solids, Vol. 13, pp. 26-336, June 1960

everal sharp absorption bands in the infrared spectrum of crys-alline α-quartz between 3200 cm^{-1} and 3655 cm^{-1} have been ssigned to defects in the lattice. Defects containing water ay cause a broad absorption through this region of the spec-rum in very imperfect parts of certain crystals, but they do ot contribute to the sharp bands observed. One band at 581 cm^{-1} is probably due to the OH stretching vibration of proton defect, but the other peaks are not. Treatments of the rystal involving X-irradiation, heat bleaching, annealing or eating in an electric field strongly affect the intensities of he bands observed, and it is concluded that the bands origi-ate in color centers with an electronic origin. Probably ore than one type of center is involved. No correlation ith the visible color centers of smoky quartz or amethyst is bserved Interstitial foreign atoms play an important role in he formation of the infrared centers but vacancies or intersti-ial Si or O atoms are probably not involved. Although much nformation relating to the infrared color centers is available, he full details of their structure are not yet known.

403 OPTICAL ABSORPTION IN IRRADIATED QUARTZ AND USED SILICA by C. M. Nelson and J. H. Crawford, Jr. Oak Ridge Natl. Lab.); J. Phys. Chem. Solids, Vol. 13, pp. 96-305, June 1960

Optical absorption measurements made from 1850 to 26,000 A n crystalline quartz and fused silica after exposure to both ast neutrons in the reactor and Co^{60} γ-rays are reported. The rominent band near 2150 A is produced by γ-rays and neutrons n fused silica but fast neutron exposures in excess of 5×10^{18} m^{-2} are necessary to cause appreciable development of the orresponding band in crystalline quartz. With shorter neutron xposures and γ-rays the absorption in quartz crystals is char-cterized by the broad visible bands and continuous absorption hich rises almost linearly toward shorter wavelength below 000 A. This continuous absorption probably corresponds to he long wavelength tail of one of the bands observed by Mit-hell and Paige in the vacuum ultraviolet region. These re-ults do not seem to agree with their interpretation of the ature of the 2200 A band in quartz. On annealing neutron-radiated quartz (5×10^8 neutrons/cm^2) at 250°C a new band t 2000 A develops. In fused silica, besides the 2150A band, he shoulder at 2400 A (resolved by appropriate optical bleach-ng as a band at 2570 A) which has previously been reported, as observed with both γ-rays and fast neutrons. The rates of oloration of quartz and fused silica as well as studies of opti-al and thermal bleaching are discussed In the fused materi-ls a mechanism of photolytic coloration which appears to be onsistent with observations provides a suitable model which based on the rupture of Si-O bonds with the formation of ee radicals as the principal product. These and other possi-le defects are discussed in the light of magnetic susceptibility nd electron spin resonance studies.

Absorption in MgO and ZnS - See 9386

Polaron Formation During Absorption of Light in Cu_2O - See 9236

9404 EXCITATION AND HIGH-TEMPERATURE ABSORPTION OF KCl:Tl by D. A. Patterson (U.S. Naval Res. Lab.); Phys. Rev., Vol. 119, pp. 962-967, Aug. 1, 1960

Absorption measurements made up to 560°C and excitation spectra for luminescence measured from liquid nitrogen temperature to 100°C on KCl crystals with a wide range of thalium concentrations are reported. These measurements, in conjunction with earlier work, lead to the conclusion that there are at least seven bands in KCl:Tl, three in the "A" band region and two each in the "B" and "C" band regions. The large shift from "C" band to "B" band at high temperatures which has been previously reported was not found here. It is noted that the addition of small amounts of Sr to KCl shifts the fundamental absorption edge to short wavelengths.

RADIATION AND LUMINESCENCE

9405 MECHANICALLY-EXCITED EMISSION IN CADMIUM SULFIDE by D. M. Warschauer and D. C. Reynolds (Wright-Patterson AFB); J. Phys. Chem. Solids, Vol. 13, pp. 251-256, June 1960

The phenomenon of radiative emission obtained by mechanical excitation of optically or thermally stimulated cadmium sulfide is described and discussed in terms of the recently proposed band structure of the material and the existence of trapping levels in the forbidden-gap region.

9406 TWO-STAGE OPTICAL EXCITATION IN SULFIDE PHOSPHORS by R. E. Halstead, E. F. Apple and J. S. Prener (GE); Phys. Rev. Lett., Vol. 2, pp. 420-421 (L), May 15, 1959

Optical evidence indicating that transitions take place in ZnS-type phosphors between the luminescent center and energy levels near or in both the conduction and valence bands and that there are impurity levels common to both types of transition is presented. Edge emission has been continuously produced at 80°K in CdS and ZnS phosphors by photons with energy less than the band gap energy. This process requires a two state excitation process with transitions which terminate in both the valence and conduction bands. The continuous generation of edge emission also requires an impurity configuration common to both transitions.

9407 A THEORY OF EDGE-EMISSION PHENOMENA IN CdS, ZnS, and ZnO by J. J. Hopfield (Bell Labs.); J. Phys. Chem. Solids, Vol. 10, pp. 110-119, July 1959

Tentative symmetry assignments of p valence bands and s conduction bands made for ZnO and CdS on the basis of a tight-binding model are discussed. The six-fold degenerate p-bands are split in hexagonal crystals into a four-fold degenerate and a two-fold degenerate band. The four-fold degeneracy is split by spin-orbit coupling. The polarization of recombination radiation depends upon which band the hole belongs to, and is almost independent of the recombination mechanism. The polarization of the edge emission should be strongly temperature-dependent. Quantitative agreement is obtained between the predictions of this band model for CdS and the edge emission polarization experiments of Dutton. It is shown that the spectra of edge emission cannot be reasonably explained without the introduction of impurities or surfaces to absorb

crystal momentum. In CdS, recombination from a shallow trap seems necessary to explain the large coupling to the lattice apparent in the observed emission spectrum. The edge emission spectrum should approximate a Poisson distribution for recombination from a trap. The mean number of emitted phonons is a measure of the radius of the trapped carrier wave function.

9408 DISPLACEMENT OF THE SULFUR ATOM IN CdS BY ELECTRON BOMBARDMENT by B. A. Kulp and R. H. Kelley (Wright Air Dev. Ctr.); J. Appl. Phys., Vol. 31, pp. 1057-1061, June 1960

The measurement of the threshold for displacement of the sulfur atom from a lattice point in CdS at 8.7 ev is reported. This has been accomplished with 115-kev electrons which is also the threshold for the production of green edge emission centers and of centers for a red fluorescence band with a maximum intensity at about 7200 A. In crystals which show edge emission before bombardment, the edge emission is removed by electron bombardment in the energy range 2.5 to 200 kev. The red luminescence is not removed by electron bombardment but increases in intensity with bombardment above the threshold. The radiation "annealing" of the edge emission is accomplished even in crystals which do not anneal thermally. A model is proposed with the sulfur interstitial atom the center for edge emission, and the sulfur vacancy the center for the red emission band.

9409 ELECTROLUMINESCENCE by W. W. Piper and F. E. Williams (GE Res. Labs.); Solid State Phys.-Adv. Res. and Appl., Vol. 6, Academic Press, 1958, pp. 96-173

The basic mechanism of electroluminescence and the interpretation of electroluminescent phenomena observed in different materials are discussed. Three distinct steps in the conversion of electrical energy into visible or near visible radiation are: (1) excitation of the crystal to an energy at least several electron volts above the ground state; (2) transport of the excitation energy through the crystal to a region where de-excitation can occur with appreciable radiative probability; and (3) radiative de-excitation. This process may involve localized states of impurity systems or interband transitions.

9410 AVALANCHE ELECTROLUMINESCENCE IN CdS SINGLE CRYSTAL by M. Kikuchi and S. Iizima (Electrotech. Lab., Tokyo); J. Phys. Soc. Japan, Vol. 14, p. 852 (L), June 1959

Electroluminescence observed in forward biased CdS diodes is discussed. The diodes are constructed with a rectifying silver paste electrode and an ohmic evaporated In layer. A linear relationship was found between the current through the cell and the light intensity. As the voltage was increased to a critical value between 25 and 50 v, the current increased rapidly and light was emitted from the periphery of the junction. It is believed that avalanche breakdown occurs in the bulk of the crystal at the critical forward voltage and the light emission is due to the recombination of the electrons and holes generated by the avalanche process.

9411 THE ELECTROLUMINESCENCE OF ZnS-Cu SINGLE CRYSTALS EXCITED WITH PULSES OF ALTERNATING POLARITY by K. Patek (Czech. Acad. Sci.); Czech. J. Phys., Vol. 10B, No. 6, pp. 452-467, 1960

The brightness waves of electroluminescence of ZnS-Cu have been measured for the case of excitation with rectangular pulses as a function of the amplitude of the pulses and the temperature. A concrete model is proposed for electronic processes in barriers in ZnS crystals, the consequences of which for the decay of electroluminescence are in agreement with measurements.

9412 THERMODYNAMIC LIMITATION ON THE CONVERSION OF HEAT INTO LIGHT by M. A. Weinstein (GE); J. Opt. Soc. Am., Vol. 50, pp. 597-602, June 1960

The problem of converting ambient heat into luminescence radiation is analyzed in terms of the thermodynamics of the electromagnetic field. The process is described in terms of the technical efficiency of a light source η, defined as the ratio of the power leaving the source in the form of luminescence radiation to the power supplied to the source in the form of work. For a source at the ambient temperature T, it is shown that the limitation imposed by thermodynamics is, in the ready state, $\eta \leq 1 + T/(T_f - T)$, where T_f is the ratio of the net rate at which the field carries energy away from the source to the net rate at which the field carries entropy away from the source as a result of the luminescence emission. Thus, $T/(T_f - T)$ is the maximum possible contribution of ambient heat to the technical efficiency of a light source. An explicit expression for T_f in terms of the ambient temperature and the spectral distribution of the luminescence emission is obtained and as an example, T_f is calculated for the green emission band of a typical ZnS phosphor.

9413 INFLUENCE OF A MAGNETIC FIELD ON THE BLUE FLUORESCENCE LINES AND ON THE ABSORPTION LINES OF CERTAIN PURE CADMIUM SULFIDE CRYSTALS AT A TEMPERATURE OF 4.2°K by E. F. Gross, E. Grillot, B. P. Zakharchenia and M. Bancie-Grillot; Optics and Spectrosc., Vol. 6, pp. 462-463, May 1959

The effect of a magnetic field on the low temperature fluorescence and absorption lines of CdS crystals grown by sublimation in a high temperature gradient is discussed. When the crystal is placed with its optical axis perpendicular to the magnetic field, splitting is observed in the fluorescence lines at λ = 4870, 4868, and at 4861 A. The spacings between the doublet components are, respectively, 0.58, 0.8, and 1.2-1.3 A. The components of these doublets are polarized perpendicular to the optical axis of the crystal. When the crystal is placed with its optical axis parallel to the magnetic field, no Zeeman splitting is observed in these fluorescence lines. A diamagnetic shift is not observed in the Zeeman splitting.

9414 FLUORESCENCE OF SOME ACTIVATED ZnS PHOSPHORS by W. van Gool, A. P. Cleiren and H. J. M. Heijligen (Philips); Philips Res. Rep., Vol. 15, pp. 254-274, June 1960

Properties of several series of ZnS phosphors prepared in H_2S atmosphere at 1150-1200°C are discussed. Activators used were Ag, Cu, Au and co-activators were Al, Sc, Ga, In. Phosphors were made with all combinations of activators and coactivators with one concentration. In other phosphors equal concentrations of selected pairs of activators and coactivators were studied at different levels. Some special series of phosphors were made in addition, and spectral distributions of all phosphors at room temperature and at -196°C are reported. The spectral distributions can be separated into parts of low and high photon energy. The high-energy parts can be attributed to the presence of the activators. The low-energy parts are of a composite structure. Part of these bands is due to an associate center of activator and coactivator. Other parts of the low-energy bands may be due to other centers which could not be identified unambiguously.

15 SELF-ACTIVATED AND Cu-ACTIVATED FLUORES-NCE OF ZnS by W. van Gool and A. P. Cleiren (Philips); ilips Res. Rep., Vol. 15, pp. 238-253, June 1960

o series of experiments on the fluorescence of ZnS are de-ibed. The first, of which only a review of the experimental ults is given, presents some additional data on the theory of S activated with Cu, made some years ago by Kröger and -workers. In the second series a limited number of phosphors ve been studied in order to settle a few questions. In partic-ar, the difference between the blue Cu emission and the ue self-activated emission of ZnS has been studied. Further-re, the temperature dependence of the fluorescence bands d the influence of the coactivator on both mentioned fluores-nces and the green copper fluorescence were determined. The ults can be interpreted by assuming that the low-temperature orescence is dependent on the coactivator. The room-tem-rature emission bands can have a composite character, in ch a way that in addition to the low-temperature emission nd another band may be important. The results are to some tent uncertain, due to experimental difficulties. These have en discussed and it is stressed that further careful experimen-work may be more important for knowledge of the ZnS orescence than detailed calculations about some special del.

16 EXCITATION SPECTRA OF VANADIUM-ACTIVATED NC AND CADMIUM SULPHIDE AND SELENIDE PHOS-IORS by G. Meuer and M. Avinor (Philips); Philips Res. p., Vol. 15, pp. 225-237, June 1960

citation spectra for the 2μ fluorescence band of vanadium tivated zinc and cadmium sulphide and selenide phosphors e reported. The emission was excited by absorption in two mposite bands due to vanadium at 1.1 and 1.6 ev, by ab-rption in an auxiliary impurity center, such as Cu or Ag, if esent, and by fundamental excitation.

17 SYMMETRY OF THE GREEN PHOSPHORESCENCE OF AT PRETREATED COLORED KCl CRYSTALS by A. Halperin d N. Lewis (Hebrew U.); Phys. Rev., Vol. 119, pp. 510-5, July 15, 1960

e effect of thermal pretreatment in the open air (at 700°C) the phosphorescence of KCl is discussed. After coloring at uid-air temperature the phosphorescence turned from violet green. While the former phosphorescence showed no ani-ropy, the green was found to become partially polarized er irradiation with [011] light. The irradiation also induced chroic absorption at 3650 A. Both the polarization in the osphorescence and dichroic absorption persisted up to nearly 0°K. The polarized light bleached the component of the 50 A absorption parallel to it, but enhanced the green phos-orescence with the main effect on the perpendicular compo-nt. It is suggested that oxygen which diffused into the crys-during the heat treatment is responsible for the asymmetric nter.

18 ENERGY-LEVEL POSITIONS OF SILVER LUMINESCENT NTERS IN SULFIDES by C.C. Klick (U.S. Naval Res. Lab.); ys. Rev. Lett., Vol. 2, pp. 418-420 (L), May 15, 1959

investigation of the energy levels introduced in CdS by ver is discussed. The CdS:Ag phosphor was cooled to 77°K d irradiated with 3650 A light. The sample was then irradi-ed with light of about 10,000 A and the emission was ob-served. Radiation at 7200 A was detected, indicating that the impurity levels introduced by silver lie near the conduction band. Since van Gool has found that emission bands change wavelength smoothly in solid solutions from CdS:Ag to ZnS:Ag, the 3900 A emission and 4500 emission in ZnS:Ag are also due to levels near the conduction band.

9419 EXCITON-INDUCED LUMINESCENT IN KI/Tl by M. Tomura and Y. Kaifu (Osaka City U.); J. Phys. Soc. Japan, Vol. 15, pp. 1295-1302, July 1960

Emissions from Tl^+ ion and a certain impurity under excitation of light in the first characteristic absorption band of KI have been observed in a single crystal of KI/Tl. These exciton-induced luminescences were measured at various temperatures for specimens of several concentrations of Tl^+ ion. The intensities of the exciton-induced luminescences attained saturated values at about liquid oxygen temperature. In consideration of the amount of energy transferred to the impurity, the saturated intensities of the exciton-induced luminescence from Tl^+ ion are almost independent of the concentration of Tl^+ ion in the range of $10^{15} \sim 10^{19}/cm^3$ and show a quantum efficiency as high as 30 per cent. Therefore the migration of an exciton through the crystal has been confirmed.

9420 SCINTILLATION PROPERTIES OF $CaWO_4$ AND $CdWO_4$ CRYSTALS by G. B. Beard, W. H. Kelly and M. L. Mallory (Michigan State U.); Bull. Am. Phys. Soc., Ser. II, Vol. 5, p. 373 (A), June 15, 1960

Because of their high densities and high Z's, $CaWO_4$ and $CdWO_4$ crystals have relatively high photoefficiencies with the disadvantage of a long decay time which renders them poor for high counting rate experiments. The effect of temperature on the scintillation efficiencies and decay times of these crystals has been studied to see if a more favorable operating temperature could be found. By using a Lucite light piper and a 6292 photomultiplier, the scintillation decay times were found to be 3.3μsec for the $CaWO_4$ and 2.9μsec for the $CdWO_4$ for both Po^{210} alphas and Cs^{137} γ rays at room temperature. The value for $CaWO_4$ agrees well with the results of Kallman and Brucker. Both decay times were found to increase by about 20 per cent when the crystals were cooled to liquid air temperature and to decrease by a factor of approximately 3 when warmed to 100°C. The apparent scintillation efficiencies, as determined from the relative pulse heights at the output of a cathode follower, were found to vary inversely with temperature. Preliminary measurements show the variations may not be monotonic. Curves were presented and the results were discussed.

PHOTOELECTRONIC PROPERTIES

9421 ELECTRICAL MEASUREMENTS ON PHOTOGRAPHIC EMULSION GRAINS. Part I. DARK CONDUCTIVITY by J. F. Hamilton and L. E. Brady (Kodak); J. Appl. Phys., Vol. 30, pp. 1893-1901, Dec. 1959

Measurements of ionic conduction on large AgBr grains from a photographic emulsion, obtained by exposure to light flashes delayed by short time intervals after the application of electric field pulses, are reported. Values of conductivity were obtained by an analysis of the transient decay of internal field pulses resulting from the application of known pulses of the external field. The internal field was measured by means of its effect in causing displacement of latent-image centers formed by the exposure flashes. The room-temperature ionic

conductance of these grains was found to be the equivalent of about $9 \times 10^{-6}\ \Omega^{-1}cm^{-1}$ with an activation energy of about 0.42 ev. This conductance is several powers of ten higher than that reported for large AgBr crystals of high purity and is thought to be primarily the result of surface effects. The implications of this result in terms of modern theories of photographic latent-image formation are discussed.

9422 ELECTRICAL MEASUREMENTS OF PHOTOGRAPHIC EMULSION GRAINS. Part II. PHOTOELECTRONIC CARRIERS by J. F. Hamiton and L. E. Brady (Kodak); J. Appl. Phys., Vol. 30, pp. 1902-1913, Dec. 1959

Pulses of electric field applied to AgBr grains of a photographic emulsion at short time intervals after the application of short light flashes cause displacement of photoelectrons and holes if their lifetimes are greater than the delay interval. The asymmetry in the location of the photoproducts - microscopically visible silver and bromine or developable latent-image specks - is an indication of the fraction of carriers free at the time the electric field is applied. As the delay interval is varied, the decay of the number of free carriers may be followed. In the emulsion system studied, the number of photoelectrons was found to decay approximately according to a $1/(1 + \alpha t)$ law, falling to half the initial value in 0.25μsec. The lack of a dependence on intensity or temperature is taken to indicate temporary trapping in a distribution of shallow traps, perhaps at the grain surface. The number of free holes decays by an exponential law, with a mean lifetime of about 15 μsec. Indications are that hole mobility is very low, owing either to temporary trapping or self-trapping. The implications of these results in terms of modern theories of latent-image formation are discussed.

9423 EXCITON-INDUCED PHOTOCONDUCTIVITY IN Cu_2O by J. H. Apfel and A. M. Portis (U. California); J. Phys. Chem. Solids, Vol. 15, pp. 33-38, Aug. 1960

Structure observed in the photoconductivity spectrum of Cu_2O which corresponds to the "yellow" exciton series observed in optical absorption is discussed. From the fact that the photoconductivity in the exciton peaks is initially stimulated by illumination and then quenched, it is concluded that distinct electronic processes are associated with the exciton-induced photoconductivity. The most likely mechanism is excitation of localized carriers by excitons. The experimental evidence is insufficient to establish that the excitons are mobile. A comparison of dc and microwave conductivity measurements of Cu_2O establishes that the conductivity is limited by barriers.

9424 PHOTOCONDUCTIVITY IN GERMANIUM by R. Newman and W. W. Tyler (GE Res. Labs.); Solid State Phys.-Adv. Res. and Appl., Vol. 8, Academic Press, 1959, pp. 49-107

A brief general review of the theory of the band structure and impurity levels, and a concise discussion of the theory of photoconductivity in Ge is presented. Three component processes are considered: (1) the generation of carriers as a result of the absorption of energy, (2) the motion of the carriers under the applied electric field, and (3) the return of the system to the unexcited state. Details of experimental studies of photoconductivity are presented. Steady state extrinsic and intrinsic properties processes, transient processes, and other complex effects such as quenching phenomenon and superlinear responses are discussed. A brief qualitative discussion of the utility of Ge as an infrared detector is given. It is mentioned that Ge is being studied both as an intrinsic or an extrinsic detector. Because of the long wavelength response possible, impurity photoconduction is given the most attention.

9425 PHOTOCONDUCTIVITY IN Cu_2O by F. L. Weichman (U. Alberta); Bull. Am. Phys. Soc., Ser. II, Vol. 5, p. 373 (A), June 15, 1960

Photoconductivity and thermoelectric effects have been measured on thin plates of multicrystalline Cu_2O mounted between two copper rods in a vacuum container. The apparatus also made it possible to detect the change in thermoelectric effect when light was incident on the Cu_2O plate. The photoconductive response as a function of incident wavelength was measured at a chopping frequency of 40 cycles per sec. The response curves obtained in this fashion at room temperature were found to be independent of the vacuum conditions. However, for a given sample the thermoelectric effects, resistance, and the time constants associated with the photoconductivity were found to be strongly influenced by the atmosphere surrounding the sample. A sample out-gassed at 10^{-5} mm Hg at 150°C had a resistance of $2 \times 10^{7}\ \Omega$ and rise times of 1×10^{-3} and 1.4×10^{-3} sec in the visible (600 mμ) and infrared (800 mμ), respectively. The thermoelectric effect is still that of a hole conductor and is enhanced upon illumination. Subsequent outgassing at 150°C at 10^{-5} mm Hg returned the sample to its original state of higher resistance and longer time constants.

9426 THE SURFACE PHOTOVOLTAIC EFFECT IN SILICON AND ITS APPLICATION TO THE MEASUREMENT OF THE LIFETIME OF MINORITY CARRIERS [in French] by A. Quilliet and P. Gosar (Lab. Magnétisme Phys. Solide); J. Phys. Radium, Vol. 21, pp. 575-578, July 1960

An experimental verification of a photovoltaic relation predicted by theory is reported. At each wavelength, the surface photovoltaic effect is proportional to $KL/(1 + KL)$, where K is the corresponding absorption coefficient, and L the diffusion length of minority carriers in the sample. Since the relation is valid in a small wavelength range, values of the minority carrier lifetime could be determined; they were in good agreement with the results given by the method of Valdes.

9427 ELECTRICAL PROPERTIES OF HYDROGEN ADSORBED ON SILICON by J. Eisinger (Bell Labs.); J. Chem. Phys., Vol. 30, pp. 927-930, Apr. 1959

The change in photoelectric threshold which accompanies the adsorption of atomic hydrogen on a silicon surface is discussed. Measurements have been made on a sample cut from a single crystal with its face parallel to the (111) plane. It is found that the photoelectric threshold increases from 4.72 ev for an uncovered surface at room temperature to 5.07 ± 0.02 ev when approximately 8×10^{14} hydrogen atoms are adsorbed per cm^2 Si surface. This corresponds to an effective dipole moment of a hydrogen atom adsorbed on silicon of $\mu = 0.15 \times 10^{-18}$ esu.

9428 SPECTRAL DISTRIBUTION OF THE PHOTOMAGNETOELECTRIC EFFECT IN Ge: EXPERIMENT by F. A. Brand, N. Baker and H. Mette (USASRDL); Phys. Rev., Vol. 119, pp. 922-925, Aug. 1, 1960

A study of the photomagnetoelectric effect in Ge as a function of the wavelength of incident radiation in the region from 0.7 to 2.0 microns is discussed. The dependence of both photoconductivity and photomagnetoelectric (PME) response has been measured in various samples, using front and back surface recombination velocities and bulk recombination as parameters.

OTOELECTRONIC PROPERTIES (Cont'd)

as been found that under certain conditions of bulk and face recombination a reversal in sign for the PME response urs over the frequency range studied. Sign reversals ob- at wavelengths in the range from 1.55 to 1.85 microns, esponding to partial optical transparency. The exact quencies at which reversal occurs depend on the surface and k recombination rates, the condition being that the Dember ld be zero corresponding to equal carrier concentrations on front and back surfaces. Furthermore, the present observa- ns are shown to be in good qualitative agreement with the oretical work reported by Gärtner. Experimental procedures described, and it is shown how this effect can be used to vantage in the study of surface recombination velocities in ous environments.

29 OPTICAL PROPERTIES OF GALLIUM-SUBSTITUTED ADOLINIUM IRON GARNETS by J. E. Jacobs, T. H. tenberg and F. E. Williams (GE Res. Labs.); Bull. Am. s. Soc., Ser. II, Vol. 5, p. 357 (A), June 15, 1960

investigation of the optical absorption and the Faraday ro- ion of gallium-substituted gadolinium iron garnets $3Gd_2O_3 \cdot a_2O_3 \cdot (5-x)\,Fe_2O_3$ was reported. Both the absorption and rotation decrease, as expected, with increasing substitu- n of gallium for the iron. Throughout the eavelength range 5000 to 10,000 A the absorption coefficients decrease ex- nentially with gallium substitution and are reduced by a tor of ten at x = 3. There is also a small shift of the 6000 the 9000 A absorption bands to longer wavelengths. For llium substitution with x > 1, Faraday rotation has been ob- ved only below room temperature. The applied magnetic ld required to orient the magnetic domains increases with llium substitution. The interpretation of these data, partic- rly as regards the contributions to absorption and rotation of tetrahedral and octahedral iron ions, and the evaluation of se materials for light valves based on the Faraday rotation, re discussed.

flectance Spectra of CdS - See 9250

THERMAL PROPERTIES

w Temperature Heat Capacity Expressions - See 9210

at Capacity of $MgNi_2$ - See 9374

ecific Heat of Alkali Halides - See 9218

30 THERMAL CONDUCTIVITY AND LATTICE VIBRATION- MODES by P. G. Klemens (Natl. Stand. Lab., Australia); id State Phys.-Adv. Res. and Appl., Vol. 7, Academic ss, 1958, pp. 1-98

e theory of heat transport by lattice vibrations is presented. e Boltzmann equation governing the distribution of phonons et up and solved on the assumption that a relaxation time be defined. Three interaction processes are considered, ., scattering by static imperfections, interactions due to armonicities, and boundary scattering. Thermal conduc- ties of nonmetals are also discussed in detail. The size ect and the effect due to lattice imperfections on thermal nductivity are considered. Theories of thermal conductivi- s of metals, semiconductors, and alloys are presented. The ice thermal conductivity is small as a consequence of the electron-phonon scattering, so it is often overshadowed by the electronic thermal conductivity. In heavily-doped semiconductors, scattering of phonons by electrons in the impurity band is an important resistive mechanism. Not enough is known about the structure to make a comparison between theory and experimental results.

9431 NONLINEAR HEAT TRANSFER PROBLEM by P. L. Chambre (U. California); J. Appl. Phys., Vol. 30, pp. 1683-1688, Nov. 1959

Time-dependent heat conduction in a semi-infinite medium subject to a boundary condition which can involve the temperature in a nonlinear manner is discussed. A formulation for the determination of the surface temperature, which is often of greatest physical interest, leads to a nonlinear Volterra integral equation. A simple iterative solution method, with an accuracy suitable for many practical purposes, is presented. As an example, the problem of the time-dependent surface temperature of a body receiving heat according to the Stefan-Boltzmann law is treated. The analysis is also applicable to physical adsorption or chemisorption processes which occur at the boundary.

9432 PULSED MEASUREMENT OF THE VARIATION OF THERMAL CONDUCTIVITY OF GERMANIUM WITH TEMPERATURE by J. I. Pankove (RCA); Rev. Sci. Instr., Vol. 30, pp. 495-496, June 1959

A rapid technique for measuring the thermal conductivity of Ge over a wide temperature range is described. The lower end of a Ge cylinder is soldered to a Cu heat sink and the upper end of the cylinder is placed in contact with a carbon filament which is heated by a 3 sec current pulse. The temperature at points along the cylinder is measured at the end of the heating cycle. The relative thermal conductivity can then be determined from $k(T) = -\frac{\phi}{A}\left(\frac{dt}{dx}\right)$ where A is the cross-sectional area of the sample, ϕ is the heat flow along the sample, and $\left(\frac{dt}{dx}\right)$ is the temperature gradient along the sample. Absolute thermal conductivity values can be determined by repeating the measurement with a sample consisting of Ge and Ni in series. Below 150°C thermal conductivity values which are in a reasonable agreement with other measurements have been obtained. At higher temperatures, values which are roughly 30 per cent lower than more refined measurements have been obtained.

Thermal Conductivity of KCl-KBr Solid Solutions - See 9270

9433 THERMAL CONDUCTIVITY OF EIGHT HALIDE CRYSTALS IN THE TEMPERATURE RANGE 220°K TO 390°K by K.A. McCarthy and S. S. Ballard (Tufts U.); J. Appl. Phys., Vol. 31, pp. 1410-1412, Aug. 1960

Measurements of the thermal conductivity of eight halide crystals over the temperature range 220° to 390°K are reported. The thermal conductivities of KBr, KCl, and NaCl vary inversely with temperature for the lower part of this temperature range, and are nearly independent of temperature for the higher temperatures of the range measured. The thermal conductivities of CsBr, CsI, and AgCl are nearly independent of temperature throughout the entire temperature range. The thermal conductivities of BaF_2 and CaF_2 vary more rapidly with temperature than anticipated from a T^{-1} relationship; however, the accuracy of the data is not sufficient to establish the exact form of the variation of thermal conductivity with temperature. The comparative method used for these measurements is described.

9434 THERMAL RESISTANCE DUE TO ISOTOPES AND OTHER POINT DEFECTS by P. G. Klemens (CSIRO); J. Phys. Chem. Solids, Vol. 8, pp. 345-347, Jan. 1959

In non-metallic crystals, including semiconductors, phonons are scattered by point defects, which thus contribute a thermal resistivity proportional to temperature. The isotopic mass variation can contribute significantly to this resistance. However, in those cases where measurements have been made, the observed point defect resistance is considerably higher than the theoretical isotope resistance. Experiments on isotopically enriched germanium and on copper-gold alloys seem to support the theory quantitatively, hence the discrepancy between the observed resistance and the isotope resistance is probably due to unknown point defects. In semiconductors they seem to have little effect on electrical conduction properties. An earlier suggestion that substitutional carbon may be responsible for the additional resistance in germanium was not confirmed experimentally.

9435 THERMAL CONDUCTIVITY OF CLEAR FUSED SILICA AT HIGH TEMPERATURES by K. L. Wray and T. J. Connolly (Avco); J. Appl. Phys., Vol. 30, pp. 1702-1705, Nov. 1959

Measurements of the thermal conductivity of clear fused silica over the temperature range 300°-2100°K, in conditions which minimized radiative energy transport, are given. This was a steady-state experiment involving the measurement of the electric current and voltage drop through a fine tungsten wire which was embedded along the axis of a cylindrical silica rod. The wire served both as a heating element and as a resistance thermometer. Thermal conductivities were calculated by graphical evaluation of the rate of change of electric power with temperature at different temperatures. The experiment yielded thermal conductivities between 2.6×10^{-3} and 2.9×10^{-3} cal/cm sec°K at room temperature, and between 4.5×10^{-3} and 5.5×10^{-3} cal/cm sec°K over the temperature range 1000°-2100°K.

9436 EXCITATION PROCESSES IN CERAMICS AND ANOMALOUS INCREASE IN THERMAL CONDUCTIVITY AT ELEVATED TEMPERATURES by D. H. Whitmore (Northwestern U.); J. Appl. Phys., Vol. 31, pp. 1109-1112, June 1960

The anomalous increase in the observed thermal conductivity of single-phase ceramics at high temperatures is discussed. At temperatures above the onset of this anomalous rise, account is taken of the possibility that phonon, electronic, and radiative heat transfer, as well as transport of thermal energy by electron-hole pairs, excitons, and dissociated gas molecules, may operate simultaneously and individually contribute significantly to the total heat flow. On the basis of reliable conductivity data on nonporous monocrystals of single-phase ceramics, estimates of the magnitudes of these high-temperature components are made which reveal that excited states of low excitation may occur in certain ceramics. In these instances, such excited energy-carrying states are able to diffuse down the temperature gradient in the specimen, thereby producing a non-negligible contribution to its observed thermal conductivity.

9437 STRAIN-INDUCED CHANGES IN THE SEEBECK COEFFICIENT OF n-TYPE GERMANIUM by J. R. Drabble and R.D. Groves (GE Ltd.); Phys. Rev. Lett., Vol. 2, pp. 451-452, June 1, 1959

Strain-induced changes in the Seebeck coefficient of oriented specimens of n-type Ge measured at 82° and 95.5°K are discussed. Large changes parallel to the applied stress were observed on [111] and [110] oriented specimens. Negligible changes were found in [100] specimens. These results indica that the changes are caused only by strain-induced changes i the carrier populations of the different valleys. The theory underlying the measurements is discussed. The ratio of the components of the phonon-drag Seebeck tensor for a single valley $Q_{P,\parallel}/Q_{P,\perp}$ has been found to be 9.6 ± 0.3 at 82°K and 9.5 ± 0.5 at 95.5°K. These values agree with the valu obtained by Herring et al. from an analysis of thermomagneti effects.

9438 EFFECT OF UNIFORM COMPRESSION ON THE ETTIN SHAUSEN-NERNST EFFECT IN ZINC AT LOW TEMPERATUR by K. S. Balain, C. G. Grenier and J. M. Reynolds (Louisi ana State U.); Phys. Rev., Vol. 119, pp. 935-938, Aug. 1 1960

The influence of hydrostatic pressure on the oscillatory Etting shausen-Nernst effect in a Zn single crystal has been studied in magnetic fields ranging from 2 to 11 kilogauss at 4.2°K. With the field along the hexagonal axis, the long period osci lations decrease in period by 5 per cent as the pressure is in creased from 300 to 2300 psi There is an average increase i amplitude of about 10 per cent for each 250-psi increase of pressure. There is no evidence of phase change with pressure

9439 THERMOMAGNETIC GENERATOR by J. F. Elliott (G J. Appl. Phys., Vol. 30, pp. 1774-1777, Nov. 1959

Calculations of the power output and the efficiency of energy conversion of a thermomagnetic generator are presented. Par ticular attention is paid to the use of the ferromagnetic element Gd as a suggested material for a practical device for the generation of electrical power from a low grade heat source (i.e., in the neighborhood of 20°C).

Thermomagnetic Properties of Zn - See 9296

9440 THERMAL EXPANSION COEFFICIENTS OF BISMUTH E. F. Cave and L. V. Holroyd (U. Missouri); J. Appl. Phys. Vol. 31, pp. 1357-1358, Aug. 1960

Measurements of the linear thermal expansion coefficients of the a and c axes of Bi from 80° to 540°K by mechanical mean and by single crystal powder X-ray methods are reported. Th mechanical and X-ray values did not differ significantly. Th expansion coefficient for the c axis was found to be 16.6 ± 0.4×10^{-6} $(C°)^{-1}$ at 100°K, 17.3 ± 0.2×10^{-6} $(C°)^{-1}$ at 150°K, and 17.6 ± 0.2×10^{-6} $(C°)^{-1}$ at 540°K. For the a axis the expansion coefficient was 10.8 ± 0.3×10^{-6} $(C°)^{-1}$ at 100°K, 11.6 ± 0.2×10^{-6} $(C°)^{-1}$ at 150°K, and 11.8 ± 0.2×10^{-6} $(C°)^{-1}$ at 540°K.

9441 THERMAL PROPERTIES OF GRAPHITE, MOLYBDENUM AND TANTALUM TO THEIR DESTRUCTION TEMPERATURES N. S. Rasor and J. D. McClelland (NA Aviation); J. Phys. Chem. Solids, Vol. 15, pp. 17-26, Aug. 1960

Measurements of the thermal expansion, specific heat and thermal conductivity from 1000°C to near the destruction tem perature of Mo (m.p. 2620°C), Ta (m.p. 3000°C) and four types of graphite (sublimes at 3650°C) are reported. The ther mal expansion data for the materials investigated show no grossly unusual features except those due to impurity evolutio The specific heat of the metals, particularly that of molybde num, appreciably exceeds the Dulong-Petit value. However

their thermal conductivities follow closely the Lorenz (Wiedemann-Franz) relation for free electrons. At intermediate temperatures (1000-2800°C) the thermal conductivity and specific heat of graphite show no unusual features. At higher temperatures, however, large and rapid increases in specific heat and thermal resistivity appear, which are consistent with the occurrence of thermally produced lattice defects, presumably vacant lattice sites. A defect concentration of about 0.5 atomic per cent at the sublimation temperature, and a formation energy in the vicinity of 7.7 ev, are indicated.

MECHANICAL PROPERTIES

9442 THE ELASTIC CONSTANTS OF CRYSTALS by H. B. Huntington (Renssalaer Polytech. Inst.); Solid State Phys.-Adv. Res. and Appl., Vol. 7, Academic Press, 1958, pp. 213-351

Elasticity and its associated definitions are discussed. Stresses, strains, and elastic constants are introduced in the notation of Voigt and Love. The current theoretical approaches to elastic constants are considered from two different points of attack, one based on a generalized force model, the other based on attempts to evaluate elastic constants from the fundamental considerations of quantum mechanics. The interrelationship of elastic constants and other physical quantities, and the methods of measurements are presented. Elastic properties and their theoretical interpretation in terms of atomic models are discussed. For the most part, interest has been focused on single crystals. A brief account of results for polycrystalline materials is included. The dependence of the elastic constants on temperature and pressure is presented for a variety of materials. The theory of the thermal variation of elastic constants is developed from the standpoint of the idealized equation of state. Two particular low-temperature effects are discussed, one associated with the superconducting transition and the other with electron damping.

9443 AN ALTERNATIVE TRANSFORMATION FOR THE ELASTIC AND PIEZOELECTRIC CONSTANTS OF ANISOTROPIC MEDIA by R. Bechmann (USASRDL); Acta Cryst., Vol. 13, Part 2, pp. 110-113, Feb. 1960

A new coordinate transformation for the tensors which represent the elastic and piezoelectric constants of anisotropic media is presented. General Christoffel moduli $\Gamma_t^{(p)}$ (t = 1...6) are introduced for the transformation of the elastic stiffnesses and general piezoelectric moduli $E_i^{(p)}$ (i = 1, 2, 3) for the transformation of the piezoelectric stress constants (in all cases p = 1...6). Other forms for these transformations are known, particularly by using general tensor relations. However, this new form is considered as particularly simple.

9444 PRESSURE VARIATION OF THE ELASTIC CONSTANTS OF SODIUM by W. B. Daniels (Case Inst.); Phys. Rev., Vol. 119, pp. 1246-1252, Aug. 15, 1960

The pressure variation of the single crystal elastic constants of Na has been measured using a modified ultrasonic pulse echo method. The values found for the pressure derivatives of the elastic constants are: $dC_{44}/dP = 1.63$, $dC'/dP = 0.226$, $dB_8/dP = 3.60$. The notation $C' = (C_{11}-C_{12})/2$ and $B_8 = (C_{11} + 2C_{12})/3$ has been used. The experimental observation that the elastic anisotropy ratio C/C' ($C = C_{44}$) does not depend on pressure indicates that one can positively neglect interaction of ion cores as a contribution to the elastic stiffness of Na. The results are interpreted in terms of Fuchs' theoretical calculation of the Coulomb contribution to the shear stiffness of the alkali metals. The interpretation indicates that as Na is compressed, the value of the electronic wave function at the boundaries of the atomic polyhedra increases more rapidly than $\Omega^{-1/2}$, where Ω is the volume of the atomic polyhedron. An expression for the volume variation of the value of the wave function of the lowest electronic state at the boundaries of the atomic polyhedra is given.

9445 PHOTOELASTIC CONSTANTS OF VITREOUS SILICA AND ITS ELASTIC COEFFICIENT OF REFRACTIVE INDEX by W. Primak (Argonne Natl. Lab.) and D. Post (U. Illinois); J. Appl. Phys., Vol. 30, pp. 779-788, May 1959

Measurements of the photoelastic constants and their dispersion for visible light for two samples of vitreous silica, Corning and Herasil No. 1, are given. The results for the Hg green line, 546 mμ, are 4.22×10^{-13} $(d/cm^2)^{-1}$ (ordinary ray) and 3.56×10^{-13} $(d/cm^2)^{-1}$ (extraordinary ray). From the ratio of Poisson's ratio to Young's modulus 0.216×10^{-12} $(d/cm^2)^{-1}$ and Young's modulus 0.76×10^{12} (d/cm^2), the pressure coefficient of refractive index 0.909×10^{-12} $(d/cm^2)^{-1}$ and the elasticity volume coefficient of refractive index $VdN/dV = 0.34$ are calculated. Comparison of these results with those reported for other glasses indicate that the oxygen ions of vitreous silica are more deformable than the oxygen ions of other siliceous glasses. In vitreous silica about 1/3 of the volume change accompanying the elastic dilatation arises from the dilatation of the oxygen ions.

9446 ELASTIC CONSTANTS OF CADMIUM FROM 4.2°K TO 300°K by C. W. Garland and J. Silverman (MIT); Phys. Rev., Vol. 119, pp. 1218-1222, Aug. 15, 1960

Measurements of the adiabatic elastic constants of Cd single crystals by an ultrasonic pulse technique are reported. The values extrapolated to 0°K are: $c_{11} = 13.08$, $c_{33} = 5.737$, $c_{44} = 2.449$, $c_{12} = 4.048$, $c_{13} = 4.145$ in units of 10^{11} dynes/cm^2. A debye characteristic temperature, θ_0, of 213° ± 1°K has been calculated from these 0°K elastic constants. The temperature dependence of the linear compressibilities, $K_\parallel$ and $K_\perp$, has also been calculated.

9447 ELASTIC CONSTANTS OF SINGLE-CRYSTAL ALUMINUM ANTIMONIDE by D. I. Bolef and M. Menes (Westinghouse); J. Appl. Phys., Vol. 31, pp. 1426-1430, Aug. 1960

Measurements of the adiabatic elastic constants of single-crystal AlSb made at 27°C, by the ultrasonic cw resonance technique are reported. The values of the elastic stiffness constants, in units of 10^{11}d/cm^2, are: $c_{11} = 8.939$, $c_{12} = 4.427$, and $c_{44} = 4.155$. A theoretical density of 4.36 g/cc was used. The values of c_{11} and c_{44} for single crystal GaSb obtained by the cw resonance technique are compared with previous values obtained by pulse-echo techniques.

9448 MEASUREMENT OF ELASTIC CONSTANTS OF RbBr, RbI, CsBr AND CsI BY AN ULTRASONIC CW RESONANCE TECHNIQUE by D. I. Bolef and M. Menes (Westinghouse); J. Appl. Phys., Vol. 31, pp. 1010-1017, June 1960

An ultrasonic cw resonance technique for the measurement of the velocity of sound in solids is described. The end correc-

tion due to the presence of the transducer and coupling film can be calculated from consideration of a transmission-line equivalent circuit. An experimental comparison is made of the cw and two pulse techniques over the frequency range 5 to 45 Mc. Application of the cw resonance technique to the measurement of the room-temperature adiabatic elastic constants of single crystals of RbBr, RbI, CsBr, and CsI is described. A tabulation of the important elastic properties of these crystals is presented.

9449 TEMPERATURE DEPENDENCE OF YOUNG'S MODULUS OF VITREOUS GERMANIA AND SILICA by S. Spinner and G. W. Cleek (Natl. Bu. Stand.); J. Appl. Phys., Vol. 31, pp. 1407-1410, Aug. 1960

The temperature dependence of Young's modulus of vitreous GeO_2 has been determined by a dynamic resonance method from -195° to 540°C. The modulus increases with increasing temperature from about -120° to 400°C. Below and above this range the modulus decreases with increasing temperature. Young's modulus for vitreous SiO_2 also increases from about -190° to 1175°C and decreases with increasing temperature outside this range. In view of the similarity in structures and bond energies of these two materials, the similarity in the elastic modulus-temperature relations is believed to be significant; especially when contrasted with the lack of agreement in another commonly measured anharmonic property, thermal expansion.

9450 THE ANELASTICITY OF NATURAL AND SYNTHETIC QUARTZ AT LOW TEMPERATURES by J. C. King; J. Phys. Chem. Solids, Vol. 13, p. 352 (A), June 1960

Certain imperfections in alpha-quartz that introduce anelastic absorption at low temperatures in crystal resonators are discussed. For a shear wave of 5 mc, absorption peaks are observed at approximately 20° and 50°K in unirradiated samples. X-irradiation effects a lowering of the amplitude of the 50°K absorption, while a new absorption is introduced at 100°K. The results of acoustic absorption measurements on a number of selected samples of synthetic quartz resonators suggest that, whereas the 50°K absorption is attributable to excess oxygen, the 100°K defect involves Al which is present substitutionally in the crystal structure. X-irradiation-induced lowering of the resonant frequency of crystal resonators is clearly the result of a lowering of the elastic modulus associated with the 100°K anelastic absorption.

9451 ULTRASONIC ABSORPTION AND ROTATIONAL DISPERSION IN YIG-CRYSTALS by H. Bommel and K. Dransfeld (Bell Labs.); Bull. Am. Phys. Soc., Ser. II, Vol. 5, p. 357 (A), June 15, 1960

When ultrasonic shear waves were passed through a thin disk of yttrium iron garnet, magnetized in the hard direction with a field around ferromagnetic resonance, a strong acoustic absorption was observed. The high field side of this absorption line is smooth and reproducible. At the low field side, however, the line shape is most irregular, varying from sample to sample. This irregularity is probably caused by nonuniform acoustic bonds between driver-quartz, sample, and receiver-quartz, leading to a nonuniform excitation of magnetostatic modes at lower fields than the uniform precession. A considerable rotation of the plane of polarization for ultrasonic shear waves propagating through the YIG crystal has also been found. For example, at 300 Mc/sec and at room temperature the plane of polarization was turned by about 45 deg in a disk only 0.010 in thick, at magnetic fields close to the main absorption. Further experiments are in progress to investigate the impurity and temperature dependence of this interaction with the spin system.

9452 BEAM METHOD FOR THE MEASUREMENT OF INTERNAL FRICTION by J. E. Thompson (English Elect.); J. Sci. Instr., Vol. 37, pp. 208-210, June 1960

Measurements on the oscillatory motion of a swinging beam used to measure the internal friction of a Si-Fe strip are reported. This motion is complicated, and consists of a small amplitude, higher frequency oscillation superimposed on a main oscillation, so that difficulty arises in obtaining a unique value for the logarithmic decrement of the strip oscillation. Reasonable agreement is found between the experimental results and the theory developed.

Announcing the Availability of Bibliographic and Information Retrieval Services

Our highly experienced scientific abstracting staff, composed of people with substantial professional qualifications and representing many branches of the sciences, is ready to work with you in these areas.

For more detailed information, write a brief description of your problem or project and a member of our scientific staff will review it. Our reply will be prompt.

Write directly to:

Dr. Geoffrey Knight, Jr., President
Cambridge Communications Corporation
238 Main Street
Cambridge 42, Massachusetts

A

brasions, Surface Damage on III-V Compounds Due to 6983
bsorption,
Acoustic 6212
Infrared 7373, 7374, 7918
Measurement of Semiconductor Properties by Microwave 6452
Optical 6197
bsorption:
Centers in Rutile Single Crystals 6629
Coefficient of Phosphors 8876
Edge, Pressure Dependence of 8270
Edge:
of Anisotropic Crystals 9398
in CdSe 8866
in Semiconductors in a High Magnetic Field 7384
of SiC 8865
(Gases) by Vacuum Evaporated Magnetic Films 6149
Lines of Cr^{3+} in Ruby 7979
of Ni^{2+} and Co^{2+} in Cubic Symmetry 7379
by Phonon-Phonon Interaction, Acoustic 6212
Spectrum of Electron in One-Dimensional Deep Trap 7930
bsorption in:
Al, Millimeter Wave 6695
Alkali Halides 6197, 8244, 8858, 9393
AlSb, Infrared 8861
$BaTiO_3$ 8854
CdS 7383, 9399, 9413
CdS Type Crystals 8591
CdSe 8866
CdTe 8870
Cu_2O 8360, 8369, 8370
GaAs-GaP 7272
GaP, Infrared 8855
Ge 6180, 6451
Ge, Infrared 8864
Ge Films 6716
Group III-V Compound Semiconductors 7380
Halide Crystals, Infrared 8363
HgTe 8867
HgTe-CdTe 8867
InSb 7673
InSb, Infrared 9400
Ionic Crystals, Infrared 7382, 8366, 9401
KBr 8839, 8857
KCl 8839, 8856, 8857, 8859, 8868
KCl:Sr 9397
KCl:Tl 9404
LiF 8367, 8393
Metals 9388
Mg, Photon 7381
MgO 9386
Mn-ZnF_2 Crystals 7980
NaCl 8362, 8868, 9396
NaCl:Sr 9397
NaF 8868
Powder Phosphors 6188
Quartz 8364, 9403, 9450
Quartz, Infrared 9402
Si, Infrared 8862, 8863
SiC 8865
SnS 7273
Te 6178
Thallous Halides, Ultraviolet 8368
Wurtzite Structure Crystals 8365
YGaG 7978
ZnO 8361, 8612
ZnS 9386
bsorption-Emission Spectra 8876, 8877
ceptor:
Levels in:
Ge, Cu 7587
Si, γ-Irradiated 8237
Occupation Statistics, Dislocation 7914
ceptors and Donors in p-n Junctions, Statistical Fluctuations of 6744
cumulators Using Transistors and Magnetic Cores 7184
Acetal Resin, Solution-Grown Crystals of an 9188
Acoustic:
Absorption:
by Phonon-Phonon Interaction 6212
in Quartz 8364, 9450
in Yttrium Iron Garnet 6147
Attenuation in:
LiF and $CrK(SO_4)_2 \cdot 12H_2O$ 8940
TiO_2 8410
Modes in ZnO, Electron Scattering Due to 6403
Acoustical Firing Indicator 8105
Activation:
Energies in Semiconducting Compounds 7907
Energy:
of Diffusion, Evaluation of 8196
for Vacancy Formation in Pt 9167
of Oxide Coated Cathodes 6252
Activators, Atomic Wave Functions of 7925
Adders 6774, 6874, 6878, 6882, 7187, 7508, 7509, 7802, 9083, 9123
Adsorption on:
Alumina, Krypton 7582
Bi_2Te_3 Surfaces, Gas 6659
Ge:
Films, Oxygen 9192
Surfaces,
Gas 6368
Oxygen 8231
Ge-Aqueous Solution Reactions, Effects of 6369
Relaxation Processes in Ge, Effect of Ion 6128
Semiconductor Surfaces, Gas 6046
Si:
Films, Oxygen 9192
Surfaces, Oxygen 8230
Adsorption Techniques, Purification of Silicon Tetrachloride by 6017
Aggregation on the Magnetic Phase Transition of Evaporated Superconducting Thin Films, Influence of 6409
Aging of $BaTiO_3$ 7288
Aircraft:
Control, Wideband FM Receiver for Remote 6852
Crashes, Radio Beacon for Locating 6565
Generators,
Controlled Rectifier Regulator for 7516
Voltage-Regulating and Static-Excitation System for 7517
Alarm, Intruder 7215
Alkali:
Alloy Systems, NMR in 7972
Metal Azides, Color Centers Due to Radiation of 7234
Metal-Gallium Alloy as Dot Material 8979
Metals, Paramagnetic Susceptibility of an Electron Gas in 7356
Ozonates, Exchange Effects in 6445
Alkali Halide:
- See also
Dielectrics,
Ionic Crystal,
and Specific Alkali Halides
Color Centers,
Radiation Required to Produce 8179
Wave Functions of 8593
Phosphors, Crystal Structure and Spectra of 7989
Points and Filaments by Controlled Dissolution, Production of 6658
Alkali Halides 9225
Alkali Halides,
Absorption in 6197, 8244, 8858, 9393
Breakdown in 9229
Color Centers in: 7235, 7915
Ag Doped 7854
Coloration Mechanism at Low Temperatures in 6933
Cuprous Halide Films Formation on 7580
Dielectric:
Absorption in 8244
Properties of 9225
Excitons in 9248
Fluorescence in 8886
Fluorescence of F-Centers in 8380
Alkali Halides, (Cont'd)
Growth of High Purity 8618
Lattice:
Dynamics of 9217
Vibrations in 9218
Luminescence of 7983, 7989, 8375
Recombination Luminescence in 8375
Reflection of 8300
Solid Solutions of 7554
Specific Heat of 9218
Spin-Lattice Relaxation in 7967
Structure and Spectra of 7989
Thermal Conductivity of 9433
Ultrasonic Attenuation in 6480
Alkali Iodides, Photoemission and Valence Band Structure of 7320
Alkaline Earth:
Fluorides, Color Centers in 7059, 7060
Pyrophosphate Phosphors, Preparation of 6189
Alkalis, Wave Representation Energy Band Calculation for 7906
Alloy-Diffused Junction Transistors, Fabrication of 9001
Alloyed Junctions,
B-Se 8973
Fabrication of 8425, 8998, 8999
Alloying, Plastic Deformation of Ge by 6748
Alloying:
Processes of Si 7846
of Semiconductor Devices, Jig for 7711
Alloys - See also Specific Alloys, Intermetallic Compounds, etc.
Alloys,
Antiferromagnetism in Dilute 7961
Electron Probe X-Ray Microanalyzer Study of 7228
NMR Intensities in 7351
Specific Heat of Dilute 7998
Theory of the Electronic Properties of 7591
Thermal Conductivity of 8000, 8403
Thermoelectric Properties of 8459
Transition Metal Content in 8156
X-Ray Fluorescent Analysis of 8156
Alnico V Magnets, Effect of Heat Treatment on 9346
Alpha of Transistors, Circuit for Measurement of 8993
Alumina,
Adsorption of Krypton on Irradiated 7582
Anomalous Dielectric Loss in 6081
Dielectric Properties of 8678
Alumina:
- See also Aluminum Oxide, Corundum, Ruby
Ceramics,
Lattice Defects in 7553
Thermoluminescence in 7553
Alumina-Chromic Oxide Systems, Lattice Spacings and Distortion in 7850
Aluminum,
Absorption in Superconducting 6695
Critical Field of Superconducting 8283
Domain Distribution in Superconducting 6117
Energy:
Band Structure of 9208
Gap of Superconducting 6695, 6696
Nuclear Spin Relaxation in Superconducting 8843
Penetration Depth in Superconducting 6696
Photoresponse of 8905
Radiation Effects in 8651
Range of Electrons in 9200
Scattering Defects in 9197
Superconductivity in 6117, 6693, 6695, 6696, 8283, 8843
X-Ray Scattering from Cyclicly Stressed 9164
Zone Refining of 8194
Aluminum:
Capacitors, Printed 6807
Films,
Characteristic Energy Losses of Electrons in 6054
Electron Energy Dissipation in 6055

Aluminum: (Cont'd)
in Ni, Diffusion of 9181
in Si,
Precipitation of Impurity 8202
Solid Solubility of 6002
Aluminum Antimonide,
Absorption in 8861
Diffusion of Cu in 8624
Elastic Constants of 9447
Energy Gap of 6623
Growth of 6362
Impurity Levels in 6362
Junction Preparation by the Decomposition of 7419
Lattice Constant of 6623
Mobility in 6362
Aluminum Antimonide Junctions, Dendritic Inclusions in 8016
Aluminum Antimonide-Gallium Antimonide,
Preparation of 6361
Preparation and Properties of 6623
Aluminum Antimonide-Gallium Antimonide System, Solid Solution in the 6361
Aluminum Antimonide-Indium Antimonide System, Conductivity and Other Properties of 7938
Aluminum-Arsenic in Ge, Interaction between 6018
Aluminum Arsenide-Gallium Arsenide, Preparation of 6360
Aluminum Boride,
Electrical Properties of 6998
Energy Gap of 6998
Semiconducting Properties of 6998
Aluminum-Copper Alloy, Neutron Irradiation Damage in an 9198
Aluminum Garnets, Paramagnetic Resonance of Ytterbium in 6446
Aluminum Nitride, Synthesis of 6038
Aluminum Oxide:
- See Also Alumina, Corundum, Ruby
Aluminum Oxide,
ESR of V in α- 8351
Flash Etching Technique for Grain Boundaries in 8189
Large Zero Field Splittings of V^{3+} in 7359
Paramagnetic Resonance of:
Ni in 8846
Transition Metals in 8847
Aluminum Phosphide,
Electroluminescence of 7589
Photovoltaic Effect and Photoconductivity of 7589
Preparation of 6359, 7589
Aluminum Phosphide in ZnS, Solid Solubility of 8161
Aluminum Tantalide Inclusions in AlSb Junctions 8016
Aluminum-Zinc, Diffusion of Zn in 7859
Ammonium Cupric Tutton Salt, Spin-Spin Relaxation in 7659, 7660
Ammonium Halides, Proton Motions in 7585
Amorphous Solids, Energy Levels in 8657
Amplifier Gain Control 7127, 7128, 9060, 9061
Amplifiers,
Audio 9064, 9065
Avalanche 7409
Bandpass 7131, 7463
Bipolar 7748
Bridge 8496
Broadband 7742
Car-Radio 6854
Carrier 7095, 8111
Cascade 6260, 9062
Chopper 8059
Class B 8080, 9071
Computer Design of 8491
Cross Modulation in 7741
Current Gain in 8021
Data 7744
dc 6295, 6596, 6824, 7194, 7203
Dielectric 6042

Amplifiers, (Cont'd)
Differentiating 7749
Diode: 6223
Loaded Helix 8061
Distortion in 7129, 7741, 8488, 9063
Distributed 6825, 7141
Electro-Optical 7145
Feedback 8494
Feedback in 8489
Ferrite 6548
Ferroelectric 8074, 8075
Ferromagnetic 7476, 8072
Functional Unit 6776
Hall Effect 8450
Hearing Aid 9065
HF 6550, 7740, 8058
High Input Impedance 6263
Hybrid: Direct Coupled 7477
IF 8062, 8063
Input Impedance of 8078
Integrating 7749
Ion Current Measuring 8146
Light 6236, 8456
Linear 6254, 6835, 7744
Low Noise 6827
Lower Cut-Off Frequency of 7468
Magnetic 8497, 9070, 9140, 9141, 9142
Magnetic-Transistor 6262
Maser - See Masers, Lasers
Microwave 6513, 8061
Narrow-Band 8057
Negative:
Conductance 8076
Impedance: 7755
Repeater 7167
Mass 8452, 8499
Resistance 6823
Parametric 6226, 6245, 6259, 6544-6546, 6548, 6549, 6827-6832, 7081, 7133-7140, 7471, 7473-7476, 7698, 7751-7754, 7777, 7845, 8007, 8046, 8060, 8065-8069, 8071-8076, 8102, 8497, 8498, 9069, 9070
Power 7145, 7750, 7755, 8451
Pulse: 9067, 9068
Regenerator 7746, 7747
Pulse-Forming 7745
Push-Pull 6826, 7750, 8064
Reactance 6547
Recording-Pen 6834
Regenerative Pulse 7168
RF 6551, 7777, 9066
Shunt-Peaked 7142
Small-Signal 7467
Solid State 7743
Stability of Tuned 7132
Stabilization of the Gain of 8070
Stereo 6275
Synthesis of 6819
Tecnetron 8031
Telephone 7756
Temperature Compensated 8492, 8493
Theory of Two-Wire 8490
Thermal Stability of 7469
Thermistor 6295
Transfer Graphs for 7452
Transmission Line 8467
Travelling Wave 7474, 7752, 7753, 8066
Tunnel Diode 6261, 6550-6552, 6833, 7143, 7467, 7472, 7739, 8009, 8010, 8054, 8063, 8077, 8079, 8096
UHF 6825, 6833
Varactor 8070
Variable Reactance 6543
Video: 6258, 7130, 7470, 7785, 8106-8108
Current 7165
Wide Band 6552, 6570
Amplitude:
Corrective System for Transmission Lines 7789
Modulation Detectors 9089

Probability Density Functions, Measurement of 6604
Analog:
Calculation of Mathematical Functions 8140
Computer:
Amplifiers, Drift Correctors for 6596
Arithmetic Units 8548
Computers, Nonlinear Electronic Elements in 8547
to Digital:
Converters 8142, 8550
Encoders 8141
Transistors,
Gallium Arsenide 7431
Ion Drift Fabrication of 6753
Anemometer, Transistorized 8149
Anisotropic:
Anomalies in Ferromagnetic Resonance of Rare Earth Garnets 6437
Conduction: 8723
in Ge 8722
in Nonstoichiometric Rutile 7618
Conductivity in SnS 7273
Elastic Constants of CdS 8004
Ferromagnetic Resonance Linewidth in Ferrites 7650
Magnetization 7644
Segregation in Indium Antimonide 6319, 6320
Anisotropy, Oriented Ferrites with Cubic 9187
Anisotropy in:
Cubic Crystals, Ferromagnetic 6429
Evaporated:
Nickel-Iron Films, Angle-of-Incidence 6430
Permalloy Films 9355
Magnetite, Magnetocrystalline 9186
a Mn-Cr-Sb System, Exchange 6432
Thin:
Films, Mechanical Model for Uniaxial Magnetic 6702
Permalloy Films, Rotatable 7043
Anisotropy of:
Electrical Properties of:
CdSb 7285
ZnSb 7286
Evaporated Nickel Films, Magnetic 7041
the Intrinsic Domain Magnetization of a Ferromagnet 7645
Line Width, Effect of Surface Irregularities on 6436
Magnetization in:
$Co_xFe_{3-x}O_4$, Effect of Cation Vacancies on Uniaxial 8317
Ferromagnetics 9352
Oblique-Incidence Permalloy Films 7042
Photoconductivity in Pyrographite 7996
Surface Breakdown of Ge in Strong Fields 7633
the Susceptibility of NiF_2 6433
Annealing:
in Impure Metals, Theory of Vacancy 7240
on the Physical Properties of Alkali Halide Soli Solutions, Effect of 7554
Annealing of:
Electron Radiation Damage in Graphite 7583
Gamma Ray Damage in Ge 6056
Irradiated Al and Cu 8651
Oblique-Incidence Permalloy Films 7042
Quenched-In Vacancies in Pt 9167
Thin Solid Films, X-Ray Reflection Studies of 7871
Volume Expansion and Color Centers in X-Ray Irradiated LiF 7238
X-Ray:
Induced Surface Hardening in NaCl 8650
Radiation Damage in LiF, Low Temperature 8647
Anodic Oxide Films on Ge, Growth of 6346
Anodization of InSb 6347
Anthracene,
Carrier Production in 8262
Drift Mobility in 8262

Anthracene, (Cont'd)
Free Carrier Generation in Photoconducting 7927
Growth of 8219
Lifetime of Positrons in 7928
Antiferromagnetic:
α-Mn, Domains in 7036
CoF_2, Transition Temperature of 8820
CrN, Ordering in 9366
Cr_2O_3,
Magnetoelectric Effect in 8334
Transition Temperature of 8334
$FeCo_3$, Ordering in 9365
$FeVO_3$, Preparation and Properties of 8631
Ground State, Theory of 7032
Metals, Superconductivity in 8290
MnF_2,
Microwave Faraday Rotation in 6709
NMR in 8808
Transition Temperature of 8820
Mn-ZnF_2, Interaction Shift in 7980
NiO,
Crystallographic Measurements in 6707
Domains in 6707, 7035
Ordering in Stacking Fault 7963
Resonance in MnO, Infrared 7048
Structure Properties of Crystalline Compounds, Theory of 6137
Susceptibility at Moderate Magnetic Fields 7962
Antiferromagnetic-Paramagnetic:
Transition in $CoBr_2 \cdot 6H_2O$ 6708
Transitions in:
$CoCl_2$ 6148
$NiCl_2$ 6148
Antiferromagnetism,
Double Exchange Effects in Magnetic Crystals Exhibiting 8332
Theory of 6136, 7998, 8331, 9321
Antiferromagnetism in:
$CoBr_2 \cdot 6H_2O$ 6158
CrF_2 and $CrCl_2$, Neutron Diffraction Studies of 8821
Dilute Alloys 7961
Rare Earth-Iron Compounds 8822
Antiferromagnets, Properties of 7634
Antiferromagnets with Large Uniaxial Anisotropy, Sublattice Magnetization and Resonance Frequency of 7047
Antimony,
Chemical Analysis of 8615
Solubility of Si in 6001, 6002
Antimony in:
Ge, Diffusion of 6332
Ge, Valley-Orbit Splitting of 7003
Pb, Determination of 8192
Si, Solid Solubility of 6002
Antimony-Doped Ge, Spin Resonance Spectrum in 7663
Antimony-Sulfur-Bromine Compound, Photoconductivity of 8901
Antimony-Sulfur-Iodine Compound, Photoconductivity of 8901
Antimony Telluride,
Dislocations in 8598, 8603
Solid Solubilities of Indium Telluride and Thallium Telluride in 6003
Antimony Telluride Containing Group III Atoms, Electrical Properties of 6003
Antimony Telluride-Bismuth Telluride Alloys,
Solid Solutions of 7401
Thermoelectric Properties of 7401
Antimony Trisulfide, Photoelectric Measurements on 9257
Antimony Trisulfide-Bismuth Sulfide Films, Electric and Photoelectric Properties of 9224
Aqueous Solutions, Reaction of Ge with 6369
Arc-Image Furnace for Growth of Crystals 6044, 7265, 7266
Arithmetic Unit 7186, 7225, 8548
Arsenic,
Purification of 6356, 7271
Solubility of Ge in 6001
Arsenic:
Alloys, Thermoelectric Power of 8407
and Aluminum in Ge, Interaction between 6018
in Ge,
Diffusion of 6333, 7228
Diffusion Coefficient of 7568
into Vapor Grown Ge, Incorporation of 6641
Arsenic-Doped Ge, Preparation of 6344
Arsenic-Selenium Films, Photoelectric and Electrical Properties of 8387
Assembler for Microcircuits 7844
Atmosphere on Surface Recombination on Si, Influence of Ambient 6391
Atomic:
Radii in Semiconducting Compounds 7907
Scattering Factor of Ge 8242
Structure Distortion in Alumina-Chromic Oxide System 7850
Wave Functions of Activators 7925
Attenuators, Ferrite 9035
Attitude Control System for Space Exploration Rockets 6566
Audio:
Amplifiers 9064, 9065
Oscillators, Sub- 9074
Volume Compressors 6276
Auger:
Effect in Semiconductors 9254
Electron Ejection from Ge and Si by Noble Gas Ions 7631
Recombination in Semiconductors, Overlap Integrals for 8697
Autodyne Detector for Paramagnetic Resonance 7827
Automatic:
Frequency Control with Reactance Transistors 6836
Gain Control 6276, 8523, 8524, 9060, 9112
Sorter 8153
Automobile Radio Receivers 7779, 7780
Automotive:
Generator Regulators 9129
Ignition System 9106
Autopilot System for Missiles, Magnetic Shift Register 6853
Autopsy Techniques for Transistors and Relays 7432
Avalanche:
Breakdown, Theory of 8025
Breakdown:
in Junction Transistors 8439
in Si Junctions 6221, 6743
Voltages of Diffused Diodes 7417
Diode:
Amplifiers 7409
Telephone Repeater 7409
Effect in Si Three-Layer Diodes 7089
Mode Operation of Si Transistors 8436
Multiplication in Junctions 8967, 8968
Transistors, Current Build-Up in 7425
Avalanching Ge Junctions, Emission of Light from 7675, 7676, 7719

B

Backward Diodes 7633, 7838
Bandpass Filters, Solid-State Sampled-Data 6563
Bandwidth in Point Contact Diodes, Increasing 8950
Barium Complex System,
Ferrimagnetic Properties of 6160
Ferroelectric Properties of 6086
Structure of 6082
Barium Ferrite, Ferrimagnetic Linewidth of 8812
Barium Fluoride, Surface Energy of 6999
Barium Fluoride-Barium Titanate System, Phase Diagram of 8224
Barium-Lead Titanate:
Ceramic Ferroelectric Memory Cells 7193
Films, Preparation of Ferroelectric 6978
Barium Oxide-Titanium Dioxide-Phosphorus Pentoxide,
Fluorescence in the System 6318
Phase Relations of the System 6318
Phosphor Preparation in the System 6318
Barium Strontium Titanate,
Electrically Variable Delay Lines Using 7727
Temperature Dependence of Piezoresistivity in 8255
Barium Titanate,
Absorption in 8854
Aging of 7288
Barkhausen Pulses in 8683
Coercive Field of 8685
Conduction Processes in 7596
Conductivity of 8682
Crystal Symmetry of the Low Temperature Phase of 6084
Cubic-Hexagonal Transition in 7548
Dielectric:
Constant of 6674, 8684
Permeability of 9232
Properties of 8686-8688
Domain:
Patterns of 6084
Wall Motions in 6677, 8249, 8250, 9240
Growth of 6041, 7920, 8224
High Temperature Discharges in 7290
Hysteresis Loops of Polarized Polycrystalline 7601
Loss Tangent of 6674
Mechanical Properties of 8414
Motion of Domains in 6386, 7958
Ohmic Contacts to 8235
Paramagnetic Resonance of Transition Metals in 8847
Permittivity of 6076, 7920
Piezoelectric:
Properties of 6307
Resonance in 9246
Polarizability of 9237
Polymorphism of 7548
Resonance Quality Factor (Q) of 8248
Space Charge:
Fields in 8680
Limited Currents in 8681
Spiral Growth Layers on Crystals of 7876
Switching in 8251
Thermal Conduction in 7289
Thin Films of 6042
UHF Spectra of 7593
Barium Titanate Ceramic Transducers for Ultrasonic Delay Lines, Thickness-Shear Mode 6533
Barium Titanate-Barium Stannate Solid Solution, Phase Transition in 7599
Barium Titanate-Strontium Titanate Solid Solution, Growth and Properties of 8225
Barium Tungstenate, Thermal Electron Emission from 7630
Barium Zirconium Metaniobite, Ferroelectric Properties of 8252
Barkhausen:
Pulses in $BaTiO_3$ 8683
Steps, Rectangular Hysteresis Loop Ferrites with 6141
Bartlett-Brune Transformation in Degenerative Amplifiers and Oscillators 8490
Base:
Connection for Junction Transistors 6233
Transfer Characteristics 8995
Beam Switching Tubes, Drivers for 7495
Beryl, Paramagnetic Resonance and Optical Spectrum of Iron in 7667
Beryllium, Elastic Constants of 6210
Beryllium Superconducting Thin Films 8757
Beryllium Oxide Flagpole Whiskers 6045
Bias Networks for Transistors 7465
Biasing Transistors 6266
Bicrystals, Anisotropy of Carrier Transport in Semiconductor 6071
Bilateral Switches 8092
Binary:
Compounds, Energy Gaps of 7907
Counter, Magnetic Switch for 8119
Counter Using Transistors and Magnetic Cores 7184

Binary: (Cont'd)
Gates, Low Voltage 8508
Multivibrator Functional Unit 6309
Semiconductors 8653
Semiconductors, Stability Limits of 8168
System, Electrical Properties of Ag_2-Group VI 8734
Binding:
in CdTe 9206
in Diamond Crystals 9204
Energies 9205
of Hydrogen in Molecules and Crystals, Chemical 7585
Properties of LiH 7681
Binistor Ring Counters 7709
Binistors, Si n-p-n Tetrode 6613
Bismuth,
Chemical Analysis of 8615
Conductivity and Properties of 8727
Energy Band Structure of 7372
Hole Component of the Fermi Surface in 7910
Infrared Studies of 7372
Magneto-Plasmas in 7372
Optical Constants of 8907
Photoelectromagnetic Effect in 8391
Solubility of:
Ge in 6001
Si in 6001
Thermal Expansion of 9440
Bismuth:
Crystal Structure at Low Temperatures 8171
Crystals, Conduction in Thin 6383
Bismuth Platinum,
Crystal Structure of 8288
Thermal Expansion of 8288
Transition Temperature of 8288
Bismuth Selenide at High Temperatures, Electrical Properties of 8268
Bismuth Telluride,
Adsorption of Gases on Cleavage Surfaces of 6659
Diffusion of Cu into 7863
Dislocations in 8598, 8603
Effective Mass Parameters of 8397
Energy Band Structure of 8919
Faraday Rotation in 8397
Heat Capacity of 8914
Infrared Absorption in 8397
Ohmic Contacts to 8235
Radiation Effects in 7402, 7403
Solid Solubilities of Indium Telluride and Thallium Telluride in 6003
Thermal:
Conductivity of 8001
Diffusivity of 7688
Properties of 8919
Thermoelectric:
Power of 8925, 8926
Properties of 7687, 7919, 8927-8929
Thermo-Junctions of 8928
Bismuth Telluride:
Cleavage Surfaces, Bonding Properties of 6659
Containing Group III Atoms, Electrical Properties of 6003
Bismuth Telluride-Bismuth Selenide Solid Solution Alloys, Lattice Constants of 7551
Bismuth Telluride-Selenide, Electrical Properties of 7919
Bistable:
Counting Circuit, Magnetic Core 8123
Switching Circuits 8451, 8506, 9083
Bleaching of Color Centers in KCl 7555
Bloch:
Wall Energy Density of Magnetoplumbite 7957
Walls in Si-Fe, Energy and Orientation of 8325
Blocking Oscillator: 6304, 7149, 7758
Discriminator 7532
Bolometers, Thermistor 7721, 7722
Bombardment:
Conductivity in Rhombic Sulfur 6113
Effects in Tunnel Diodes 7083
Bond Structure of ZnS Structure Crystals 8654
Bonding Scheme:
for CdI_2-Type Compounds 8169
of ZnSb, Atomic 8589
Boron,
Oxide Masking of SiO_2 against Diffusion of 6329
Preparation of 8226
Boron:
from Boron Carbide, Preparation of 6355
in Si, 6013, 7563
Diffusion of 6637, 8621
for Silicon Oxide, Affinity of 6335
in Steel, Detection of 7563
Boron-Aluminum Alloys 8973
Boron Carbide, Preparation of Boron from 6355
Boron-Lithium Ions in Si, Relaxation Process for Recombination of 7867
Boron Nitride,
Crystal Potential of 6066
Energy Band Structure of 6066, 7281
Boron Nitride Electroluminescent Devices 6235
Boron Phosphide,
Electroless Contacts to 6666
Semiconducting Properties of Cubic 8732
Boron-Silicon Alloyed Junctions 8973
Bragg Reflections:
from Polygrain Metals 8592
in Scattering, Double 9157, 9163-9165
in Single Crystals, Theory of Double 9161
Brass, Radiation Enhanced Diffusion in 7861
Breakdown, Effect of Statistical Fluctuations of Donors and Acceptors on 6744
Breakdown:
Avalanches in Ge, Optical Radiation from 7675, 7676, 7719
Characteristics of Si p-Sp-n Rectifiers 8015
Dendrites on LiF Cleavage Faces, Dielectric 7255, 7256
Point in Transistors, Bias Methods to Increase 6266
Strength of KCl 6998
Breakdown in:
CdS at Low Temperatures 6112
Dielectrics, Theory of 7594
Diffused Silicon Junctions, Localized 6495
Nonpolar Semiconductors, Internal 7315
Porous Ceramics 9228
Semiconductors, Circuit Protection Employing 8443
Silicon Rectifiers, Effect of Surface Angle on 7416
Transistors, Avalanche 8439
Uniform Silicon p-n Junctions, Broad Area 6745
Breakthrough Junction Diodes 6490
Bridge:
Amplifiers, Magnetic 8496
Clamp for Millivolt Signals, Diode 6845
Bridgman Method,
Growth of:
GaAs by the Horizontal 7253
HgSe-HgTe by 6931
of Single Crystal Growth, Horizontal Modification of 7878
Brittleness, Effect of Atmospheric Conditions on 9201
Brittleness of NaCl Crystals, Environmental Effects on the 7695
Broadband Nonreciprocal Transmitters 8041
Bromine on Se, Effects of 7828
Buffers, Solid State 6774
Burnout of Crystal Diodes 7699

C

Cadmium,
Elastic Constants of 9446
Photoresponse of 8905
Solubility of Ge in 6001
Cadmium:
Doping in InAs 7878
Layers, Electrical Conductivity of 7392
Cadmium in:
AgBr, Diffusion of 6639
AgBr-CdBr Solid Solutions, Diffusion of 6639
AgCl, Diffusion of 6950
GaAs, Diffusion of 8623
Ge, Diffusion of 7569
Cadmium Antimonide,
Anisotropy of Electrical Properties of Single Crystal 7285
Cyclotron Resonance Absorption in 8768
Dissociation Pressure and Heat of Dissociation of 8159
Preparation of 7285
Cadmium Arsenide,
Electrical Properties of 7027
Hall Field in 6121
Cadmium Arsenides, Solid-Vapor Equilibria for 8582
Cadmium Indium Telluride,
Optical Properties of 6198
Purification and Crystal Growth of 6015
Cadmium Iodide-Type Compounds, Bonding Scheme for 8169
Cadmium Oxide-Manganese Oxide-Ferric Oxide, Switching Properties of 9351
Cadmium Selenide,
Absorption Edge in 8866
Emission of 8891
Mechanism for Electrical Conduction in 8276
Optical Properties of 7396
Cadmium Selenide Radiation Detectors, Fabrication of 9023
Cadmium Sulfide,
Absorption in 6197, 7383, 8365, 9399, 9413
Absorption Edge in 9398
Breakdown in 6112
Conductivity in 6112, 7310
Contact Noise in 9309
Contacts Applied by Diffusion to 6667
Current Noise in 6095
Debye Temperature of 8400
Dielectric Susceptibility of 9231
Dislocations in 6011
Distribution of Electrons in 7005
Edge Emission in 8873, 9406, 9407
Elastic Constants of Hexagonal 8004
Electric Field Induced Light Absorption in 6450
Electrical Properties of 6133
Electroluminescence in 8376
Electron Paramagnetic Resonance of Eu in 7058
Emission in 9405
Energy:
Levels of Ag Luminescent Centers in 9418
Model for Edge Emission in 7385
Transport in 6192
Etch Pits in 8182
Excitons in 7604, 8850, 9250
Fluctuations in 6192, 6419
Fluorescence in 8887, 8888, 9150, 9413, 941
Fluorescence Polarization in 6456
Growth of 6961, 6962, 6967, 7880, 8213, 8214
Intensity in 7824
Lattice Vibrations in 9231
Luminescence in 9408
Luminescence Polarization in 6455
Magnetoresistance of 8767
Photoconductivity in 6192, 7391
Photosensitive Ultrasonic Attenuation in 8942
Photovoltaic Effects in 6470, 8388
Piezoelectric Constants of 8257
Piezoelectric Scattering in 8693
Preparation of 8388
Production of Dislocation Etch Pits on 7855
Recombination Centers in 6419
Reflectance Spectra of 9150
Space Charge Limited Currents in 8681
Surface Noise in 7951
Surface Recombination in 9261
Transparent Contacts to 6667, 6780
Trapping Noise in 7319

dmium Sulfide, (Cont'd)
Traps in 6095, 6419, 7802
Traps to Noise Relation in 7022
dmium Sulfide:
Detectors in Crystal Counters 6967
Diodes, Electroluminescence in 9410
as an Infrared Optical Material 6474
Photoconducting Films 7393, 8384
Photoconductor Storage Light Intensifier Display Panel 7718
Photovoltaic:
Cells, Photoemission in 6721
Solar Energy Converters 6519
Powder Cells, Photoconductivity in 7069
and Selenide Phosphors, Vanadium Activated 6461
Type Crystals, Photoelectric Analysis of Imperfections and Properties of 8591
dmium Sulfide-Electrolyte Interface, Photovoltaic Effects at a 6720
dmium Sulfide-Mercury Sulfide, Preparation of Solid Solutions of 6030
dmium Sulfide:Mn, Paramagnetic Resonance Absorption in 8356
dmium Sulfide-Selenide, Photoconductive Spectral Response of Cu-Activated 8385
dmium Sulfide-Selenide:
Photoconductive Device, Fabrication of 9028
Photosensitive Cells, Fabrication of 9024
dmium Sulfide-Zinc Sulfide Mixed Crystals, Photoconductivity of 8899
dmium Telluride,
Absorption in 8870
Binding in 9206
Decay Times of X-Ray Excited Carriers in 6684
Hall Properties of 8764
Latent Heat of Fusion of 6317
Optical Properties of 8764
Refractive Index of 9206
Spin Resonance of Mn^{2+} in 8771
dmium Telluride:
Junctions, Quantum Efficiency of 7717
Layers, Photoelectric Properties of 7392
in PbTe and SnTe, Solid Solutions of 7231
dmium Telluride-Mercuric Telluride Alloys, Solid Solution in 6624
dmium Telluride:Mn, Paramagnetic Resonance Absorption in 8356
dmium Telluride-Zinc Telluride Alloys, Solid Solution in 6624
dmium-Tellurium, Phase Diagram for 6317
dmium Tin Arsenide, Properties of 6108
dmium Tin Arsenide by Directional Freezing, Preparation of 6108
dmium Tungstate, Scintillation Properties of 9420
lcium in NaCl, Measurement of Concentration of 8244
lcium Carbonate, Surface Energy of 6999
lcium Chloride Impurity in KCl Crystals, Vacancy Association with 7868
lcium Fluoride,
Coloration of 7059
Maser Action from U^{3+} Ions in 7669
Paramagnetic and Optical Spectra of Yb^{3+} in 7976
Paramagnetic Resonance of 8832
Surface Energy of 6999
lcium Fluoride at Low Temperatures, Specific Heat and Elastic Constants of 6475
lcium-Iron-Oxygen Compounds, Ferrimagnetic 7651
lcium Orthosilicate Phosphors, Tin-Activated 6464
lcium Sulfide:Cu, Eu Electroluminescent Phosphors of 6462
lcium Tungstate,
Paramagnetic Resonance of Mn^{2+} and Gd^{3+} in 8353

Calcium Tungstate, (Cont'd)
Scintillation Properties of 9420
Spin Echo Experiments in Cerium and Erbium Doped 7668
Calcium Tungstate Containing Paramagnetic Ions, Growth of 8222
Cameras,
Power Supply for Television 7821
Transistor Television 6863
Capacitance:
Diodes, Fabrication of High-Power Nonlinear 8959
Intruder Alarm 7215
Capacitor Storage Element 8128
Capacitors,
$BaTiO_3$ 6042
Evaporated Ge-Ta Film 9051
Printed Al 6807
SiN Thin Film Dielectric 6366
Storage Circuits Employing Ferroelectric 8545
Thiourea Ferroelectric 6531
Capacitors with Semiconductor Electrolyte, Tantalum 6922
Capture Cross Sections in Si and Ge 7804
Carbon:
Films,
Electron Energy Dissipation in 6055
Preparation of Unsupported 7269
in GaAs, Behavior of 7253
by Heat Treatment, Formation of Spin Centers in 7238
from SiC, Study of Amorphous 6645
Carbonyl Iron Powder, Magnetization Curve in 7955
Card Reader Using Photoelectric Sensing Devices 8125
Cardiac Pacemaker 6849
Cardiotachometer 7161
Carrier:
Absorption in Semiconductors, Free 7376, 7380
Behavior in Molecular Solids, Domain Theory of 7008
Concentration, Fluctuations in 9252
Concentration in:
Cd_3As_2 7027
InSb 7831
Semiconductors 6099, 6682
Vitreous Materials 7949
Zn_3As_2 7027
Current in a Linearly Graded Drift Field, Minority 6102
Decay Time in Junction Transistors 6507
Density of:
AlSb-InSb 7938
GaAs-Ga_2Se_3 7942
Diffusion, Influence of Grain Boundaries on Minority 6073
Diffusion in a Magnetic Field 7307
Distribution in Semiconductors 8696
Generation in Photoconducting Anthracene, Free 7927
Interaction in Semiconductors 9251
Lifetime:
Measurement Using Transients in Junction Diodes 6223
by Microwave Absorption, Measurement of 6452
Lifetime in:
p-Type Si 6104
Semiconductors, Determination of 6093, 6223
Transistor Bases 8024
Transistors, Control of 7707
Mobilities in:
Cd_2As_3 7027
Ge-Si Alloys 7619
Zn_2As_3 7027
Mobility in Si and Ge, Field-Dependence of 6101
Multiplication in Ge, Microwave Induced 9253
Production in Anthracene 8262

Carrier: (Cont'd)
Properties of Semiconductors with Traps, Theory of 8261
Recombination in:
a Cylindrical Transistor Base Region 6503
Homopolar Semiconductors, Plasma Mechanism of 6092
Irradiated Ge 9262
Surface Transport 8710
Systems, Feedback Amplifiers for 8111
Transport, Dislocation Effects on 8708
Transport in:
Ge 8709
Semiconductor Bicrystals, Anisotropy of 6071
Solids 8707
Trapping by Surface Energy States 7267
Carrier-Carrier Scattering on Mobility in Semiconductors, Theory of the Effects of 7612
Carriers,
Cyclotron Resonance of Negative Mass 6122, 9301
Decay Rate of Excess 6094
Diffusion of Minority 6073
Magnetic Susceptibility of Photogenerated 9371
Carriers - See also Electrons, Holes
Carriers in:
Filaments, Photoconductive Decay of 6392
Ge,
Drift Mobility of 7609
Polarizability of Free 7010
Scattering of Hot 6109
Junctions, Multiplication of 6399
Semiconductors,
Measurement of Decay Times of X-Ray Excited 6684
Microwave Heating of 6090
Si, Plarizability of Free 7010
Cartridge Impedance of Microwave Diodes 6217
Cascaded Amplifiers 7739, 9062
Cascode:
Configuration, Analysis of the Transistor 6260
Transistor Trigger Circuits 7153
Casting, Preparation of AlSb and GaSb Alloys by Progressive and Zone 6623
Catalysis at a Semiconductor Surface 6980, 8232
Cathodes, Mobile Acceptor Model for Oxide Coated 6252
Cathodoluminescence, Voltage Dependence of 8730
Cations in Spinels, Distribution of 9153
Cavity Masers, Characteristics of Reflection 8472
Cellulose, Temperature Dependence of Conductivity of 7936
Center Law of Lattice Vibration Spectra 7917
Ceramic:
Electroluminescent Lamps 7439
Transducers for Ultrasonic Delay Lines, $BaTiO_3$ 6533
Ceramic Oxides, Heat Transfer Mechanisms in 8405
Ceramic Rutile, Stability and Aging of 7901
Ceramics,
Characteristic Improvements by Diminishing Inhomogeneity in 8676
Dielectric:
Breakdown in Porous 9228
Constant of Ferroelectric 6675
Ferroelectric Characteristics of $PbZrTiO_3$ 6085
Magnetic 6155
Mechanical Properties of Ferroelectric 8414
Thermal:
Conduction in Ferroelectric 7289
Conductivity of 9436
Thermoluminescence in Alumina 7553
Transducer Properties of Lead Titanate Zirconate 6532
Ceramics Containing Nb or Ta, Properties of Lead Titanate 6678
Cerium-Doped $CaWO_3$, Spin Echo Experiments in 7668

Cesium Antimony Films,
  Electrical Resistivity of 6070
  Formation of 6070
Cesium Bromide,
  Color Centers in 7239
  Elastic Constants of 9448
  Ionic Conductivity and Diffusion in 8245
  Photoemission from 7320
Cesium Chloride,
  Cohesive Energy of 8236
  Color Centers in 7239
  Growth of 6966
  Photoemission from 7320
Cesium Chloride Whiskers, Growth of 6034
Cesium Fluoride, Lattice Vibrations in 9218
Cesium Iodide,
  Color Centers in 7239
  Elastic Constants of 9448
  Ionic Conductivity and Diffusion in 8245
  Photoemission from 7320
Chalcopyrite Crystals, Energy Band Structure of 8656
Channel Converter for Carrier Frequency Telephone Systems 7506
Channels on Silicon p-n Junctions, Anomalous Surface 6741
Character Recognition, Magnetic Pulse Sequence Detector for 7775
Characteristic:
  Energy Losses in Metal Films 6177
  Frequencies for Semiconductors 6416
  Frequency and Center Frequency, Equivalence of 7917
Characteristics of:
  Epitaxial Junctions Formed between Ge and GaAs 8421
  GaAs Diodes 8419
  Power Transistors, Measurement of 8430
Characterization of Transistors 7462
Charge, Influence of Ambient Atmosphere on Surface 6391
Charge:
  Control Parameters:
    in Transistor Switching Circuit Design 8091
    of Transistors 7094
  Densities, Effect of Crystalline Fields on 7926
  Distributions, Static Space- 6423, 6481
  Screening, Classification of Solids by Free Electron 7903
  Transport through Organic Polymer Films 7013
Chemical:
  Analysis of Bi-Sb-Te-Se Systems 8615
  Composition of Pyrrhotites 6316
  Etching, Mechanism of 6372
  Etching of Si 6373
Chemisorption:
  of Oxygen Gas on Ge Surfaces, Reduction of 6368
  Properties of Ge Surfaces 9283
Chlorine, Reaction of SiC Single Crystals with 6645
Chlorine:
  in InAs, Solubility of 8203
  Ions in:
    AgCl, Diffusion of 6950
    NaCl, Self-Diffusion of 7251
Chopper, Micro- 6926
Chopper:
  for dc Amplifier 8059
  Type dc Amplifier 6824
Choppers for Low-Level Direct Current Signals 6558
Chromic Bromide, Magnetic Properties of 8818
Chromic Oxide,
  Antiferromagnetic Transition Temperature of 8334
  Magnetoelectric Effect in Antiferromagnetic 8334
Chromic Oxide-Alumina Systems, Lattice Spacing and Distortion in 7850
Chromite Spinels, Ferrimagnetic 9324
Chromium:
  Fluorescence Line, Strain-Induced Splitting of a 7386
  Ions in:
    Guanidine Alum, Paramagnetic Resonance Spectrum of 6167
    Potassium Cobalticyanide, Microwave Paramagnetic Resonance Spectrum of 6163
    Ruby, Spin-Lattice Relaxation Times of 6169
  in Ruby, Absorption Lines of 7979
Chromium-Containing Spinels, Low Magnetic Moments in 9325
Chromium-Doped Titania Maser, Operation of a 8474
Chromium^{3+}:
  in Al_2O_3, Paramagnetic Resonance Line Width Broadening of 8339
  Doped Corundum, Spin-Lattice Relaxation in 8343
  Ions in Magnesium Oxide Crystals, Zeeman Effect of the Purely Cubic Field Fluorescence Line of 7360
  in $K_3Co(CN)_6$, Electron Spin-Lattice Relaxation of 8344
  in Ruby,
    Paramagnetic Resonance of 8845
    Relaxation Times of 7655
  Spin-Phonon Interaction in Ruby 8341
  in TiO_2 as a Maser Material 6806
  in YGaG, Paramagnetic Resonance of 8350
  in ZnF_2, Paramagnetic Resonance of 8352
Chromium $^{53}3+++$ in Ruby, Hyperfine Structure of 6447
Chromium Dioxide, Preparation of Ferromagnetic 8630
Chromium Nitride, Antiferromagnetic Ordering in 9366
Chromium Pentoxide, Magnetic Properties of 8335
Chromium Potassium Sulfate, Acoustic Attentuation in 8940
Chromous Chloride, Antiferromagnetic 8821
Chromous Fluoride, Antiferromagnetic 8821
Circuit:
  Analysis 8052, 8485
  Breakers, Energizer for 8579
  Protection, Semiconductor Breakdown Device for 8443
  Techniques, Thin Film 6821
Circulators,
  Ferrite 6242, 6525, 6793, 6794, 7222, 8114, 8462, 8463
  Large Bandwidth Tunnel Diode Amplifiers Using 8079
  Strip Line L Band Compact 6243
Circulators with Masers, Use of 7724
Clamp for Millivolt Signals, Diode Bridge 6845
Class:
  A-B Amplifiers, Distortion in 8488
  B Amplifiers 9071
Cleaned Ge Surfaces,
  ac and dc Field Effects on 6129
  Properties of 6422
Cleaning:
  Ge Surfaces, Ion-Bombardment Method for 6422, 8637
  InSb Surfaces, Ion-Bombardment Method for 8638
Cleavage:
  Faces of LiF Single Crystals, X-Ray Observation of 7872
  Planes of the III-V Compounds and Ge 7559
  Whiskers in Crystals 8206
Climb of Dislocations in Si, Gold-Induced 7242
Clock Pulse Circuits 9128
Clocks, Electronic 9149
Cluster Formation in Crystal Lattices, Determination of 6945
Cobalt,
  Magnetic Structure Thickness Dependence in 8800
  NMR in 6146, 8806, 8807
Cobalt, (Cont'd)
  Polarization of Conduction Electrons in 7643
  Structure and Magnetic Properties of 6994
Cobalt:
  Compounds, Ferrimagnetism of AB_5 7349
  Film, External Fields from Domain Walls of 6434
Cobalt^{2+}, Spin Hamiltonian of 7654
Cobalt^{2+}:
  in Cubic Symmetry, Optical Absorption of 7379
  Ions in Mixed Paramagnetic Crystals 8337
  in Single Crystals of MgO, ZnO, ZnS, $MgAl_2O_4$ and YGaG, Crystalline Field for 7379
Cobalt Acetate, Susceptibility of 8819
Cobalt Chloride, Magnetic Phase Transitions of 7653
Cobalt Dichloride Hexahydrate, Crystal Structure of 8172
Cobalt Ferrite, Semiconducting Properties of 9214
Cobalt Fluoride,
  Antiferromagnetic Transition Temperature of 8820
  Curie Temperature of 8820
Cobalt-Iron Permanent Magnets, Elongated Single Domain 9332
Cobalt-Iron Ferrite, Magnetoelastic Effects in 7327
Cobalt-Iron Oxide, Effect of Cation Vacancies on Uniaxial Anisotropy in 8317
Cobalt-Manganese Alloys, Exchange Anisotropy in 7338
Cobalt Metaniobates, Ferroelectric Properties of 9245
Cobalt-Molybdenum Alloys, Electrodeposition of 6996
Cobalt-Nickel:
  Alloys, Effect of Plating Parameters on the Structure and Magnetic Properties of 6994
  Alloys from a Pyrophosphate Bath, Electrodeposition of 6995
Cobalt Oxide, Oxygen Surplus in Monocrystals of 6642
Cobalt Pyroniobates, Ferroelectric Properties of 9245
Cobalt Tantalates, Ferroelectric Properties of 9245
Cobalt Zinc Ferrite, X-Ray Study of Ferromagnetic Domains in 6139
Cobaltous Bromide,
  Antiferromagnetism in 6158
  Néel Temperature of 6708
  Specific Heat of 6158
  Susceptibility of 8314
Cobaltous Chloride, Specific Heat of 6148
Coercive:
  Field of $BaTiO_3$ 8685
  Force:
    of Fe_2C 8220
    of Ferromagnetic Powders and Films 9328
    on Imperfections, Dependence of 6703
Coercivity, Application of Neil Spike Formation to 9361
Coherer Information Storage Device 6584
Cohesive:
  Energies of CsCl and KCl 8236
  Properties of Solids, Free Electron Bond Effect on 7903
Coincidence Circuits 6904, 6905, 7532, 8507
Cold Cathode Light Sources, Fabrication and Properties of 8455
Colemanite,
  Ferroelectric Properties of 9243
  Intrinsic Bias in Ferroelectric 9242
  Model for Switching and Plarization Reversal in 6087
Collector:
  Avalanche Breakdown, Theory of 8025
  Contact Effects on Parameters of Ge Junction Transistors 8438
Colloids in:
  Additively Colored NaCl 9169
  KCl, Electron Microscope Studies of 6981

or:
Center:
Absorption in:
Alkali Halides, Pressure Effect on 8858
KBr 8857
KCl 8857, 8859
KCl:Sr 9397
NaCl 9396
NaCl:Sr 9397
Absorption and Emission in NaCl 8362
Concentration by Microwave Faraday Rotation, Measurement of 7666
Fluorescence in Alkali Halides, Infrared 8886
Spin Resonance at Low Temperatures, Optical Effects on 8345
Wavefunctions 8895
Centers,
Bleaching of 7555
Photo-Ionization of 8860
Centers in:
Ag-Doped Alkali Halides, Effect of Pressure on 7854
Alkali Halides 8178
Alkali Halides,
Infrared Fluorescence of 8380
Radiation Energy Required to Produce 8179
Wave Functions of 8593
Alkaline Earth Fluorides 7059, 7060
Cesium Halide Single Crystals 7239
Irradiated Alkali Halide Crystals after Annealing, Spontaneous Generation of 7235
KCl,
Bleaching of 7236, 9168, 9395
Diffusion of 6934
Effects of Plastic Deformation on X-Ray Production of 6005
NaCl 7237, 8177, 9169
X-Irradiated Alkali Metal Azides 7234
oration of Alkali Halides at Low Temperatures, Mechanism for 6933
umbium - See also Niobium
umbium Oxide Rectifiers, Fabrication of 8989
mmon Emitter Amplifier Stage, Design of 8489
mmunication:
Receivers, Parametric Radio Frequency Amplifier for 7777
Systems, Maser 9109
mmutators 6595, 7480, 7507
mparators, Coincidence Sensing 7481
mplementary Transistor Circuits 6822
mplexes in Si, Lithium-Oxygen 6337
mponents, Review of Micromodule 6537
mpound:
Junction Transistor 8513
Semiconductors, Analysis of Impurities in 6944
mpounds,
Preparation of Mixed Valence 6524
Thermal Properties of Mixed Valence 6524
Thermoelements Using Mixed Valence 6524
mpressibility of F and M Centers in Alkali Halide Crystals 7915
mpressors, Audio Volume 6276
mputer, Digital-Analog Pulse Amplitude Interpolation 7195
mputer:
Circuits - See also Specific Circuit
Circuits,
Complementary Transistor 6822
Cryotron 7511
Instrumentation for the Application of Microwave Energy to 7795
Parametron 7800
Surface Barrier Transistor 7172
Components, Reliability of 8532
Control Circuit 8136, 8137
Counters - See Counters
Design of Amplifiers 8491
or Doppler Radar, Pulse Amplitude Interpolation 7195
Computer: (Cont'd)
with Elementary Structure, General-Purpose Microprogram-Controlled 6868
Elements,
Switching Properties of Ferrite 9350
Tunnel Diode Locked Pair 7180
Logic Circuits - See Logic Circuits
Memory Units - See Memory
Optimization of Transistor Logic Circuits 7794
Shift Registers - See Shift Registers
Storage - See Storage, Memory
Switching Circuits - See Switching Circuits
Computers,
Applications of Magnetic Tape Recording to Digital 6283
Hybrid 8549
Solid State:
Leprechaun 6279
Micrological Elements for Digital 6774
Computing, Modulation-Demodulation Scheme for Ultrahigh Speed 6570
Computing:
System from a Basic Transistor Circuit, Construction of a 6278
Systems, dc Amplifier Misalignment in 7194
Concentration Profile of Diffused Layers, Calculation of 6635
Conduction, Dielectric Theory of Impurity 8721
Conduction:
- See also Conductivity
Band:
of GaAs 6378
of GaSb 6060, 6378
of InP 6378
Occupancy Function after Collision 7908
Counting of Alpha Particles Using Rhombic Sulfur 6113
at Low Concentrations, Impurity 7015
Processes in Ceramic $BaTiO_3$, Transitional dc 7596
Conduction in:
Ge, Shear Effects on Impurity 7614
Insulators 9290
Nonstoichiometric Rutile, Anisotropic 7618
Organic Solids 7621
Si, Low Temperature Impurity 7943
Thin Bismuth Crystals, Effect of Size on 6383
Conductivity,
Anisotropy in 8723
Four-Point Probe Measurement of 6400
Heitler-London Mechanism of 8718, 9272
Measurement of Microwave Surface 8298
Monte-Carlo Calculation for a Size Effect in Electrical 7611
Pressure Dependence of 8270
Theory of Electrical 6110
Voltage Dependence of Electron Bombardment Induced 8730
Conductivity:
- See also Resistivity, Conduction
Pulses in Irradiated Zinc Sulfide 6688
Types, Infrared Techniques for Determining 6634
Conductivity of:
Ag_2-Group VI Binaries 8734
AgBr Emulsions, Dark 9421
α-Fe_2O_3 8275
$BaTiO_3$ 8682
Bi 8727
CdS: 6112, 7310
Type Crystals, Photoelectric Analysis of 8591
CdSe 8276
CdTe Layers 7392
Cellulose 7936
Contacts to SiC 6689
CsBr and CsI 8245
Dy 8736
Films Produced by Electrostatic Charging, Changes in Normal-State 8282
GaAs 8273
Conductivity of: (Cont'd)
GaAs-Ga_2Se_3 7942
GaSb, Effect of Pressure on 6068
Ge: 6672, 7940, 7941, 8720, 8722, 9280, 9282, 9285
Surfaces 6422, 9281
Ge-Si 7619
Glass:
(Sodium Aluminosilicate) 7939
(Vanadium Phosphate) 7944
InAs 7826
InSb 7937, 8731
Ionic Crystals 8713
KCl 7868
KCl-KBr Solid Solutions 9270
Li-Ni-O 8719
Low-Impedance Materials, Measurement of 7592
Magnetite 8733
NaCl 8729
Organic Polymer Films 7013
p-Phenylenediamine-Chloranil Complex 8735
PbS and PbSe 8918
PbTe 7849
Polar Semiconductors 9271
Rhombic Sulfur 6113
Semiconductor Surfaces 9284
Semiconductors 7935
Si 9278, 9279, 9286
Si-Co System 7620
SnS 7273
Wustite 8733
Zeolite Powder Compacts 9289
ZnO 8612
ZnTe Layers 7392
Conductors, Resistivity Constants of Anisotropic 9276
Connection of Leads, Identification of Phases Formed during 7228
Constant Resistivity, Growth of Single Crystals with 6024
Contact:
Electrification of Semiconductors 6673
Noise in CdS 9309
Phenomena in Ge at Low Temperatures 6405
Contacts,
Diffused 9010
Electroplated 9017
Evaporated 6757
Point 8994
Superconducting 6812
Surface Barrier Rectifying 8976
Contacts to:
BP 6666
CdS 6667, 6780
Semiconductors 8235
Si 7097, 8981
SiC 6666, 6689, 7026
Contamination of Si, Crucible 6027
Contractometer 7078
Control,
Photovoltaic Moiré Fringe System for Machine Tool 7435
Wideband FM Receiver for Remote Aircraft 6852
Control:
Circuit, Computer 8136, 8137
Elements, Systems Using Transistors and Transductors as 7144
Relays 8557, 8558
Systems,
Applications of Transfluxors to Electromechanical 7522
Theater Lighting 6296
Controlled:
Rectifier:
Circuits 6840
Frequency Multiplier 7773
Logic Circuits 8533
Reactor Safety System 7214
Regulator for Aircraft dc Generators 7516
Rectifiers, Trinistor 7837
Rectifiers Using Triode Transistors, Design of 6893

Controls, Motor 8556
Conversion Loss of GaAs Microwave Diodes 6732
Converters,
  Analog-Digital 8142, 8550
  Broad-Band Hybrid Coupled Tunnel Diode Down- 7492
  dc-ac 6295, 7819, 8510, 8525, 9098
  dc-dc 7201, 8144, 8555, 9138
  Frequency 8514
  Gain-Bandwidth of 6543
  Gain Optimization in Parametric Up- 7491
  Infrared Quantum 6237
  Noise Figure of 6543
  Parametric 7135
  Phase 8514
  Power 7201, 7819, 8112, 8144
  Pulse Height to:
    Digital Signal 6290
    Time 6274
  Time to:
    Amplitude 8575
    Pulse Height 7210
  Transceiver Application of 8525
  Tunnel Diode 6561, 7156
  Variable-Reactance 6543
  Voltage to Pulse-Width 7486
Conveyor, Selective 8153
Cooling:
  of Junction Devices, Peltier 7075
  of Power Rectifiers 7421
  Semiconductor Devices, Methods of 7697
  of Superconductors by Adiabatic Magnetization 9295
Copper,
  Effect of Oxygen on the Magnetoresistance of 7628
  Grain Boundary and Lattice Diffusion of Zn Vapor into 9180
  Paramagnetic Resonance Spectrum of 6162
  Photoresponse of 8905
  Radiation Effects in 8651
  Scattering Defects in 9197
  Small-Angle X-Ray Scattering from Neutron Irradiated 9157
Copper:
  Alloys,
    NMR in 9383
    Nuclear Resonance in 9381
    Thermoelectric Power of 8407
  under Cyclic Stress, X-Ray Scattering from 9164
  Films, Density Measurements of Thin 9156
  Whiskers by the Hydrogen Reduction of Cuprous Iodide Vapor, Growth of 6970
Copper in:
  AlSb, Diffusion of 8624
  Bi_2Te_3, Diffusion of 7863
  GaAs,
    Diffusion of 6357
    Thermal Conductivity Conversion Due to 8273
  Ge,
    Acceptor Levels of 7587
    Heat of Solution of 6620
  InAs, Determination of 6014
  Mg-Cr Ferrites, Addition of 7896
  Semiconductors, Solubility of Interstitial 6020
  Si, Precipitation of 6336
Copper-Aluminum Alloy, Neutron Irradiation Damage in a 9198
Copper Chloride, Antiferromagnetic Susceptibility of 7962
Copper-Gold, Elastic Constants of Ordered and Disordered 7406
Copper Gold Alloys, Thermoelectric Effects in 6205
Copper Halides, Optical Properties of 7671
Copper-Nickel, Nuclear Resonance Study of Electronic Magnetism in 7350
Copper-Nickel Alloys, Resistivity of 9288
Copper Phthalocyanine, Electrical Properties of Poly- 6424
Copper Tungstate,
  Crystal Structure of Tri-Clinic 6998
  Electrical Properties of 6998
Corbino:
  Disk, Theory of 7106
  Disk Voltage Regulators 7106
  Disks in:
    Magnetic Power Amplifiers 8451
    Two State Digital Elements 8451
Correlator, Transistorized Silica Delay-Line Memory for a 40-MC Deltic 6582
Correlators Using Hall Effect Multipliers 6903
Corundum - See also Alumina, Aluminum Oxide, Ruby
Corundum,
  Elastic Compliances and Constants of 8936
  Etching of Dislocations in 8183
  Growth of 6041
  Paramagnetic Resonance:
    Line Width Broadening of Cr^{3+} in 8339
    of Mn^{2+} in 6714
    of Ti^{3+} in 8355
  Spin-Lattice Relaxation in Cr^{3+} Doped 8343
Costa-Ribeiro Effect, Anisotropy in Single Crystal Naphthalene of the 7897
Counter Tubes, Blocking Oscillators for Driving 6304
Counters 6280, 9122
Counters,
  Binary 6309, 6881, 7435, 7801
  Binistor Ring 7709
  Fission Probe 6608
  High Energy Particle 6606
  Magnetic Core 8120, 8123, 8124
  Multiple Diode 6280
  Nuclear 8574
  100 Mc Transistor 7839
  Steering Circuits for Controlling Reversible 6281
  Surface Barrier 6301-6303, 6908
  Tunnel Diode 6557, 7179
Counting Circuits, Magnetic 8537, 8568
Critical:
  Current in Superconducting Sn Films 8286
  Field of Superconducting:
    Al 8283
    Hg 8284, 8748
    In 7312, 8748
    Nb_3Sn 7946
    Sn 6118, 7312, 8285, 8747, 8748
    Ta 7312
    Zn 8283
  Fields of:
    Superconductors 8741
    Thin Superconducting Films 7626
  Temperature of Superconductors 8745, 8746
Cross Relaxation:
  in Dilute Paramagnetic Systems 7366
  Effect of Cr and Fe in Potassium Cobalticyanide 7661
  by a Four Spin Flip Mechanism 7965
  in Spin Systems 7950
Crossover Transitions for a Spin 3/2 System 7355
Crowe Cells,
  Characteristics of 7450
  Lead Film 6591
  Superconducting 6289
Crucible Technique of Growing Single Crystals, Floating 6024
Crucibles,
  Contamination of Si by 6027
  Growth of Si Crystals from Fused Quartz 6028
Cryostat for:
  Crystal Orientation by Neutron Diffraction 6321
  Electrical Measurements on Semiconductors 8267
Cryotron:
  Catalog Memory, Thin-Film 7512
  Circuits, Evaporated-Film 6554
  Gating Circuits 8094
  Loops, Operation of 7449
  Memory Circuits 7511
  Shift Register 6808
Cryotron: (Cont'd)
  Storage Circuit 6808
  Switches 7446, 7447
  Switching:
    Circuits for Computers 7447
    and Storage Devices 7192
  Trigger Circuits 6810
Cryotrons,
  Characteristics of 7511
  Crossed Film 6808, 7448
  Fabrication of:
    Multiple-Characteristic 8476
    Thin Film 7192
  Increasing the Speed of 7446
  Superconducting Contacts for 6812
  Temperature Dependence of Current Amplification Factor of Thin Film 8477
  Thin Film 6809-6811, 7447
Crystal:
  Calibrator Employing Tunnel Diodes 8151
  Counters, Cadmium Sulfide and Zinc Sulfide 6967
  Deterioration of Diodes 7699
  Distortion in Mn^{3+} Spinels 8590
  Field Splitting in $KNiF_3$ 7358
  Growth - See Growth of
  Imperfections, Changes in Lattice Parameters Due to 7237, 7238, 7241
  Imperfections:
    See also Dislocations, Defects, etc.
    in Si and Ge 6007
  Model, Surface States in a One-Dimensional 6381
  Orientation by Neutron Diffraction, Cryostat for 6321
  Perfection, Determination of 6945
  Potential of Semiconductors 6066
  Puller, Synthesis and Crystal Pulling of GaAs in a Magnetic 6956
  Structure - See Structure
  Symmetry of:
    the Low Temperature Phase of $BaTiO_3$ 6084
    Metal Chelate Salt Crystals 6367
  Type Resistors 6918
  Wafer Slicer 6306
Crystalline:
  Field:
    Effects on Charge Densities and Magnetic Form Factors 7926
    for Ni^{2+} and Co^{2+} in Single Crystals of MgO, ZnO, ZnS, $MgAl_2O_4$ and YGaG 7379
  Fields in Solids, Theory of 6161
Crystallographic Properties of:
  Ag_2Se 7077
  Rubidium Bisulfate 6387
  Square Loop Materials 9184
Crystallography of FeNiN 7575
Crystals,
  Cleavage Faces of LiF 7872
  Effect of Screw Dislocations on the Yield Strength of 7694
  Electronic Spectra of 9390, 9391
  Growth of - See Growth of
  Houston's Method of Face-Centered Cubic 6004
  Infrared Absorption in Ionic 7382
  Lattice Constants of 8170
  Mosaic Structure of 7245
  Plastic Resistance in 8186
  Position of Atoms in 9223
  Radiation Damage in 6997
  Surface States of Ionic and Valence 8238
  Theory of Double Bragg Reflections in Single 9161
Cupric Sulfide, X-Ray Spectra of Superconducting 8371
Cuprous Halide:
  Films, Diffusion in 7580
  Films on Alkali Halide Crystals, Formation of 7580
Cuprous Halides, Energy Band Structure of 6067

uprous Iodide Vapor, Mechanism of Hydrogen Reduction of 6970
uprous Oxide,
Absorption in 8360, 8369, 8370
Diffusion of:
Ag in 6951
Zn in 7567
Exciton Absorption in 8360
Photoconductivity of 8903, 9423, 9425
Thermal EMF of 6204
Cuprous Oxide Rectifiers, Encapsulation of 8991
Curie:
Points in Dilute Iron Alloys 9336
Temperature of Fe-Ni Alloys, Hydrostatic Pressure Changes in the 7334
Temperatures of MnF_2 and CoF_2, Pressure Effects on 8820
urrent:
Amplification Factor, Frequency Dependence of 6231
Drift Calculation in Junction Transistors 8055
Flow - See also Conduction, Conductivity
Flow in:
Dielectric Layers between Cylindrical Electrodes 6079
Insulators, Theory of 6098
Junctions,
High Forward 6494
High Injection Level 8963
Reverse 8965
Junctions between Semiconductors Having Different Energy Gaps 8422
Fluctuations in Lead Sulfide Cells 6468
Gain in Transistors, Measurement of 8021
Growth in p-n Junctions in Moist Atmospheres 6482
Limiter Galvanometer 6844
Noise in CdS Due to Multiple Retrapping 6095
Regulators 6597, 7200, 7518
Stabilizers for Electromagnets 6293, 7813
Switching and Routing Techniques 6874
Currents in:
Dielectrics, β-Particle Transmission in 9230
Diodes, Reverse 8966
Curve Tracers,
Transistor 6924
Tunnel Diode 6312, 6617, 6817
Cutoff:
Characteristics of Si p-Sp-n Rectifiers at Breakdown 8015
Frequencies, Transistor 6536, 8024
Cyclotron:
Resonance, Infrared 9302
Resonance:
Absorption in ZnSb and CdSb 8768
of Negative:
Effective Mass Carriers, Nonequilibrium 6122
Mass Carriers 9301
Negative Effective Mass Experiments 8769
Resonance in:
Ge 8295, 8296
an Oriented Magnetic Field 7318
Polyvalent Metals 9209
Semiconductors 6416
Si 6123, 8296, 8706
Resonances in the Valence Band of Ge, Power-Induced Shifts of 8295
Czochralski Method of Crystal Growth 6647, 6971, 7877

D

D-Bands in Cubic Lattices 7001
Damage of Si Surfaces Due to Lapping 6370
Damping of Ge and Si Containing Impurity Oxygen, Mechanical 6213
Data:
Conversion Circuits for Earth Satellite Telemetry 6274
Instrumentation, Transistor Building Blocks for 7173
Storage on Magnetic Tape 8130-8132
dc:
to ac:
Converters 6295, 7819, 8510, 8525, 9098
Inverters 8554
Currents, Semiconductor Diode Modulator for Measurements of 7202
to dc Inverters 8555
Debye Temperature of:
CdS 8400
Solids 8913
Decay:
of Excess Carriers in Semiconductors 6094
Time of:
PbS Photodetectors 8453
X-Ray Excited Carriers, Measurement of 6684
Decoration of Dislocations inside Large Crystals 7557
Defects,
Low Temperature Thermal Resistivity of Point 6200
Structure of 7852
Defects:
- See also Dislocations
with Dislocations in Si, Interaction of Point 7573
on Lattice Thermal Conductivity, Influence of Point 6201
Produced by γ Irradiation, Hole-Capture Cross Section of 7605
Defects in:
FeO 8204
Ge, Neutron Irradiation 6627, 7929
Glass (Lead Silicate) 8648
InSb, Deformation Induced 6632
KCl 7556
LiF 7556, 7856
Quartz 7853
Si: 8174
Junctions 8445
Sn, Quenched-In 9166
ZnS 7561
Deflection Circuits, TV 8109, 8527, 9113
Deformation:
of Ge 7690
Potentials in Ge 7586
Deformation-Induced Defects in InSb 6632
deHaas-van Alphen:
Effect in:
Graphite, Field Dependence of 7931
Polyvalent Metals 9209
Oscillations in:
Mg 8849
Sn 6120
Delay:
Circuits 6846, 6848
Generators, Multivibrators as 6562
Line Storage, Silica 6582, 7804
Lines,
Sonic 6282
Ultrasonic 6533
Variable 7727, 8124
System for Transmission Lines 7789
Delineation of:
Ferroelectric Domains in Triglycine Sulfate by Etching 7291
Junction Defects 8445
Junctions 8444, 9009
Demagnetization in Ferrimagnets, Adiabatic 7952
Dember Effect in AgCl 7025
Demodulators, Pulse-Position 9094
Dendrites,
Dislocations in Ge 7893
Etch Pits on Ge 6664
Growth of:
Atomically Flat Surfaces on Ge 6349
GaAs 6657
Dendrites, Growth of: (Cont'd)
Ge 6033, 7270, 7888, 7890, 7892, 7893
InSb 6348
Si 6964
Growth Steps on the Surfaces of 6963
Propagation of Ge 6350, 6656
Dendritic:
Growth, Twin Generation and Seeding Mechanism in 6351
Growth:
on Ge Dendrite Surfaces 7891
Studies by Pulse Plating Techniques 6353
Theory 6352, 7889
Inclusions in AlSb Junctions 8016
Density:
Meters, Thermistor 8148
Reduction in Neutron Irradiated Ge 6627
Deposition of:
Au on Various Base Metals, Electroless 6992
Fe-Ni Films, Influence of Thiourea on the 6993
Ge Thin Films 7885, 7887
Metals on Si, Mechanisms of Electroless 6991
Desorption of H_2 from Ge Surfaces 8231
Dessicants in Hermetically Sealed Gas Filled Semiconductor Rectifiers, Solid 8427
Detection with Multiple Frequencies, Phase-Sensitive 7488
Detectors,
Alpha Particles 6609
AM 9089
Frequency 8511, 9091
Gamma-Ray 8573
Health Physics Monitoring 7212
Microwave Spectrometer 7205
Millimeter Wave 7490
Nuclear Particle 6909
Paramagnetic Resonance Autodyne 7827
Particle 6606, 6607, 6609, 8569, 8570, 8572
Phase 8511, 8513, 9093
Radiation 7715
Radio Receiver 9112
Tunnel Diode 8096
Video 6267
Deuterium, NMR of Solid 8346
Device Reliability, Method for Evaluating Semiconductor 6730
Devices,
Equipment for Encapsulating Semiconductor 6772
IRE Standards on Solid State 6729
Negative Resistance in Semiconductor 6731
Diamagnetic Susceptibility of:
Graphite 9215
Si and Ge 8848
Diamagnetism, Theory of 7670
Diamagnetism of Graphite, Electron 6715
Diamond,
Binding in 9204
Decay of Persistent Polarization in 7995
Electron Diffraction and Secondary Electron Emission Studies of a (100) Semiconducting Surface of 7870
Energy Band Structure of 7281
Four Spin Flip Mechanism in 7965
Gas Etching Effects on Single Crystals of 8643
Intrinsic Recombination Radiation in 8372
Luminescence in Semiconducting 7987
Scratching of 9196
Surface States of 7004
Synthesis of 7898, 7899
Diamond:
Lattice, Grain Boundaries in 8611
Structure Crystals, Lattice Vibrations in 9219
Thermistors, Fabrication and Properties of Semiconducting 8457
Dicing, Semiconductor 7900
Dictating Machines 8115
Dielectric, SiN Thin Film 6366
Dielectric:
Absorption in Alkali Halides 8244
Amplifiers, $BaTiO_3$ Thin Film 6042

Dielectric: (Cont'd)
Breakdown:
in Alkali Halides 9229
Dendrites on LiF Cleavage Faces 7255, 7256
in Porous Ceramics 9228
Constant, Measurement of 8670, 8671
Constant of:
$BaTiO_3$ 6674, 7593, 8684
Ferroelectric Ceramics 6675
Ge 6075, 8672, 8673
HgSe 6130
LiF 9226
Mixed Titanate Systems 6088
Si 6075, 8672
YIG 9368
Dispersion and Loss in Ferroelectrics, Microwave 6076
Layers between Cylindrical Electrodes, Space Charge and Current Flow in 6079
Loss in Alumina, Anomalous 6081
Permeability of:
$BaTiO_3$ 7288, 9232
Insulators 8674
$SrTiO_3$-Bi_2O_3·TiO_2 9232
Polarization of Ferroelectric Solid Solutions Based on Sodium Niobate 6680
Properties, Theory of Lattice Effects on 8243
Properties of:
Alumina, High Temperature 8678
$BaTiO_3$ 8686-8688
Ferroelectric Lead Metatantalate 6679
Ga-Sr and Ba-Pb Titanates 8225
Insulating Ceramics 8676
Insulators, Radiation Effects on 8675
Lead Titanate Ceramics Containing Nb or Ta 6678
Lead Titanate Zirconate 7603, 8258
MnO_2 8689, 8690
Organic Polymer Films 7013
Pb-Ba Niobates 8254
Rutile at Low Frequencies 7287
Solid Solution Systems Based on $NaNbO_3$ 8677
Some Semiconducting Oxide Glasses 7311
YGaG 9227
Resonator for Inductive Capacity Measurement 7921
Susceptibility of:
CdS 9231
Triglycine Sulfate 6043
Theory of Impurity Conduction 8721
Dielectrics,
β-Particle Transmission Currents in 9230
Ferroelectric Ceramics as Nonlinear 7602
Space Charge:
Distribution in 8679
Fields in 8680
Theory of Breakdown in 7594
Thermal Conductivity Tensor of 7999
Differentiating Amplifier, Transistor 7749
Diffraction Studies of Pyrographite, X-Ray 7851
Diffused:
Junctions, Fabrication of 8978
Layers,
Calculation of the Properties of 6635
p-n Junction Method for the Measurement of 6637
Surface Carrier Density in 7300
Layers in Ge, Evaluation and Control of 7249
Shot-Melting Technique for Making Junction Devices 6749
Si,
Evidence of Surface Damage and Precipitation in 6330
Preservation of Lifetime in 6393
Diffusion,
Carrier 6073, 6214, 7307, 9252, 9268
Effect of Pressure on 7860
Exciton 6398
Radiation Enhanced 7861
Diffusion:
After Effect 9356
Coefficients,
Effects of Strain upon 7859
Electron Probe Method of Measuring 7228
Coefficients:
in Crystals, Evaluation of 8196
of Ionized Impurities in Semiconductors 7566
Constants by Ion Drift, Measurement of 6753
Controlled Process in InSb Oxidation 8229
Equation, Solution of a 6512
of Ge Transistors 8028, 8441
Diffusion in:
AgBr, Cd 6639
AgBr-CdBr, Cd 6639
AgCl, Ion 6950
AlSb, Cu 8624
Au-Ni System, Isothermal 7864
Bi_2Te_3, Cu 7863
Crystals, Statistical Dynamics of Atomic 8195
CsBr and CsI, Ionic 8245
Cu, Zn 9180
Cu_2O, Ag 6951
Cu_2O, Zn 7567
Cuprous Halide Films 7580
GaAs 6356
GaAs,
Cd 8623
Cu 6357
Se 7865
Sulfur 7865
Zn 7228, 7566, 7572
GaSb 6069
Ge,
Ag 7569
As 6333, 7228, 7568
Au 8622
Cd 7569
Cu 6620
Fe 7569
Hydrogen 7250
In Surface Concentration in 6331
Mask for 6327
Oxygen 7570
Sb 6332
Ta 7569
Te 7569
InSb, Zn 7252
KCl, Color Center 6934
NaCl, Chloride Ion Self- 7251
Ni, Metal 9181
Se,
Hg 8198
Sn 7547
Semiconductors, Substitutional and Interstitial 8620
Si 6326, 6328, 6636, 6637, 6757, 7858
Si,
Boron 6637, 6949, 8621
Group III and V Elements 6335
Li 6638, 7571, 8199
Oxygen 7570
Phosphorous 6334, 7862
SiC, Nitrogen 6948
Sn-In Alloys, Sn 9182
Solid Solutions, Theory of 7852
Solids, Vacancy 8594
ZnO, Li 7227
Digital-Analog Pulse Amplitude Interpolation Computer 7195
Diode:
Connection Assembly, Polarized 8984
Curve Tracers, Tunnel 6312, 6817
Impedance, Measurement of 7124
Diodes,
Ag Bonded 8007
Al Bonded 8951
AlSb 8016
Assembly Process for 7705, 8974
AsTe 8990
Avalanche 7089, 7409, 7417
Backward 7218, 7838
Diodes, (Cont'd)
Breakdown of 6490, 6495, 6744-6746, 6753, 7088, 7089, 7417
Computer 6225, 6265
Cooling of 7075, 7421, 7697, 8426
Current-Voltage Characteristics of 6483, 6700, 7087
Encapsulation of 6772, 8952, 8953
Forward Current in 6494
Four Layer 6733, 8954
Fuses for 7460
GaAs 6226, 6308, 6356, 6612, 6739, 7091, 7150, 7410, 7431, 7836, 8956, 8964
GaP 6500, 7703
Heat Sinks for 8446
Impedance Characteristics of 6492, 6493, 7085, 7124, 7414, 7696, 8962
InSb 6499, 6747, 7086, 7633
Junction:
AlSb 8016
Anomalous:
Barrier Capacitance of InSb 7086
Surface Channels on 6741
Approximating the Ideal Logarithmic Characteristics of 7415
Avalanche:
Breakdown Voltages of Diffused 7417
Effect in Si Three-Layer 7089
Behavior of Doped Contacts in 6491
Breakdown in: 6745, 6746
Si 7088
Breakthrough 6490
Capacitance of Graded 7085
Carrier Lifetime at Arbitrary Injection Levels in 7418
Cartridge with Disk-Shaped Electrodes for 7752
Current-Voltage Characteristics of SiC 7087
Dendritic Inclusions in AlSb 8016
Diffused Shot-Melting Technique for Making 6749
Doped Contacts in 6491
Double Diffusion Oxide Masking in Diffused 8017
Effect of:
Ambient Atmospheres on 6421
Dislocations in 7420
Moist Atmospheres on Noise Spectra and Current Growth in 6482
Surface Angle on Voltage Breakdown in 7416
Tunneling on I-V Characteristics of 6700
Equivalent Circuit of Parametric 7458
Evaluation of Si Single Crystals for 7092
Excess Reverse Current Due to Metal Precipitates in 6754
External Photoelectric Emission from Back Biased Si 6722
Fabrication:
by Epitaxial Deposition of SiC Films of 6960
of SiC 7093
by Thermal Oxidation of 6751
by Thin Film Evaporation Techniques of 7090
GaAs 6226, 6356, 7091, 7150, 7836, 8964
GaP 6500, 7703
Ge 6748, 7410
Guard Ring 7088
Hemispherical 6498
High:
Forward Current Flow in 6494
Frequency Varactor 7698
Inductance 6493
Power: 7407
(Current) - See also Rectifiers
Si 7702
Voltage Breakdown 6753
Impedance of Diffused Si Mesa Varactor 7124
Imperfections in 7704

es, Junction: (Cont'd)
Increased Speed of Recovery Transient 6496
Inductance of 6492, 7414
InSb 6499, 6747, 7086, 7633
Internal Field Emission in Narrow InSb 6747
Ionization Rates for Electrons in 6746
Light Emission from 6742, 6745
Localized Breakdown in Diffused Si 6495
Location of Junctions in 6752
Low Breakdown Spots in 6744
Micro-Etch Techniques on Millimeter Wave-Length Diodes, Use of 6502
Microplasmas in 6742, 6743, 6745
Multiplication of Carriers by Impact Ionization 6399
Negative Resistance 6484, 6485, 6733
Neutron Bombardment of Tunnel 7083
Noise:
Performance of Tunnel 7700, 7701
Properties of Varactor 7115
Parameters of Si Single Crystals for 7263
Peltier Effect in 7075
Performance Parameters of Si Power 6497
Plastic Deformation of Ge by Alloying 6748
p-n-p-n 6733
Potential Distribution in Graded 7085
Preparation:
by the Decomposition of Compounds in 7419
of Uniform 6745
Rectifying Barrier at an AlC-SiC Interface in 7026
Reverse Bias in 7084
Shot and Thermal Noise at High Current Levels in 6766
Si 6495, 6497, 6722, 7088, 7089, 7124, 7410, 7702, 7835
SiC 6037, 6501, 6960, 7087, 7093
Spreading Resistance in 7696
Statistical Fluctuations of Donors and Acceptors in 6744
Surface:
Effects in 6421
Stabilization of 7420
Theory of: 6481
Current-Voltage Characteristics of 6483
Thermal Spreading Resistance in 7696
Transient:
Behavior of 6223, 6224
Processes at Arbitrary Injection Level in 7418
Response of Variable Capacitance in 6735
Trinistor Controlled Rectifier 7837
Tunnel:
Characteristics of 6535, 6617
Currents in InSb 7633
Vapor Grown 6734, 6750
Varactor Package for Microwave Frequencies in 7698
Variable Capacitance 6734
Voltages and Electric Fields of Diffused 7413
ulti-Layer: Fabrication of 8959
oise in 6740, 6766, 7115, 7459, 7700, 7701, 8969
ackaging of 8983
arallel Operation of Power 7497
oint Contact:
As-Te 8990
Dipole Mode of Minority Carrier Diffusion in 6214
Fabrication of 8949
Forming of 8948
GaAs 6612
Increasing Bandwidth in 8950
Microwave Switches for 6216
Surface Currents in Inversion Layers of 7080
Whisker Mounting on 9016
wer – See Rectifiers
otection of 7125
otective Coatings for 6773, 8019, 8985

Diodes, (Cont'd)
Reverse Current in 6754, 7084, 8965, 8966
SiC 6037, 6501, 6960, 7087, 7093
Space Charge Limited Currnets in Insulator 8961
Survey of 8526
Thermal Test Set for 6925
Thin Film Circuit Techniques Using 6821
Tunnel 6181, 6219, 6220, 6484-6489, 6535, 6617, 6737-6740, 6747, 7082, 7083, 7150, 7218, 7410-7412, 7431, 7459, 7633, 7700, 7701, 7838, 8009, 8010, 8012, 8054, 8956
Turnover Behavior of Ge 6731
Varactor: 6226, 6308, 6734, 7081, 7115, 7124, 7698, 7835
Figures of Merit of 8960
Zener 6736, 7535
Dipole Mode of Minority Carrier Diffusion 6214
Directional Freezing, Preparation of Cadmium Tin Arsenide by 6108
Directivity of Crystal Properties, Theory of 7905
Discriminators 7487, 7532, 8513, 9090
Discriminators, Pulse 8520, 9092
Dislocation:
Acceptor Occupation Statistics 7914
Climb in Plastically Deformed InSb 6632
Cross-Glide in LiF Crystals 7856
Damping in:
NaCl 9175
Si and Ge 8946
Densities in GaAs, Reduction of 6342
Density in:
Si 6025
Si, Optical Determination of 6008
Effects on Carrier Transport 8708
Etch:
Pit Relation in SiC 6937
Pits:
in Ge, Effect of Cu Precipitation on 6662
on InSb 6371
in Te 6936
Models of Grain Boundaries 8610, 8611
Motion, Plastic Resistance of Crystals to 8186
Multiplication in LiF Crystals 7856
Nets in Sb_2Te_3 and Bi_2Te_3 8603
Networks in Alloy Foils 9171
Nucleation in LiF 9173
Structure of NaCl Whiskers 6009
Theory, Implications of the Dangling Bond Model for 7000
Velocities in Ge and Si, Stress Dependent 8187
Dislocation-Free:
Ge Crystals, Growth of 7260
Si and Ge Crystals, Growth of 7243
Dislocations,
Climb Motion of 8605
Continuous Distribution of 8597
Edge 8184
Frictional Stress on Moving 6939
Graphitization Stress as a Source of 9172
Interactions between: 8608
Fixed and Moving 8607
Parallel Edge and Tilt 8606
Kinetic Theory of Stress-Assisted Precipitation on 9174
Lattice Statics of 8596
Motion of 8604
Dislocations:
and Etch Pits in GaAs, Correlation between 7244
Introduced during Growth, Reduction of 6343
of Like and Unlike Signs, Forces between 7560
by Spark Discharge, Formation of 8599
Dislocations in:
Ag 8180
AgCl 7557
Bi_2Te_3 8603
CdS 6011, 7855, 8182
Corundum 8183
Crystal Growth, Role of 6937
Crystals, Sources of 9173
GaAs 6342, 7244, 8641

Dislocations in: (Cont'd)
Ge: 6007, 6651, 6662, 6748, 6935, 7243, 8187, 8208, 8946
Dendrites 7893
Graphite 6633, 6938
Fe: 9362
Whiskers 9176
Ferroelectric Glycine Sulfate 8609
the Growth of SiC Crystals, Role of 6937
InSb 6371, 6632
KI 9170
LiF 6643, 7856, 8185, 9173
NaCl 6009, 9175
NaI 9170
Nonmetallic Layer Structures 8598
PbTe 8642
Sb_2Te_3 8603
Si 6008, 6010, 6025, 6630, 7242, 7243, 7558, 7573, 8181, 8187, 8946
SiC 6007, 6631, 6937, 6989
Solids, Theory of 7903
Spinel Structures 6932
Te 6096, 6936
ZnO 7227
ZnS 6967
Dislocations on:
Diode Characteristics, Effect of 7420
Hardening, Effect of 8601
Plastic Flow in Crystals, Effect of 7694
Strength of Crystalline Materials, Effect of 8602
the Strength of Sodium Chloride Whiskers, Effect of 6009
Work-Hardening in fcc Metals, Effect of 8600
the Yield Strength of Crystals, Effect of Screw 7694
Disorder Phenomenon, Theory of Electroluminescence as a 7062
Dispersion:
Curve of Spin Waves in a Metal 7332
in Ferroelectrics, Microwave Dielectric 6076
Relations, General Spin-Wave 7331
of Spin Waves in YIG 7333
Display Panel, Storage Light Intensifier 7718, 7719
Displays 7445, 7810
Displays,
Electroluminescent Alphanumeric 6291
Review of Panel-Type 6892
Dissociation:
Mechanism for the Diffusion of Substitutional Cu in Ge 6620
Pressure of CdSb 8159
Pressures of Cd_3As_2 8582
Dissolution, Effect of Cold Work on 6983
Dissolution:
of Ge,
Influence of Hydrofluoric Acid on the 7278
Orientation-Dependent 6984
Kinetics of Ge in Electrolytes 6369
of Quartz by Ga 6928
Distillation Purification of Ge 8619
Distortion in:
Almost-Linear Networks, Nonlinear 7095
Alumina-Chromic Oxide Systems 7850
Class A-B Push-Pull Amplifiers 8488
Transistor:
Amplifier Stages, Calculation of the 7129
Amplifiers, Nonlinear 9063
Stages 7741
Distortions Produced by Ni^{2+} on Tetrahedral Lattice Sites 6174
Distributed:
Amplifiers, Design of Transistor 1741
Parameter Microminiature Structures 7123
Distribution:
Coefficient:
of In in Ge, Temperature Dependence of 8165
of Sn in Se 7547
of Te in Melt Grown InSb Crystals 7847
of Zn in GaAs 8166
in Zone-Refining Processes, Variation of the Effective 7248

Distribution: (Cont'd)
Coefficients of:
Impurities in:
GaAs 7233
Ge 7232
InSb 6036
Si 7232
Te in InSb Crystals, Orientation-Dependent 6320
Function in Dilute Electron Gases 7296
of Impurities during Zone Equalization 7866
Distributions in Mg-Mn Ferrites, Ion 8584
Dividers,
Frequency 7153, 7158, 8097, 9095
Pulse 7415
Domain:
Arrays Produced in Triglycine Sulfate by Thermal Shock, Ferroelectric 7291
Distribution in Superconducting Sn and Al 6117
Growth, Kinematic Theory of Ferroelectric 7923
Magnetization of a Ferromagnet, Anisotropy of the Intrinsic 7645
Motion in Ferromagnetic Thin Films 9349
Nucleation Centers in $BaTiO_3$, Motion of 7958
Patterns of $BaTiO_3$ 6084
Structure, Effects of Heat Treatment on Magnetic 7873
Structure:
of Mg-Mn Ferrites 9360
of Ni Films 8322
in YIG 7646
Theory of Carrier Behavior in Molecular Solids 7008
Tube Structures in Si-Fe 9361
Wall Motion: 8801, 8805
in $BaTiO_3$ 6386, 6677, 8249, 8250, 9240
Walls,
Co^{59} NMR Broadening in Co 8806
Energy and Entropy of 8802
Zigzagging in 8804
Walls in:
Antiferromagnetic Nickel Oxide Crystals 6707
$BaTiO_3$ 6386
Co Films, External Fields from 6434
Ferrites, Fast Switching by 6796
Permalloy:
Films 8803
Films, Cross-Tie 9359
Si-Fe 8323-8325
Thin Ni-Fe Films 6435
Width of Magnetoplumbite, Thickness Dependence of 7957
Domain-Dislocation Relationship in Ferroelectric Glycine Sulfate 8609
Domains in:
α-Manganese and its Alloys, Antiferromagnetic 7036
Iron Whiskers under High Fields, Observation of 7034
Nickel Oxide, Neutron and Optical Studies of 7035
Thin Magnetic Films Observed by Electron Microscopy 7345
X-Ray Damaged Rochelle Salts 8247
Donor State Wave Functions, Strain-Induced Changes of 7614
Donor-Acceptor:
Pairs, Energy Levels of 6380
Pairs in SiC, Polarization of Luminescence of 6454
Donors:
and Acceptors in p-n Junctions, Statistical Fluctuations of 6744
in Compensated Si, EPR of 8358
Doping, Infrared Techniques for Determination of Local 6634
Doping:
Ge with As 6344
of Group III-V Compounds with Group IV Elements 8197
Doping: (Cont'd)
of InAs with Cd 7878
Problems, Application of Statistical Techniques to 6947
of Semiconducting Compounds, Mobility 7012
Si by Diffusion 7858
Dose Rate Meters, Miniature 7163
Dosimeters, Thermoluminescent 7502
Double:
Refraction in Wurtzite-Type Binary Compounds 6194
Tetrode Transistor 8023
Drift:
Correctors for Analog Computer Amplifiers 6596
Field, Minority Carrier Current in a Linearly Graded 6102
Mobilities of Anthracene 8262
Mobility, Use of the Field Effect Modulation of Photoconductors to Measure 7070
Mobility:
of Carriers in Ge 7609
for Electrons and Holes, Evaluation of the Ratio of Hall Mobility to 6683
as a Function of Concentration of Scattering Centers 6104
Transistors 6102, 6761
Transistors, TV Signal Amplifiers Using 8106
Driving Circuits for Counter Tubes 6304
Duplexers, Ferrite 6793, 8114, 8462
Duplexing:
a Ruby Maser 6273
Systems, Microwave 8528
Systems with Masers, Use of 7724
Dysprosium,
Conductivity of 8736
Electrical Resistivity of Polycrystalline 7016
Dysprosium^{161}, Nuclear Resonance Absorption in 7353

E

Echo-Sounder, Underwater 6867
Edge:
Dislocations 8184
Emission in:
- See also Emission
CdS 7385, 8873, 9407
SiC 6453
Sulfide Phosphors 9406
ZnO 9407
ZnS 9407
Effective:
Mass,
Cyclotron Resonance Measurement of 8769
Faraday Effect Method of Measuring 8911
Theory of Electron 7606
Mass:
Carriers, Nonequilibrium Cyclotron Resonance of Negative 6122
of Carriers in:
Bi_2Te_3 8397
CdS 8768
CdTe 6198
Gray Tin 7298
HgSe 6130
InAs 8912
InP 8912
InSb 6130
Semiconductors 8705
Si 6065, 6123, 8706
Si-Ge 8824
SnS 7273
SnSe 6132
Ti_2O_3 7309
ZnSb 8768
Ratio in Semiconductors, Measurement of the 6384
Tensor of Electrons in Semiconductors 8395
Elastic:
Compliances of Corundum 8936
Constants,
Theory of 9442
Ultrasonic Measurements of 9448
Constants of:
AlSb 9447
Anisotropic Media 9443
Be 6210
β Tin 7405
Corundum 8936
CaF at Low Temperatures 6475
Cd 9446
CdS 8004
Cu_3Au 7406
KBr 8409
Na 9444
NaI 6724
Triglycine Sulfate 6043
Y 8411
YIG 7691
Moduli of:
KCl 8937
Rutile 8935
TiO_2 8410
Strain on the Anomalous Transmission of X-Rays in Ge, Effect of 7371
Waves in Trigonal Crystals 9222
Electret, Photorectifier Combining a Photoconductor and an 6518
Electric:
Field, Theoretical Variation of Electron Mobility with 6397
Field:
Effect on Electron Mobility in InSb 7933
in Ge and Si Samples, Effect of a High 6388
Induced Light Absorption in CdS 6450
Fields, Properties of InSb in Pulsed High 7934
Fields on Hydrogen-Like Excitons, Effect of 6389
Power Generators, Photovoltaic 8551
Strength of Insulators, Radiation Effects on 8674
Electrification of:
KCl Crystals, Influence of β Rays on 6385
NaCl Crystals, Influence of X-Rays on 6078
Electrochemiluminescence of Si 8884
Electrodeposited:
Co and Co-Ni Alloys, Effect of Plating Parameters on the Structure of 6994
Films of Fe-Ni Alloys, Initial Growth of Plating in Thin 7078
Thin:
Magnetic Films, Influence of Substrates on 7039
Ni-Fe Films, Effects of Composition and Thickness on the Magnetic Properties of 7040
Electrodeposition of:
Co-Mo Alloys 6996
Ni-Co Alloys from the Pyrophosphate Bath 6995
Thin Magnetic Films in a Magnetic Field 7039
Electrodeposits, Measurement of Stress in Very Thin 7078
Electrodes 6374, 6375, 6668, 6757, 6769, 6770, 8425, 8982
Electroenhancement of X-Ray Excited Luminescence 6191
Electroless:
Deposition of:
Au on Various Base Metals 6992
Metals on Si, Mechanisms of 6991
Plated Contacts to SiC and BP 6666
Electroluminescence,
Irreversible Thermodynamics of Injection 6185
Mechanisms of 9409
Temperature Dependence of 7985
Theory of 7062
Very Low Frequency Excitation of 7985
Electroluminescence of:
AlP 7589

ectroluminescence of: (Cont'd)
CdS: 8376
Diodes 9410
Diamond 7987
GaP 7990, 8882
Insulated Particles, Model for 7984
(Zn,Hg)S and (Zn,Cd,Hg)S Phosphors 7988
ZnS 6458, 8881, 8883
ZnS:Cu 8377, 9411
ectroluminescence under Pulsed Square-Wave Excitation 6184, 6459
ectroluminescent:
Alphanumerical Displays 6291
Cells,
Area-Type 6522
Light Waveforms Emitted from 8374
Device for Observing Pulse Trains 8454
Devices, Boron Nitride 6235
Display Screens, Ferroelectric Ceramic Devices for Controlling 7445
Lamps, Ceramic 7439
Light Amplifier 8456
Panels: 6618
in Light Amplifiers, Use of 6236
Phosphors,
CaS:Cu,Eu 6462
Fatigue in 6186
Maintenance of 7063
Microscopic Observations on 6182
Preparation of (Zn, Hg)S and (Zn,Cd,Hg)S 7677
Voltage Dependence and Particle Size Distribution of 6183
Television Screens, Polychromatic 6567
Typewriter 9124
Zinc Sulfide, Ionic Properties of 6080
lectrolysis, Production of Boron by 8226
lectrolytes, Dissolution Kinetics of Ge in 6369
lectrolytic:
Al Capacitors 6807
Rectification, Theory of 7017
lectromagnet, Current Stabilizer for an 6293
lectromagnetic:
Properties of Insulators 6074
Wave Polarization by Gyormagnetic Rods 8042
Waves, Hall Effect Device for 6195
lectromechanical Coupling Coefficients of Nickel Zinc Ferrites 6365
lectrometers 8146, 8560
lectron:
Beam Zone Refiner 6305
Bombardment, Production of Color Centers in Alkaline Earth Fluorides by 7059, 7060
Bound States, Calculation of Wave Functions and Energies of 7930
Capture by a Lattice Vacancy in Si 6097
Density:
Distribution in Ge 8242
Maps of CdS Crystal Structure 7005
Detection in Si Junctions 7831
Diffraction, Measurement of Intensity in 7824
Diffraction:
Measurement of the Magnetic Induction at the Surface and Interior of Fe Particles 8309
of a (100) Semiconducting Diamond Surface 7870
Effective Mass in Solids, Theory of 7606
Ejection from Ge and Si by Noble Gas Ions, Auger 7631
Emission:
from Barium Tungstanate, Thermal 7630
from MgO Single Crystals, Secondary 7023, 7024
of a (100) Semiconducting Diamond Surface 7870
from Si, Thermionic 6388
from Si Junctions, Hot 6222
Energy:
Bands in Solids 9207
Electron: Energy: (Cont'd)
Dissipation and Secondary Emission in Solids, Relation between 6055
Impact Ionization, Occupancy State Probability Function in 7908
Irradiated:
PbS Films, Photoelectromotive Forces in 7678
Si, Infrared Studies of 6050, 6051
Microscopy, Domains in Thin Magnetic Films Observed by 7345
Microscopy in Surface Structure Determination 8205
Mirror Microscopy of Magnetic Stray Fields on Grain Boundaries 9331
Mobility:
in AgBr 7610
with Electric Field, Theoretical Variation of 6397
in InSb 7933
in Si 7608
Multiplication in CdTe Photocells 7717
in One-Dimensional Deep Trap, Absorption and Emission Spectra of 7930
Paramagnetic Resonance:
of Color Centers in KCl 7665
of Donors in Compensated Si 8358
of Mn^{2+} 9387
Spectra of $K_3Co(CN)_6$, Polytype Effects in the 8831
Spectrometer, Analysis of a 6901
in Studies of Activated Phosphors 8878
Probe:
Method of Measuring Diffusion Coefficients 7228
X-Ray Microanalyzer, Study of Semiconductor Alloys Using the 7228
Relaxation in Si and Ge 8945
Scattering Due to Acoustic Modes in ZnO 6403
Spin:
Paramagnetic Resonance in LiF 6417, 8836
Relaxation in Ferromagnetic Insulators 8328
Resonance:
of F-Centers in KCl 8840
in Ge, Effect of Strain on 6062
of Mn^{2+} in Ionic Crystals 9306
of S-State Ions 8826
in Semiconducting Rutile 6170
Spectra of Si 8176
of V in α-Al_2O_3 8351
Spin-Lattice Relaxation in:
$K_3Co(CN)_6$ 8344
Phosphorus-Doped Si 6171
Transport in:
GaAs 7282
Solids 6395
Tunneling:
Measurement of Superconducting Energy Gap 8749
between Two Superconductors 7627
Electron-Electron Scattering in n-p Tunneling 6700
Electron-Phonon Scattering: 7611
in Normal Metals 8266
Electronegativities in Semiconducting Compounds 7907
Electronic:
Counters Using Multiple Diodes 6280
Structure of:
Crystals, Hartree-Fock Equations of 8668
Group IV and III-V Semiconductors 7002
Electrons, Lattice Displacements by Fast 6376
Electrons:
- See also Carriers
and Holes, Evaluation of the Ratio of Hall Mobility to Drift Mobility for 6683
Electrons in:
an Electric Field, Wave Functions and Effective Hamiltonian for Bloch 6091
Ferromagnetic Metals 7643
Ge and Si, Spin-Lattice Interaction for Donor 6168
Electrons in: (Cont'd)
Nonpolar Crystals 7304
Semiconductors 6090, 6390, 6683
Solids 6053, 6054, 9200
Electro-Optic Constants of Zincblende 7369
Electro-Optical:
Power Amplifiers 7145
Switches 7221
Electroplated Base Connections for Junction Transistors 6233
Electroplating for Revealing Variations of Resistivity, Use of Pulse 6353
Electroquenching of X-Ray Excited Luminescence 6191
Electrostrictive Effect in Rutile Single Crystals 6998
Emission, Secondary 9315
Emission:
- See also Edge Emission
of Auger Electrons from Ge 9314
from Back Biased Silicon Junctions, External Photoelectric 6722
Band of Electron Bombarded Ge, Radiative Recombination 8373
Bands of:
Sn, Pb and Sb Activated Phosphors 7925
Zn-Hg Phosphors 7988
from $BaWO_4$, Thermal Electron 7630
in CdS,
Edge 8873
Mechanically Excited 9405
from CdSe Phosphors 8891
in NaCl, Color Center 8362
from Si:
Junctions, Hot Electron 6222
Surfaces, Thermionic 6388
Spectrographic Method of Impurity Analysis 6940
Spectrum of:
Electron in One-Dimensional Deep Trap 7930
a Ge Tunnel Diode 6181
Luminescent ZnS-In 7991
from Ta, Field Dependence of Photoelectric 6193
from TiO_2, Field 9317
from ZnS:Cu, Infrared 8871
Emissivity, Peltier Method of Measuring Radiation 7072
Emitter:
Efficiency Characteristics 8995
Junction, Characteristics of Imperfect 8026
Encapsulation of Devices 6772, 8952, 8953, 8983, 8991
Encoders,
Analog to Digital 8141
Optical 8141
Energy, Calculation of Lattice Free 7916
Energy:
Band:
Calculation in Solids, Technique for Electronic 7906
Dynamics of Semiconductors 8705
Structure,
Many Electron State 8655
Reflectance Method of Measuring 7394
Structure of:
Al 9208
AlP 7589
Alkali Halide Phosphors 7989
Alkali Iodides 7320
Amorphous Solids 8657
Bi 7372
Bi_2Te_3 8919
CdS 6456, 9250
Chalcopyrite Crystals 8656
$CoFe_2O_4$ 9214
Cuprous Halides 6067
GaAs 7282
GaSb 6068
Ge in External Magnetic Field 7909
Graphite 9215
Group III-V Compounds 6058
InP 6111
InSb 9400

Energy: Band: Structure of: (Cont'd)
PbTe 6413
Polyvalent Metals 9209
Semiconductors 6066
Si 7394
Si-Ge 8824
Solids 7281, 9207
Te 6178
ZnS 6456
ZnS-In 7991
Theory 6059
Converters,
Thermoelectric 6310
Thermomagnetic 9439
Gap of:
AIB 6998
AlSb 6623
AlSb-GaSb 6623
Bi_2Se_3 8268
Cd_3As_2 7027
CdI_2-Type Compounds 8169
CdTe 8764
GaAs-GaP Alloys 7272
GaAs-Ga_2Se_3 7942
GaSb 6623
Ga_2Te_3-ZnTe 7230
Ge 7913
In_2Te_3-Group II-VI Telluride Solid Solutions 7546
Iodine 6998
Organic Molecular Solids 7029
Pb 6061
Semiconducting Compounds 7907
SiC 8865
SnS 7273
Superconductors 6695, 6696, 8749
Zn_2As_3 7027
ZnS Structure Crystals 8658
Gap Alloy-$GaAs_xP_{1-x}$, Preparation of a Graded 7076
Level Density in Superconductors 8746
Level-Surface Recombination Relationship 9258
Levels,
Adsorption Effects on Surface 9211
Surface 8660-8664, 9212, 9213
Levels:
of Ag Luminescent Centers in Sulfides 9418
in CdS Type Crystals 8591
of Donor-Acceptor Pairs 6380
in Ge 6064, 8373
of Holes 7911
in InSb-GaSb Alloys 8262
in Paramagnetic Crystals 7977
Losses of Electrons in Solids, Interpretation of 6054
Spectrum of Ge and Si, Effect of Deformation on Hole 7912
Transport in:
CdS, Neutral 6192
Disordered Lattices 7590
Enthalpy of Formation of III-V Compounds 6626
Entropy in Spin Systems 7950
Epitaxial:
Diodes, Si 7835
Films,
Ge 6651, 7268, 7885, 8215
Si 7268, 8201, 8216, 8628
Growth onto Silicon Carbide Seeds 6960
Junctions between Ge and GaAs 8421
Transistors 7219, 9007
Vapor Deposition, Surface Preparation for 6650
Equivalent:
Circuit for:
Drift Transistors 6761
Gyrators 8056
p-n-p-n Junction Diodes 6733
Parametric Diodes 7458
Tecnetrons 8032
Transistors 6254, 6255, 6258, 7463, 7464, 8027, 8440
Tunnel Diodes 8012
Equivalent: (Cont'd)
Circuit Analysis of Generation - Recombination Noise in Semiconductors 6126
Erbium,
Electrical Resistivity of Polycrystalline 7016
Magnetic and Resistivity Properties of 6151
Erbium-Doped $CaWO_4$, Spin Echo Experiments in 7668
Error Detectors, Magnetic Core 8519
Esaki Diodes - See Tunnel Diodes
Etch:
Pits:
in CdS 7855
Due to a Precipitated Phase, Saucer 6935
in Ge Dendrites, Orientation of 6664
in Pyrolytic Graphite, Ion-Bombardment Produced 6663
Rates, Correlation of Shape of Etch Hillock and Pits with 6047
Studies of Dielectric Breakdown Dendrites in LiF 7256
Etching,
Delineation of Ferroelectric Domains in Triglycine Sulfate by 7291
Jet 9014
Junction Delineation 9009
Etching:
Effect of Gas on Semiconductor Surfaces 8643
on Fast Ge Surface States, Effect of Chemical 6670
on Surface Structure, Effect of 6644
Techniques, Diode 6502
Techniques for:
Examining Dielectric Breakdown Dendrites on LiF Cleavage Faces 7255, 7256
Fabricating Silica Windows 8629
Preparing Thin Filaments of Ge, Photoelectric 7267
Etching of:
Dislocations 6935
Dislocations in:
Ag 8180
CdS 8182
Corundum 8183
Ge 6662
GaAs 7244, 8641
PbTe 8642
Si 8181
SiC 6937
Te 6936
Ge 6049, 6670, 6982, 6984-6987, 7278
Grain Boundaries in Al_2O_3, Flash 8189
Group III-V Intermetallic Compounds 8639,8640
Growth Patterns in Quartz 8190
InSb 6371
Intermetallic Compounds 6340, 6371
Semiconductors 6661
Si 6049, 6373, 6665, 6982, 6985, 6987, 6988
SiC 6048, 6989, 6990
Te 6096
Twin Boundaries 8188
Ettingshausen Effect in:
Semiconductors, Theory of the 7404
Si at High Temperature 6479
Ettingshausen-Nernst Effect in:
Sn, Oscillations in the 6120
Zn 9438
Europium,
Magnetic Susceptibility of 9372
Resistivity of 8274
Europium in CdS, Electron Paramagnetic Resonance of 7058
Europium Garnets, Magnetism in 9369
Europium-Iron Garnet, Ferrimagnetic Resonance in 7346
Evaporated:
Film Cryotron Circuits 6554
Ge Films, Preparation of Vacuum 7257
High Conductance Metal Electrodes 6757
Nickel-Iron Films, Angle-of-Incidence Anisotropy in 6430
Evaporated: (Cont'd)
Photoconductive Cells, Influence of Crystals Siz on the Spectral Response Limit of 6465
Evaporation of Sb during Heat Treatment of InSb, Preferential 6021
Evaporator,
Electron Gun 8627
Residual Gases in a High Vacuum 6345
Exchange:
Anisotropy in:
Co-Mn Alloys 7338
a Mn-Cr-Sb System 6432
$(Ni,Fe)_3$ Mn Alloys 7339
Constant of Magnetoplumbite 7957
Effects in Alkali Ozonates 6445
in Ferromagnets, Direct 7335
Interaction:
in Conductive Organic Solids 7621
of Fe^{3+} and Mn^{2+} in Spinel Structures 796
on Paramagnetic Relaxation Times, Influenc of 6172
Exchange-Inversion:
Magnetization, Model of 7336
in $Mn_{2-x}Cr_xSb$ 7033
Excited Levels of Activator Ions in Alkali Halides 7983
Exciton:
Absorption in Cu_2O 8360
Effect in Strained and Unstrained Ge 7370
Energy Levels in Ge and Si 8695
Migration 6389
Motion in CdS, Observation of 7604
Spectra of ZnO 8361
Exciton-Induced:
Luminescence in KI:Tl 9419
Photoconductivity in Cu_2O 9423
Excitons,
Effect of Electric Fields on Hydrogen-Like 6385
Kinetics of the Destruction of 6398
Optical Spectrum and Magneto-Optical Prope ties of 9249
Excitons in:
Alkali Halides 9248
CdS 8850, 9250, 9399
Expansion of Si, Thermal 6207
Exposure Meters 9147
Extinction Coefficient of:
a Highly Doped Si Surface 6723
Si 7394

F

F-Band Absorption in KCl 8856
F-Center:
- See also Color Centers
Concentration by Microwave Faraday Rotation, Measurement of 7666
Electrons, Spin Relaxation of 7664
F-Centers, Photo Ionization of 8860
F-Centers in:
KCl, ESR of 8840
KCl, Growth of 6006
LiF,
Concentration of 6201
PMR of 8837
F-Centers on Lattice Thermal Conductivity in LiF, Influence of 6201
Fabrication of:
As-Te Point Contact Diodes and Rectifiers 899
Boron-Silicon Junctions 8973
CbO (NbO) Rectifiers 8989
Cold Cathode Light Sources 8455
Composite Se-Ge Rectifiers 8987
Four-Layer Triodes 9006
GaAs Diffused Diodes 8964
Ge p-n Junction Rectifiers 8424
Hall Effect Memory Devices 8449
Hook Collectors 9002, 9003
Junction:
Diodes 8424, 8964

Fabrication of: Junction: (Cont'd)
Transistors 7219, 8431, 8999, 9001, 9004, 9005, 9007
Junctions:
(Alloy) 8972-8975, 8999, 9000
(Alloy-Diffused) 9001
(Diffused) 8964, 8978, 9004, 9005
(Epitaxial) 7219, 7835, 8421, 9007
(Eutectic) 8977
(Grown) 8970, 8971
(Vapor Deposited) 9007
Microalloy Junctions in Si 8974
Multielement Photocells 9030
Photocells 9025, 9026
Photoconductive Devices 9028
Photosensitive Cells 9024
Point Contact:
Diodes 8948, 8949, 8990
Transistors 8998
Power Transistors 9008
Radiation Detectors 9023
Se Rectifiers 8986, 8988
Semiconducting Diamond Thermistors 8457
Si Power Rectifiers 8423
Solid Metallic Rectifiers 8992
Surface Barrier:
Rectifying Contacts on Si and Ge 8976
Transistors 9014
Surface-Protected Photoconductive Cells 9029
Tetrode Transistors 8433
Tunnel Diodes 8955
Fabry-Pérot Interferometer 8475
Faraday:
Effect, Generation of Microwave Using the 6195
Effect:
Method of Measuring Effective Mass in InSb 8911
in Si and Ge, Microwave 6998, 7395
in $Y_3Fe_5O_{12}$, Infrared 8396
Rotation, Measurement of F-Center Concentration and Relaxation Time by Microwave 7666
Rotation in:
Antiferromagnetic MnF_2, Microwave 6709
Bi_2Te_3 8397
Cerium Phosphate Glass, Measurement of the Intermediate State in Superconductors by 8287
Garnets 9429
InAs and InP 8912
Magnetic Thin Films 9330
Rotator, Quadruply-Ridged Circular Waveguide 7113
Fatigue in Electroluminescent Phosphors 6186
Feedback:
Amplifiers, Stabilization of 8494
in Amplifiers 8489
Amplifiers for Carrier Systems 8111
Quadrature Suppressor, Transistor-Thermistor 6600
Repeaters, Stability of 8495
Fermi:
Contact Interaction of the Magnetic Field at the Nucleus in Ferromagnets 7638
Surface in Bi, Hole Component of the 7910
Surfaces: 9210
of hcp Metals, Effect of Spin-Orbit Splitting on the 7591
of Polyvalent Metals 9209
Fermion Systems 9210
Ferreeds in Switching Circuits, Application of 6246
Ferric Oxide,
Conductivity of 8275
Morphology of γ 7550
Ferrielectricity 7294
Ferrimagnetic:
to Antiferromagnetic Phase Transition in Mn-Cr-Sb System 7033, 7339
Ba Complex Systems, Properties of 6160
Ca-Fe-O Compounds 7651
Compounds Containing Fluorine, Properties of 7904
Ferrimagnetic: (Cont'd)
$FeCr_2O_4$ Spinels 9324
Garnets, Superexchange Interaction in 8791
Linewidth of $BaFe_{12}O_{19}$ 8812
Rare Earth Iron Garnets, Statistics of Superexchange Interaction and Ionic Distribution in Substituted 7340
Resonance,
High Power Effects on 6438
Nonlinear Effects of Crystalline Anisotropy on 7049
Saturation Effects in 6439
Wall Effect in 8810
Resonance in:
Eu-Fe Garnet 7346
Ferrite Spheres 9363
Ni Ferrites 6441
Three-Sublattice Systems 7648
YIG 6440, 7052, 7053, 7347, 7647
Ferrimagnetism of AB_5-Co Compounds 7349
Ferrimagnets,
Adiabatic Demagnetization and Specific Heat in 7952
Molecular Field Coefficients in 6140
Ferrite:
Amplifiers, Double Pump Degenerate 6548
Attenuators 9035
Circulators 6242, 7222, 8462
Core:
Memory Systems with Rapid Cycle Times 7189
Parametron Computer Circuits 7800
and Transistor Memory System 6883
Cores,
Effect of Rare Earth Oxides on the Magnetic Behavior of 9041
Fluxlok Memory Technique Using 6884
High-Speed Coincident Current 6803
Inhibited Flux Operation of 9038
Partial Switching of 6577, 6587, 6588
Preparation of 6585
Residual States in 9039
Reversible Magnetization in 9040
Devices,
Broad-Band Ridge Waveguide 7113
High Power Effects in 6241
Nonreciprocal Single Crystal 6240
Radar Duplexing with 8114
Devices for Computers 9037
Duplexers 6793
Films, Preparation and Properties of 6974, 6976
Films for Logic and Storage, Open Flux Path 6801
Hall Generators 8033
Isolators 6616, 7538, 9036
Limiters 7114
Loaded Waveguide:
Junction, Tetrahedral 6525
Microwave Transverse Switches 9035
Transmitters, Broadband Nonreciprocal 8041
Memory Planes for Extreme Environmental Conditions, Miniature 6798
Micropowders, Magnetic Properties of 9327
Microwave Frequency Doublers 8100
Modulators 7841
Particles, Growth of 6972
Phase:
Modulators 8461
Shifters 6527, 7723
Resonance Isolators, Theory of 6526
Resonators, Oscillations of 8037
Ring Cores for Fast Non-Destructive Read Stores 6587
Rotating Half-Wave Plate, High-Speed 6530
Samples, Walker Modes in Large 6792
Scansors, Properties and Applications of 8040
Slab Loaded Rectangular Waveguides, Modes of a 6249
Spheres,
Ferrimagnetic Resonance Modes in 9363
Susceptibility of 7954
Switches, Broad-Band 6529, 9043
Ferrite: (Cont'd)
Switching Properties 9350
Systems, $CdO \cdot MnO \cdot Fe_2O_3$ 9351
Systems Containing Cu, Square Loop Materials in 9184
Toroids, Flux Reversal of 9348
Transducer Heads 7171
Transducers, Mechanical Filters with 7539
Ferrite-Diode Logic Circuits, Synthesis of 8539
Ferrites,
Alloys for Bonding Thermocouples into 6668
Anisotropic Ferromagnetic Resonance Linewidth in 7650
Compositions and Properties of 7896
Demagnetization of 8792
Ferromagnetic:
Domains in Cobalt Zinc 6139
Resonance in 6144, 7045, 7959
Hall Effect in 8763
Ion Distributions and Valencies in Mg-Mn 8584
Magnetic:
After-Effect in Mg-Mn 7642
Polarity Reversal in 6142
Properties of Mixed 8815
Magnetization in Mn 8787
Magnetoelastic Effects in Co-Fe 7327
Magnetostatic Properties in Ni-Zn 8788
Magnetostriction of Ni-Zn 6365
Measurement at High Signal Levels of Microwave 7641
Paramagnetic Susceptibilities of Fe-Rare Earth 8338
Permeability in 8313
Permeability and Permittivity of 8315
Phase Equilibria of $FeO-MgO-Fe_2O_3$ 8581
Preparation:
of Fine-Particle 7275
and Properties of Low Loss 7056
Production of Ni-Zn 6365
Relaxation Processes in 7964
Resonance Absorption Linewidths in Mg-Mn 7960
Specific Heat of MnZn and NiZn 6477
Stability of 9044
Switching:
by Domain Walls in 6796
Rate in 6795
Ferrites:
with Cubic Anisotropy, Oriented 9187
by the Czochralski Method, Growth of Single Crystal Fe 6971
at High Signal Levels, Measurement of Microwave 7641
in Isolators, Prediction of High Power Performance of 6145
with Large Barkhausen Steps, Rectangular Hysteresis Loop 6141
for Microwave Devices, Preparation and Properties of 8221
Ferroelectric, Resonance Spectrum of a Paramagnetic 6167
Ferroelectric:
and Antiferroelectric Properties of Solid Solutions of $NaNbO_3$-$PbZrO_3$ 7293
$BaTiO_3$-Based Solid Solutions, Preparation and Properties of 9245
Capacitors, Thiourea 6531
Ceramic Devices for Controlling Electroluminescent Display Screens 7445
Ceramics,
Determination of the Nonlinear Characteristics of 7602
Effects of Stress on the Mechanical Properties of 8414
High Temperature Discharges in 7290
Measurment of the Dielectric Constant of 6675
Thermal Conduction in 7289
Characteristics of $PbZrTiO_2$ Ceramics 6085
Colemanite,
Displacement Current Transients Obtained from 6087

Ferroelectric: Colemanite, (Cont'd)
Intrinsic Bias in 9242
Curie Temperature of $PbNb_2O_6$-Type Compounds 6676
Delay Lines, Electrically Variable 7727
Deuterium-Doped Rochelle Salt, Electro-Optic Kerr Effect and Polarization Reversal in 7007
Digital Information Storage and Switching 6592
Domain:
Delineation in Triglycine Sulfate 7291
Effects in the Deuteron NMR Spectrum of KD_2PO_4 9234
Growth, Kinematic Theory of 7923
Films, Preparation of 6978
Glycine Sulfate, Dislocations in 8609
$LiH_3(SeO_3)_2$, Crystal Structure of 8173
Memory Cells 7193
Monocrystals by Zone Recrystallization, Preparation of 6041
Parametric Amplifiers 8074, 8075
$PbNb_2O_6$, Phase Transitions in 7600
$Pb(Ta_2O_5)_2$, Properties of 6679
Properties of:
$BaLi_{2x}Al_{2-2x}F_{4x}O_{4-4x}$ 7292
$BaZr(Nb_2O_6)_2$ 8252
Colemanite 9243
a Complex Ba System 6086
$([N(CH_3)_4]\cdot HgCl_3)$ 8253
$PbTiO_3$ Ceramics Containing Nb or Ta 6678
$Pb(Ti\cdot Zr\cdot Sn)O_3$ Thin Films 7922
Triglycine Sulfate, Temperature Variation Effects on 8691
Triglycine Sulfate and Selenate, Effect of Hydrostatic Pressure on 6083
Rochelle Salt, Paramagnetic Resonance Spectrum of 6166
Solid Solutions Based on $NaNb_2O_6$, Properties of 6680
Storage:
Devices, Nondestructive Technique for Reading Out Information from 6593
Units 8545
Switching 6592
Transition in $Rb(SO_4)_2$ 6387
Triglycine Sulfate,
Preparation of Large Single Crystals of 6043
Transitions in 8692
Ferroelectricity of $K_4Fe(CN)_6\cdot 3H_2O$ 9244
Ferroelectrics,
Applications of 7726
Isotopic Effects in 9233
Microwave Dielectric Dispersion and Loss in High-Permittivity 6076
Paramagnetic Resonance in 6166, 6167
Resonance Quality Factor (Q) of 8248
Structure of 6082
Theory of the Electric Field Variation of Incremental Permittivity in Perovskite-Type 6077
Ferromagnetic:
Anisotropy in Cubic Crystals 6429
to Antiferromagnetic Exchange-Inversion 7336
Co, Nuclear Magnetic Resonance in 6146, 8807
Cores, Reversal of Loaded 7441
Cores with Rectangular Hysteresis Loops, Preparation of 6585
CrO_2, Preparation of 8630
Domains in Co-Zn Ferrite, X-Ray Study of 6139
Fe, Correlation between the Magnetization and the Effective Magnetic Field in 8311
Films,
Electrical Readout from Thin 7808
Flux Reversal by Noncoherent Rotation in 6431
Insulators, Electron Spin Relaxation in 8328
Interaction in Tb 9335
Ferromagnetic: (Cont'd)
Magnetic Anisotropy, Temperature Dependence of 8794
Metals, Polarization of Conduction Electrons in 7643
Parametric:
Amplifiers 6245, 7476, 8072
Amplifiers, Reduction of Pump Power in 8073
Particles,
Anisotropy Energy and Remanent Magnetization of 8790
Superparamagnetism of 9370
Powders, Coercive Force of 9328
Properties, Structure of a System Having 6082
Properties of Garnets 8163, 8329
Resonance,
Anisotropic Elastic Stress Effects on 8809
Effect of Circularly Polarized Radiation on 7959
Resonance:
Absorption Linewidth, Ferrite Size and Shape Effects on 8811
Due to Magnetic Fields Generated by Displacement Current in Ferrites 7045
Experiments, Generation of Phonons in High Power 6706
Experiments at High Peak Power Levels, L-Band 6145
at High Power Levels, Theory of 6710
Line Shape in Insulators, Theory of 7649
Linewidth:
in Ferrites, Anisotropic 7650
Maximum in YIG 7051
Linewidths in Ga Substituted YIG 6143
Parameters, Effect of Surface Irregularities on Single Crystal 6436
in Piezoelectric $Ga_{2-x}Fe_xO_3$ 7046
in Rare Earth Garnets 6705
in Rare Earth Garnets, Giant Anisotropy of 6437
of Thin Ferromagnetic Sheets 8326
at X-Band in Polycrystalline Garnets and Ferrites, High Power 6144
Semiconductors, Recombination in 9264
Sheets, Ferromagnetic Resonance of 8326
Structure Properties of Crystalline Compounds, Theory of 6137
Superconductors,
Intermediate State of 8738
Properties of 7625
Thin:
Film Computer Storage Matrix 7190
Films,
Magnetic Induction of 8310
Magnetization Reversal in 9349
Preparation and Properties of 6655
Properties of 9329
Ferromagnetics,
Anisotropy of Magnetization in 9352
Electron Diffraction Measurement of the Magnetic Gradient at Surfaces of 8308
Flux Reversal Process in 9347
Internal Friction in 8943
Longitudinal Oscillations in 8005
Magnetization of a Dilute Suspension of Multidomain 7955
Magnetoelastic Properties of 8301
Magnetostatic Modes in 9323
Magnetostriction in 9352
Polarization of Nuclei in Nonmetallic 8320
Young's Modulus of 8943
Ferromagnetism,
Anisotropic Superexchange Interaction and Weak 7341
Equivalence of the Critical Concentrations in the Ising and Heisenberg Models of 8306
Theory of: 9321
Spin-Wave Interactions in 6136
Ferromagnetism:
to Antiferromagnetism in Dy 7016
in Dilute Alloys, Critical Concentration for Existence of 8785
in $NaNiF_3$ 8336
and Superconductivity, Coexistence of 6138
of Thin Films 9329
Ferromagnets,
Anisotropy:
in Cubic 6429
of the Intrinsic Domain Magnetization of 7645
Degree of Texture Perfection in 8799
Direct Exchange in 7335
Fermi Contact Interaction of the Magnetic Field at the Nucleus in 7638
Flux Reversal in Soft 8798
Green's Function Applied to 8780
Magnetic State Stability in 8786
Magnetization:
Curve of Heisenberg 8782
in Si-Fe 8805
Magnetocrystalline Anisotropy in 7644
Magnetostrictive Constants of 8775
Refractive Indices of 8906
Spin Waves in 8781
Transverse Magnetization in 8781
Ferromagnets with General Spin, Properties of Heisenberg 7634
Ferrospinel Compositions 6365
Ferrous Fluoride, NMR of F^{19} in 9385
Ferrous Oxide, Defect Structure of 8204
Ferro-Vanadium Oxide, Preparation and Properties of Antiferromagnetic 8631
Field:
Amplification in Zn-CdS-Mn Phosphors 7982
Dependence of:
de Haas-van Alphen Effect in Graphite 7931
Domain Motion in $BaTiO_3$ 7958
Exciton Creation in InSb 7934
Photoelectric Emission from Ta 6193
Spin-Lattice Relaxation in Nd-Ethyl-Sulfate 7968
Effect,
High Frequency 8773
Relaxation Processes in the 6128
Effect:
on Cleaned Ge Surfaces, ac and dc 6129
in Ge 9318
in Ge, Effect of Ion Adsorption on Relaxation Processes in the 6128
at High Frequency 6420
Measurements on Cleaned Ge Surfaces 6422
Modulation of Photoconductors, Measurement of Drift Mobility Using the 7070
in Semiconductors, Frequency Dependence of the 6127
Transistors 6504, 8029
Effects on Mobility of Surfaces 8264
Emission:
Microscope for Surface Studies 8633
at Narrow p-n Junctions in InSb, Internal 6747
from TiO_2 9317
Field-Ion Microscope for Surface Studies 8633
Figure of Merit for Varactors 8960
Filamentary Crystals, Growth of 7895
Filaments, Influence of Transverse Modes on Photoconductive Decay in 6392
Filaments:
by Controlled Dissolution, Production of Alkali Halide 6658
of Ge, Photoelectric Etching Technique for Preparing Thin 7267
File Drum as a Computer Storage, High Density 6285
Film:
Boiling Technique for Preparing Semiconductor Grade Si 6325
Memories, Cryogenic 7543
Resistors, Fabrication and Applications of Deposit 8415

Films - See also Specific Materials
Films,
  Deposition of 7886
  Evaporation of:
    Ge 6652, 7257
    Phosphor 6968, 7894
    Si 6653
  Growth of Anodic Oxide Ge 6346
  Oxidation of Thin 8636
  Preparation of:
    $BaTiO_3$ 6042
    Carbon 7269
    Epitaxial:
      Ge 7268
      Si 7268
    Ferromagnetic 6655
    Ge 6649, 7885, 7887
    Si 6649, 7578
  Semiconductor 7276
Filter:
  Circuits 8521
  Structures for Parametric Amplifiers 8066
Filters,
  Bandpass 6563, 6820, 7451, 7498
  Low Frequency 8036
  Low Pass Subaudio 6269
  Ripple 7811
  Stabilization of 9102
  Tunable Microwave 6791
  Twelfth-Order Tchebycheff Parameter Bandpass 6820
Filters:
  with Ferrite Transducers 7539
  for Multiplexed Telemetry 6269
  for Pulsed Sinusoids 6270
Fission:
  Fragment Detectors 8570
  Probe, Semiconductor 6608
Flagpole Whiskers, BeO 6045
Flame Fusion Process of Growing YIG 6040
Flash Etching Technique for Al_2O_3 8189
Flat Surfaces on Ge Dendrites, Growth of Atomically 6349
Flaws in:
  Heavily Doped Semiconductors, Solubility of 7545
  YIG Crystals, Detection of 6322
Flip-Flop Cryotron Circuit 8476
Flip-Flops, Switching and Memory Criteria in 7763
Float Zoning of Si, Shape of Melt-Crystal Interfaces during 6958
Floating:
  Crucible Technique of Growing Single Crystals 6024
  Zone:
    Growth of:
      Crystals, Arc Image Furnace 7265,7266
      GaP 6359
    Refining of GaAs, Apparatus for the 7576
    Techniques, Modified RF Coil to Facilitate 7264
  Zones in Rods with Various Zone Shapes 7262
Flow:
  Graphs Using Array of Non-Touching Loops 9054
  Meters, Thermistor 8148
  Stress of Mg, Parameters Influencing 8412
Fluctuations:
  of Donors and Acceptors in p-n Junctions 6744
  from the Nonequilibrium Steady State 6125
Fluorescence:
  in Alkali Halides, Color Center 8380, 8886
  Line, Strain-Induced Splitting of Cr 7386
  Line of $MgO:Cr^{3+}$, Zeeman Effect of the Purely Cubic Field 7360
Fluorescence of:
  $BaO-TiO_2-P_2O_5$ System 6318
  CdS 6456, 8887, 8888, 9150, 9413, 9416
  CdSe 7396, 9416
  Ho in Scheelite Structure Crystals 8381
  NaI 7064
Fluorescence of: (Cont'd)
  ZnO 8361
  ZnS 6456, 9414-9416
  ZnSe:V 9416
Fluorescent Tubes, Transistor Power Supplies for 6598
Fluoride Crystals, Optical Absorption in 7980
Fluorine in Hexagonal Ferrimagnetic Compounds 7904
Fluorine^{19} in FeF_2, NMR of 9385
Flux:
  Measurement of Thin Magnetic Films 7953
  Meters, Hall Effect 9019
  Reversal by Noncoherent Rotation in Magnetic Films 6431
  Trapping in a Superconducting Ring 9294
Fluxlok:
  Memory Technique Using Ferrite Memory Cores 6884
  Technique in a Random-Access Memory, Use of the 6589
Forbidden Zone Width of ZnS Structure Crystals 8658
Forming Circuits, Magnetic Pulse 8568
Forward Characteristics of Junctions 6494, 8014
Four-Layer:
  Diode Switching Circuits 7823
  Diodes 8954
  Semiconductor Device, Fabrication of 8432
Four-Point Probe Measurement of Resistivity 6400, 9273, 9274
Fracture in Elemental and Compound Semiconductors, Brittle 7559
Free:
  Carrier Generation in Photoconducting Anthracene, Extrinsic Model of 7927
  Energy of:
    the Fe-Al System 9326
    Formation of:
      Group III-V Compounds 6626
      PbSe, Standard 8158
      SiC, Standard 6625
  Radicals, Spin-Lattice Relaxation in 6172
Frequency:
  Characteristics of Tunnel Diodes 8012
  Converters 6560, 8062, 8122, 8514
  Counting Circuits 6839
  Detectors 8511
  Dividers 6488, 7153, 7158, 8097, 8098, 9095
  Doublers 8099, 8100
  Inverters 8498
  Meters 7525, 8561
  Mixers 8100
  Modulators 9088, 9101
  Multipliers 7773, 8097, 8101, 9253
  Response:
    of Infrared Detectors, Measurement of the 9027
    Meters 7843
  Stabilization for Reflex Klystrons 7815
  Standard:
    Oscillators 7478
    Units 9148
Friction:
  of Metals in Reciprocating Sliding, Low 9195
  by Sonic Vibrations, Reduction of 9194
Fringe Comparator Employing Photodevices 8147
Functional Units,
  Electronic 6516, 6774, 6776, 7104, 7121, 8487
  Multivibrator 6309
  Shift Register 6775
  Twin-T Network 6776
Fused Contacts to SiC 7026
Fuses for Rectifiers 7460
Fuzing Systems, Use of Four-Layer Diodes in 7822

G

Gadolinium,
  Electrical Resistivity of Polycrystalline 7016
Gadolinium, (Cont'd)
  Magnetic Properties of Evaporated Thin Films of 9330
  Magnetostriction Temperature Dependence of 8777
  Thermal Expansion of 8777
Gadolinium^{3+} in:
  $CaWO_4$, Paramagnetic Resonance of 8353
  Single Crystal Oxides, Paramagnetic Resonance of 8847
Gadolinium Iron Garnets,
  Magnetostriction of 6428
  Optical Properties of Ga-Sbustituted 9429
Gain:
  Control Techniques, Semiconductor 7127
  Controls, Amplifier 7128, 9060, 9061
  in Double Tetrode Transistor 8023
  Stabilization of Varactor Amplifiers 8070
Gallium,
  Anisotropy of the Magnetic Sysceptibility of 7326
  Dissolution of Quartz by 6928
  Nuclear Quadrupole Resonance in Superconducting 7030
  Purification of 6356, 7271
  Solubility of Ge in 6001
Gallium:
  Alloys as Electrodes 6668
  in Ge, Solubility of 7228
  in the Normal and Superconducting States, Thermal Conductivity of 8917
  and Quartz, Reactions between 6928
  in Si,
    Diffusion of 6335
    Solid Solubility of 6002
Gallium Antimonide,
  Conduction Band of 6060, 6378
  Diffusion of Impurities in 6069
  Effect of:
    Impurities on the Electrical Properties of 6069
    Pressure on the Electrical Properties of 6068
  Electrical Properties of 6060
  Energy Band Structure of 6068
  Piezoresistance of 8724
  Properties of 6623
  Reflection Spectrum of 8392
Gallium Antimonide-Aluminum Antimonide:
  Alloys,
    Electrical Properties of 6361, 6623
    Preparation of 6361, 6623
  System, Solid Solution in the 6361
Gallium Antimonide-Germanium Alloys, X-Ray Diffraction Study of 6622
Gallium Antimonide-Indium Antimonide, Physical Properties of 8725
Gallium Arsenic Phosphide, Preparation of a Graded Energy Gap Alloy- 7076
Gallium Arsenide,
  Behavior of Carbon in 7253
  Calculation of Mobility in n-Type 6107
  Commercial Availability of 6610
  Conduction Bands of 6378
  Correlation between Etch Pits and Edge Dislocations in 7244
  Cu Effect in Heat Treatment of 6669
  Diffused Junctions in 6356
  Diffusion of:
    Cd in 8623
    Cu in 6357
    S and Se in 7865
    Zn in 7228, 7566, 7572
  Direct Recombination in 7009
  Distribution:
    Coefficient of Zn in 8166
    Coefficients of Impurities in 7233
  Effect of Crystallographic Polarity on the Perfection of 8209
  Electrical Properties of 6356
  Electron Transport in 7282

Gallium Arsenide, (Cont'd)
Energy Band Structure of 7281, 7282
Etchants for Revealing Dislocations in 8641
Excitons in 6389
Floating Zone Refining of 7576
Growth of 6342, 6356, 6956, 7253, 7271, 7431, 7882
Growth Mechanism of 8207
Hall Coefficients of Si Doped 8762
Heat Treatment of 6669
Impurity Levels in 6357, 7271
Magnetic Crystal Puller for Growth of 6956
Magnetoresistance of 8765
Mobility in 6357, 7271, 7253
Mobility Killer in 6105
Ohmic Contacts to 8235
Photoelectric Measurements on 9257
Photoemission from 8389
Preparation of Junctions by the Decomposition of 7419
Purification of 6356
Reflection Spectrum of 8392
Surface Damage in 6660
Thermal:
Conductivity Conversion Due to Cu in 8273
and Physical Properties of 8932
Gallium Arsenide:
Dendrites, Growth and Properties of 6657
Detectors, γ-Ray 8573
Diodes 6226, 6308, 6612, 6732, 6739, 7150, 7431, 7836, 8419, 8956, 8964
Electrolyte Interface, Photovoltaic Effect at a 6720
Microwave Diodes, Conversion Loss of 6732
Photodiodes for the Visible Region 6782
Photovoltaic Energy Converters 6519
Power Rectifiers 7091
Solar Converters 6786
Transistors 7431
Tunnel Diodes 6739, 7150, 7431, 8956
Varactor Diodes 6226, 6308, 7836
Gallium Arsenide-Aluminum Arsenide Alloys,
Electrical Properties of 6360
Homogeniety and Composition of 6360
Preparation of 6360
Gallium Arsenide-Gallium Phosphide Alloys, Properties of 7272
Gallium Arsenide-Germanium Alloys, Device Applications and Growth of 8980
Gallium Arsenoselenides, Conductivity and Other Properties of 7942
Gallium Garnets, Paramagnetic Resonance of Ytterbium in 6446
Gallium-Indium Antimonides, Properties of 8725
Gallium Iron Oxide, Ferromagnetic Resonance in Piezoelectric 7046
Gallium Iron Oxide Resonators, Piezoelectric and Magnetostrictive Properties of 6681
Gallium Phosphide,
Crystallization of 6965
Electrical Properties of 6358
Electroluminescence in 8882
Growth of 6359, 7882
Impurities in 8203
Infrared:
Absorption in 8855
Properties of 8852
Luminescence of 7990
Photovoltaic Effects in 7990
Preparation of 6358, 6359, 7703
Properties of 6358, 7703, 8882
Thermal Expansion of 8852
Gallium Phosphide:
Diodes, Radiative Recombination in 8872
Junctions, Preparation and Characteristics of 6500
Gallium Phosphide-Gallium Arsenide Alloys, Properties of 7272
Gallium Phosphide-Silicon:
Alloys, Solubility Enhancement in 6621
Growth of 6621
Gallium Sulfo-Selenide, Photoconductivity of 8900
Gallium Telluride with II-VI Tellurides, Solid Solution of 7230
Gallium Telluride-Zinc Telluride, Variation of Energy Gap Width with Composition in the System 7230
Galvanomagnetic:
- See also Magnetoelectric
Effect in Crystals, Theory of 7905
Effects in:
Ge 9299
Sn at Low Temperatures, Oscillations in 6120
Properties, Effect of Random Inhomogeneities on 7019
Properties of:
Pyrographite 7948
Zn 9296
Galvanometer:
Current Limiters 6844
Driver Amplifiers 7203
Gamma-Ray:
Detectors 8570, 8573
Spectrometers 7528
Garnet Resonators, Magnetically Tunable Microwave Filters Employing Single Crystal 6791
Garnets,
Effect of Pressure on the Spectrum of 9394
Ferromagnetic:
Properties of 8329
Resonance:
of Rare Earth 6437
at X-Band in Polycrystalline 6144
Magnetic Properties of 6159
Microwave Properties and Applications of 7054
Paramagnetic Resonance of Yb^{3+} in Al and Ga 6446
Permeability Characteristics of Mixed Y-Ga-Fe 6444
Preparation of:
High Permeability 8330
Polycrystalline 6443
Solid Solutions in 8163
Superexchange Interactions in Ferrimagnetic 8791
Synthetic 6646
Garnets for Microwave Applications 7216
Gas
Absorption by Vacuum Evaporated Magnetic Films 6149
Adsorption on Ge Surfaces 6368
Etching and its Effect on Semiconductor Surfaces 8643
Gases Adsorbed on Semiconductor Surfaces, Mass-Spectrometric Determination of 6046
Gates,
Binary 8508
Cryotron 7447
Solid State 6774
Zener Diode Bridge 7480
Gating:
Circuits 9084, 9085
Circuits, Diode 8507
Elements, Zener Diodes as Voltage Breakdown 7765
Systems,
Parametric 8122
Superconductive 8094
Gauge Invariance in the Theory of Superconductivity 6406
Generation of Microwaves Using the Faraday Effect 6195
Generation-Recombination Noise in Semiconductors 6126
Generator:
Regulators 9129
Generator: (Cont'd)
Supply, Tunnel Diode 7544
Generators - See also Oscillators
Generators,
Diode UHF 8099
Hall 6298
Harmonic 6496, 8099, 8101, 9096, 9097
Microwave 8087
Millimeter Wave 8088
Pulse 8515-8517, 9099
Ramp Function 9100
Sawtooth 8527
Thermoelectric 6310
Tone 8112
Ultrasonic-Frequency Power 6294
Waveform 9101
Germania, Young's Modulus of 9449
Germanium,
Absorption in 6180, 8864
Absorption of Light by Charges Liberated by th
Photoelectric Effect in 6451
Acceptor Levels of Cu in 7587
Acoustic Absorption by Phonon-Phonon Interac
tion in 6212
Aggregative Reactions of Oxygen in Solid Solu
tion in 6338
Annealing of Gamma Ray Damage in 6056
Anodic Oxide Film Growth on 6346
As Doped 6344
Atom Ejection Patterns in Sputtering of Single Crystal 7279
Atomic Scattering Factor of 8242
Attachment of Gold Electrodes to 6374
Capture Cross Sections in 8704
Carrier:
Multiplication in 9253
Recombination in 6092, 9262
Transport in 8709
Cleavage Planes of 7559
Conductivity of 8720, 9280, 9281, 9285
Conductivity:
Anisotropy of Hot Electrons in 8722
Fluctuations in 7940, 7941
Contacts for 9010
Cyclotron Resonance in 6122, 8295, 8296
Decay Times of X-Ray Excited Carriers in 668
Defects in 6627, 6935, 7929
Deformation of 7690
Deformation Potentials in 7586
Delineation of Diffused p-n Junctions in 8444
Density Reduction in 6627
Dielectric:
Constant of 8672, 8673
Constant Measurements in 6075
Diffusion in 8620
Diffusion of:
Ag in 7569
As in 6333, 7228, 7568
Au in 8622
Cd in 7569
Cu in 6620
Fe in 7569
Hydrogen in 7250
Minority Carriers in 6073
Oxygen in 7570
Sb in 6332
Ta in 7569
Te in 7569
Dislocations in 6007, 6662, 7234, 8187, 820
Dissolution of 6984
Distribution:
Coefficient of In in 8165
Coefficients of Impurities in 7232
Function in 7296
Drift Mobility of Carriers in 7609
Effect of Shear on Impurity Conduction in n-T
7614
Electrical:
Conduction at Low Temperatures in 6405
Effects of Oxygen in 6179
Properties of 6998

ermanium, (Cont'd)
Electrical Properties of Grain Boundary Layers in 6072
Electrolytic Etching of 6661
Electron:
Density Distribution in 8242
Emission from 8390
Mobility in 6397
Emission of Auger Electrons from 7631, 9314
Energy:
Band Structure of 7281
Gap in 7913
of Grain Boundaries in 6323
Levels in Gold-Doped 6064
Epitaxial:
Film Growth of 7268
Ge Layers on 8215
Etching of 6372, 6982, 6986, 6987
Evaluation and Control of Diffused Impurity Layers in 7249
Exciton Energy Levels in 8695
Excitons in 7370
Faraday Effect in 6998, 7395
Field:
Dependence of Carrier Mobility in 6101
Effect in 6128, 6420, 9318
Galvanomagnetic Effect in 9299
Gas Etching Effects on Single Crystal of 8643
Growth of 6024, 6640, 6641, 6651, 6955, 7243, 7260, 7261, 8200, 8211
Growth Striations in 8191
Hall:
Coefficients of 8294, 8761
Effect in 6415, 9282
Mobility in 7932
Heat of Solution of Cu in 6620
High Energy Electron Irradiation of 8649
Hole Energy Spectrum of 7912
Hollow Cylindrical Seeds Used in Growth of 8210
Hot Electrons in 6388
Impurities in 6196
Impurity:
Bands in 6379
Conduction in 7613, 7614
States in Doped 6379
Influence of Hydrofluoric Acid on the Dissolution of 7278
Interaction between Arsenic and Aluminum in 6018
Internal Friction in 8945-8947
Ion:
Bombardment Etching of 6049
Radius of 8242
Lifetime of 7605, 8700, 8701, 8864
Magnetic Susceptibility of:
Fe and Zn Doped 6425
p-Type 7324
Photogenerated Carriers in 9371
Magneto-Optic Effect in 7370, 7909
Magnetoplasma Resonance in 9303
Magnetoresistance of 7316, 7613, 7947
Mechanical Damping of 6213
Nernst Effect in 6206
Neutron Radiation Effects in 6627, 6672, 7929
Noise in 9307, 9308
Optical:
Constants of 6473
Effects of Oxygen in 6179
Oxidation of 7581, 8637
Peltier Effect in 8003
Photoconductivity of: 8259, 8386, 8864, 8894, 9424
Grain Boundaries in 8896
Photoelectric Etching Technique for Preparing Thin Filaments of 7267
Photoelectrical Properties of Grain Boundary Layers in 6072
Photoemission from 8389, 8390
Photomagnetoelectric Effect in 9428
Piezoresistance of 7003, 8724
Polarizability of Free Carriers in 7010

Germanium, (Cont'd)
Production of 8155
Properties of Vapor Grown 6640, 6641, 6651
Purification of 8619
Radiation:
from Breakdown Avalanches in 7675, 7676
Effects in 6755
Radiative Recombination in Electron Bombarded 8373
Reaction:
with Aqueous Solutions of 6369
of Oxygen in 6338
Recombination:
Centers in 6196
of Electrons and Donors in 7297
Radiation in 6181
Reflectivity of 7010, 8392
Refractive Index of 7994
Relaxation Processes in 6128
Resistivity:
of Heavily Doped n-Type 6686
Homogeneity of 6401
Variations in 6648
Role of Twin Planes in Rapid Dendritic Propagation of 6656
Scattering in 6109, 7301, 8265
Seebeck Coefficients of 6478, 9437
Solid Solubilities of Impurity Elements in 6002
Solubilities of 6001
Solubility of:
Ag, Fe, Cd, Te, and Ta Radioisotopes in 7569
Ga in 7228
Interstitial Impurities in 7869
Spin Resonance in 7663, 9220
Spin-Lattice:
Interaction for Donor Electrons in 6168
Relaxation in 9304, 9305
Statistics in 7295
Structural Defects in 6935
Surface:
ac and dc Field Effect on Cleaned 6129
Adsorption of Gases of 6046, 6368
Breakdown of 7632
Chemisorption of Oxygen Gas of 6368
Concentration of In in 6331
Conductivity of 7321, 8284, 8299, 9282
Levels of 9213
Mobility of Carriers in 7267
Properties of 6422, 8160, 8233, 8774, 9311, 9312
Recombination Velocity of 9283
Relaxation in 9319
States on 6129, 6670, 8664
Structure of 6644
Tension of 8160
Susceptibility of: 8823, 8848
Donors in 7325
Thermal:
Conductivity of 6202, 7071, 7398, 7683, 9432
Diffusivity of 6726
Thermoelectric Power of 7398
Transmission of X-Rays in 7371
Tunneling Probability in 8418
Twin Boundaries in 8188
Valence Band Structure in External Magnetic Field of 7909
Valley-Orbit:
Splitting in 6062
Splitting of Sb in 7003
Germanium:
by Alloying, Plastic Deformation of 6748
Dendrites,
Growth of: 6033, 7270, 7888-7893
Atomically Flat Surfaces on 6349
Growth Steps on the Surface of 6963
Orientation of Etch Pits on 6664
Propagation Mechanism of 6350, 6656
Use of Pulse Plating Techniques to Study the Growth of 6353
Diodes, Surface Effect in 6421

Germanium: (Cont'd)
in Electrolytes, Dissolution Kinetics of 6369
Films,
Absorption and Refraction in 6716
Adsorption of O_2 on 9192
Formation of 6032, 6649, 7268, 7885, 7887
Preparation of Vacuum Evaporated 6652, 7257
Texture in Evaporated 7257
Liquidus Curves 6001
at Low Temperatures, Contact Phenomena in 6405
p-n-p-n Switch, Sandwich Structure for 6760
Saturated with III-V Compounds, Preparation of 8162
Germanium-Gallium Antimonide System, Metastable Solid Solutions in the 6622
Germanium-Gallium Arsenide Alloys, Device Applications and Growth of 8980
Germanium-Silicon,
Comparison of the Etch Rate of 6985
Electrical Conductivity and Hall Effect of 7619
Mobilities in 7619
Preparation of 7619
Reflection Spectrum of 8392
Susceptibility of 8824
Germanium Telluride, Thermoelectric Properties of 7400
Glass, Radiation-Induced Defects in Lead Silicate 8648
Glass Coatings for Junctions, Protective 8985
Glasses,
Electrical Properties of Certain Semiconducting Oxide 7311
Optical Properties of Semiconducting 7674
Thermoelectric Power of Some Semiconducting Oxide 7311
Glow:
Curves, Evaluation of Thermal Activation Energies from 6208
Curves of Thermoluminescence of ZnS 8379
Glycine Sulfate, Dislocations in Ferroelectric 8609
Gold,
Electroless Deposition of Au on 6992
Point Defects in 9197
Range of Electrons in 9200
Zone Refining of 8194
Gold:
Activated Zn-CdS-Mn Phosphors 7982
Electrodes to Si and Ge, Attachments of 6374
Films Grown by Vacuum Deposition, Structure and Mechanical Properties of Single Crystal 7079
in Ge,
Diffusion of 8622
Optical Studies of 6196
Gold-Doped Ge, Energy Levels in 6064
Gold-Induced Climb of Dislocations in Si 7242
Gold-Aluminum Electrodes to Si, Attachment of 6375
Gold-Copper Alloy, Effect of Neutron Irradiation on 9199
Gold-Germanium Eutectic Junctions 8977
Gold-Nickel System, Kirkendall Effect in the 7864
Gold-Tin Electrodes to Si, Attachment of 6375
Grain:
Boundaries,
Destruction of Excitons by 6389
Electroluminescent 8882
Magnetic Stray Fields at 9331
Photoconductivity of Ge 8896
Photoresponse of 6788
Structure and Properties of 8610
Boundaries:
in Al_2O_3, Etching of 8189
on Barrier Potential, Dependence of the Capacitance of 9179
in CdS, Etch Pits of 8182
in Diamond Lattice 8611
in Ge, Energy of 6323
on Minority Carrier Diffusion, Influence of 6073

Grain: (Cont'd)
Boundary Layers in Ge, Electrical and Photoelectrical Properties of 6072
Growth, Growth of Large CdS-Type Crystals by 6962
Graph Plotter, Transistorized 8152
Graphite,
Annealing of Electron Radiation Damage in 7583
Band Structure of 6715
de Haas-van Alphen Effect in 7931
Diamagnetic Susceptibility of 9215
Diamagnetism of 6715
Dislocations in 6633, 6938, 8598
Energy Band Structure of 9215
Etch Pits in Pyrolytic 6663
Hall Coefficient of 8291
Magnetoresistance of 8291
Radiation Damage Annealing in 7583
Spin Resonance of Charge Carriers in 8772
Surface States of 7004
Thermal Properties of 9441
Graphitization Stress as a Source of Dislocations 9172
Group:
I^b-In-VI^b_2 Compounds, Phase Diagrams of 7274
II-VI Telluride Alloys, Solid Solution in 6624
II^b-In_2-VI^b_4 Compounds, Phase Diagrams of 7274
III-V:
Compounds,
Crystal Growth Phenomena for 6341
Group IV Doping of 8197
Ohmic and Rectifying Contacts for 9010
Preparation of Ge Saturated with 8162
Surface Damaged Layers and Crystalline Perfection in 8234
Techniques for Revealing Twin Boundaries in 8188
Thermodynamic Properties of 6626
Vapor Pressures of 6626
Intermetallic Compounds, Inhibition of {111} Surfaces of 8640
V-VI-VII Compounds, Photoconductivity of 8901
VI-Silver Compounds, Properties of 8734
Grown Junctions, Fabrication of 8996
Growth, Reduction of Dislocations Introduced during Crystal 6343
Growth:
Mechanism in Dendrites, Lateral 6352
from the Melt, Cellular Interface Morphology during 6957
Patterns of Quartz 8190
Phenomena for III-V Compounds, Crystal 6341
Poisoning of LiF from Aqueous Solutions 7579
Steps on the Surfaces of Dendrites 6963
Striations in Ge, Detection of 8191
Studies by Pulse PlatingTechniques, Dendritic 6353
Growth of:
- See also Preparation of, Synthesis of
AgSe 7077
Alkali Halides 8618
AlP 7589
AlSb 6362
Anodic Oxide Films on Ge 6346
Anthracene 8219
Atomically Flat Surfaces on Ge Dendrites 6349
$BaTiO_3$ 7920, 8224
$BaTiO_3$-$PbTiO_3$ 8225
$BaTiO_3$-$SrTiO_3$ 8225
$CaWO_4$ 8222
CdS 6961, 6962, 7880, 8213, 8214
Crystals, Theory of 7875
Cu Whiskers 6970
Cu_2O 7883
Dendrites - See Dendrites, Growth of
Epitaxial Si 8201, 8216, 8628
Ferrite Particles 6972
Ferrites 6971
Films 7886
GaAs: 6342, 7253, 7431, 7576
Dendrites 6657
GaAs-Ge 8980
Growth of: (Cont'd)
GaP: 6359
Phosphors 7990
GaP-Si 6621
Ge: 6344, 6640, 6641, 6651, 6955, 7261, 8162, 8200, 8210, 8211, 8955
Dendrites 6033, 7270, 7888, 7890-7893
Films 6649, 7885, 7887
Group III-V Compounds 7882
HgS 7881
HgSe-HgTe 6931
InAs 6036, 7878, 7882
InP 7882
InSb 6026, 6036
Metal Chelate Salt Crystals 6367
MnBi Films 7873
PbS 8214
PbTe 7877
Phosphors 7894, 7988, 7991
Polyoxymethylene Single Crystals 9188
Quartz 7884, 8223
Se 8908
Semiconductors 6029
Si: 6013, 6025, 6027, 6028, 6324, 6325, 6647, 7261, 8211
Films 6649, 7879
by Thermal Decomposition of $SiCl_4$ 8212
SiC 6937, 6960
Single:
Crystals, Arc-Image Furnace for 6044
Crystals with Constant Resistivity 6024
Whiskers from Solid Metal 7895
YIG 6040, 6364
Yttrium-Gallium Garnet 6364
ZnF_2:Mn 8217
(Zn,Hg)S Phosphors 7988
ZnO 8218
ZnS 6039, 6354, 7874, 8213, 8214
ZnS-In Phosphors 7991
Zn_3Sb_2 6363
Guanidine Alum, Paramagnetic Resonance Spectrum of Cr^{3+} in 6167
Guanidine Aluminum Sulfate Hexahydrate, Reversal of the Spontaneous Polarization in 7598
Gyrators 6240, 6525, 8056
Gyromagnetic:
Media, Characteristics of Wave Guides with 8466
Ratio of:
Fe 9333
Ni 9333
Supermalloy 7343
Rods,
Multimode Propagation in 6528
Polarization of Electromagnetic Waves by 8042

H

Half-Wave Plate, Ferrite Rotating 6530
Halides, Structure of 8587
Hall:
Coefficient, Cryostat for the Measurement of 8267
Coefficient 9269, 9277
Coefficient of:
Bi_2Se_3 8268
CdS 6133, 8591
CdTe 8764
GaAs 8762
GaSb 6068
Ge 8294, 8761
Graphite 8291
InSb 6414, 7937, 8731
PbTe 6413
Polar Semiconductors 9271
Si 7943, 8237, 8293
SnS 7273
Ti_2O_3 7309
Effect,
Identification of Impurities Using the 6941
Hall: Effect, (Cont'd)
Longitudinal 6415
Measurement of the 7308
Effect:
Amplifier 8450
Devices 6195, 8760, 9018-9020
Impedance Relays 6601
Magnetometer for Measuring Ion Beam Currents 6297
Measurements on Semiconductors at Microwave Frequencies 6699
Memory Devices 8449
Microwave Mixer for Measuring Carrier Mobility 6100
Multipliers 6903, 7105
Effect in:
Ag-Sb-Te 7020
AlSb-InSb 7938
Ferrites 8763
Ge 9282, 9299
Ge-Si 7619
InSb 9300
NaCl 7597
PbTe 8292
Poly-Copper Phthalocyanine 6424
Pyrographite 7948
Semiconductors at Microwave Frequencies, Measurement of the 6699
Si 6104
Sn 6120
Superconductors 7314
Vitreous Materials 7949
Field, Frequency Dependence of the Complex 6699
Field in Cd_2As_3 6121
Generator with Large Ratio of Length to Width 6698
Generators,
Characteristics of 8034
Frequency Dividers Utilizing 8098
InAs 6298, 7220
InSb 6298
Magnetic Field Measurements with 8034
Output Multiplication in 8033
Mobility, Measurement of High Temperature 7597
Mobility:
to Drift Mobility for Electrons and Holes, Evaluation of the Ratio of 6683
in Ge, Microwave 7932
of Holes in AgBr 6106
in Molecular Solids 7008
in Neutron Irradiated Ge 6672
Probes, Magnetic Flux Pattern Measurements Using 7527
Probes:
with Large Outputs 8563
for Measuring Magnetic Flux Density in the Air Gap of Rotating Machines 8562
Voltage:
Generators 6412
in an Inhomogeneous Magnetic Field 6698
Hall-Voltages, Elimination of Thermoelectric Voltage Errors in the Measurement of 6412
Hamiltonian for:
Bloch Electrons in an Electric Field 6091
the Paramagnetic Spectrum of Fe in $SrTiO_3$ 6712
Hardening, Dislocation Effects on 8601, 8606
Hardware, Transistor 6313
Harmonic:
Approximation Calculation of Lattice Specific Heat and Free Energy 7916
Coupling in Ruby 7970
Generation with "Gradual Grade" Diffused Si Junction Diodes 7115
Generators 6496, 6843, 7157, 7490, 7835, 8099 - 8101, 9096
Health Physics Monitoring, Use of Semiconductor Detectors in 7212

Hearing Aid:
  Amplifiers 9065
  Capacitors 6922
Hearing Aids 7542
Hearing Aids, Solar Powered 9118
Heat:
  Capacity, Low Temperature 9210
  Capacity of:
    Bi_2Te_3 8914
    $MgNi_2$ 9374
    $MnCl_2 \cdot 4H_2O$ 8401
  Dissipation of Power Transistors, Method for 9011
  Dissipators for Transistors 8447
  of Dissociation of CdSb 8159
  of Formation of SiC 6625
  of Fusion of Cd-Te 6317
  Pumps, Peltier 8460
  Sinks for:
    Diodes 8426, 8446
    Transistors 8446
  of Solution of Cu in Ge 6620
  of Sublimation, Correlation of Solid Solubility with 6002
  Transfer Mechanisms in Ceramic Oxides 8405
  Treatment, Formation of Spin Centers in Carbons by 7368
  Treatment:
    on Alnico V Magnets, Effect of 9346
    of CdS Films 8384
    of GaAs 6669
    of InSb 6021
    of Si 7617
    of ZnS 6354
Heating of Carriers in Semiconductors, Microwave 6090
Heisenberg Magnets with General Spin, Properties of 7634
Heitler-London Conductivity Mechanism 8718
Helical Spin Configuration, Magnetization Process of a 7031
Hexagonal Solids, Debye Temperature of 8913
Hexammine Nickel Chloride, Paramagnetic Resonance in 8357
Hexammine Nickel Halides, Low-Temperature Magnetic Behavior of 7652
High Frequency:
  Amplifiers, Design of 8058
  Equivalent Circuits for Junction Transistors 6255
  Transistors, Fabrication of 8998, 9004, 9005
High Power Switching Circuits 9086
High Voltage Power Supplies 8553, 8564
Hole:
  Component of the Fermi Surface in Bi 7910
  Energy Spectrum of Ge and Si, Effect of Deformation on 7912
  Mobility in:
    Doped Si 7608
    Se 7607
Hole-Capture Cross Section of Defects Produced by γ Irradiation 7605
Holes, Energy Levels of 7911
Holes:
  - See also Carriers
  in Semiconductors, Measurement of Excess 6683
Holmium, Electrical Resistivity of Polycrystalline 7016
Holmium:
  in Crystals with the Scheelite Structure, Fluorescence of 8381
  Metal, Low-Temperature Magnetic Remanence, Molecular Field, and Approach to Saturation of 6150
Homogeneity of:
  Gallium Arsenide-Aluminum Arsenide Alloys 6360
  the Resistivity of Ge, Photovoltaic Evaluation of the 6401
Hook Collectors, Fabrication of 9002, 9003
Hot:
  Carriers in Ge, Scattering of 6109
  Electron Emission from:
    Ge 8390
    Si Junctions 6222
  Electrons in:
    Ge 6388, 8722
    Nonpolar Crystals 7924
    Si 6388
Humidity, Use of Peltier Cooling to Measure 7206
Hybrid Computers 8549
Hybrid-π Circuit for Junction Transistors 8027
Hydrogen, NMR of Solid 8346
Hydrogen:
  in Ge, Diffusion of 7250
  on Ge Surfaces, Desorption Processes of 8231
  Reduction of CuI Vapor, Mechanism of 6970
  in Semiconductors, Solubility of Interstitial 6020
Hydrothermal:
  Crystal Growth of ZnO 8218
  Preparation of Solid Solutions from II-VI Compounds 6030
Hygrometers Using Peltier Cooling, Automatic Dew-Point 7206
Hyperfine Structure:
  of the Cr^{53+++} Ion in Ruby by Double Resonance 6447
  in the Electron Paramagnetic Resonance of Mn:ZnF_2 6449
Hysteresis:
  Loop:
    of $BaTiO_3$ 8685
    of MnO_2 8690
    Tracer for Thin Magnetic Films 7953
    of Triglycine Sulfate, Aging Process Effects on 9241
  Loops of Polarized Polycrystalline $BaTiO_3$ 7601
  in NiFe Thin Films 9183
  in X-Ray Damaged Rochelle Salts 8247

I

IF Amplifiers 8062, 8063
Ignition System, Transistorized 7776, 9106
Image Intensifiers 7110, 9032, 9033
Impact Ionization in Semiconductors 8717
Impedance:
  of Diodes,
    Inductive Character of 8962
    Measurement of the 7124
  of Microwave Diodes, Cartridge 6217
  Transformation from a Mesa Diode to a Transmission Line 7124
Impedances, Transistor Matching 6256
Imperfections, Dependence of the Coercive Force on 6703
Imperfections:
  in CdS Type Crystals, Photoelectric Analysis of 8591
  in Ge Junctions, Direct Viewing of 7704
  on Lattice Thermal Conductivity, Effect of Point 7074
Impulse Selection for Ferrite Core Logic 7183
Impurities,
  Analysis of 6940, 6942, 8613, 8615
  Carrier Properties in Semiconductors Containing Multiply-Ionized 6682
  Hall Effect Identification of 6941
  Interstitial Solubility in Ge and Si 7869
  Zone Equalization and Distribution of 7866
Impurities in:
  GaSb, Diffusion of 6069
  Ge, Optical Studies of 6196
  InAs 6014, 6339
  NaCl, Phonon Scattering by 7684
  Semiconductors 6020, 6944, 7376, 7545, 7566
  SiC 6943, 8614
Impurities during Epitaxial Vapor Growth of Ge, Introduction of 6651
Impurity:
  Band:
    Conduction Model for Rutile 6404
    Theory 6379
Impurity: (Cont'd)
  Concentration Dependence of Refractive Index of Ge 7994
  Conduction, Dielectric Theory of 7821
  Conduction:
    in Ge 7613, 7614
    at Low Concentrations 7015
    in Si 7943
  Diffusion Parameters in Si Lapping Process 6370
  Distributions in InSb Crystals, Inhomogeneous 7247
  Effects on Mobility in Si 6103
  Energy Levels in GaAs and InP 7271
  Induced Infrared Lattice Vibration Absorption at Isolated Frequencies 7918
  Interactions in Si, Li-Oxygen 8625
  Ions in Si, Spin Resonance of 6164
    Layers in Ge, Evaluation and Control of Diffused 7249
  Levels in:
    AlSb 6362
    GaAs 6357
    Semiconductors 8659
    Si 6065
  Precipitation on Dislocations, Kinetic Theory of Stress-Assisted 9174
  Redistribution in Ge by Thermal Oxidation 6751
  Relaxation in Si and Ge 8945
  Resistance in Metals, Theory of 7014
Inclusions in AlSb Junctions 8016
Indicating Instruments, Transistor-Oscillator Limit Switch for 7523
Indium,
  Critical Field of Superconducting 7312
  Solubility of:
    Ge in 6002
    Si in 6001
  Superconducting 8748
Indium:
  in Ge,
    Solid Solubility of 8165
    Surface Concentration of 6331
Indium Antimonide,
  Anodization of 6347
  Conductivity and Other Properties of 7937
  Dendritic Growth of 6348
  Diffusion of Zn in 7252
  Dislocation Climb in Plastically Deformed 6632
  Distribution Coefficients of:
    Impurities in 6036
    Te in 6320, 7847
  Effective Mass of Electrons in 6130
  Electrical Properties of 8731
  Electron Mobility in 7933
  Etching of 6371
  Evaporation of Antimony during Heat Treatment of 6021
  Faraday Effect in 8911
  Growth of 6026, 6036
  Hall:
    Coefficient of 6414
    Effect in 9300
  High Field Properties of 7934
  Impurity Distributions in 7247
  Infrared Absorption in 9400
  Internal Field Emissions at Narrow Junctions in 6747
  Junction Preparation and Properties in 6499
  Lattice Absorption Bands in 7673
  Lifetimes in 8698
  Magnetic Susceptibility of Photogenerated Carriers in 9371
  Magnetoelectric Effect in 8759
  Magnetoplasma Reflection in 6130
  Magnetoresistance of 7317, 9297, 9300
  Magnetoresistive:
    Effects in 8766
    Voltage Regulator Employing 8143
  Melting Point of 8271
  Noise in 8698

Indium Antimonide, (Cont'd)
Oxidation of 6979, 8228, 8229
Photoconductivity of 8897
Photoemission from 8389
Piezoelectric Scattering of Electrons in 7305
Piezoresistance of 8724
Quadratic Deviations from Ohm's Law in 7306
Reflection Spectrum of 8392
Resistivity of 8271
Segregation in 6319
Spin Resonance of Conduction Electrons in 6124
Surface:
Adsorption of Oxygen on 8638
Characteristics of 6021, 6340
Damage in 6660
Thermal Conductivity of 8001
Thermoelectric Properties of 7400
Thermomagnetic Effects in 8933
Tunnel Currents in 7633
Tunneling in: 6701
Narrow Junctions Formed in 8278
Voight Effect in 7679
Zener Tunneling in 6131
Indium Antimonide:
Devices Using the Faraday Effect 6195
Films, Preparation and Properties of 6654
Hall:
Effect Magnetometer 6297
Generators 6298, 6412
Photodiodes, Noise in 6781
Photovoltaic Cell, Alloyed Junction 6520
Indium Antimonide-Gallium Antimonide, Mobilities and Energy Levels of 8262
Indium Antimonide-Indium Telluride,
Electrical and Optical Properties of 7323
Solid Solutions of 7323
Indium Arsenide,
Cl Impurities in 8203
Conductivity of 8726
Cu in 6014
Effective Mass of Charge Carriers in 8912
Faraday Rotation in 8912
Growth of 6036, 7882
In as a Source of Impurities in 6339
Magnetoresistive Effects in 8766
Mobility Killer in 6105
Pb in 6014
Preparation of 7878
Properties of 7878, 8760
Reflection Spectrum of 8392
Solubility of Al in 8203
Thermal:
Conductivity of 6202, 7685
and Physical Properties of 8932
Voight Effect in 7679
Indium Arsenide Hall:
Effect Multiplier for Use at Radio Frequencies 7105
Generators 6298, 6412, 7220
Indium-Germanium Junctions, Properties of 8013
Indium-Mercury Alloys, Superconductivity of Dilute 6119, 6411
Indium Phosphide,
Conduction Bands of 6378
Effective Mass of Charge Carriers in 8912
Energy Band Structure of 6111
Growth of 7271, 7882
Impurity Energy Levels in 7271
Mobility in 7271
Mobility Killer in 6105
Piezoresistance in n-Type 6111
Preparation of: 6359
Junctions by the Decomposition of 7419
Indium Telluride:
in Bi_2Te_3 and Sb_2Te_3, Solid Solubility of 6003
with Group III-VI Tellurides, Energy Gap of Solid Solutions of 7546
in PbTe and SnTe, Solid Solution of 7231
Indium Telluride-Cadmium Telluride, Solid Solutions of 7546
Indium Telluride-Indium Antimonide, Solid Solutions of 7323
Indium Telluride-Mercuric Telluride, Solid Solution of 7546
Indium Telluride-Zinc Telluride, Solid Solutions of 7546
Inductance:
Diodes, High 6493
of Junction Diodes 6492, 7414
Inductive Capacities in Millimeter Range, Measurement of 7921
Inductors, Operation of Thin Magnetic Film as Time Variable 6802
Information:
Capacity of Radiation Detectors 7715
Storage:
Devices, Coherer 6584
and Switching, Use of Ferroelectrics for 6592
Infrared, Voice Communication by 6927
Infrared:
Absorption:
of Oxygen in Silicon, Evidence for Internal Rotation in the Fine Structure of 7378
by a Semiconductor in an Electric Field 7374
of Solid Lithium Hydride, Effect of Isotopic Composition on 7375
Absorption in:
AlSb 8861
Bi_2Te_3 8397
Crystals 7373
GaP 8855
Halide Crystals 8363
InSb 9400
Ionic Crystals 7382, 8366, 9401
Quartz 9402
Si 8862, 8863
Synthetic Quartz 8364
Wurtzite Structure Crystals 8365
Antiferromagnetic Resonance in MnO 7048
Color Center Fluorescence in Alkali Halides 8886
Cyclotron Resonance 9302
Detectors, Measurement of the Frequency Response of 9027
Emission in ZnS:Cu 8871
Faraday Effect in $Y_3Fe_5O_{12}$ 8396
Fluorescence of F-Centers in Alkali Halides 8380
Impurity Photoconductivity in CdS Induced by Preliminary Illumination 7391
Microscopy, Localization of Dislocations in Si and Ge by 6007
Optical:
Material, CdS as an 6474
Properties of Semiconductors, Theory of 6176
Photocells, Fabrication of 9026
Properties of:
Au in Ge 8864
GaP 8852
Quantum:
Converters 6237
Counters, Time Discrimination in Solid State 6789
Reflection of:
Ionic Crystals 8910
NaCl 6472
Spectra of Crystals 7672
Studies of:
Bi 7372
Electron Irradiated Si 6050, 6051
Techniques for Determining Conductivity Types 6634
Transmission through Normal and Superconducting Films 8853
Inhomogeneities on Electrical and Galvanomagnetic Properties, Effect of Random 7019
Injection:
Electroluminescence, Irreversible Thermodynamics of 6185
of Electrons from Collector, Effects of Contact Material on 8438
Heat Transfer 7075
Instrumentation, Transistor Building Blocks for Data 7173
Insulated Particles, Model for Electroluminescence of 7984
Insulators,
Characteristic Improvements by Diminishing Inhomogeneity in 8676
Conduction in 6098, 9290
Dielectric Properties of 8674, 8675
Electromagnetic Properties of 6074
Ferromagnetic Resonance Line Shape in 7649
Integrated Circuits 6538, 7434, 8486
Integrating Amplifier 7749
Interaction:
between As and Al in Ge 6018
of Conduction Electrons with Acoustic Waves 9251
Interactions between Li and Oxygen in Si 6337
Intercardiac Catheter Tip Peizoresistive Pressure Gauge 7117
Interface:
Curvature and Rotation Rate, Relation between 6025
during Float Zoning of Si, Shape of a Melt-Crystal 6958
during Growth from the Melt, Microscopic Shape of a Solid-Liquid 6957
Motion, Theory of 7875
Shape upon Melt-Grown Pure Metal Crystals, Effect of Solid-Liquid 8632
Intermetallic:
Compound Dendrites, Growth Steps on the Surface of 6963
Compounds,
Band Structure of 6058
Conditions Governing Formation of 8164
Crystal Model Studies of Growth Phenomena in 6341
Etching of 6340, 6371, 6661, 8639, 8640
Filled and Empty Dangling Bonds in III-V 7000
Free Carrier Absorption Due to Polar Modes in 7380
Hydrothermal Preparation of Two-Component Solid Solutions of 6030
Optical Properties of 6030
Oxidation Kinetics of III-V 8635
Surface Characteristics of III-V 6340, 6983
Compounds between Lanthanons and Transition Metals, Preparation and Structure of 7259
Semiconductor Compounds, Use of a High Pressure Furnace in the Preparation of 7577
Internal:
Friction, Beam Method Measurement 9452
Friction in:
Ferromagnetics, Temperature Dependence of 8943
Ge and Si 8945-8947
Synthetic Quartz 8944
Interstitial:
Impurities in Semiconductors, Theory of Solubility of 6020
Oxygen in Si 7378
Interstitials in Alkali Halides, Formation of 7556
Intervalley Noise 9307
Intrinsic Regions by Ion Drift, Production of 6753
Intruder Alarm, Capacitance 7215
Inversion:
Layers on Semiconductors, Surface Currents in 7080
of Spin Populations by Simultaneous Passage 8468
Inverters 6840, 6895-6897, 7521, 7819, 8554, 8555, 9139
Iodine, Electrical Properties of 6998
Iodine in:
GaP, Solubility of 8203
Ge, Concentration of 6640
Ion:
Adsorption on Relaxation Processes in Ge, Effect of 6128
Beam Currents, Measurement of 6297

on: (Cont'd)
Bombardment:
Cleaning of:
Ge Surfaces 6422, 8637
InSb Surfaces 8638
Etch Pits in Pyrolytic Graphite 6663
Etching of Si and Ge 6049
Counters, Surface Barrier 6301
Current Measurement, Amplifier for 8146
Distributions and Valencies in Mg-Mn Ferrites 8584
Drift, Diffusion Constants Measurement by 6753
Drift in:
Si, Effect of Li-Boron Ion Pairing on Li^+ 7574
Si Junctions, Investigation of Li-Boron Pairing by 6019
Gauge for Surface Studies 8633
Lattices, Polarization Energy in 8669
Pairing in Si, Effect of Li-Boron 7574
Radius of Ge 8242
nic:
Conductivity:
of CsBr and CsI 8245
on the Electric Strength of KCl and NaCl, Effect of 7594
Crystals - See also Alkali Halides, Specific Ionic Crystals
Crystals,
Conductivity of 8713, 9271
Dielectric Properties of 9225
ESR of Mn^{2+} in 9306
Hall Constant of 9271
Infrared:
Absorption in 8366, 9401
Reflection of 8910
Luminescence in 8875
Mechanism for Far Infrared Absorption in 7382
Mobility in 8713
Nuclear Magnetic Relaxation in 8842
Polaron Formation in 9236
Surface States of 8238
Thermoelectric Power of 8921
Diffusion in CsBr and CsI 8245
Distribution in Substituted Ferrimagnetic Rare Earth Iron Garnets, Statistics of 7340
Hall Effect in NaCl 7597
Lattice Vibrations 8667
Properties of Electroluminescent ZnS 6080
Radii, Theory of 7006
nization,
Classification of Solids by Ease of 7903
Occupancy State Probability Function in Electron Impact 7908
nization:
Chamber, Solid State 6910, 8569
Energy of Traps, Method of Determining 6190
Potential of Atoms 8164
Rates for Electrons in Uniform Si p-n Junctions 6746
in Semiconductors, Impact 8717
nizing Particle Detectors, Si Junction 7831
ns, Sputtering of Semiconductors by Low Energy Argon 6052
ns in:
Crystals, Electronic Spectra of 9391
Si, Spin Resonance of Impurity 6164
on,
Gyromagnetic Ratio of 9333
Magnetic:
Properties of Evaporated Thin Films of 9330
Viscosity in 9362
Paramagnetic:
Resonance of 9376
Susceptibility of 9375
Phase Transformation by Differential Thermal Analysis of α-γ 7848
Polarization of Conduction Electrons in 7643
Self Diffusion Coefficient during Compression of 7859
Specific Heat of High Purity 6199

Iron, (Cont'd)
Thermal Diffusivity of Armco 6726
Yield Stability in 8939
Iron:
Alloys, Saturation Magnetization and Curie Points in Dilute 9336
in Beryl, Paramagnetic Resonance and Optical Spectrum of 7667
Films by Impact Evaporation, Preparation of 6975
in Ge,
Diffusion of 7569
Solubility of 7569
Magnets, Elongated Single Domain 9332
Particles by Electron Diffraction, Measurement of the Magnetic Induction at the Surface and Interior of 8309
Permanent Magnets, Elongated Single Domain 9332
Powder, Magnetization Curve in Carbonyl 7955
in Rutile, Paramagnetic Resonance of 6713
in Spinel Structure, Exchange Interaction of 7966
in $SrTiO_3$, Hamiltonian for the Paramagnetic Structure of 6712
Whiskers,
Dislocations in 9176
High Temperature Oxidation of 9191
Whiskers under High Fields, Observation of Domains in 7034
Iron-Doped Ge, Magnetic Susceptibility of 6425
$Iron^{3+}$ in:
Sapphire, PMR of 8348
TiO_2, PMR of 8349
Iron-Aluminum:
Alloys, Permeability of 9345
System, Free Energy of the 9326
Iron Carbide, Preparation and Coercive Force of Fine Powder Hexagonal 8220
Iron-Cobalt:
Ferrite, Magnetic Anisotropy of 9354
Magnets, Elongated Single Domain 9332
Iron Ferrites, Growth by Czochralski Method of 6971
Iron Garnets at Low Temperatures, Specific Heat of Some 6476
Iron-Magnesium Oxide Ferrites, Phase Equilibria of 8581
Iron Monosulfide, Composition of Natural Crystals of 6316
Iron-Nickel,
Magnetic Properties of 8793
Magneto-Optic Infrared Properties of 8851
Iron-Nickel Alloys,
Curie Temperature of 7334
Initial Growth of Plating in Thin Electrodeposited Films of 7078
Iron-Nickel Ferrite, Magnetic Properties of 9357
Iron-Nickel Films, Influence of Thiourea on the Deposition of 6993
Iron-Nickel-Cobalt Alloys, Electroless Deposition of Gold on 6992
Iron Nickel Nitride, Preparation and Crystallography of 7575
Iron Oxide Particle Size on Nickel Ferrite Formation, Effect of 6155
Iron Oxide-Lanthanum Oxide System in Air, Phase Equilibria of 8157
Iron-Rare Earth Ferrites, Paramagnetic Susceptibility of 8338
Iron-Silicon, Dislocation Formation by Spark Discharge in 8599
Iron-Yttrium Ferrites, Paramagnetic Susceptibility of 8338
Irradiation:
Damage in a Cu-Al Alloy, Neutron 9198
Defects in Ge, Neutron 7929
Effects on Resistivity of W, Deuteron 7902
Produced Color Centers in NaCl 8177
Ising:
Model,
Magnetic Properties of the 8307
Monte Carlo Computations on the 7639
Model of Ferromagnetism 8306
Problem for Rectangular Lattice, Solution of 8779
Islands in Semiconductor Slices, Production of 7900
Isolators: 6145, 6240, 6525, 6526, 6616, 6851, 6921, 7112, 7113, 7115, 9036
Isotope Effects on Thermal Resistance 9434

J

Jahn-Teller Effect in KCl:Tl Phosphors 8874
Junction:
Capacitors, Evaporated Ge-Ta 9051
Counters for Nuclear Spectroscopy, Multi-Channel 8574
Fabrication by Masking 8443
Layer Microcircuits, Laminar 7736
Particle:
Detectors 8570, 8572
Spectrometers, Design and Performance of Si 9150
Junctions,
Alloy-Diffused: Fabrication of 9001
Alloyed:
Fabrication of 8972-8975, 8998, 8999
Hook: Fabrication of 9002, 9003
Avalanche Breakdown in 6221, 8439
Current Flow Equations of Se-CdO 8422
Defects and Weaknesses in Si 8445
Delineation of 6752, 8444, 9009
Detection of Minimum Ionizing Particles in 7831
Diffused:
Fabrication of 6356, 7100, 7858, 8017, 8978, 9004
Ohmic and Rectifying 9010
Emission of Light from 7675, 7676, 7719
Epitaxial:
Fabrication of 9007
Ge-GaAs 8421
Eutectic: Au-Ge 8977
Ferrite-Loaded Waveguide 6525
Formation by:
the Decomposition of Compounds of 7419
Thermal Oxidation of 6751
Forward Current in 8014
GaAs 6356
GaP 6500
Grown: Fabrication of 8970, 8971, 8996
High Current Characteristics of 8963
Hot Electron Emission from Si 6222
Li-Boron Pairing in Si 6019
Minority Carrier Diffusion Lengths in 8008
Multiplication of Carriers in 6399
Photoeffect in Nonuniformly Irradiated 6784
Photoelectric Emission from Treated Si p-n 6722
Photoemission in Undiffused Metal-Semiconductor 6721
Properties of In-Ge 8013
Protective Glass Coatings for 8985
Quantum Efficiency of CdTe 7717
Reverse Current in 8965, 8966
SiC 8018, 8030
Stabilization of 9012
Theory of 6481
Thermoelectric Behavior of 6218
Transient Temperatures in 6230
Tunneling in:
InSb 6701, 8278
Sb-As Doped Ge 8958
Vapor-Grown 6640
Junctions:
- See also Diodes, Junction; Transistors, Junction
between Semiconductors Having Different Energy Gaps 8422

K

Kerr:
Effect in Deuterium-Doped Rochelle Salt, Electro-Optic 7007
Magneto-Optic Effect to the Observation of Magnetic Domain Development, Application of the 7034

Kinematic Theory of Ferroelectric Domain Growth 7923
Kinetic Phenomena, Statistical Theory of 6396
Kinetics of:
the Destruction of Excitons 6398
Luminescence of Alkali Halides 7983
Phthalocyanine Photoconductivity 7992
Kirkendall:
Diffusion, Nonequilibrium Vacancy 8594
Effect in the Au-Ni System 7864
Knight Shift in Ta Metal 7973

L

Lamp Flashing Generator 9143
Landau Levels upon Tunnel Currents in InSb, Effect of 7633
Lanthanum,
NMR of La^{139} in 8347
Superconducting Transition Temperature of 8744
Lanthanum Ethyl Sulfate, Paramagnetic Resonance of Nd^{3+} in 8827
Lanthanum Oxide-Iron Oxide System in Air, Phase Equilibria of 8157
Lapping of Si, Precision 6370
Large-Signal Parameters of Transistor Triodes 8440
Lasers, Resonant Modes in 8475
Lasers: 7540
- See also Masers
Lateral Growth Mechanism in Dendrites 6352
Lattice:
Constant of:
AlSb 6623
AlSb-GaSb 6623
Bi_2Te_3-Bi_2Se_3 7551
Conduction of Cellulose 7936
FeO-MgO-Fe_2O_3 8581
GaAs-GaP 7272
GaSb 6623
Single Crystals, Measurement of 8170
Defects,
Low Temperature Thermal Resistivity of 6200
Scattering of Phonons by 6200
Defects:
in Alumina Ceramics 7553
on Lattice Thermal Conductivity, Influence of 6201
in Si Crystals, Observation of 8174
Dilatation Due to Point Defects 7241
Dispersion Frequencies of NaCl and KCl 6671
Displacements by Fast Electrons 6376
Dynamics, Slow Neutron Interaction Analysis of 8666
Dynamics of Alkali Halides 9217
Effects on Dielectric Properties 8243
Free Energy, Calculation of 7916
Gas, Equation of State and Phase Transition of the Spherical 7328
Grain Boundaries in Diamond 8611
Parameters, X-Ray Measurement of 9154
Parameters:
of Bi at Low Temperatures 8171
of $CoCl_2 \cdot 6H_2O$ 8172
due to Crystal Imperfections, Changes in 7237, 7238, 7241
of $LiH_3(SeO_3)_2$ 8173
Phase Transition on F and M Centers in Alkali Halide Crystals, Effect of 7915
Position of Atoms 9223
Potential of Si 9216
Scattering in Si 8716
Sites, Distortions Produced by Ni^{2+} on Tetrahedral 6174
Spacings in Alumina-Chromic Oxide Systems 7850
Specific:
Heat, Calculation of 7916
Heats of Superconducting and Normal Nb 8399
Sums, Extension of the Madelung Method for the Evaluation of 6382
Lattice: (Cont'd)
Thermal Conductivity 6201, 8916
Vacancies in Neutron Irradiated Ge 6627
Vibration:
Absorption, Impurity Induced Infrared 7918
Spectra, Center Law of 7917
Vibrational Modes 8241
Vibrations, Ionic 8667
Vibrations in:
Alakli Halides 9218
CdS 9231
CdTe 8764
Diamond Structure Crystals 9219
Si 8665
Wave Scattering by Point Defects 8403
Lattices,
D Bands in Cubic 7001
Energy Transport in Disordered 7590
Layer:
Geometry in Pyrographite 7851
Structure in Dislocation Free Si Crystals, Observation of 6012
Layered SiC, Crystal Structure of 174 6023
Lead,
Determination of Sb and Tl in 8192
Energy Gap in 6061
Solubility of Si in 6001
Superconductivity in 6693
Transition Hysteresis in Superconducting 9292
Lead:
Film Superconductive Storage Elements, Relaxation Times in 6591
Films,
Penetration of Magnetic Field through 6061
Time Delays in the Superconducting Transition of 6697
in Ge, Solid Solubility of 6002
in Indium Arsenide, Determination of 6014
Superconductors,
Isotope Effect in 8756
Resistivity Limit of 8755
Lead-Barium Niobates, Dielectric Properties of 8254
Lead Fluoride-Zinc Oxide System, Eutectic Point and Composition in 8218
Lead-Indium Alloys, Time Delays in the Superconducting Transition of 6697
Lead Metatantalate, Properties of Ferroelectric 6679
Lead Metatantalate with Nb, Ba, and Sr, Solid Solutions of 6679
Lead Niobate, Phase Transitions in Ferroelectric 7600
Lead Niobium-Type Compounds,
Crystal Structure of 6676
Ferroelectric Curie Temperature of 6676
Lead Selenide,
Electrical Properties of Sintered 6959
Mobility and Scattering in 7399
Optical Absorption in 6197
Photoconductivity of 8898
Standard Free Energy of Formation of 8158
Thermal Properties of 8918
Thermoelectric Properties of 6059, 7399
Lead Selenide Photoconductive Cells, Influence of Crystal Size on the Spectral Response Limit of Evaporated 6465
Lead-Selenium, Thermoelectric Properties of 9034
Lead Sulfide,
Controlling Deviations from Stoichiometry in 7254
Growth of 8214
Mobility and Scattering in 7399
Optical Absorption in 6197
Photoconduction Mechanisms of 9022
Thermal Properties of 8918
Thermoelectricity and Thermal Conductivity of 7399
Lead Sulfide:
Cells,
Current Fluctuations in 6468
Lead Sulfide: Cells, (Cont'd)
Diffusion Length in Chemically Deposited 6466
Radiation Limited 6517
Films,
Crystal Size in 7011
Electric Properties of Chemically Deposited 7284
Photoconductivity of 7284
Photoelectromotive Forces in Electron Irradiated 7678
Signal Response in 6469
Photocells 9025, 9026, 9030
Photocells, Operating Characteristics of 6234
Photoconductive:
Cells, Time Constant of 6466
Films,
Hole Mobility and Crystal Size in 7011
Minority-Carrier Effects in Chemically Deposited 6466
Noise and Signal Response in 6469
Photoconductors,
Role of Surface States in 6467
Traps in 6467
Photodetectors, Relaxation Time of 8453
Lead-Sulfur, Thermoelectric Properties of 9034
Lead Telluride,
Composition Limits of Stability of 7849
Etches for Revealing Dislocations in 8642
Growth of 7877
Hall Effect in 8292
Magnetic-Field Dependence of the Hall Coefficient of p-Type 6413
Magnetoresistance of 8292, 9298
Mobility and Scattering in 7399
Piezoresistivity of 6402, 8256
Radiation Effects in 7402, 7403
Solid Solutions of InTe and CdTe in 7231
Thermal:
Conductivity of 8001
Properties of 6238
Thermoelectric Properties of 8927, 8928
Thermoelectricity and Thermal Conductivity of 7399
Thermo-Junctions of 8928
Lead Telluride Photoconductive Cells, Influence of Crystal Size on the Spectral Response Limit of Evaporated 6465
Lead-Tellurium, Thermoelectric Properties of 9034
Lead-Tellurium-Selenium, Thermoelectric Properties of 9034
Lead $(Ti \cdot Zr \cdot Sn)O_3$, Ferroelectric Properties of Thin Films of 7922
Lead Titanate, Thermal Conduction in 7289
Lead Titanate Containing Nb or Ta, Properties of 6678
Lead Titanate Zirconate,
Dielectric:
Breakdown in 9228
Properties of 7603, 8258
Ferroelectric Characteristics of 6085
High Temperature Discharges in 7290
Properties of 8414
Resonance Quality Factor (Q) of 8248
Transducer Properties of 6532
Lead Zirconate, Thermal Conduction in 7289
Lead Zirconate and $NaNbO_3$, Solid Solutions of 7293
Life Expectancy of Transistors 8020
Lifetime,
Measurement of 6093
Microwave Measurement of 6452, 8260, 9255
Photoconductive Measurement of 8699, 8700
Photovoltaic Measurement of 9426
Lifetime:
- See also Recombination
at Arbitrary Injection Levels in Junction Diodes, Calculation of 7418
in Diffused Si 6393
in Transistors, Control of Carrier 7707

Lifetime of:
Anthracene, Positron 7928
Ge 8701, 8864
InSb 8698
Semiconductors 9254
Si 6104, 9426
Si, Preservation of 6393
Te 6096
Light:
Absorption:
in CdS, Electric Field Induced 6450
by Photoelectrons 6451
Amplifiers 6236, 8456
Emission from Si Junctions 6742, 8445
Intensifier Display Panel, Storage 7718
Meters 9147
in Paramagnetic Crystals, Microwave Modulation of 7720
Pulses, Transistors as Generators of High-Speed 7719
Scattering by Neutron Irradiated Fused Silica 8646
Stimulation in Luminescence Kinetics 7986
Light-Activated p-n-p-n Switches 7840
Lighting Control Systems, Theater 6296
Lightning Protection for Transistor Repeaters 8154
Limit Switch for Indicating and Recording Instruments, Transistor-Oscillator 7523
Limiters 6564, 6844, 6862, 7114, 7499, 9103, 9104
Line Broadening, Phonon 9220
Linear:
Networks 8483, 8484
Sweep Circuits 8085
Wave Generator 7493
Linewidth, Effects of Surface Irregularities on Ferromagnetic Resonance 6436
Linewidth:
Narrowing in Ga Substituted YIG 6143
Variations in the Magnetic Spectrum of Divalent Ni in Sapphire 7657
Liquid-Solid Interface Studies of Ge Dendrites 7892
Liquidus Curves for Ge and Si 6001
Lithium:
on Dislocations in ZnO, Precipitation of 7227
as a Donor and an Acceptor in ZnO 7227
and Oxygen in Si, Interactions between 6337
in Si, Diffusion of 6638, 7571, 8199
in Si Containing Oxygen, Precipitation of 7226
in ZnO, Diffusion of 7227
Lithium-Aluminum Ferrites, Magnetic Properties of 8816
Lithium-Boron:
Ions in Si, Relaxation Process for Recombination of 7867
Pairing in Si 6019, 7574
Lithium Chloride, Absorption in 8858
Lithium-Chromium Ferrites, Magnetostriction in the Neighborhood of the Compensation Point of 8776
Lithium Fluoride,
Absorption in 8393
Acoustic Attenuation in 8940
Annealing of Volume Expansion and X-Ray Induced Color Centers in 7238
Cleavage Faces of Single Crystals of 7872
Dielectric Constant of 9226
Dislocation:
Multiplication in 7856
Sources in 9173
Dislocations in: 8185
Surface Layers of 6643
Electron Spin:
Paramagnetic Resonance in 8836
Resonance Studies of Metallic Li in Neutron-Irradiated 6417
Interstitials in 7556
Mechanical Properties of 7689
Paramagnetic Resonance:
of F-Centers in 8837
Lithium Fluoride, Paramagnetic Resonance: (Cont'd)
in Irradiated 8835
Study of X-Ray Radiation Damage in 8647
Plastic Properties of 7693
Recovery Properties of 7692
Reflection Spectra of 8393
Surface Energy of 6999
Thermal Conductivity of 6201, 6725, 7074
Ultraviolet Absorption in 8367
Lithium Fluoride:
from Aqueous Solutions, Growth Poisoning of 7579
Cleavage Faces, Dielectric Breakdown Dendrites on 7255, 7256
Lithium Hydride,
Binding Properties of 7681
Infrared Absorption of Solid 7375
Preparation and Properties of Single Crystals of 7681
Lithium-Nickel Oxides, Conductivity of 8719
Lithium-Oxygen Interaction in Si 8625
Logic,
Back-Transient Diode 6573
High-Speed Magnetic Film 6578
Logic:
Circuits 6573-6576, 6871, 6874-6876, 7175, 7182, 7765, 7794, 7797, 7798, 8118, 8486, 8533, 8534, 8539, 9083, 9121
Circuits,
Backward Diodes for 7218
Comparison of Magnetic and Transistor 8536
Direct Coupled 6279
Elliott Sheffer Stroke Static Switching 7176
High-Speed Magnetic-Film 6578
Impulse Selection for Ferrite Core 7183
Integrated 8486
Magnetic: 7183, 7799, 8119-8121, 8535, 8537, 8538
Analogs of Relay Contact Networks for 6800
Open Flux Path Ferrite Films for 6801
Optimization by Computer of 7794
Tunnel Diode 6572, 6870, 6872, 6873, 7178, 7179, 7218, 7796
Design, Transistor Adaptive 6576
Devices, Magnetic Film Parametrons as 6878
Element,
Ferrite Film 6801
Multi-Aperture Magnetic 6799
Tunnel Diode as a 6571
Elements, Solid State Micro- 6580, 6774
Gates, Design of Transistor Resistor 7181
Networks,
Statistical Analysis of Transistor-Resistor 6876
Theory of 7174
Systems, Multielement High-Speed 6569
Logimag Ferromagnetic Switching Device 8465
Logistor Relays 8558
Loop Scatterer for Microwave Field Distribution Measurements, Diode 6902
Loss:
in High-Permittivity Ferroelectris, Microwave 6076
Mechanisms in Ferrites, Dielectric and Magnetic 8221
Tangent of $BaTiO_3$, Measurement of the 6674
Low:
Frequency Wave Filters, Thermistors in 8036
Temperature Solid State Physics 8652
Luminescence,
Electroenhancement and Electroquenching of X-Ray Excited 6191
Experimental Studies of 6197
Pressure Effects in 7387
Very Low Frequency Excitation of 7985
Luminescence of:
AgCl 7981
Alkali Halides 7983, 7989
CdS 6455, 9408
CdSe 8891
GaP 7990
Impurity Centers 8876, 8877
Ionic Crystals 8875
KCl:Tl 7390, 8874, 9404
KI:Tl 9419
Semiconducting Diamond 7987
SiC: 6454
Junctions 6501
Silica Gel 8892
ZnO 8382, 8612, 8880
ZnS 6354, 6455
Luminescence Kinetics, Light Stimulation in 7986
Luminescent:
Center in Sulfides, Energy Levels of Ag 9418
Display Devices, Review of Panel-Type 6892
Emission States of the Rare Earths, Factors Influencing the 7061
Films, Formation by Evaporation of 7894
Light Source, Cold Cathode 8455
Properties of Silver-Activated Magnesium Borate Phosphors 6463
Lutetium, Electrical Resistivity of Polycrystalline 7016

M

Machine Tool Control, Photovoltaic Moiré Fringe System for 7435
Madelung Method for the Evaluation of Lattice Sums, Extension of the 6382
Magnesium,
Flow-Stress of 8412
Magnetoresistance of 7591
Photon Absorption by Valence Electrons in 7381
Susceptibility of 8849
X-Ray Scattering by Plastically Deformed 9165
Magnesium:
Binary and Ternary Alloys, Thermoelectric Power of 8930
Films, Surface Structure of 8205
in Ni, Diffusion of 9181
Magnesium-Group IV Compounds, High Pressure Furnace for the Preparation of 7577
Magnesium Aluminate, Crystalline Field for Ni^{2+} and Co^{2+} in Single Crystals of 7379
Magnesium Borate Phosphors, Luminescent Properties of Silver-Activated 6463
Magnesium-Ferrite-Manganite System, Magnetization of the 8312
Magnesium-Manganese Ferrites,
Domain Structure of 9360
Ferrimagnetic Resonance in 8810
Ion Distributions and Valencies in 8584
Magnetic After-Effect in 7642
Resonance Absorption Linewidths in 7960
Magnesium $Nickel_2$, Paramagnetic Susceptibility of 9374
Magnesium Oxide,
Crystalline Field for Ni^{2+} and Co^{2+} in Single Crystals of 7379
Effects of Neutron Bombardment on 6377
Gas Interaction with 9190
Paramagnetic Resonance:
Absorption in 9386
of Transition Metals in 8847
Plastic Properties of 7693
Radiation Effects in 6377
Secondary Electron Emission from 7023, 7024
Spin-Phonon Interaction in 9377
Surface Energy of 6999
Magnet Current Regulators, Transistor 6597
Magnetic:
After-Effect in Magnesium Manganese Ferrites 7642
Amplifier Control Systems 6292, 6566, 9140
Amplifiers, Computer Design of 9141
Amplifiers: 8496, 8536, 9142

Magnetic: Amplifiers: (Cont'd)
for Magnetic Memory Sensing, Miniature High Frequency 6244
Analogs of Relay Contact Networks for Logic Circuits 6800
Anisotropy: 9356
Constants of Single-Crystal Films, Measurement of 7956
Anisotropy in:
Fe 6135
Fe-Co Ferrite 9354
Ferrimagnetic Spinel 8319
Ferromagnetics 8794
Films 6702, 7956
Ni Films 8797
Ni-Fe Films 7041, 8795
Ni_3Mn 8318
Permalloy Films 8796, 8797
Annealing in:
Co-Substituted Magnetite, Kinetics of 7344
Perminvar 9343
Si-Fe 9344
Behavior of Some Cubic Crystals, Low-Temperature 7652
Cartridges, Transistor Stereo Preamplifier and Tone Control for 6275
Ceramics 6155
Contribution to Shear of Fe-Al Alloys 9326
Control Circuit 8137
Cores 8464
Cores,
High-Speed Coincident Current 6803
Magnetization in Tape-Wound 7442
Reversal of Loaded 7441
Coupling in Crystalline Compounds 6137
Crystal Puller, Synthesis and Crystal Pulling of GaAs in a 6956
Crystals, Double Exchange Effects in 8332
Delay Lines 8124
Devices - See also Hall Effect Devices, Masers
Diagrams, Use of a Hall Generator for Static Interrogation of 6298
Dipole Interactions in Semiconductors 8778
Energy Losses 9358
Field, Hall Voltage in an Inhomogeneous 6698
Field:
Attenuation, Measurement by Thin Superconducting Films of 6408
at the Iron Nucleus, Correlation between the Magnetization and the Effective 8311
Measurements, Hall Generators for 6298, 8034
Meters 7826, 8562, 8563
of Twistors, Representation of the 6797
in the Vicinity of a High Permeability Parallelepiped, Determination of 8784
Fields, Antiferromagnetic Susceptibility at Moderate 7962
Fields in Superconductors, Measurement of 6116
Film:
Parametrons, Operation of 6802
Parametrons as Logical Devices 6878
Films,
Domains in Thin 7345
Effects of Heat Treatment on Growth and Domain Structure of MnBi 7873
Flux:
Measurement of Thin 7953
Reversal by Noncoherent Rotation in 6431
Gas Absorption by Vacuum Evaporated 6149
Impact Evaporation Preparation of 6975
Nanosecond Switching in Thin 6579
Spiral Walls in Thin 7038
Structure of Thin 6974, 6976
Films Electrodeposited in a Magnetic Field, Influence of Substrates on Thin 7039
Flux Pattern Measurements Using Hall Probes 7527

Magnetic: (Cont'd)
Form Factors, Effect of Crystalline Field on 7926
Gradient at Surfaces of Ferromagnetics by Electron Diffraction, Measurement of the 8308
Induction:
of Ferromagnetic Thin Films, Measurement of the 8310
at the Surface and Interior of Iron Particles, Electron Diffraction Measurement of the 8309
Logic Element, Multiaperture 6799
Material for Permanent Magnets 9045
Materials,
Elastic Switching Properties of Toroidal Square Loop 8039
Generation of Microwave Electromagnetic Radiation in 7169
Materials for High-Speed Storage, Low Flux Density 6804
Moment Arrangements in Manganese Spinels, Triangular 7037
Moments in Cr-Containing Spinels, Origin of Low 9325
Phase:
Transition of Evaporated Superconducting Thin Films, Influence of Aggregation on 6409
Transitions of $CoCl_2$ 7653
Polarity Reversal of Mn-Mg and Ni-Zn Ferrites 6142
Properties of:
Alkali Ozonates 6445
Co and Co-Ni Alloys, Effect of Plating Parameters on the 6994
Core Materials, Effect of Temperature on the 9341
$CrBr_3$ 8818
Cr_2O_5 8335
Er 6151
Fe-Ni Alloys, Radiation Effects on 8793
Ferrite:
Micropowders 9327
Thin Films 6974, 6976
Fine-Particle Ni Ferrites 7275
a Garnet System 6159
Graphite 6715
Heavy Rare Earth Metals 7016
the Ising Model 8307
Li-Al Ferrites 8816
Mixed Ferrites 8815
Mn Chromite-Aluminates 6157
$Mn_xCo_{80-x}C_{20}$ Alloys 9185
Mn-Zn Ferrite 6442, 9189
Ni-Fe:
Ferrite 9357
Thin Films 7040, 9183
Ni-Zn Ferrites 7056
Permalloy:
Films 6971,6973, 7042
Films, Use of Magnetoresistance Measurements to Study the 7044
Solids Using Configuration Interaction, Determination of 6134
Square Loop Materials 9184
Ultra Fine Ferrite Particles 6973
YIG Containing:
Nd 6977
Sm 6443
the Y-Yb Garnet System 8817
Recording Tapes, Particle Interaction in 6250
Remanence of Ho Metal, Low-Temperature 6150
Resonance,
Measurement Broadening in 9379
Thermodynamics of 7950
Resonance:
Observations, Transistor Oscillator for Nuclear 6900
Spectrometer, Analysis of a 6901
Spectrum in Deuterated Rochelle Salt 9235

Magnetic: (Cont'd)
Resonance to Study Surfaces, Use of 9193
Saturation Moment of Ferrimagnetic Garnets 8791
Spin:
Configurations, Determination of Ground-State 7329
Configurations in the Cubic Spinel, Classical Theory of 7636
State, Effect of Magnetization Reversal on 8316
State Stability in Ferromagnets 8786
Stray Fields, Electron Mirror Microscopy of 9331
Structure of:
Co, Thickness Dependence of the 8800
$(Mn,Co)_4C$ 6153
$MnCO_3$ 6154
MnN_2 6704
Superconductors, Properties of Some 7625
Susceptibility, Induction Apparatus for Measurement of 9339
Susceptibility of:
a-MnS 6427
$CoBr_2 \cdot 6H_2O$ 6158
Eu 9372
Fe 9375
Fe-Si Alloys, Paramagnetic 9375
Ga, Anisotropy of the 7326
Ge 6425, 7324, 7325
$MgNi_2$ 9374
Ni, Recovery of 9340
Organic Solids 7621
Pd- and Pt-Transition Metal Complexes 9373
Photogenerated Carriers 9371
Switching in Permalloy Films 7044
Systems with Dilution, Behavior of 7635
Tape,
Assessment of Data Storage on 8131
High Storage Capacity of 8116
Storage of Analog and Digital Data on 8130
Tape:
Cartridges 9120
Recorders 6276, 6277, 6283, 7792, 8132, 8133, 9119
Recording Heads 7171, 7793, 8117
Torque of:
Si-Fe 9334
YIG 7640
Transducer Heads, Fine-Grained Ferrite for 7171
Transitions in:
Dy 8736
$TiCl_3$ 8305
Viscosity in Fe 9362
Magnetically:
Polarized Media, Magnetoelastic Wave Propagation in 8783
Tunable Microwave Filters Employing Single Crystal Garnet Resonators 6791
Magnetism, Monte Carlo Computations on the Ising Model of 7639
Magnetism of:
Cu-Ni, Nuclear Resonance Study of Electronic 7350
Eu Garnets 9369
NiF_2 6433
3d Metals 6137
Magnetism-Spin Wave Dispersion Relations 9322
Magnetite,
Conductivity and Thermoelectric Power of 8733
Kinetics of Magnetic Annealing in Co-Substituted 7344
Magnetite Powders, Shape Distribution of 9186
Magnetization,
Anisotropic 7644
Asymmetrical 9338
Model of Exchange-Inversion 7336
Magnetization:
Curve of Heisenberg Ferromagnet 8782
Curves for TiFe 6152
in Dilute Iron Alloys, Saturation 9336
and Effective Magnetic Field in Ferromagnetic Iron, Correlation between 8311

Magnetization: (Cont'd)
in Ferromagnetics, Anisotropy of 9352
in Mn Ferrites, Ultrasonic Measurement of 8787
Process of a Helical Spin Configuration 7031
Reversal:
Effect on the Magnetic State 8316
of Ferrite Toroids 9348
in Ferromagnetic Thin Films 9349
of Permalloy Films 8321
Process in Ferromagnetics 9347
Magnetization of:
Co-Mn Alloys 7338
a Dilute Suspension of a Multidomain Ferromagnetic 7955
a Ferromagnet, Anisotropy of the Intrinsic Domain 7645
Mg-Cr-Sb 6432
the Mg-Ferrite-Manganite System 8312
Mg-Mn Ferrites 9360
$Mn_{2-x}Cr_xSb$ 7033
Nb_3Sn 7946
Ni, Effect of Chemisorbed H_2 on the 9337
Si-Fe Ferromagnets 8805
Single Crystals of Ni_3Mn 8318
Tb, Saturation 9335
YiG 6977, 9368
Magnetocrystalline:
Anisotropy, Linear Decrease in the 7342
Anisotropy in Hexagonal Oxides 9353
Magnetoelastic:
Effects in Co-Fe Ferrite 7327
Properties of Ferromagnetic Single Crystals 8301
Waves, Propagation of 8783
Magnetoelectric:
Effect in:
Antiferromagnetic Cr_2O_3 8333, 8334
InAs 8760
InSb 8759
Properties of Bi 8727
Magnetometer,
Ferromagnetic 7826
Use of a Second Harmonic Phase-Sensitive Detector in a Flux-Gate 7488
Magnetometer for:
Satellites 7526
Satellites, Transistorized Search Coil 7526
Magnetometers, Hall Effect 6297, 9018
Magneto-Optic:
Effects:
on Excitons in CdS 8850
in Ge 7370, 7909
Infrared Properties of Ni-Cu and Fe-Ni 8851
Studies of Bi 7372
Magneto-Optical Properties of Excitons 9249
Magneto-Oscillatory Effect in the Electron-Hole Plasma in a Semiconductor 6777
Magnetoplasma:
Reflection in Solids 6130
Resonance in Ge 9303
Magnetoplasmas in Bi 7372
Magnetoplumbite, Thickness Dependence of Domain Structure of 7957
Magnetoresistance of:
AuCu 9199
CdS 8767
Cu 7628
GaAs 8765
Ge 7316, 7613, 7947, 9299
Graphite 8291
InAs 8766
InSb 7317, 7937, 8766, 9297, 9300
Mg 7591
PbTe 8292, 9298
Permalloy Films 7044
Si 7302, 8293
Zn 9296
Magnetoresistive:
Multipliers 7514
Trigger Circuits 6842
Voltage Regulators 8143
Magnetoresistors 6614, 7514
Magnetostatic:
Modes in Ferromagnetics 9323
Properties in Ni-Zn Ferrites, Temperature Dependence of 8788
Resonance Modes in Large Ferrite Samples 6792
Waves and Spin Waves, Propagation and Generation of 7330
Magnetostriction of:
Ferromagnetics 9352
Ga-Fe Oxides 6681
Gd 8777
Gd-Fe Garnets 6428
$Li_{0.5}Fe_{0.8}Cr_{1.7}O_4$ 8776
Ni 9367
NiO 8303
Ni-Zn Ferrites 6365
YIG 8304
Magnetostrictive:
Elastic Coefficients in a Cubic Crystal 7327
Resonance Units, Band-Pass Filters Using 7451
Strains 7327, 8302
Magnetothermal Effects in Si-Fe Alloys 8406
Manganese:
and its Alloys, Antiferromagnetic Domains in 7036
Binary Structures, Superconductivity of 8758
in Corundum, Paramagnetic Resonance of 6714
in Spinel Structure, Exchange Interaction of 7966
Spinels, Triangular Moment Arrangements in 7037
in TiO_2, Paramagnetic Resonance of 7364
Manganese^{2+}, EPR of 9387
Manganese^{2+} in:
$CaWO_4$, Paramagnetic Resonance of 8353
CdTe, Spin Resonance of 8771
Ionic Crystals, ESR of 9306
$ZnSiF_6{:}6H_2O$, Paramagnetic Resonance Spectrum of 7365
Manganese Acetate, Susceptibility of 8819
Manganese Antimonide, Neutron Diffraction Studies of Chromium-Modified 7337
Manganese Bismuthide Films, Effects of Heat Treatment on Growth and Domain Structure of 7873
Manganese Chloride, Antiferromagnetic Susceptibility of 7962
Manganese Chromite-Aluminates,
Magnetic Properties of 6157
Preparation of 6157
Manganese Chromium Antimonide, Exchange Inversion in 7033
Manganese Chromium Antimony System, Exchange Anisotropy in the 6432
Manganese Cobalt Carbide, Preparation of the Ternary Alloy 6153
Manganese-Cobalt-Carbide Alloys, Crystal Structure of 9185
Manganese-Cobalt-Carbon Alloys, Magnetic Properties and Crystal Structure of 9185
Manganese Dichloride, Antiferromagnetic-Paramagnetic Transition in 8401
Manganese Difluoride, Microwave Faraday Rotation in Antiferromagnetic 6709
Manganese Dioxide,
Dielectric Properties of 8689, 8690
Effect of Thorium Doping on Resistivity Variations in 6687
Manganese Ferrites,
High Power Effects on Ferrimagnetic Resonance in 6438
Magnetization in 8787
Oxidation of 8634
Manganese Fluoride,
Antiferromagnetic Transition Temperature of 8820
Curie Temperature of 8820
NMR in 8808
Spin Flopping in 7050
Manganese^{2+}-Fluorine^{1-} in NaCl, PMR of 8354
Manganese-Magnesium Ferrites,
Magnetic Polarity Reversal of 6142
Relaxation Processes in 7964
Manganese Metaniobates, Ferroelectric Properties of 9245
Manganese Nitride, Magnetic Structure of 6704
Manganese Oxide,
Infrared Antiferromagnetic Resonance in 7048
Oxygen Surplus in Monocrystals of 6642
Manganese Pyroniobates, Ferroelectric Properties of 9245
Manganese Sulfide, Magnetic Susceptibility of Sintered Alpha- 6427
Manganese Tantalates, Ferroelectric Properties of 9245
Manganese Zinc Ferrite,
Ferromagnetic Resonance Parameters in 6436
Magnetic Properties and Grain Structure of 9189
Process of Making 6442
Manganese-Zinc Fluoride,
Hyperfine Structure of F^{19} in the Electron Paramagnetic Resonance of 6449
Optical Absorption in 7980
Manganous Carbonate, Magnetic Structure of 6154
Manganous Sulfide, Specific Heats of Polymorphic Forms of 7963
Manometers, Piezoelectric Oscillator 6299
Maser:
Action, Effect of:
Impurity Concentration on 6248, 6448
Temperature on 6248
Communication Systems 9109
Operation at High Temperatures 7725
Masers,
$CaF_2{:}U^{3+}$ 7669
Characteristics of 7467, 8046, 8472-8474
Circulators for 7724
Design of 6805
Duplexing in 6273
HF 6247
Microwave 8044, 8045
Millimeter Wave 6169, 9049
Negative Temperature in Semiconductor 8470
Nuclear Polarization Effects on 9047
Optical - See Lasers
Pumping in 7965
Recovery Technique for Saturated 7444
Reflection Cavity 7443
Resonant Modes in 8475, 9046
Ruby 6169, 6273, 8342, 8471, 9050
Semiconductor 8470
Theory of 8043, 8469
Titania 8474
Traveling Wave 7115, 8043, 8473, 9048
Tunable X-Band 8045
Masking, Fabrication of Double Diffused Junction Transistors by Oxide 9004
Masking:
in Si Using the Box Method, Oxide 6328
by SiO_2 Layers 6329, 6335
Technique for Vacuum Evaporation 6769
Mass:
Spectrometric Analysis of Molecules in Equilibrium with SiC 6929
Transport during Whisker Growth, Mechanism for 6034
Mathematical Functions, Analog Calculation of 8140
Matrices, Diode: Vapor Grown 6750
Matrix:
Switch for Coincident Current Memory 8121
Switches, Optimal Load-Sharing 7767
Synthesis 9058
Measuring Set for Telephone Message Circuit Noise 6865
Mechanical:
Properties:
- See also Elastic Constants, Plastic Properties
of Ceramics, Effects of Stress on 8414
of LiF 7689, 7692
Rate Meters 8567

Medical:
Applications:
Pulse Rate Monitors 7500, 7501
Radio Transmitter for Remote Heartbeat Measurements 7500
Thermoluminescent Dosimeter 7502
of Transistors:
Cardiac Pacemaker 6849
Cardiotachometers 7161
Intercardiac Catheter Tip Piezoresistive Pressure Gauge 7117
Physiological Stimulators 6850
Stimulus Isolator 6851
Electronics: Telemetering System for Stomach Pressure 8529
Measurements, Transistor Application in 8104
Meissner Effect in the Quasi-Chemical Equilibrium Theory of Superconductivity 7624
Melting:
of $AgSeTe_2$, Incongruent 6954
Point of InSb, Pressure Dependence of 8271
Memories - See also Storage Units
Memories,
Crowe Cell 7450
Cryogenic 7511, 7512, 7543
Ferroelectric 7193
Magnetic:
Core 6590, 6883-6885, 7189, 7806, 8134, 8135, 8464
Disc 6287
Film 6578, 6586, 6655, 6886-6888, 7191, 9126
Matrix 8543
Rod 9042
Maximization Techniques for Design of 6581
Transistor and Ferrite Core 6883
Twistor 7510
Memory,
Indexing System for Magnetic Drum 8541
Magnetic Core Matrix Switch for 8121
Memory:
Address Selector, Parametric 8122
Cells, Ferroelectric 7193
Cores,
High-Speed Coincident Current 6803
Inhibited Flux Operation of 9038
Residual States in 9039
Reversible Magnetization in 9040
Devices, Hall Effect 8449
Element for Perceptron System 8129
Elements,
$BaTiO_3$ Thin Film 6042
Capacitor 8128
Core Switching 7809
Cryotron 6808, 6813
Ferrite 6801, 6803, 6804, 8464
Magnetic Rod 9042
Semiconductor 6889, 9127
Tunnel Diodes as 6583
Planes for Extreme Environmental Conditions, Miniature 6798
Sensing, Miniature High Frequency Magnetic Amplifiers for Magnetic 6244
Transfer Circuits 8546
Mercuric Telluride-Zinc Telluride, Solid Solution in 6624
Mercury,
Critical Field of Superconducting 8284
Superconducting 6693, 8748
Mercury in Se, Diffusion Rate of 8198
Mercury Indium Alloys, Superconductivity of Dilute 6411
Mercury Selenide,
Dielectric Constant of 6130
Effective Mass of Electrons in 6130
Magnetoplasma Reflection in 6130
Mercury Selenide-Mercury Telluride,
Electrical Properties of 6931
Growth of 6931
Mercury Sulfide, Growth of 7881
Mercury Telluride, Optical Properties and Preparation of 8867
Mercury Telluride-Cadmium Telluride, Optical Properties and Preparation of 8867
Metal:
Alloys,
Resistivity of 8272
Thermoelectric Properties of 8920
Chelate Salt Crystals,
Crystal Symmetry of 6367
Growth of 6367
Films, Characteristic Energy Losses in 6177
Oxide Powder Compacts, Seebeck Coefficient of 6203
Precipitates, Excess Reverse Current in Junction Diodes Due to 6754
Metallic:
Bonds, Classification of Solids by 7903
Films, Vacuum Deposited 8415
Metals,
Absorption in 9388
Energy Band Structure of Polyvalent 9209
Fermi Surfaces of the Hexagonal Close-Packed 7591
Impurity Resistance in 7014
Mutual Solubility of 8164
Optical Properties of 9388
Polycrystalline Double-Bragg Reflections from 8592
Range of Electrons in 6053
Refraction in 9388
Resistivity Measurements by Eddy-Current Method in 9275
Superconductivity in Antiferromagnetic 8290
Theory of Electronic Properties of 7591
Thermal:
Conductivity of 8000
Resistivity of 8403
Transport Coefficients in Alkali 7299
Twin Faults in fcc 9177
Ultrasonic Attenuation in 8413
Vacancy Annealing in Impure 7240
Work-Hardening in fcc 8600
X-Ray Scattering from Fatigued 9163
Metals:
Grown from Melt, Effect of Solid-Liquid Interface on Pure 8632
by Low Energy Argon Ions, Sputtering of 6052
at Low Temperatures, Ultrasonic Attenuation and Dispersion in 6211
on Si, Mechanisms of Electroless Deposition of 6991
Meteorological Meters, Anemometer 8149
Meter, dc: Zener Diodes in 7524
Microcircuits,
Assembler for 7844
Laminar Junction Layer 7736
Microelectronics 6257, 6539, 7103, 7122
Micrologic Elements, Solid State 6580, 6774
Microminiaturization of Transistor Modules 6257
Micromodule Components, Review of 6537
Microphones, Piezoelectric 8105
Microphonism in Microwave Crystal Mixers 6215
Microplasma Phenomena in Si Junctions 6221, 6742, 6743, 8445
Microplasmas in Si 7088
Microwave:
Absorption,
Measurement of:
Carrier Lifetime by 6452
Semiconductor Properties by 6452
Absorption Switch, Broadband 6528
Amplifiers 6513, 8060, 8061, 8474
Applications, Garnets for 7216
Carrier Injection Modulators, Semiconductor 7109
Computer Circuits, Instrumentation for 7795
Crystal Mixers, Microphonism in 6215
Dielectric Dispersion and Loss in Ferroelectrics 6076
Diode Cartridge Impedance 6217
Microwave: (Cont'd)
Electromagnetic Radiation in Magnetic Materials, Generation of 7169
Energy through a Semiconductor, Effect of Absorption and Multiple Reflections on the Transmission of 6779
Faraday Effect in Si and Ge 7395
Ferrites at High Signal Levels, Measurement of 7641
Field:
on Conductivity in Ge, Effect of 9280
Distributions, Measurement of 6902
Filters Employing Single Crystal Garnet Resonators, Magnetically Tunable 6791
Frequencies, Fabrication of Semiconductor Devices for 8017
Generation and Amplification, Atomic and Molecular Resonances for 7725
Generators 6866
Hall Mobility in Ge 7932
Heating of Carriers in Semiconductors 6090
Methods of Measuring Mobility in Semiconductors 6100
Modulation of Light in Paramagnetic Crystals 7720
Modulators,
Excess Carrier Injection 7109
Semiconductor 6778, 6779
Paramagnetic Resonance Spectrum of Chromium Ions in Potassium Cobalticyanide 6163
Power Absorption in Yttrium Garnets 8038
Projectile Telemetry 7164
Properties:
and Applications of Garnets 7054
of Semiconductors 6416
of YIG 9364, 9368
Resistivity by Eddy Current Loss in Small Spheres, Measurement of 7616
Spectrometer, Precision Zeeman Modulation 6603
Spectrometers, Detectors for 7205
Switches, Diode 6216, 6265
Microwaves, Hall Effect Device for the Generation of 6195
Migration of Excitons 6389
Military:
Electronics, Piezoelectric Firing Indicator for 8105
Electronics: Thermoelectric Refrigerating System for Submarines 8576
Millimeter:
Cyclotron Resonance in Si 6123
Wave:
Generation, Parametric 8088
Harmonic Generator and Detector 7490
Modulator, Fabrication and Performance of a Ge p-i-n 8006
Oscillators 8090
Pulsed Field Masers 9049
Millivoltmeters 6899, 8559
Miniaturization of Devices and Circuits, Study of 6539
Minority:
Carrier:
Diffusion, Dipole Mode of 6214
Diffusion Lengths in p-n Junctions, Measurement of 8008
Sweep-Out Effect 9265
Carriers, Effect of Magnetic Field on the Diffusion of 7307
Missile:
Applications, Magnetic Amplifier-Transistor Power Supply for 6292
Autopilot System, Magnetic Shift Register 6853
Control Valves, Circuit for Determining Closure Time in 8150
Tracking, Transponder for 7791

Mixed:
Valence Compounds,
Thermal Properties of 6524
Thermoelements Using 6524
Mixer Diodes, GaAs 6612
Mixers,
Analysis of 6560
Microphonism in Microwave Crystal 6215
N-Frequency Parametric 7489
Noise Figure of 8067
Optimum Source Conductance of Crystal 7118
Mobility,
Bardeen-Shockley Formula of 8711
Field:
Dependence of 9269
Dependent 7283, 7304, 7306
Microwave Measurement of 8714
Surface 6421, 7267, 7300, 8264
Theory of 9266
Mobility:
- See also Scattering
Doping of Semiconducting Compounds 7012
with Electric Field, Theoretical Variation of Electron 6397
of an Electron in Donor Band of Compensated Semiconductors 8263
for Electrons and Holes, Evaluation of the Ratio of Hall Mobility to Drift 6683
using the Field Effect Modulation of Photoconductors, Measurement of Drift 7070
in Intrinsic and Narrow Band Gap Semiconductors 9267
Killer in Gallium Arsenide, Indium Arsenide, and Indium Phosphide, Evidence for a 6105
Variation with Applied Electric Field 8712
Mobility of:
AgBr, Hall 6106
AlSb 6362
AlSb-InSb 7938
Anthracene, Drift 8262
CdSnAs, Electron 6108
GaAs 6107, 6357, 7253, 7271
GaAs-GaP 7272
GaAs-Ga_2Se_3 7942
Ge 6101, 6109
Ge,
Hall 6672
Surface 7267
Ge-Si Alloys 7619
Hot Electrons 6388
InP 7271
InSb, Electron 7933
InSb-GaSb Alloy 8262
Ionic Crystals 8713
PbS: 7399
Photoconductive Films, Hole 7011
PbSe 7399
PbTe 7399
Polarons 9247
Se, Hole 7607
Semiconductors, 7612
Microwave Methods of Measuring 6100
Si 6101, 6103, 6104, 7608, 8237, 8715
Ti_2O_3 7309
Vitreous Materials 7949
ZnAs 7027
Modes:
of a Ferrite Slab Loaded Waveguide 6249
in Linear Circuits 7457
Modulation, Voltage to Pulsewidth Converters for Linear Pulsewidth 7486
Modulation of Light in Paramagnetic Crystals, Microwave 7720
Modulation-Demodulation Scheme for Ultrahigh-Speed Computing and Wideband Amplification 6570
Modulators,
Ferrite 7841, 8461
Microwave 6778, 6779, 7109
Millimeter Wave 6559, 8006
Radar 7160
Modulators: 6223, 6558, 6596, 6926, 7155, 8510, 9088
for dc Current Measurement 7202
Moisture Gettering with Porous Vycor 7713
Molecular:
Crystals,
Electronic Spectra of 9392
Paramagnetic Resonance in Hydrated and Deuterated 8838
Engineering, Concept of 6516
Field:
Coefficients in Ferrimagnets, Determination of 6140
of Ho Metal, Low-Temperature 6150
Solids, Domain Theory of Carrier Behavior in 7008
Molecules in Crystals, Electronic Spectra of 9390
Molybdenum,
Thermal:
Conductivity of 8000
Properties of 9441
Molybdenum-Cobalt Alloys, Electrodeposition of 6996
Molybdenum Si Contacts, High Temperature 8981
Monte Carlo:
Calculation for a Size Effect in Electrical Conductivity 7611
Computations on the Ising Model 7639
Morphology of Synthetic Submicroscopic Crystals of FeOOH and Fe_2O_3 7550
Mössbauer Effect in Crystals 8889
Motor Controls 6898, 8556
Mounting Washers, Transistor 6313
Multiaperture Magnetic Logic Element 6799
Multi-Layer Semiconductor Device, Fabrication of 8432
Multimode Propagation in Gyromagnetic Rods 6528
Multiplexers 7507, 8113, 8530
Multiplication, Use of Magnetoresistors for Analog 7514
Multiplication:
in Junctions 6399
in Junctions, Avalanche 8967, 8968
of Surface Current 6421
Multipliers,
Hall Effect 7105, 8033, 8760
Magnetoresistive 7514
Pulse 7415
Multiterminal Network Elements, Analysis of Circuits by 8052
Multivibrator Functional Unit, Binary 6309
Multivibrators 6268, 6562, 6613, 7148, 8083, 9073, 9078
Multivibrators,
Effect of Saturation on 7148
Output Pulse Duration of 6268
Recovery Time of 9079
Stability in Time Delay 6838
Temperature Stability of 8084
Trigger Sensitivity of 7757
Muscle Potential, Detection Circuit for 8104
Muscovite, Dislocations in 8598
Musical Instruments, Oscillators for 9072

N

N-Port Networks, Transmission and Hybrid Parameters for 9055
Nanosecond Pulses, Non-Saturating Transistor Circuitry for 6605
Naphthalene, Anisotropy of the Costa-Ribeiro Effect in 7897
Néel Points of the Heavy Rare Earth Metals 7016
Negative:
Conductance Amplifiers, Tunnel Diode 8079
Impedance Converter, Synthesis of Active Networks with One 7120
Negative: (Cont'd)
Mass:
Amplifiers,
Conditions for Amplification by 8452
Stability of 8499
Amplifiers as Noise Generators 8499
Carriers, Cyclotron Resonance of 9301
Effect in Semiconductors, Theory of the 6416
Resistance:
Amplifiers, Noise in 6823
Devices, Static Characteristics of Combinations of 7408
Diodes, p-n-p-n 6733
as an Equivalent Circuit Element 7733
in Network Synthesis 8050, 8053
Oscillators 8086
in Semiconductor Devices 6731
Temperature in Semiconductor Masers 8470
Neil Spike Formation in Si-Te 9361
Neodymium in:
Lanthanum Ethyl Sulfate, Paramagnetic Resonance of 8827
YIG, Incorporation of 6977
Neodymium Ethyl Sulfate, Spin-Lattice Relaxation in 7968
Nernst:
Effect, Methods of Measuring the 6206
Effect in Si at High Temperatures 6479
Network:
Analysis 7455, 7456
Synthesis 6819, 7120, 8050, 8053, 8480-8483, 9058, 9059
Theory 7119, 7452, 7454, 7457, 7734, 9054-9057
Networks, Parametric: Frequency-Domain Theory for 7453
Neutron:
Activation Analysis of Impurities 6942,6943
Bombardment Damage in Ge, Stability of 6672
Circuit for Use in Self-Organizing Systems, Solid-State 6568
Detectors 7209, 8570
Diffraction, Cryostat for Crystal Orientation by 6321
Diffraction:
Studies of Chromium-Modified Mn_2Sb 7337
Study of the Magnetic Structure of $(Mn,Co)_4C$ 6153
Irradiated:
Al, Microscopic Damage in 9197
Cu, Small-Angle X-Ray Scattering from 9157
Ge,
Defects Produced in 6627
Density Reduction in 6627
Electrical Conductivity in 6672
Hall Mobility in 6672
Lattice Vacancies in 6627
LiF, Electron-Spin Resonance Studies of Metallic Li in 6417
Irradiation:
Damage in a Cu-Al Alloy 9198
Defects in Ge 7929
of Gray Tin 7280
of PbTe, Bi_2Te_3, and ZnSb 7402, 7403
Radiation Damage, Resistance of Microalloy Diffused Base Transistor to 6767
Scattering in Lattices, Slow 8666
Transport in CdS 6192
Nickel,
Diffusion of Metals into 9181
Effect of Chemisorbed H_2 on the Magnetization of 9337
Electroless Deposition of Gold on 6992
Gyromagnetic Ratio of 9333
Magnetic:
Properties of Evaporated Thin Films of 9330
Susceptibility of 9340
Magnetostriction in 9367
Paramagnetic Resonance Lines of 7656
Polarization of Conduction Electrons in 7643
Zone Refining of 8194

Nickel:
Films,
Deposition of 7886
Magnetic:
Anisotropy in 7041, 8797
Domain Structure of 8322
Magnetoresistance in 8322
Spin Wave Resonance in 8327
Films by Impact Evaporation, Preparation of 6975
during Tension, Diffusion of H through 7859
Nickel in:
Al_2O_3, Paramagnetic Resonance of 8846
Cubic Symmetry, Optical Absorption of 7379
$KNiF_3$, Crystal Field Splitting of 7358
MgO, ZnO, ZnS, $MgAl_2O_4$ and YGaG, Crystalline Field for 7379
ZnF_2, Paramagnetic Resonance of 8352
$Nickel^{2+}$ in Sapphire, Linewidth Variations in the Magnetic Spectrum of 7657
Nickel Acetate, Susceptibility of 8819
Nickel-Cadmium Ferrites, Susceptibility of 8825
Nickel Chloride, Specific Heat of 6148
Nickel-Chromium Ferrites, Composition Effects on Characteristics of 8813
Nickel-Cobalt Alloys from a Pyrophosphate Bath, Electrodeposition of 6995
Nickel-Copper, Magneto-Optic Infrared Properties of 8851
Nickel-Copper Ferrites, Resonance Linewidth of 8814
Nickel Ferrite Formation, Effect of Iron Oxide Particle Size on 6155
Nickel-Ferrite-Aluminate, Ferromagnetic Resonance Absorption in 6145
Nickel Ferrites,
Electrical Resistivity of 8269
Ferrimagnetic Resonance in 6441, 8810
Magnetic Properties of Fine-Particle 7275
Preparation of Fine-Particle 7275
Thermomagnetic Behavior of Pure 6156
Nickel Fluoride, Magnetism of 6433
Nickel-Gold System, Kirkendall Effect in the 7864
Nickel-Iron:
Alloys, Temperature Dependence of the Magnetic Properties of 9342
Films,
Angle-of-Incidence Anisotropy in Evaporated 6430
Domain Walls in 6435
Induced Magnetic Anisotropy in Evaporated 8795
Magnetic Properties of Electrodeposited 7040
Texture and Magnetic Properties of Evaporated 9183
Nickel-Iron Ferrite, Magnetic Properties of 9357
Nickel-Iron Manganese Alloys, Exchange Anisotropy in 7339
Nickel Manganese,
Magnetic Anisotropy in 8318
Magnetization of 8318
Volume Changes on Ordering in 8167
Nickel Metaniobates, Ferroelectric Properties of 9245
Nickel Monoxide, Magnetostriction in 8303
Nickel Oxides,
Antiferromagnetic Domains in 6707, 7035
Conductivity of 8719
Crystallographic Measurements in Antiferromagnetic 6707
Oxygen Surplus in Monocrystals of 6642
Nickel Pyroniobates, Ferroelectric Properties of 9245
Nickel Tantalates, Ferroelectric Properties of 9245
Nickel-Zinc Ferrites,
Deposition of Thin Films of 7886
Magnetic Polarity Reversal of 6142
Magnetostatic Temperature Dependence of 8788
Magnetostriction of 6365
Preparation and Properties of Low Loss 7056
Production of 6365
Niobium, Lattice Specific Heats of Superconducting and Normal 8399
Niobium Oxide Rectifiers, Fabrication of 8989
Niobium Stannide,
Critical Field for Superconductivity in 7946
Isotope Effect on the Superconducting Transition of 7313
Nitric Oxide in KCl, Paramagnetic Resonance of 7363
Noise, Intervalley 9307
Noise:
Consideration for the Variable Capacitance Parametric Amplifier 6829
Figure:
Meters, Thermistor 8145
in Parametric:
Amplifiers 8065, 8067, 8068
Converters 8065
Mixers 8067
Generators, Negative Mass Amplifiers as 8499
Performance of:
Parametric Amplifiers 6544
Tunnel:
Diode Amplifiers 6261, 6740
Diodes 7459, 7700, 7701
Properties of Varactor Diodes 7115
Ratio of Si Crystal Rectifiers 8420
Spectra of p-n Junctions in Moist Atmospheres 6482
Suppression for Digital Signals 7745
Temperature Ratio of GaAs Microwave Diodes 6732
to Traps in CdS and ZnO, Relation of 7022
Noise in:
CdS,
Contact 9309
Shallow Trap 6419
Surface 7951
Trapping 7319
Ge, 1/f 9308
Ge Diodes 8969
InSb: 8698
Photodiodes 6781
Junction:
Diodes, Shot and Thermal 6766
Transistors, Shot 6232
Negative-Resistance Amplifiers 6823
a Nonlinear R-C System 7021
PbS:
Cells 6468, 6517
Photoconductive Films 6469
Semiconductors · 6125
Semiconductors,
1/f 6418
Excess 7022
Generation-Recombination 6126, 7629
Nonequilibrium Superconductive Phase in Cu-Bi Alloys 8289
Nonlinear:
Electronic Computer Elements for Analog Computers 8547
Networks, Random Process in 8484
Nonmetals, Optical Properties of 9389
Nonpolar Crystals, Variational Treatment of Warm Electrons in 7924
Nonreciprocal Single Crystal Ferrite Devices 6240
Nonunilateral Electron Devices in Narrow-Band Amplifiers, Analysis of 8057
NOR Circuits, Diode-Transistor 6871
Nuclear:
Coincidence Circuits 6904, 6905
Instruments: 7207
γ-Ray Spectrometers 7528
Pulse Height Analyzer 7211
Time-to-Pulse-Height Converters 7210
Magnetic:
Relaxation in Ionic Crystals 8842
Resonance:
Measurement of Superconducting Pb Resistivity Limit 8755
Observations, Transistor Oscillator for 6900
Nuclear: Magnetic: Resonance: (Cont'd)
Studies of Dislocations in NaI and KI 917
Resonance in:
Alkali Alloy Systems 7972
Alloys 7351
Antiferromagnetic MnF 8808
Crystal Analysis 8588
Cu Alloys 9383
Ferromagnetic Co 8807
Multidomain Ferromagnetic Cobalt Particle 6146
Organic Crystals 9155
Ta Metal 7352
Resonance of:
Co^{59} in Domain Walls of Co 8806
F^{19} in FeF_2 9385
Fluorine in $KMnF_3$ 9384
La^{139} in La 8347
Sc^{45} in Sc 8347
Solid H_2 and D_2 8346, 8844
Ta^{181} in Ta 7973
Paramagnetic Resonance of Na^{23} and Cl^{35} 7974
Particle:
Counters, Surface-Barrier 6908
Detectors,
Si Junction 6909, 6912, 6913, 6915, 7208, 7212
Si Surface Barrier 7209
Spectrometers,
Si Junction 6910, 6914
Si Surface-Barrier 6911
Quadrupole:
Interactions in Crystals, Volume Dependence of 7974
Resonance, Selective Spin Excitation and Relaxation in 7354
Resonance:
Absorption in Dy^{161} 7353
in Cu Alloys 9381
Study of Electronic Magnetism in Copper-Nickel 7350
Spectroscopy, Multi-Channel Junction Counters for 8574
Spin-Lattice Relaxation via Quadrupole Coupling 6175
Spin Relaxation in Superconducting Al 8843
Techniques for Measuring Magnetic Field in Superconductors 6116
Nucleation Mechanisms of Interface Motion 7875
Nuclei in Nonmetallic Ferromagnetics, Polarization of 8320

O

Occlusions on the Resistivity of Heavily Doped n-Type Ge, Effect of p-Type 668
Occupancy State Probability Function in Electron Impact Ionization 7908
Occupation Statistics, Dislocation Acceptor 7914
Ohmic Contact Method for Obtaining Sheet-Conductance Profile of Diffused Layers 6635
Ohm's Law in:
InSb, Deviations from 7306
Nonpolar Crystals, Deviations from 7304
Olivine, Effect of Pressure on the Spectrum of 939
Optical:
Activity in Te 7680
Bleaching in KCl 9395
Constants of:
Bi 8907
Ge 6473
Se 7997, 8908
Si 7394
Effects on F-Center Spin Resonance at Low Temperatures 8345
Encoders, Analog to Digital 8141
Filters 8869
Masers - See Lasers
Properties - See also Absorption

Optical: (Cont'd)
Properties of:
Carbon Films 7269
Cd-In-Te 6198
CdS 6474, 7385
CdSe 7396
CdTe 8870
Cu Halides 7671
Ga-Substituted GdIG 9429
Group II-VI Compound Solid Solutions 6030
Hg Te and HgTe-CdTe 8867
InSb Layers 6654
$InSb-In_2Te_3$ Alloys 7323
KCl:Tl in the Extreme Ultraviolet Region 7390
Luminescent ZnS-In 7991
Metallic Films 8394
Metals 9388
Nonmetals 9389
Phosphors 8876
Pyrographite 7996
Semiconductors 6176, 8869
SnSe 6132
Solids 6197
Vitreous Semiconductors 7674
ZnS 8883
ZnSe and ZnTe 7397
Radiation from Breakdown Avalanches in Ge 7675, 7676
Spectra in Paramagnetic Crystals 7977
Spectrum of:
Excitons 9249
Yb^{3+} in CaF_2 7976
Studies of Impurities in Ge 6196
Tape Sound Recording System, Transistorized 8531
Transmissivity and Characteristic Energy Losses, Relation of 6177
Order-Disorder in Ni_3Mn Alloy 8167
Organic:
Crystals,
Electronic Spectra of 9392
NMR and Thermal Expansion in 9155
Deposits, Trapped Radicals in 7367
Molecular Solids, Variation of Energy Gap with Size of the Conjugated System in 7029
Polymer Films,
Dielectric Properties of 7013
Electric Charge Transport through 7013
Photocurrents Excited by Visible Light in 7013
Semiconductors,
Characteristics of p-Phenylenediamine-Chloranil Complex 8735
Preparation of 6690
Resistivity of 6690
Solids,
Electronic Conduction and Exchange Interaction in a Class of Conductive 7621
Surface Trapping in 7029
Orientation:
of Etch Pits on Ge Dendrites 6664
of Evaporated Tin Telluride Films, Crystallographic 6953
by Neutron Diffraction, Cryostat for Single Crystal 6321
Oscillation Conditions 8081
Oscillations in:
Ferromagnetic Materials, Internal Friction of Longitudinal 8005
Quartz Crystals 8478
the Thermomagnetic Effect in Sn at Low Temperatures 6210
Oscillator-Generator, Multi-Frequency 6272
Oscillators - See also Generators
Oscillators, 6837, 6900, 7147, 7759, 8082, 8500, 8502
Automatic Frequency Control 6836
Beta-Phase-Shift 7151
Oscillators, (Cont'd)
Blocking: 6304, 7149, 7758
Discriminator 7532
Class-C 6555
Cryotron Ring 6554, 6811
Crystal-Controlled Precision 7478
dc to ac Converter 7818
Degenerative 8490
Functional Unit 6776
Hall Effect 9019
Harmonic 7479
HF: 8081
to UHF 7760
High Power 6264
Maser 8471
Microwave Parametric 8087
Multivibrator 7757, 9078, 9079
Negative Resistance 8086
Oscillistor 6777
Parametric 7698, 8504
Phase-Locked 7698, 9075
Piezoelectric 7730
Pulse 9072
Radiation Effects on Quartz 9052
Relaxation 8503
Resonant Circuit 9077
Sub-Audio 9074
Transistor:
Effect of Collector Junction Thickness on 8505
Limiting in Saturation Region of 8501
Tunnel Diode 6550, 7150, 8009, 8010, 8054, 8089, 8090
Variable Amplitude 9074
VLF 7146
Voltage Controlled 6553, 9076
Oscillistor 6777
Oscilloscope, Transistor Sampling Pulse 7825
Outdiffusion in Junction Transistor Fabrication 9006
Overload Safety Circuit 7199
Oxidation of:
Fe Whiskers, High Temperature 9191
Ge: 7581, 8637
Films 9192
Group III-V Intermetallic Compounds 8635
InSb 6979, 8228, 8229
Mn Ferrites 8634
Si Films 8227, 9192
SiC 8636
Thin Solid Films, X-Ray Reflection Studies of 7871
Oxidation-Induced Diffusion in Si 6326
Oxide:
Coated Cathodes, Mobile Acceptor Model for 6252
Films on Ge, Growth of Anodic 6346
Layers, Effect on Diffusion of P in Si 7862
Masking:
in Si by the Box Method 6328
of Solid SiO_2 against Boron 6329
Monocrystals, Modified Bunsen Method for Determination of Stoichiometric Deviations in 6642
Oxides,
Properties of Solid 6057
Structure of 8587
Oxygen,
Mechanical Damping of Ge and Si Containing 6213
Precipitation of Li in Si Containing 7226
Radiation Damage in n-Type Si Containing Dissolved 8645
Oxygen:
Adsorption on Clean InSb Surfaces 8638
Content on Electrical and Thermoelectric Properties of $Bi_2Te_{3-x}Se_x$, Influence of 7919
Dissolved in Si 6050, 6051
Ion Dilatation in Vitreous Silica 9445
and Lithium in Si, Interactions between 6337
Oxygen in:
Ge,
Diffusion Coefficient of 7570
Electrical and Optical Effects of 6179
Si,
Diffusion Coefficient of 7570
Evidence for Internal Rotation in the Fine Structure of the Infrared Absorption of 7378
Interstitial: 7378
versus Substitutional 7246
Solid State Reactions of 7226
Solid Solution in Ge, Aggregative Reactions of 6338
Oxygen on:
Ge Surfaces, Adsorption of 8231
the Magnetoresistance of Cu, Effect of 7628
Si Surfaces, Adsorption of 8230
Sintered CdS Photoconducting Films, Effect of 7393
Oxygen-Lithium Interaction in Si 8625

P

P-Phenylenediamine-Chloranil Complex, Electrical and Thermoelectric Properties of the 8735
Packaging of:
Diodes 8983
Diodes,
Dessicants Used in 8427
Heat Sink Configuration for 8426
Point Contact Diodes 8952, 8953
Transistors 9013
Transistors, Heat Dissipators for 8447
Pairs, Energy Levels of Donor-Acceptor 6380
Pairs in SiC, Polarization of Luminescence of Donor-Acceptor 6454
Palladium-Transition Metal Complexes, Magnetic Susceptibility of 9373
Paramagnetic:
Absorption of Polymeric Deposits 7367
Amplifiers, Design of Directional 6805
Behavior of Polycrystalline Sa 7057
Crystal Field Splitting in $KNiF_3$ 7358
Crystals,
Energy Levels in 7977
Microwave Modulation of Light in 7720
Optical Spectra in 7977
Spin-Phonon Interaction in 8340
Defects in Potassium Azide, Radiation Induced 7362
Energy Spectrum of Ruby, Effect of Configuration Mixing and Covalency on the 7357
FeO, Defect Structure of 8204
Ions, Growth of $CaWO_4$ Crystals Containing 8222
Ni^{2+} Ions, Calculation of the 3d-Electronic State of 6174
Particles, Anisotropy Energy and Remanent Magnetization of 8790
Properties of Cr^{3+} in TiO_2 6806
Relaxation:
Effect of Cr and Fe in Potassium Cobalticyanide 7661
Rates Determined by Pulsed Double Resonance Experiments 6448
Time Measurements 7655
Times, Influence of Exchange Interaction on 6172
Resonance,
Exchange-Narrowed 8828
Nuclear and Electron 8841
Passage Effects in 6711
Resonance:
Absorption,
Observation of Energy Storage in Phosphors by 8383
Saturation of Inhomogeneously Broadened 8830

Paramagnetic: Resonance: (Cont'd)
Absorption in:
CdTe:Mn and CdS:Mn 8356
Si 8359
ZnS 9386
Absorption of:
Fe^{2+} in MgO 9386
Fe^{3+} and Mn^{2+} in Spinel Structures 7966
Nickel^{2+} in Sapphire 7657
Line Shape 7656
Lines, Spin-Flip Narrowing of 6162
Linewidth in Dilute Crystals with Anisotropic g-Factor 8827
Study of X-Ray Radiation Damage in LiF 8647
Resonance in:
Al Garnets 6446
Al_2O_3 8339, 8355, 8846
Beryl 7667
CaF_2 7976, 8832
$CaWO_4$ 8353
CdS 7058
Corundum 6714
Ferroelectric Materials 6166, 6167
Ga Garnets 6446
Guanidine Alum 6167
Hydrated and Deuterated Molecular Crystals 8838
KBr 8839
KCl 7363, 7665, 8345, 8839
$K_3Co(CN)_6$ 8831
$KFe_2(CN)_6$ 6163
La Ethyl Sulfate 8827
LiF 6417, 8835, 8837
Metal Chelate Salt Crystals 6367
$Ni(NH_3)_6Cl_2$ 8357
Non-Cubic Crystals 7361
Rochelle Salt 6166
Ruby 8845
Rutile 6165
Sapphire 8348
Solids 6161
SrS 8879
TiO_2 7364, 7975, 8349
YGaG 8350
ZnF_2 6449, 8352
$ZnSiF_6 \cdot 6H_2O$ 7365
Resonance of:
Color Centers in:
KCl 7665
KCl, Optical Effects on 8345
Co^{2+} 7654
Cr in Potassium Cobaltcyanide, Microwave 6163
Cr^{3+} in:
Al_2O_3 8339
Guanidine Alum 6167
Ruby 8845
YGaG 8350
ZnF_2 8352
Eu:
Activators in SrS 8879
in CdS 7058
F-Centers in LiF 8837
Fe: 9376
in Beryl 7667
Fe^{3+} in:
Rutile 6165
TiO_2 8349
Gd^{3+} in:
$CaWO_4$ 8353
Single Oxide Crystals 8847
Li in LiF 6417
Mn in:
TiO_2 7364
ZnF_2 6449
Mn^{2+} in:
$CaWO_4$ 8353
Corundum 6714
$ZnSiF_6 \cdot 6H_2O$ 7365
Nd^{3+} in Lanthanum Ethyl Sulfate 8827
Paramagnetic: Resonance of: (Cont'd)
Ni in Al_2O_3 8846
Ni^{2+} in ZnF_2 8352
NO in KCl 7363
Sm Activators in SrS 8879
Ti^{3+} in Al_2O_3 8355
Transition Metals in Single Crystal Oxides 8847
V^{2+} in ZnF_2 8352
V^{4+} in TiO_2 7975
Yb and Ga Garnets 6446
Yb^{3+} in:
Al and Ga Garnets 6446
CaF_2 7976
Salts, Spin-Lattice Relaxation in 8833
Solute in Metals, Antiferromagnetic Ordering of 7961
Spin:
Coupling 6173
Relaxation of F-Center Electrons 7664
Resonance by Microwave Faraday Rotation, Measurement of 7666
Spin-Spin Relaxation, Theory of 7658-7660
Spins and the Crystal Lattice, Power Transfer between 7662
Stimulated Infrared Emission from Trivalent Uranium 7669
Susceptibility in Si and Ge 8848
Susceptibility of:
an Electron Gas in Alkali Metals 7356
Fe and Fe-Si Alloys 9375
Fe-Y and Fe-Rare Earth Ferrites 8338
$MgNi_2$ 9374
Mixed Paramagnetic Crystals 8337
Ni-Cd Ferrites 8825
Systems, Cross Relaxation in Dilute 7366
Three and Four Level Systems, Saturation in 8829
Zero Field Splitting of V^{3+} in Al_2O_3 7359
Paramagnetics, Resistivity of 9287
Paramagnets, Refractive Indices of 8906
Parametric:
Amplification:
by Junction Diodes 7471
along Nonlinear Transmission Lines 6546
Using Surface Space Charge Varactors 6251
Amplifier:
Performance, Theoretical Limitations to Ferromagnetic 6245
Transistor Operating in an Up-Conversion Mode 7137
Amplifiers 6226, 6832, 7133, 7135, 7467, 7752, 7754, 7845, 8007, 8065, 8071, 8102, 8498, 9069, 9070
Amplifiers,
Degenerate Mode 6548, 7473, 7475, 7751
Distributed 6259
Ferrite 6548
Ferroelectric 8074, 8075
Ferromagnetic 7476, 8072
Filter Structures for 8066
Helix 6831
Low-Noise 6827
Magnetic Film 8497
Noise in 6544, 6829, 7134, 7136, 7473, 8066-8068
Pumping of 6549, 8073
RF 7777
Strip Line 7698
Traveling-Wave 6545, 7138, 7139, 7474, 7752, 7753, 8066
Tunable 7140
Wide Band 8066
X-Band 8069
X- and S-Band 8060
Converters 8065, 8102
Device as a Nonreciprocal Element 7735
Diode, Equivalent Circuit of a 7458
Diode Figure of Merit and Optimization 6830
Frequency Multipliers 8097
Parametric: (Cont'd)
Generators,
Microwave 8087
Millimeter Wave 8088
Harmonic Generators, Large Signal Analysis of 7157
Limiters, Passive 6564
Mixers,
Evaluation of N-Frequency 7489
Noise Figure of 8067
Modulators 7155
Networks, Frequency-Domain Theory for 7453
Oscillators 8504
Phase Shifters 8051
Switching Circuits 7769
Trigger Circuits 7768, 7769
Up-Converters, Gain:
Inconsistencies in Low-Frequency Reactance 6828
Optimization in 7491
Parametron:
Binary Adders 6878
Computer Circuits 7800
Shift Registers 6878
Parametrons,
Application in Computer Circuitry 8122
Operation of Magnetic Film 6802
Parametrons as Logical Devices, Magnetic Film 6878
Partial Switching of Ferrite Cores 6577, 6587, 6588
Particle:
Counters 6967
Detectors 7208, 7212, 8569, 8570, 8572
Growth during ZnS Phosphor Preparation 6969
Interaction in Magnetic Recording Tapes 6250
Particles, Growth of Ultra Fine Ferrite 6972
Passivation of Micro-Components, Surface 7706
Pedestal Method for Growing Ge and Si Crystals 8211
Peltier:
Coolers, Properties of 8460
Cooling, Automatic Dew-Point Hygrometer Using 7206
Effect:
for Cooling Diodes, Use of the 7075
in Ge, Resistivity Gradient Dependence of Volume 8003
Method of Measuring Radiation Emissivity 7072
Penetration Depth in Superconducting Al 6696
Perceptron System, Magnetic Memory for 8129
Perfection of Crystals, Determination of the 6945
Peritectic:
Compounds,
Electrical Properties of 7274
Zone Refining and Crystal Growth of 6015
Semiconducting Compounds, Preparation of 7274
Permalloy:
Films,
Anisotropy in Evaporated 9355
Annealing of Oblique-Incidence 7042
Cross-Tie:
and Chain Walls in 8803
Walls in 9359
Initial Susceptibility Spectra of 6426
Magnetic Anisotropy in 8796, 8797
Magnetization Reversal of 8321
Magnetoresistance and Magnetic Switching in 7044
Rotatable Anisotropy in 7043
Films Evaporated at Grazing Incidence 6971, 6973
Permanent Magnets, Magnetic Material for 9044, 9045
Permeability, Temperature Variation of 8313
Permeability:
- See also Susceptibility
Characteristics of Mixed Y-Gd Iron Garnets, Initial 6444
of Fe-Al Alloy, Heat Treatment-Magnetic Field Effects on 9345

Permeability: (Cont'd)
of Ferrites, Measurement by Resonant Cavity Techniques of 8315
of $SrTiO_3$-$Bi_2O_3 \cdot BiO_2$, Dielectric 9232
Permeation Rates of Hydrogen in Ge 7250
Perminvar, Magnetic Annealing in 9343
Permittivity, Measurement of 7592
Permittivity:
-See Dielectric Constant
of $BaTiO_3$, Effect of Si Ion Replacement on 7920
in Millimeter Range, Measurement of 7921
in Perovskite-Type Ferroelectrics, Theory of the Electric Field Variation of Incremental 6077
Perovskite-Type Ferroelectrics, Electric Field Variation of Incremental Permittivity in 6077
Perovskites, Antiferromagnetic Rare Earth-Fe 8822
Persistent-Current Superconducting Devices, Study of 7728
Persistor Superconducting Memory Element 6813
Perturbation Theory of Antiferromagnetism 8331
Phantastron Delay Circuits 6848
Phase:
Converters 8514
Detectors 8511-8513, 9093
Diagram:
for Cd-Te 6317
Determination in Alkali Alloy Systems 7972
of HgSe-HgTe 6931
Diagrams:
of I^b In VI^b_2 and II^b In_2 VI^b_4 Alloys 7274
in a Pseudoquinary System 7229
of Si 7846
Discriminators 9092
Equilibria:
for $CdAs_2$ and Cd_2A_3, Solid-Vapor 8582
of FeO-MgO-Fe_2O_3 Ferrites 8581
of La_2O_3-Iron Oxide Systems in Air 8157
in the ZnO-TiO_2 System 8580
Modulators, Reciprocal Ferrite 8461
Relations in the System BaO-TiO_2-P_2O_5 6318
Shifters,
Ferrite 6527, 7723
Nonreciprocal 7735
Variable Capacitance Diode 8051
Transformation, Effect of High Pressures on α-γ Iron 7848
Transformations in:
Mn^{3+} Spinels 8590
Transition Metal Spinels, Cubic-to-Tetragonal 9151
Transition:
in $BaTiO_3$-$BaSnO_3$ Solid Solutions 7599
of Evaporated Superconducting Thin Films, Influence of Aggregation on the Magnetic 6409
Transitions in:
Ferroelectric $PbNb_2O_6$ 7600
Teflon, Polymorphic 9152
Solid Solutions 8583
Solids, Gradual 8585
Phase-Locked Oscillators 9075
Phase-Sensitive Detection with Multiple Frequencies 7488
Phase-Shift Modulators, Hall Effect 9018
Phonon:
Drag:
Measurements in Si, Transmitted 8922
in Si, Transmitted 9221
Scattering:
by Chemical Impurities in NaCl 7684
in KCl-KBr Solid Solutions 9270
in Nonpolar Crystals 7924
Phonon-Assisted Transitions in Tunnel Currents 6701
Phonon-Phonon:
Interaction, Acoustic Absorption by 6212
Transitions in Si 8716
Phonon-Spin Interaction in YIG 6147
Phonons:
in High Power Ferromagnetic Resonance Experiments, Generation of 6706
by Lattice Defects, Scattering of 6200
Phosphate Glass, Conductivity of High Vanadium 7944
Phosphor:
Decay, Effect of Pressure on 6457
Films:
by Evaporation, Formation of ZnS 6968
Formation by Evaporation 7894
Preparation, Particle Growth during ZnS 6969
Radiation Detectors, Dual 7829
Screens 9031
Phosphor BaO-TiO_2-P_2O_5, Preparation of the 6318
Phosphorescence:
of KCl 9417
Mechanisms, Theory of 7065-7068
Phosphorometer 7066
Phosphors,
Boron Nitride Electroluminescent 6235
CaS:Cu, Eu Electroluminescent 6462
$CaSiO_4$:Sn 6464
Charge Compensation Theory in 8161
Crystal Structure and Spectra of Alkali Halide 7989
Electroluminesce:
under Pulsed Square-Wave Excitation in 6184
in ZnS:Cu 8377
Electron Paramagnetic Resonance Studies of Activated 8878
Emission Bands in Sn, Pb, and Sb Activated 7925
EPR Studies of Eu and Sm Activators in SrS 8879
Fatigue in Electroluminescent 6186
Field Amplification of Zn-CdS-Mn 7982
Fluorescence of BaO-TiO_2-P_2O_5 6318
Growth of 7988, 7991
Light Stimulation of ZnS-Cu 7986
Luminescent Properties of $3MgO \cdot B_2O_3$:Ag 6463
Maintenance of Electroluminescent 7063
Mechanism and Efficiency of Electroluminescence in ZnS 6458
Microscopic Observations on Electroluminescent 6182
Optical Properties of 8876
Paramagnetic Resonance Absorption Observation of Energy Storage in 8383
Photo- and Electroluminescence in (Zn,Hg)S and (Zn,Cd,Hg)S 7988
Preparation of:
Alkaline Earth Pyrophosphate 6189
(Zn,Hg)S and (Zn,Cd,Hg)S Electroluminescent 7677
Quantum Efficiency and Absorption of Powder 6188
Range of Electrons in 6053
Vanadium Activated Zinc and Cadmium Sulfide and Selenide 6461
Voltage Dependence and Particle Size Distribution of Electroluminescent 6183
X-Ray Photoconductivity of Sulfide 6191
Phosphors:
of KCl:Tl, Jahn-Teller Effect in 8874
under Pulsed Square Wave Excitation, Electroluminescence of 6459
Phosphorus, Purification of 7271
Phosphorus in Si, Diffusion of 6334, 7862
Photocell Applications in Card Readers 8125
Photocells,
Diffusion Layer Measurements in Si 7300
Fabrication:
and Characteristics of 9025
of Coolable PbS 9026
of Multielement 9030
and Performance of Position Sensitive 8035
Reflection Coefficient of Antireflection Coated Surfaces of Si 6521
Photoconduction in PbS, Mechanisms of 9022
Photoconductive:
Cells,
Fabrication of Surface-Protected 9029
Influence of Crystal Size on the Spectral Response Limit of Evaporated 6465
Time Constant of PbS 6466
Decay in Filaments, Influence of Transverse Modes on 6392
Detectors, Operating Characteristics of PbS 6234
Devices, Fabrication of 9028
Films,
Hole Mobility and Crystal Size in PbS 7011
Minority-Carrier Effects in Chemically Deposited PbS 6466
Noise and Signal Response in PbS 6469
Sintered CdS 7393, 8384
Processes in CdS 6192
Trapping in ZnS, Paramagnetic Resonance Studies of 8893
Photoconductivity, Experimental Studies of 6197
Photoconductivity of:
AgBr Emulsions 9421, 9422
AlP 7589
CdS 6112, 7391, 7951
CdS-ZnS Mixed Crystals 8899
Cu-Activated Cd(S:Se), Spectral Response of the 8385
Cu_2O 8903, 9425
Cu_2O, Exciton-Induced 9423
GaS-Se 8900
Ge: 8259, 8386, 8864, 8894, 9424
Grain Boundaries 8896
Group V-VI-VII Compounds 8901
InSb 8897
KBr 7993
KCl 6717
Metal-Free Phthalocyanine Films 7992
Microcrystalline Powders, Mechanism of 7069
PbS Films 7284
PbSe 8898
Rhombic Sulfur 6113
Semiconductors with Traps, Theory of 8261
Sulfide Phosphors, X-Ray 6191
ZnO 8612
Photoconductor:
and an Electret, Photorectifier Combining a 6518
Response, Contact Geometry and Detector Orientation Considerations in Maximizing 6780
Photoconductors,
High Electric Fields in Shadow Regions on 6718
Measurement of Drift Mobility Using the Field Effect Modulation of 7070
Surface States in PbS 6467
Thermally Stimulated Currents in 6190
Traps in PbS 6467
Photocurrents Excited by Visible Light in Organic Polymer Films 7013
Photodetectors,
Grain-Boundary 6788
Relaxation Time of PbS 8453
Photodevice:
Applications: Radiation Tracking 7529
Dose Ratemeter 7163
Photodevices,
Application in Fringe Comparator 8147
Operating Characteristics of PbS 6234
Radiation Limited PbS 6517
Spectral Response of Solar Cell 7438
Two Color Input-Two Color Output Image Intensifier 7110
Photo-Dielectric Effect in ZnS-(Cu,Fe) 8890
Photodiodes,
Graded Junction 7436
Noise in InSb 6781
Photodiodes for the Visible Region, GaAs 6782
Photoeffect on Diffused Junctions with Integral Field Gradients 7436
Photoeffects in Nonuniformly Irradiated Junctions 6784

Photoelastic Constants of Vitreous Silica 9445
Photoelectric:
  Binary Counter 7435
  Card Reader 8125
  Emission from Ta, Field Dependence of 6193
  Etching Technique for Preparing Thin Filaments of Ge 7267
  Measurements on High Resistivity Crystals 9257
  Properties of:
    Cd and ZnTe Layers 7392
    Grain Boundary Layers 6072
    Metallic Films 8394
    Se and AsSe Films 8387
    ZnSe and ZnTe 7397
  Punched:
    Card Reading System 7435
    Tape Reader 8126
  Sensitivity of Se Cells Subjected to a Magnetic Field 7716
  Threshold in Si, Hydrogen Adsorption Effects on 9427
Photoelectromagnetic Effect in:
  Bi 8391
  Ge 9428
Photoelectromotive Forces in Electron Irradiated PbS Films 7678
Photoelectronic Properties of ZnS 8902
Photoemission:
  of Alkali Iodides 7320
  from Back Biased Si Junctions, External 6722
  from Ge, Field Induced 8390
  in the Phtovoltaic Response of Cu-CdS Cells 6721
  from Semiconductors 8389
Photoflash Power Converters 6599
Photoluminescence:
  of SiC, Polarized Edge Emission in 6453
  in (Zn,Hg)S and (Zn,Cd,Hg)S Phosphors 7988
Photomagnetic Effect in Semiconductors, Measurement of the 6471
Photometric Determination of Sb and Tl in Pb 8192
Photomultipliers,
  Power Supply for 8553
  Transistor 8564
Photon Absorption by Valence Electrons in Mg 7381
Photorectifier Combining a Photoconductor and an Electret 6518
Photoresponse of:
  Junctions 8008
  Si Junction Surfaces 6741
Photosensitive:
  Cells, Fabrication of 9024
  Ultrasonic Attenuation in CdS 8942
Photosensitivity of Photo-Cathodes 8905
Phototransistor:
  Card Readers 8125
  Photocells 8035
  Punched Tape Readers 8126
  Relays 7437
Phototransistors,
  Fabrication of an Array of 9030
  Thermal and Optical Beahvior of 7437
Photovoltages:
  from Anodic Films on InSb 6347
  in Si Films, Larger-than-Bandgap 7578
Photovoltaic:
  Cell, Alloyed Junction InSb 6520
  Cells for Instrumentation and Control Applications 7435
  Devices, Diffused Si 6949
  Effect:
    from the Carnot Cycle, Derivation of the 6783
    at a GaAs-Electrolyte Interface 6720
  Effect in:
    AlP 7589
    Binary Compounds, Becquerel 6720
    CdS 6470
    GaP 7990
    Si, Surface 9426
  Electric Power Generators 8551
  Evaluation of the Homogeneity of Resistivity of Ge 6401
Photovoltaic: (Cont'd)
  Moiré Fringe System for Machine Tool Control 7435
  Power Supplies, Multiple Junction 6542
  Response of Cu-CdS Cells, Photoemission in the 6721
  Solar Energy:
    Conversion, Effect of Temperature on 6519
    Converters,
      Efficiency of 6785
      GaAs 6786
      Improvement of 6787
Phthalocyanine, Electrical Properties of Poly-Copper 6424
Phthalocyanine Films, Photoconductivity of Metal-Free 6719, 7992
Physiological:
  Stimulator 6850
  Stimulus Isolator, Transistor 6851
Piezoelectric:
  Constants of:
    Anisotropic Media 9443
    CdS, Measurement of 8257
    Ga-Fe Oxide 6681
  Crystals,
    Production of Sound in 8694
    Reduction of Temperature Frequency Shift by Stressing 8047
  Excitation of Quartz Oscillators 7730
  Force Gages 7729, 7730
  $Ga_{2-x}Fe_xO_3$, Ferromagnetic Resonance in 7046
  Microphones 8105
  Moduli of Crystals of Triglycine Sulfate 6043
  Oscillator Manometers 6299
  Plates, Excitation of 6816
  Properties, Effect of Random Inhomogeneities on 7019
  Properties of:
    $BaTiO_3$ 6307, 7596
    a Mixed Titanate System 6088
    Some Ferroelectric Solid Solutions Based on $NaNbO_3$ 6680
  Quartz Crystals, Reduction of Transverse Oscillations in 8478
  Resonance in $BaTiO_3$ 9246
  Resonators, Properties of Synthetic Quartz 8479
  Scattering in:
    CdS 8693
    InSb 7305, 7306, 7317
    ZnO 8693
  Substances, Search for New 6089
Piezoelectricity, Effect of Random Inhomogeneities on 7019
Piezo-Optic Constants of Zincblende 7369
Piezoresistance of:
  Sb Doped Ge 7003
  GaSb, Pressure Effects on 6068, 8724
  Ge, Pressure Effects on 8724
  InSb, Pressure Effects on 8724
Piezoresistance in InP 6111
Piezoresistive:
  Devices, Design of 6402
  Effect in Semiconductors 6402
  Pressure Gauge, Intercardiac Catheter Tip 7117
  Strain Transducers 6534
Piezoresistivity, Survey of 6534
Piezoresistivity of:
  $(Ba \cdot Sr)TiO_3$, Temperature Dependence of 8255
  InSb 8271
  PbTe 8256
  Rutile 6404
Pipes, Association of Breakdown with Doping 6495
Pirani Gauge Utilizing Thermistors 8566
Plasma:
  Effects in Bi 7372
  Mechanism of Carrier Recombination in Homopolar Semiconductors 6092
  in a Semiconductor, Magneto-Oscillatory Effect in the Electron-Hole 6777
Plastic:
  Deformation:
    of Ge by Alloying 6748
    on X-Ray Production of Color Centers in KCl, Effects of 6005
  Flow in Crystals 7694
  Properties of LiF and MgO Single Crystals 7693
  Resistance to Dislocation Motion in Crystals 8186
Plasticity of Mg, Parameters Influencing 8412
Plates, High-Speed Ferrite Rotating Half-Wave 6530
Plating:
  Parameters on the Structure of Co and Co-Ni Alloys, Effect of 6994
  Techniques, Dendritic Growth Studies by Pulse 6353
  in Thin Electrodeposited Films of Fe-Ni Alloys, Initial Growth of 7078
Platinum, Kinetics of Quenched-In Lattice Vacancies in 9167
Platinum-Transition Metal Complexes, Magnetic Susceptibility of 9373
Point:
  Contact:
    Rectification, Dipole Mode of Minority Carrier Diffusion with Reference to 6214
    Transistors, Fabrication and Properties of 8429
  Defect Effects on Thermal Resistance 9434
  Defects in:
    NaCl, K^+ 8175
    Quenched Ag and Au 9197
Points by Controlled Dissolution, Production of Alkali Halide 6658
Polar:
  Crystals, Slow Electrons in 9247
  Semiconductors,
    Conductivity of 9271
    Hall Constant of 9271
Polarizability of:
  $BaTiO_3$ 9237
  Free Carriers in Ge and Si 7010
Polarization:
  in Diamond, Decay of 7995
  Effect in Electrical Conductivity of Al_2O_3 7595
  Energy in Ion Lattices 8669
  in Guanidine Aluminum Sulfate Hexahydrate, Reversal of the Spontaneous 7598
  Reversal in:
    Colemanite 6087
    Deuterium-Doped Rochelle Salt 7007
    Rochelle Salt 9238
    Triglycine Sulfate 9239
Polarization of:
  Conduction Electrons in Ferromagnetic Metals 7643
  Fluorescence in CdS and ZnS 6456
  the Luminescence of Donor-Acceptor Pairs in SiC 6454
  Luminescence in ZnS and CdS 6455
  Microwaves, Rotation of the Plane of 6195
  Nuclei in Nonmetallic Ferromagnetics 8320
  Triglycine Sulfate, Spontaneous: Pyroelectric Technique for Determination of 8246
Polarized:
  Edge Emission of SiC 6453
  Light Determination of Optical Constants of Se Crystals 7997
Polaron, Parameters of 9247
Polaron Formation in Ionic Crystals 9236
Polishing:
  of Quartz Crystal Surfaces 8048, 8049
  YIG Spheres 7277
Poly-Copper Phthalocyanine, Electrical Properties of 6424
Polycrystalline Garnets, Preparation of 6443
Polygonization in Plastically Deformed InSb 6632
Polygrain Metals, Double-Bragg Reflections from 8592

Polymeric Deposits,
  Paramagnetic Absorption of 7367
  Preparation of 7367
Polymerization Reaction of Oxygen with Si 7226
Polymorphism:
  in Alkali Halide Phosphors 7989
  of $BaTiO_3$ 7548
  of the Thallium Halides 7549
Polyoxymethylene Single Crystals, Growth and Properties of 9188
Polyphase Oscillators, Oscillation Conditions for 8081
Polystyrene Films, Electric Charge Transport through 7013
Polytype in SiC Whiskers, Determination of 6022
Polytypism in SiC Crystals 6937, 6952
Positive-Gap Diode Adders 7508
Positive Temperature Coefficients of Electrical Conductivity, Temperature Distribution in Materials with 6727
Positrons in Anthracene, Effect of Disorder on Lifetime of 7928
Postal Sorters 8153
Potassium$^+$ Point Defects in NaCl 8175
Potassium Azide,
  Radiation Induced Paramagnetic Defects in 7362
  Thermoluminescence of 7389
Potassium Bromide,
  Absorption in 8839, 8857
  Color Centers Created in 7235
  Infrared Absorption in 8363
  Paramagnetic Resonance in 8839
  Pulse Photoconductivity of Additively Colored KBr 7993
  Secondary Emission of Cleaved 9316
  Temperature Dependence of the Elastic Constants of 8409
Potassium Chloride,
  Absorption in 8839, 8856, 8857, 8859, 8868, 9397, 9404
  Bleaching of:
    Color Centers in 7236, 9168, 9395
    Irradiated 7555
  Breakdown Strength of 6998
  Cohesive Energy of 8236
  Color:
    Center Diffusion in 6934
    Centers in 6005, 7235
  Defects in 7556
  Dislocations in 8596
  Elastic Moduli of 8937
  Electric Strength of 7594
  Electrical Properties of 6998
  Electrification of 6385
  Electron:
    Microscope Studies of Colloids in 6981
    Paramagnetic Resonance of Color Centers in 7665
  ESR of F-Centers in 8840
  F-Center Photoconductivity in 6717
  Fundamental Lattice Dispersion Frequency of 6671
  Growth of F-Centers in 6006
  Infrared Absorption in 8363
  Paramagnetic Resonance in 7363, 8839
  Phosphorescence of 9417
  Photoconductivity of 8904
  Radiation Effects in 6385
  Secondary Emission of Cleaved 9316
  Specific Heat of 8937
  Sr Concentration in 8244
  Thermo-Activation Energies in 6209
  Ultrasonic Attenuation in 6480
  Vacancy Association with $CaCl_2$ Impurity in 7868
Potassium Chloride Surfaces, Electron Microscope Studies of Cleaved 6981
Potassium Chloride-Potassium Bromide Solid:
  Solution, Effect of Annealing on 7554
  Solutions, Phonon Scattering and Conductivities of 9270
Potassium Chloride:Tl in the Extreme Ultraviolet Region, Optical Properties of 7390
Potassium Chloride:Tl Phosphor, Jahn-Teller Effect in 8874
Potassium Chrome Alum, Acoustic Attenuation in 8940
Potassium Chromicyanide, Electron Spin-Lattice Relaxation in 8344
Potassium Cobalticyanide,
  Cross Relaxation Effect of Cr and Fe in 7661
  Electron Paramagnetic Resonance Spectra of 8831
  Microwave Paramagnetic Resonance Spectrum of Cr Ions in 6163
  Paramagnetic Relaxation Rates in Cr-Doped 6448
Potassium Ferrocynamide Trihydrate, Ferroelectricity of 9244
Potassium Halides, Lattice Vibrations in 9218
Potassium Iodide,
  Color Centers in 7235
  Luminescence of 9419
  Nuclear Magnetic Resonance Investigation of Dislocations in 9170
  Photoemission from 7320
  Secondary Emission of Cleaved 9316
Potassium Manganese Fluoride, Nuclear Magnetic Resonance of Fluorine in 9384
Potassium Nickel Fluoride,Crystal Field Splitting in 7358
Potentiometer Tracks, Application of Deposited Film Resistors to 8415
Powder:
  Compacts, Effect of Pressure on the Seebeck Coefficient of 6203
  Metallurgy Techniques, Preparation of PbSe by 6959
Power:
  Conversion Gain of Si Crystal Rectifiers 8420
  Converters 6599, 7201, 7818, 8112, 8144
  Dissipation, Transistor 7466
  Dissipation:
    of Diodes, Method for Increasing 8426
    Limits in Bistable Transistor Pulse Circuits 6556
  Effects in Ferrite Devices, High 6241
  Flow in Reactive Elements 8485
  Gain of Narrow-Band Amplifiers Employing Nonunilateral Electron Devices 8057
  Generation, Precise Frequency 7519
  Generators,
    Photovoltaic 8551
    Regulators for 7516, 7517, 9130
    Thermoelectric 8459
    Ultrasonic-Frequency 6294
  Inverters, Diode-Magnetic Amplifier 7819
  Measurement, Use of a Hall Generator for 6298
  Measurements, Error in RF 7828
  Meters 6619
  Meters, RF 9146
  Performance of Ferrites in Isolators, Prediction of High 6145
  Rectifiers, Performance Parameters of 6497
  Regulators 7812, 8112, 9133
  Regulators, Transistor dc 7196
  Sources for Semiconductor Devices, Photovoltaic 6542
  Supplies,
    Constant Current 7518
    Discharge Lamp 7820
    Fluorescent Tube 6598
    Mass Spectrometer 7814
    Photomultiplier 8553, 8564
    Photovoltaic 6542
    Stabilizers for Transistor 6541
    Static Control for Mechanically Regulated 7515
    TV Receiver 8526
  Supplies: 6292, 6541, 6736, 7200, 7814, 7821, 8552, 9135-9137
    - See also Voltage Regulators
  Supply for Missile Applications, Magnetic Amplifier-Transistor 6292
  Switches, Comparison of Three and Four Layer Devices as 6227
Power: (Cont'd)
  Switching Circuits 8506, 8509
  Transistors,
    Fabrication of 9008
    Increasing Power Handling Capacity of 8442
    Measurement of Characteristics of 8430
    Transient Junction Temperatures in 6230
  Transmission Systems, Protection of 6601
Precipitated Phases in Crystal Lattices, Determination of 6945
Precipitation in:
  Ag-Sb-Te, Widmanstatten 6954
  Ge 6935
  Si 6330, 7573, 8202
  Si, Cu 6336
  Si, Li 7226
  ZnO, Li 7227
Precipitation on Dislocations, Kinetic Theory of Stress-Assisted 9174
Preparation of:
  - See also Growth of, Synthesis of
  Alkaline Earth Pyrophosphate Phosphors 6189
  Aluminum Antimonide-Gallium Antimonide Alloys 6623
  $BaTiO_3$-Based Solid Solutions 9245
  Boron 8226
  CdSnAs by Directional Freezing 6108
  Ce-Sb Films 6070
  CrO_2 8630
  Ferrites 8221
  Ferroelectric Monocrystals by Zone Recrystallization 6041
  Fe_2C 8220
  $FeVO_3$ 8631
  Garnets 8330
  Ge by:
    Distillation 8619
    Titration 8155
  HgTe-CdTe 8867
  Intermetallic Semiconductor Compounds, High Pressure Furnace for the 7577
  Mn Chromite-Aluminates 6157
  NiFe Films by Evaporation 9183
  Semiconducting Materials, Compensation Method for the 6029
  SiC by the Periodic Shock Wave Technique 6031
  SnSe 6132
  Solid Solution Group II-VI Compounds, Hydrothermal 6030
  the Ternary Alloy MnCo Carbide 6153
  Triglycine Sulfate 6043
Preset Counters 8124
Pressure Gauges,
  Intercardiac Catheter Tip Piezoresistive 7117
  Pirani 8566
Printed Circuits, Fabrication of 8448
Printers, Control Circuit for 9125
Projectile Telemetry with Microwaves 7164
Propagation in Gyromagnetic Rods, Multimode 6528
Protection:
  Circuits, Overvoltage and Underfrequency 7533
  of Metal Surfaces from Atmospheric Oxidation, Use of Silicon Nitride Thin Film for 6366
  of Power Transmission Systems 6601
  of Repeating Equipment from Lightning 8154
  of Semiconductor Rectifiers 6540, 6919, 7125, 7460
  for Transistor Voltage Regulators, Overload 7520
  of Transistors in Circuits 7199
Pulse:
  Amplifiers 7168, 9067, 9068
  Amplitude Interpolation Computer for Doppler Radar 7195
  Characteristics, Measurement of Fractional Nanosecond 7496
  Circuitry, Non-Saturating Nanosecond 6605
  Circuits,
    Complementary Transistor 6822
    Diode Clamp 6845

Pulse: Circuits, (Cont'd)
Microwave 7795
Power Dissipation Limits in Bistable Transistor 6556
Code Modulation:
Repeaters 7168
System for Video Transmission 7786
Converters 8519, 9084, 9085
Counting and Forming Circuits, Magnetic 8568
Discriminators 8520
Forming Amplifiers 7745
Gating Systems 7765
Generators 6496, 7159, 7160, 7425, 7719, 7774, 7795, 7802, 8103, 8436, 8515-8517, 9072, 9073, 9099, 9101
Height:
Analyzers 7211
to Digital Signal Converters 6290
Modulators 7772
Multipliers and Dividers 7415
Photoconductivity of Additively Colored KBr 7993
Position Demodulators 9094
Rate Monitors 7500, 7501
Regenerators 7746, 7747
Sensing Systems 7807
Sequence Detectors 7775
Shaping with Variable Capacitance Diodes 8548
Steering Circuit for Binary Counters 6881
Systems, Analysis of 8518
Trains, Electroluminescent Device for Observing 8454
Width Modulators 8095
Punched Tape Reader, Phototransistor Application in 8126
Purification, Modified Boat for Zone 8617
Purification Factor Characterization of Zone Refining 7564
Purification of:
Alkali Halide Crystals 8618
As 6356, 6946, 7271
Ga 6356, 7271
GaAs 6356
Ge, Distillation 8619
High Vapor Pressure Elements, Vapor-Zone Refining Method of 8616
Phosphorus 7271
Si, Iodide Process 6324
Si Zone Refining 8193
$SiCl_4$ 6017
SiI_4 6016, 6325
Push-Pull Amplifiers,
Distortion in 8488
Driving Source for 6826
Pyrographite,
Galvanomagnetic Properties of 7948
Optical Properties of 7996
X-Ray Diffraction Studies of 7851
Pyrolytic Graphite, Etch Pits in 6663
Pyrophosphate Phosphors, Preparation of Alkaline Earth 6189
Pyropolymers, Semiconduction in Aluminum-Doped 7028
Pyrrhotites, Chemical Composition of 6316

Q

Q Factor Increase in Quartz Crystals 8049
Q Value, Measurement of Microwave 8298
Quadrupole Coupling, Nuclear Spin-Lattice Relaxation via 6175
Quantizers 9105
Quantum:
Converters, Infrared 6237
Counters, Time Discrimination in Solid State Infrared 6789
Effects on Valence Band Structure in Ge 7909
Efficiency of:
CdTe Junctions 7717
Powder Phosphors 6188
Quarternary Se and Te Semiconductors 8653
Quartz,
Absorption in 9403
Acoustic Absorption in 8364, 9450
Defects in Natural and Synthetic 7853
Elastic Waves in 9222
Growth of 7884, 8223
Growth Patterns of 8190
Hypersonic Waves in 8941
Infrared Absorption in 8364, 9402
Internal Friction in Synthetic 8944
Preparation of VHF 8048
Q of 8049
Reduction of Transverse Oscillations in Piezoelectric 8478
Thermal Conductivity of Fused 7682
X-Ray Reflectivity of 9160
Quartz:
Crucibles, Growth of Si Crystals from Fused 6028
Delay Lines 6282
by Ga, Dissolution of 6928
Oscillators,
Piezoelectric Excitation of 7730
Radiation Effects on 9052
Piezoelectric Resonators, Properties of Synthetic 8479
Plates, Effect of Initial Stress in Vibrating 6815
Plates by Use of Parallel Field, Excitation of 6816
Surfaces, Polishing of 8048, 8049
Quasi-Particles in the Theory of Superconductivity 6406

R

Radar, Pulse Amplitude Interpolation Computer for Doppler 7195
Radar:
Duplexers, Ferrite 8114, 8462
Ionospheric Echo Sounding, High Frequency Spectrometer for 7790
Modulators, Magnetic Pulse Generator for Use as a 7160
Systems, Use of a Maser in 6273
Transponders 7223, 7791
Radiation, Angular Dependence of 8644
Radiation:
from Breakdown Avalanches in Ge 7675, 7676
Detectors 6300, 6606-6609, 6916, 7213, 7714, 7715, 7829, 9023, 9024
Effect in Gray Tin 7280
Emissivity Using the Peltier Effect, Measurement of 7072
Energies Required to Produce Color Centers in Alkali Halides 8179
Enhanced Diffusion 7861
Induced:
Defects in Lead Silicate Glass 8648
Paramagnetic Defects in Potassium Azide 7362
Monitors 6300, 6916, 7213
Noise, Effect on Detectivity of Detectors of 7714
from Phosphors, Paramagnetic Resonance Absorption Observations of 8383
Receivers, Threshold Sensitivity of 8565
Survey Meters 6906
Tracking Transducers 7529
Radiation-Powered Thermoelectric Generators, Analysis of 7440
Radiative Recombination in:
Diamond 8372
Electron Bombarded Ge 8373
Radical-Anion Salts, Thermoelectric Power of Some 7621
Radio:
Beacon for Locating Aircraft Crashes 6565
Circuits 7779
Circuits,
Car 6854
FM Limiter 6862
Testing Device for Transistor 7541
Communication System, Personal Two-Way VHF 7503
Radio: (Cont'd)
Frequency:
Amplifiers 9066
Power Meters 9146
Receivers,
AGC in 8523, 8524
AGC:
Characteristics in 6857
and Detector Stages of 9112
AM 6856
AM-FM 7782
Battery Operated 9110
FM 6855
Portable 7778
Receiving Systems, Calibration of 9111
Transmitter for Remote Heartbeat Measurements 7500
Tuning Circuits, Varactor Diode 7780, 7781
Railway Track Signaling System 9107
Ramp Function Generators 9100
Random Process in Linear and Nonlinear Systems, Poles and Zeros of 8484
Range of Electrons in Solids 6053
Rare Earth:
Doped Yttrium Iron Garnet, Ferrimagnetic Resonance in 7347
Metals, Resistivity of the 7016
and Transition Metals, Preparation and Structure of Intermetallic Compounds between the 7259
Rare Earth Garnets,
Anisotropy Anomalies of Ferromagnetic Resonance in 6437
Ferromagnetic Resonance in 6705
Rare Earth Ions, Growth of $CaWO_4$ Crystals Containing 8222
Rare Earth Iron Garnets, Statistics of Superexchange Interaction and Ionic Distribution in Substituted Ferrimagnetic 7340
Rare Earth-Iron Perovskites, Antiferromagnetic 8822
Rare Earth Oxides on the Magnetic Behavior of Ferrite Cores, Effect of 9041
Rare Earths, Factors Influencing the Luminescent Emission States of the 7061
Ratemeters, Design of 7162
Raysistors 7221
Reactance Amplifiers, Low-Frequency 6547, 7752
Reaction of Ge with Aqueous Solutions 6369
Reactions:
between Ga and Quartz 6928
of Oxidized Li with ZnO 7227
of Oxygen in:
Si 7226
Solid Solution in Ge, Aggregative 6338
Reactive Elements, Power Flow in 8485
Reactor Safety System 7214
Reader for:
Cards, Photoelectric 8125
Punched Tape, Photoelectric 8126
Readout, Nondestructive Memory 8134
Readout Head for Digital Computer 8127
Recombination,
Carrier Concentration Fluctuations Due to 9252
Plasma 6092
Recombination: 9268
- See also Lifetime
Luminescence in Alkali Halides 8375
Radiation and Optical Absorption in Semiconductors 7377
Radiation in:
Diamond, Intrinsic 8372
GaP Diodes 8872
Ge, Influence of Degeneracy on 6181
Velocity of Ge, Surface 9283
Recombination in:
CdS 6419
CdS, Surface 9261
Ferromagnetic Semiconductors 9264
GaAs 7009
Ge 6196, 7297, 8259, 8373, 9262

Recombination in: (Cont'd)
High Resistivity Crystals 9257
Semiconductors 6682
Semiconductors, Auger 8697
Si,
Li-B Ions 7867
Surface 6391, 8703, 9259
Si 9263
Si-Electrolyte Interfaces 9260
Te 6096, 6394, 6936
Transistor Base Region 6503
Recorders, Magnetic 6277, 7792
Recording:
Channle, Magnetic Film 7170
Heads, Mechanical Limitations of Multi-Track 8117
Heads Using Bonding Glass Spacers, High-Resolution Ferrite 7171
Instruments, Transistor-Oscillator Limit Switch for 7523
Systems,
Optical Tape Sound 8531
Sensitivity of Reproducing Heads in Magnetic 7793
Recording-Pen Amplifiers 6834
Recovery:
Properties of LiF 7692
Time in Multivibrators, Reduction of 9079
Rectification, Theory of Electrolytic 7017
Rectification:
in AlP, Point Contact 7589
in Polycrystalline Phthalocyanines 7018
of Ratios of Fused Junctions in SiC 8030
Rectifier Parameters, Measurement of High Current 6923
Rectifiers,
As-Te 8990
Breakdown Characteristics of 8015
CbO (NbO) 8989
Characteristics of 6540, 8423
Cooling of Power 7421
Dessicants in Hermetically Sealed Gas Filled Semiconductor 8427
Encapsulation of 8991
Fabrication 6037, 8423, 8424
Fuses for 7460
GaAs 7091
Ge 8424, 8972
High Current: Measurement of the Parameters of 6923
Noise Ratio 8420
Parallel Operation of 7497
Power Conversion Gain of 8420
Protection of 6540
Se 8986, 8988
Si 6919, 8015, 8420
SiC 6037, 7263
Solid Metallic 8992
Surge Protector for 6919
Test Set for 6923
Rectifiers: 7407
- See also Diodes
Using Triode Transistors, Design of Controlled 6893
in Voltage Tuned Resistance-Capacitance Oscillators, Se Dry-Disk 6553
Rectifying:
Barrier at an AlC-SiC Interface 7026
Circuits 8526, 9131
Contacts to SiC 7026
Refining, Continuous Zone 7857
Reflectance Method of Measuring Energy Band Structure 7394
Reflectance of:
CdS 9150
Ge 7010, 8392
Ionic Crystals, Infrared 8910
LiF 8393
Metallic Films 8394
NaCl, Infrared 6472
NaI 7064
Quartz, X-Ray 9160
Si 7010, 7394
ZnO, Exciton 8361
Reflection:
Coefficient of:
Antireflection Coated Surfaces of Si Photocells 6521
Ge, Measurement of the 6473
Curves of Annealed or Oxidized Metal Films 7871
of Electrons from Alkali Halides 8300
Equations, Fresnel 8909
Refraction in:
Metals 9388
Wurtzite-Type Binary Compounds, Double 6194
Refractive:
Index of:
CdTe 9206
Ge: 7994
Films 6716
Si 6723, 7394
Vitreous Silica, Elastic Coefficient of 9445
Indices of Ferro- and Paramagnetic Solids 8906
Refrigerating Thermocouples, Stationary and Transient Behavior of 6523
Refrigeration Units, Thermoelectric 6615, 8576-8578
Regenerative Wave Shaping Circuit 6839
Registers, Magnetic Shift 8138
Regulators,
Corbino Disk 7106
Current 6597, 7196, 7518, 7813, 7816, 8112, 9134
Overload Protection for 7520
Power 7196, 8112, 9133, 9134
Voltage 7106, 7198, 7520, 7816, 7821, 9132
Regulators for Aircraft Generators 7516, 7517
Relaxation, Spin-Spin 7658-7660
Relaxation:
Oscillators 8503
Processes in the Field Effect 6128
Rates Determined by Pulsed Double Resonance Experiments, Paramagnetic 6448
Time:
by Microwave Faraday Rotation, Measurement of 7666
of PbS Photodetectors 8453
Times,
Influence of Exchange Interaction on Paramagnetic 6172
Paramagnetic 7655
Times in:
CdInTe 6198
Pb Film Superconductive Storage Elements 6591
Ruby, Spin-Lattice 6169
Relaxation in:
Alkali Halides 7967
MgMn Ferrites 7964
Neodymium Ethyl Sulfate 7968
Ruby 7969-7971, 9380
Relay:
Amplifiers, Computer Design of 8491
Contact Networks for Logic, Magnetic Analogs of 6800
Relays for Signaling and Control, Diode and Transistor 7823
Relays,
Control 8557
Delay Circuit for 6846
Electro-Optical 7221
Hall Effect Impedance 6601
Logistor 8558
Phototransistor 7437
Reliability of:
Computer Components 8532
Transistors 6730, 8020
Repeaters,
Equivalent Circuit for 8495
Lightning Protection for 8154
Negative Impedance 7167
Pulse Code 7168
Stability of Feedback 8495
Telephone 7505
Reproducing Heads in Magnetic Recording Systems, Sensitivity of 7793
Reset Circuit for Sequential Stepping Devices 8136
Resistance,
Injection-Controlled Variable 7485
Nonlinear Controlled Semiconductor 9021
Resistance:
Due to Isotopes and Other Point Defects, Thermal 9434
in Metals, Theory of Impurity 7014
Resistivity,
Eddy-Current Measurement of 9275
Four-Point Probe Measurements of 9273, 9274
Measurement of 7308, 9277
Microwave Measurement of Volume 7615
Superconducting Sn Films of Low Residual 6410
Resistivity:
- See also Conductivity
Gradient Dependence of Volume Peltier Effect in Ge 8003
Measurements on Tunnel Diode Materials, Anomalous 6685
at Microwave Frequencies, Measurement of Volume 7615
to Néel Point in the Heavy Rare Earth Metals, Relation of Electrical 7016
Test Set 7834
Variations in MnO_2, Effect of Thorium Doping on 6687
Resistivity of:
AgAuCd Ternaries 8277
AgSe 7077
Anisotropic Conductors, Measurement of 9276
Bi_2Se_3 at High Temperatures 8268
Cu-Au Alloys 6205
Cu-Ni Alloys, Temperature Dependence of 9288
Er 6151
Eu 8274
Ge 6401, 6648, 6686
InSb, Pressure Dependence of the 8271
Metallic Alloys, Order and Temperature Effects on 8272
MnO_2, Effect of Thorium Doping on 6687
Ni Ferrite 8269
Organic Semiconductors 6690
Paramagnetics 9287
Rare Earth Metals 7016
Semiconductors, Cryostat for the Measurement of 8267
Si 7617, 8237
SiC 6948
Ti_2O_3, Temperature Dependence of the 7309
Yb 8274
ZnO, Effect of Pressure on the 6403
Resistors,
Crystal Type 6918
Current-Voltage Characteristics of Semiconductor 8416
Dynamic Current-Voltage Characteristics of Silicon Carbide 7108
Fabrication and Applications of Deposited Film 8415
Resistors for Microsystems Electronics, Ti Thin Film 7107
Resonance,
High Power Effects on Ferrimagnetic 6438
Nonlinear Effects of Crystalline Anisotropy on Ferrimagnetic 7049
Saturation Effects in Ferrimagnetic 6439
Resonance:
- See also Ferrimagnetic, Ferromagnetic, Paramagnetic
Absorption Linewidths in Mg-Mn Ferrites 7960

Resonance: (Cont'd)
in Alkali Alloy Systems 7972
Experiments, Paramagnetic Relaxation Rates Determined by Pulsed Double 6448
of Fe^{3+} in Rutile 6713
Frequency of Antiferromagnets with Large Uniaxial Anisotropy 7047
Linewidth of:
Ni-Cu Ferrites 8814
Polished Single Crystal YIG Spheres 7277
Modes in Large Ferrite Samples 6792
Quality Factor (Q) of Ferroelectrics 8248
Tuning of Spherical Resonators 8037
of V^{4+} in TiO_2 7975
in YIG 7348
Resonant:
Circuit Oscillators 9077
Modes in Optical Masers 8475
Resonator for Inductive Capacity Measurement, Dielectric 7921
Resonators,
Magnetically Tunable Microwave Filters Employing Single Crystal Garnet 6791
Oscillations of 8037
Properties of Gallium Iron Oxide Single Crystal 6681
Quartz 8479
Reverse:
Characteristic of Ge Tunnel Diode, Pressure Dependence of 8011
Current in Junctions, Jumps in 8965
Currents in Diodes 8966
RF Power, Error in the Measurement of the 7828
Rhodochrosite, Magnetic Structure of 6154
Ring:
Counters, Magnetic 8138
Oscillators Using Evaporated-Film Cryotrons 6554
Ringing Generators, Transistor Multi-Frequency 6272
Rochelle Salt,
Electro-Optic Kerr Effect in Deuterium-Doped 7007
Hysteresis and Domains in X-Ray Damaged 8247
Magnetic Resonance Spectrum in Deuterated 9235
Paramagnetic Resonance of X-Irradiated 6166
Polarization Reversal in 7007, 9238
Rotation in Magnetic Films, Flux Reversal by Noncoherent 6431
Rotational Hysteresis in Some Mn-Cr-Sb Alloys 6432
Rubidium Bisulfate,
Crystallographic Properties of 6387
Ferroelectric Transition in 6387
Rubidium Bromide, Elastic Constants of 9448
Rubidium Halides, Lattice Vibrations in 9218
Rubidium Iodide,
Elastic Constants of 9448
Infrared Absorption in 8363
Photoemission from 7320
Ruby,
Absorption Lines of Cr^{3+} in 7979
Concentration Dependence of the Relaxation Time in 7971
Cross Relaxation in 9380
Elastic Waves in 9222
Energy Spectrum of 7357
Hyperfine Structure of the Cr^{53+++} Ion in 6447
Microwave Modulation of Light in 7720
Paramagnetic:
Relaxation Rates in 6448
Resonance of Cr^{3+} in 8845
Phosphorescence of 7068
Quadrupole Coupling Constant in 9378
Relaxation:
Time in 7971
Times of Cr^{3+} in 7655
Resonant Linewidths in 9378
Spin Coupling in 8342
Ruby, (Cont'd)
Spin-Lattice:
Relaxation:
and Harmonic Coupling in 7970
Times in 6169
Relaxation in 7969
Spin-Phonon Interaction in 8341
Ruby:
- See also Aluminum Oxide, Alumina Corundum 8846
Maser Operation at High Temperatures 7725
in Masers, Use of 8471
Masers,
Applications and Characteristics of 9050
Duplexing Systems for 7724
Nuclear Polarization Effects on 9047
Pulsed Field 9049
Resonance Condition Calculations for Three-Level 9046
Traveling-Wave 9048
Tunable:
L-Band 8044
X-Band 8045
Rutile,
Absorption Centers in 6629
Anisotropic Conduction in Nonstoichiometric 7618
Dielectric Properties of 7287
Elastic Moduli of 8935
Electron Paramagnetic Resonance of Mn in 7364
Electron-Spin Resonance in 6170
Electrostrictive Effect in 6998
Field Emission from 9317
Paramagnetic Resonance of Fe^{3+} in 6165, 6713
Piezoresistivity of 6404
Stability and Aging of Ceramic 7901
Rutile as a Maser Material, Chrome-Doped 6806

S

Samarium, Paramagnetic Behavior of Polycrystalline 7057
Samarium-Sulfur System, Preparation and Structure of Compounds in the 7258
Sampled-Data Bandpass Filters, Solid-State 6563
Sampling Function to Circuit Analysis of Diode Modulators and Demodulators, Application of the 6560
Sapphire,
Electrical Conductivity of 7595
Linewidth Variations in the Magnetic Spectrum of Nickel^{2+} in 7657
Paramagnetic Resonance of Fe^{3+} in 8348
Thermal Conductivity of Synthetic 7073
Satellite:
Applications,
Harmonic Generator for 6843
Miniature Transistorized Crystal-Controlled Precision Oscillator for 7478
Communication Systems, Maser 9109
Instrumentation Systems 9108
Search Coil Magnetometer 7526
Tape Recorders 6898, 7792
Telemetry, Data Conversion Circuits for Earth 6274
Saturable Reactor and Transistor Systems 7144
Saturation Effects in Ferrimagnetic Resonance 6439
Sawtooth Generators, TV Deflection 8527
Scalers 6880, 7185
Scalers, Tunnel Diode 6879, 7224
Scaling:
Reactions, Theory of Diffusion-Limited 6979
Theory, Transistor 6762
Scandium, NMR of Sc^{45} in 8347
Scanners, Input 6315
Scansors, Properties and Applications of 8040
Scattering:
- See also Mobility
on Mobility in Semiconductors, Theory of the Effects of Carrier-Carrier 7612
of Phonons by Lattice Defects 6200
Scattering in:
AgBr 7610
Al, Defect 9197
Alkali Metals 7299
Cu, Defect 9197
Cubic Solid Solutions, X-Ray 9162
Ge 7316
Ge, Hot Carrier 6109, 7301
InSb, Piezoelectric 7305, 7306, 7317
Lattices, Slow Neutron 8666
Metals, Electron-Phonon 8266
NaCl, Phonon 7684
Nonpolar Crystals 7304
PbS, PbSe, and PbTe 7399
Semiconductors, Group Theory of 8265
Si 7302, 7303
Si, Phonon-Phonon 8716
Tunneling, Electron-Electron 6700
ZnO, Electron 6403
Scattering from:
Cu and Al under Cyclic Stress, X-Ray 9164
Cubic Powders, X-Ray 9158
Fatigued Metals, X-Ray 9163
Mg, Small-Angle X-Ray 9165
Neutron Irradiated Cu, Small-Angle X-Ray 9157
Scheelite Structure Crystals, Fluorescence of Ho in 8381
Scintillation:
Counter Spectroscopy, Amplifier for 6835
Properties of $CaWO_4$ and $CdWO_4$ 9420
Screw Dislocation Mechanism of Interface Motion 7875
Secondary:
Electron Emission: 9315
from MgO 7023, 7024
Emission:
of Cleaved Alkali Halide Crystals 9316
and Electron Energy Dissipation in Solids, Relation between 6055
Seebeck:
Coefficient of:
Ge 6478, 9437
Powder Compacts, Effect of Pressure on the 6203
Effect 8408
Seeding Mechanism in Dendritic Growth 6351
Segregation:
Coefficients:
- See also Distribution Coefficients of Impurities in InSb 6036
in Crystal Lattices, Determination of 6945
in InSb, Anisotropic 6319, 6320
Selenium,
Chemical Analysis of 8615
Diffusion:
Coefficient of Sn in 7547
of Hg in 8198
Electrical Properties of 8728
Growth of 8908
Hole Mobility in 7607
Optical Constants of 7997, 8908
Selenium:
from As, Separation of 6946
Cells Subjected to a Magnetic Field, Photoelectric Sensitivity of 7716
Diffusion in GaAs 7865
Films, Photoelectric and Electrical Properties of 8387
Radiation Detectors, Fabrication of 9023
Rectifiers,
Encapsulation of 8991
Fabrication of 8986, 8988
and Tellurium, Solid Solutions of 7552
Selenium-Cadmium Oxide Junctions, Current Flow Equations of 8422
Selenium-Germanium Composite Rectifiers 8987
Semiconducting:
Phases in Systems with Transition Metals, Formation of 7584
Properties, Microwave Absorption Measurement of 6452

Semiconducting: (Cont'd)
Properties:
of $CoFe_2O_4$ 9214
of Cubic Boron Phosphide 8732
in the Si-Co System 7620
Semiconductor:
Bicrystals, Anisotropy of Carrier Transport in 6071
Compounds,
Furnace for the Preparation of Intermetallic 7577
Mobility Doping of 7012
Device Reliability, Method for Evaluating 6730
Devices,
Electrodes for 8425
Equipment for Encapsulating 6772
Fabrication of Four-Layer 8432
Low-Melting Glasses for Sealing 6773
Methods of Cooling 7697
Negative Resistance in 6731
Sound Movies on 6611
in an Electric Field, Absorption of Infrared Radiation by a 7374
Masers, Negative Temperature in 8470
Materials, Compensation Method of Preparing 6029
Memory Element with Non-Destructive Read-Out 6889
Microwave:
Generators 6866
Modulators 6778, 6779
Resistors, Current-Voltage Characteristics of 8416
Statistics 7295
Strain Transducers 6814
Surfaces,
Catalysis at 6980
Properties of 6421
Surfaces and Films 7276
Thermoelectric Elements 8458
Type, Infrared Techniques for Determination of 6634
Variable Resistance, Injection-Controlled 7485
Semiconductors,
Absorption:
Edge in 7384
and Recombination Radiation in 7377
Alloys for Bonding Thermocouples to 6668
Auger:
Effect in 9254
Recombination in 8697
Band Dynamics of 8705
Binary and Quarternary 8653
Breakdown in Nonpolar 7315
Carrier:
Distribution in 8696
Interaction in 9251
Properties of 8261
Recombination in Homopolar 6092
Classification Rules for 9202
Conductivity in 7935
Contact Electrification of 6673
Cryostat for Electrical Measurements on 8267
Decay:
of Excess Carriers in 6094
Times of X-Ray Excited Carriers in 6684
Dielectric Constant Tensor of 8395
Diffusion in 8620
Diffusion Coefficients of Ionized Impurities in 7566
Effective:
Mass of 8705
Mass:
Ratio in 6384
Tensor of 8395
Electrical Properties of Thin-Film 6384
Electrodes for Controlled Valency 6668
Electrolytic Etching of 6661
Electron Mobility Variations with Applied Electric Field in 6397
Semiconductors, (Cont'd)
Electronic Structure of Group IV and III-V 7002
Ettingshausen Effect in 7404
Excess Holes and Electrons in 6683
Field Effect in 6127
Hall Effect Microwave Measurements on 6699
Impurity Levels in 8659
Infrared:
Measurement of:
Inhomogeneity in 6634
Type of 6634
Properties of 6176
Lifetime in 9254
Lifetime Measurements by Microwave Absorption Technique of 8260
Location of Junctions in 6752
Magnetic:
Dipole Interactions in 8778
Susceptibility of Donors in 8823
Magneto-Oscillatory Effect in the Electron-Hole Plasma in 6777
Measurement of:
Properties by Microwave Absorption in 6452
Thermal Diffusivity in 7688
Microwave Heating of Carriers in 6090
Minority Carrier Lifetime in 6093
Mobility of: 6100, 8264
Electrons in Compensated 8263
Negative-Mass Effect in 6416
Noise in 6126, 6418, 7022
Photoconductivity of 8261
Photoemission from 8389
Preparation and Properties of Organic 6690
Pressure Dependence of Properties of 8270
Recombination in 9254
Skin Effect in 8297
Slicing of 7217
Solubility of:
Charged Impurities in 7545
Flaws in Heavily-Doped 7545
Interstitial Impurities in 6020
Space Charge:
and Added Carrier Concentrations in 6099
Distributions in 6481
Statistical Theory of Kinetic Phenomena in 6396
Statistics of Electrons in 6390
Stoichiometry in Compound 7254
Surface:
Properties of 8774
Space Charge Calculations for 7322
Thermoelectric Efficiency of 8002
Thomson Effect in 8923, 8924
Transmission of Microwave Energy through 6779
Tunneling in 6416
Voight Effect in 7679
Zener:
Effect in 8705
Tunneling in 6131
Semiconductors:
Containing Multiply-Ionized Impurities, Properties of 6682
Having Different Energy Gaps, Junctions between 8422
by Low Energy Argon Ions, Sputtering of 6052
Sensistor Stabilization of Transistor Circuits 7126
Servo Systems, Transistor-Thermistor Feedback Quadrature Suppressors for 6600
Setting of a Magnetic Core by Transistors 6877
Shaping Method for Si 8629
Shift:
Register: 6774, 6775, 6874, 7802, 7803, 8135
Autopilot System for Missiles, Magnetic 6853
Interstage Coupling Circuitry 6890
Registers,
Cryotron 6554, 6808
Magnetic: 8120, 8138, 8139, 8537
Film 6578, 6594, 6891
Parametric 8122
Parametron 6878
Shift: Registers, (Cont'd)
Solid Circuit Binary Multivibrators for Use in 6309
Tunnel Diode 6557, 6870, 7179
Twistor 9053
Shockley Equation, Imperfect Emitter Junction Characteristics Applied to 8026
Short-Circuiter for Protecting Semiconductor Rectifiers 7125
Shot Noise in Junction Transistors 6232
Siderite, Antiferromagnetic Ordering in 9365
Signal:
Converters,
Pulse Height to Digital 6290
Tunnel Diode 6561
Pulse Converters, Magnetic Core 8519
Transfer Circuits 8093
Signaling, Use of a Hall Generator for Contactless 6298
Signaling:
Device Utilizing Infrared 6927
System, Railway 9107
Silanes, Production of Si by Decomposition of 7879
Silica,
Photoelastic Constants of Vitreous 9445
Radiation Damage in Fused 8646
Thermal Conductivity of 9435
Young's Modulus of 9449
Silica:
Gel, Luminescence of 8892
on Mo, Deposition of Thin Films of 7886
Windows, Selective Etching Technique for Fabricating 8629
Silicides, Thermoelectric Power and Electrical Conductivity of 8931
Silicon,
Absorption in 8862, 8863
Acceptor Levels in 8237
Adsorption of Gases on 6046, 8230
Alloying Processes of 7846
Attachment of Au Electrodes to 6374
Auger Electron Ejection from 7631
Capture Cross Sections in 8704
Conductivity of 7943, 9278, 9279, 9286
Cyclotron Resonance in 6123, 8296
Damage in 6370
Determination of Boron in 7563
Dielectric Constant of 6075, 8672
Diffusion in 6326, 6370, 6636, 6757, 8620
Diffusion of:
Boron in 6637, 6949, 8621
Group III and V Elements in 6335
Li in 6638, 7571, 8199
Minority Carriers in 6073
Oxygen in 7570
Phosphorus in 6334
Phosphorus through Oxides in 7862
Diffusion Doping of 7858
Dislocation:
Climb in 7242
Interactions in 8608
Velocities in 8187
Dislocations in 6007, 6008, 6010, 6025, 6630, 7558
Distribution Coefficients of Impurities in 7232
Drift Mobility in 6104
Effective Masses in 6065, 6123
Electrical Properties of 6998, 7617, 8193, 8237
Electrochemiluminescence of 8884
Electroless Deposition of Metals on 6991
Electrolytic Etching of 6661
Electron:
Capture by a Lattice Vacancy in 6097
Emission from 6222
Energy Band Structure of 7281, 7394
Epitaxial Vapor Deposition of 6650
EPR of Donors in Compensated 8358
Etch Patterns of Dislocations in 8181
Etching of 6372, 6373, 6665, 6982, 6987

Silicon, (Cont'd)
Evaporation of 8627
Exciton Energy Levels in 8695
Extinction Coefficient of Highly Doped 6723
Faraday Effect in 6998, 7395
Gas Etching of 8643
Growth of: 6013, 6025, 6647, 7243, 7261, 8211
Epitaxial 7268, 8201, 8216, 8628
$SiCl_4$ by Thermal Decomposition of 8212
SiI_4 by Thermal Decomposition of 6324,6325
Hall:
Coefficient of 8293
Effect in 6104
High:
Field Effects in 7088
Purity 6013
Temperature Mo Contacts for 8981
Hole Energy Spectrum of 7912
Hot Electrons in 6222, 6388
Impurity:
Concentrations in 6941
Variations in 6947
Infrared Studies of Electron Irradiated 6050, 6051
Internal:
Friction in 8945-8947
Impurity Levels in p-Type 6065
Interstitial:
Oxygen in 7378
versus Substitutional Oxygen in 7246
Ion Bombardment Etching of 6049
Lattice:
Defects in 8174
Potential of 9216
Vibrations in 8665
Layer Structure in Dislocation Free 6012
Li and Oxygen Interactions in 6337, 8625
Li-Boron Pairing in 6019, 7574
Lifetime in 6104, 6393, 9426
Liquid-Solid Interface:
during Czochralski Method Growth of 6647
Reactions during Etching of 6988
Magnetoresistivity of 8293
Mechanical Damping of Oxygen Containing 6213
Microplasmas in 7088
Mobility of 6101, 6103, 7608, 8715
Nernst and Ettingshausen Effects in 6479
Ohmic and Rectifying Contacts for 9010
Optical Constants of 7394
Oxidation Mechanisms in Steam and Oxygen for 8227
Oxygen:
Dissolved in 6050, 6051
Effects on Radiation Damage in n-Type 8645
Paramagnetic Resonance Absorption in 8359
Phase Diagrams of 7846
Phonon Drag in 8922, 9221
Phonon-Phonon Scattering in 8716
Photoelectric Threshold in 9427
Photovoltaic Effect in 9426
Polarizability of Free Carriers in 7010
Precipitation in 6330, 7573
Precipitation of:
Cu in 6336
Impurities in Al Doped 8202
Li in Oxygen Containing 7226
Precision Lapping of 6370
Preparation by:
Decomposition of Silanes of 7879
Film Boiling Technique of 6325
Radiochemical Techniques of 7562
Zone Purification of SiI_4 of 6035
Preparation of High-Purity 6324
Radiation Damage in 8645
Reactions of Oxygen in 7226
Recombination in 6092, 9263
Reflectivity of 7010
Refractive Index of 6723
Scattering in 8265

Silicon, (Cont'd)
Scattering:
Anisotropies in 7302
of Conduction Electrons by Lattice Vibrations in 7303
Shape of Melt-Crystal Interfaces during Float Zoning of 6958
Shaping Method for 8629
Solubility of:
Interstitial Impurities in 7869
in Various Elements of 6001, 6002
Specific Heat of 8665
Spin:
Resonance in 6164, 9220
Resonance of Group VIII Impurities in 8770
Spin-Lattice:
Interaction for Donor Electrons in 6168
Relaxation in 6171, 9304, 9305
Strain Aging in 7573
Surface:
Adsorption of Oxygen on 8230
Damage in 6330
Energy of 6999
Levels of 9212
Properties of 7283, 8233, 9320
Recombination in 6391, 8703, 9259
States on 8663, 8664
Susceptibility of 8823, 8848
Thermal:
Conductivity of 6202, 8402
Expansion of 6207, 8934
Thermionic Emission from 6388
Twin Boundaries in 8188
Vacancy Interaction in 8176
Valence Band Parameters in 8706
Zone Refining Purification of 8193
Silicon:
Contacts, Improved 7097
by the Crucible, Contamination of 6027
Crystals, Effects of Seed Rotation on Growth of 6025
Dendrites, Growth:
and Evaluation of 6964
Steps on the Surface of 6963
Devices, Surface Treatment of 6771
Diodes, Surface Effect in 6421
Doped GaAs, Hall Coefficients of 8762
Electrolyte Interfaces, Recombination at 9260
for Fabricating Diffused Junction Devices, Method of Evaluating 7092
Films,
Adsorption of O_2 on 9192
Evaporated 6653
Growth of 6649
Photovoltages in 7578
Preparation and Properties of 7578
in Ga, Solubility of 6928
and Germanium, Comparison of the Etch Rate of 6985
Integrated Circuits 7434
Junctions,
Avalanche Breakdown in 6221
Defects and Weaknesses in 8445
Hot Electron Emission from 6222
Localized Breakdown in Diffused 6495
Liquidus Curves 6001
into Ni, Diffusion of 9181
p-Sp-n Rectifiers, Breakdown Characteristics of 8015
Photocells, Reflection Coefficient of Antireflection Coated Surfaces of 6521
Photovoltaic Devices, Diffused 6949
Power Rectifiers,
Fabrication and Characteristics of 8423
Parameters of 7263
Surge Protector for 6919
Resistor for Stabilization of Transistor Circuits, Use of 7126
Solar Energy Converters 6519
Transistors, Field Effect on 6504

Silicon-Boron Alloyed Junctions 8973
Silicon Carbide,
Absorption Edge of 8865
Chlorine Reaction with 6645
Crystal Structure of 174 Layered 6023
Deposition of Thin Films of β- 7886
Dislocation-Etch Pit Relation in 6937
Dislocations in: 6631
Crystal Growth of 6937
Edge Emission of 6453
Electroless Contacts to 6666
Energy Gap of 8865
Etching of 6989, 6990
Formation of Junctions in 8018, 8030
Free Energy and Heat of Formation of 6625
Fused Contacts to 7026
Grown p-n Junctions in 6501
Heat of Sublimation of 6929
Impurities in 6940
Luminescence of Donor-Acceptor Pairs in 6454
Mass Spectrometric Analysis of Molecules in Equilibrium with 6929
Neutron Activation Analysis of 6943
Ohmic and Rectifying Contacts for 9010
Oxidation of 8636
Preparation of 6031, 6037
Resistivity of Granular 6948
Spectrographic Analysis of 8614
Study of Amorphous Carbon from 6645
Surface Properties of 6048
Transient Conductivity of Contacts to 6689
Silicon Carbide:
Crystals, Polytypism in 6937, 6952
Device Fabrication, Thermocouple Furnace for 7093
Films,
Electrical Properties of 6960
Fabrication of Junctions by Epitaxial Deposition of 6960
Grains, Diffusion of Nitrogen in 6948
Rectifiers, Fabrication of 6037
Resistors, Dynamic Current-Voltage Characteristics of 7108
Transistors, Analysis of Bipolar and Unipolar High Temperature 7101
Unipolar Transistors 7433
Varactor Diodes 7087
Whiskers, Determination of Twist and Polytype in 6022
Silicon-Cobalt:
Compounds, Thermoelectric Power of 7620
System, Semiconducting Properties of Compounds in the 7620
Silicon Dioxide, Light Scattering Study of Neutron Radiation Damage in Fused 8646
Silicon Dioxide:
against Boron, Oxide Masking of Solid 6329
Diffusion Masks, Fabrication of Double Diffused Mesa Ge Transistors Using 6327
Films, Growth Mechanisms for 8227
Protective Films for Photoconductive Cells 9029
Silicon-Gallium Phosphide Alloys, Solubility Enhancement in 6621
Silicon-Germanium, Susceptibility of 8824
Silicon-Iron,
Domain Walls in 8323
Magnetic:
Annealing in 9344
Stray Fields in 9331
Torque Curves in 9334
Magnetization in 8805
Magnetothermal Effects in 8406
Neil Spike Formation in 9361
Optimum Domain Width of 8324
Paramagnetic Susceptibility of 9375
Susceptibility of 8789
Silicon-Iron Bloch Walls, Energy and Orientation of 8325
Silicon Nitride:
Receptacle, Horizontal Growth of Ge Single Crystals Using a 6955

Silicon Nitride: (Cont'd)
Thin Film Dielectric Capacitors 6366
Silicon-Silicon Dioxide Interface System 7276
Silicon Tetrachloride, Growth of Si by Decomposition of 7879
Silicon Tetrachloride by Adsorption Techniques, Purification of 6017
Silicon Tetra-iodide, Preparation of Transistor Grade Silicon by Zone Purification of 6035
Silicon Tetra-iodide by Zone Melting, Continuous Multi-Stage Purification of 6016
Silver,
Method for Detecting Edge and Screw Dislocations in 8180
Point Defects in 9197
Self Diffusion Coefficient during Compression and Torsion of 7859
Silver:
Alloys, Thermoelectric Power of 8407
into Cuprous Oxide, Diffusion of 6951
Doped Alkali Halides, Effect of Pressure on Color Centers in 7854
Films, Twin Formation in Evaporated 9178
in Ge,
Diffusion of 7569
Solubility of 7569
Ions in AgCl, Diffusion of 6950
$(S,Se,Te)_2$, Thermoelectric Power of 8921
Silver$_2$-Group VI Compounds, Electrical Properties of 8734
Silver Antimony Telluride,
Anomalous Hall Effect in 7020
Structure of 6954
Thermal Conductivity of 7020
Silver Bromide,
Diffusion of Cd in 6639
Electron Mobility and Scattering Processes in 7610
Hall Mobility of Holes in 6106
Silver Bromide Emulsions, Photoconductivity of 9421, 9422
Silver Bromide-Cadmium Bromide Solid Solutions, Diffusion of Cd in 6639
Silver Chloride,
Dember Effect in 7025
Diffusion of Ions in 6950
Dislocations in 7557
Luminescence Decay in 7981
Silver-Gold-Cadmium Ternaries, Resistivity of 8277
Silver Halides, Optical Absorption in 6197
Silver Selenide,
Crystal Structure of 7077
Preparation and Properties of 7077
Silver Selenium Telluride, Incongruent Melting of 6954
Sintering of ZnO Spheres 8626
Sinusoidal Oscillators 8082
Skin:
Depth, Standards of Microwave 8298
Depth in Superconducting Al 6696
Effect in:
Polyvalent Metals 9209
Semiconductors 8297
Superconductors 8279, 8750
Slicer, Crystal Wafer 6306
Slicer for Analyzing Signal Amplitude 6604
Slicing Semiconductors, Machine for 7217
Sodium, Elastic Constants of 9444
Sodium Aluminosilicate Glass, Conductivity of 7939
Sodium Bromide, Photoconductivity of 8904
Sodium Chloride,
Absorption in 8362, 8363, 8868, 9396, 9397
Annealing of X-Ray Induced Surface Hardening in 8650
Brittleness of 9201
Ca Concentration in 8244
Colloids in Additively Colored 9169
Color Center Formation in 7235, 7237, 8177
Sodium Chloride, (Cont'd)
Conductivity of 8729
Dislocation Damping in 9175
Electric Strength of 7594
Electrification of 6078
Emission in 8362
Excitons in 9248
Hall Effect in 7597
Infrared:
Absorption in 8363
Reflection Spectrum of 6472
Lattice Dispersion Frequency of 6671
Phonon Scattering by Chemical Impurities in 7684
Point Defects in 8175
Secondary Emission of Cleaved 9316
Self-Diffusion of the Chloride Ion in 7251
Specific Heat of 8915
Thermoactivation Energies in 6209
Thermoluminescence of 7388, 8378, 8885
Ultrasonic Attenuation in 6480
Vacancies in 6628
Yield Stress of 8938
Sodium Chloride Whiskers, Dislocation Structure, Formation, and Strength of 6009
Sodium Chloride-Sodium Bromide Solid Solution, Effect of Annealing on 7554
Sodium Fluonickelate, Ferromagnetism in 8336
Sodium Fluoride 7534
Sodium Fluoride, Absorption in 8868
Sodium Iodide,
Dislocations in 9170
Elastic Constants of 6724
Fluorescence of 7064
Photoemission from 7320
Reflection Spectra of 7064
Specific Heat of 6724
Sodium Niobate,
Dielectric Properties of Solid Solution Systems Based on 8677
Properties of Some Ferroelectric Solid Solutions Based on 6680
Sodium Niobate:
Ferroelectric Memory Cells 7193
Films, Preparation of Ferroelectric 6978
Sodium Niobate-Lead Zirconate, Ferroelectric and Antiferroelectric Properties of Solid Solutions of 7293
Solar:
Cell Structures, Spectral Response of 7438
Energy:
Conversion, Effect of Temperature on Photovoltaic 6519
Converters,
Efficiency of 6785
GaAs 6786
Improvement of 6787
Powered Hearing Aids 9118
Solid:
Circuit Binary Multivibrators 6309
Oxides, Properties of 6057
Solution Ceramics Containing Nb or Ta, $PbTiO_3$ 6678
Solutions,
Conditions Governing Formation of 8164
Optical Properties of Some II-VI Compounds 6030
Physical Properties of Alkali Halide 7554
Properties of Ferroelectric Sodium Niobate 6680
Structure of 8583
Solutions in:
the Bi_2Te_3-Bi_2Se_3 System 7551
the CIS-YIG System 6159
a Garnet System 6159, 8163
the GaSb-AlSb System 6361, 6623
the GaSb-Ge Pseudo-Binary System 6622
the Ge Aggregative Reactions of Oxygen 6338
the HgSe-HgTe System 6931
a Pseudo-Quinary System 7229
Solid: Solutions in: (Cont'd)
the ZnO-TiO_2 System 8580
the ZnS-AlP System 8161
Solutions of:
Fe_2O_3 and $FeVO_3$ 8631
Ga_2Te_3 with Group II-VI Tellurides 7230
Group II-VI:
Compounds, Hydrothermal Preparation of 6030
Tellurides 6624
InSb and In_2Te_3 7323
InTe and CdTe in PbTe and SnTe 7231
In_2Te_3 with II-VI Tellurides, Energy Gap of 7546
Lead Metatantalate with Nb, Ba, Sr 6679
Metals and Tungsten Trioxide 6998
$NaNbO_3$ and $PbZrO_3$ 7293
Oxygen in Ge 6338
Semiconductors with Deviations from Stoichiometry 7401
Te and Se 7552
(Zn,Hg)S 7677
State, Low Temperature 8652
State:
Devices, IRE Standards on 6729
Micrologic Elements 6774
Transducers 6311
Solids,
Electrons in 6053
Energy Losses of Electrons in 6054
Magnetoplasma Reflection in 6130
Optical and Electrical Properties of 6197
Paramagnetic Resonance in 6161
Phase Transitions in 8585
Relation between Electron Energy Dissipation and Secondary Emission in 6055
Specific Heat of Isotropic 8398
Transport Processes in 6395, 8707
Solubilities of:
InTe and TlTe in BiTe and SbTe 6003
Interstitial Impurities in Semiconductors, Theory of 6020
Solubility of:
Ag in Ge 7569
Cd in Ge 7569
Fe in Ge 7569
Flaws in Heavily-Doped Semiconductors 7545
Ga in Ge 7228
Ge in Various Elements 6001, 6002
Impurities in:
Ga 6928
Ge 7228, 7569, 7869, 8165
Semiconductors 7545
Si 7869
ZnO 7227
In in Ge 8165
Li in ZnO 7227
Metals, Mutual 8164
Si in:
Ga 6928
Various Elements 6001, 6002
Ta in Ge 7569
Te in Ge 7569
Solubility Enhancement in GaP-Si Alloys 6621
Solutions, Reaction of Ge with Aqueous 6369
Solvent Evaporation Technique for Growing Low Resistivity Ge Crystals 8200
Sonic Delay Lines 6282
Sorters, Automatic Postal 8153
Space Charge:
Calculations for Semiconductors, Surface 7322
in Dielectric Layers between Cylindrical Electrodes 6079
Distributions,
Effects of Charge Mobility on 8679
Semiconductor 6481
Solid and Liquid 8679
Static 6423, 8679
Fields in $BaTiO_3$ 8680

Space Charge: (Cont'd)
Layer:
Varactors 6251
Widening in Junction Transistors, Analysis of 8437
Limited Currents in:
$BaTiO_3$ and CdS 8681
Insulator Diodes 8961
in Semiconductors, Transient 6099
Spacistors,
Fabrication and Properties of High-Frequency 8435
Low-Frequency Parameters of 8434
Specific:
Heat,
Calculation of Lattice 7916
Method of Determining 6199
Heat of:
Alkali Halides 9218
β Tin 7405
CaF at Low Temperatures 6475
$CoBr_2 \cdot 6H_2O$ at Low Temperatures 6158
Dilute Alloys 7998
Ferrimagnets 7952
Iron 6199
Iron Garnets at Low Temperatures 6476
Isotropic Solids 8398
KCl 8937
Magnetic Materials 6148
MnZn- and NiZn-Ferrite 6477
NaCl 8915
NaI 6724
$NiCl_2 \cdot 6H_2O$ and $ClCo_2 \cdot 2H_2O$ at Low Temperatures 6148
Polymorphic Forms of Manganous Sulfide 7963
Si 8665
Spectral Response Limit of Evaporated Photoconductive Cells, Influence of Crystal Size on 6465
Spectrographic Analysis of:
Impurities 8613
SiC 8614
Spectrometer for Ionospheric Echo Sounding, High Frequency 7790
Spectrometers,
Analysis of Electron Paramagnetic Resonance 6901
Detectors for Microwave 7205
γ-Ray 7528
Si Junction Particle 9150
Spectroscopy, Multi-Channel Junction Counters for 8574
Speech-Path Switches for Direct Coupled Connections 8092
Spin:
Alignment in Superconductors 6694
Centers in Carbons Formed by Chemical Attack 7368
Configurations,
Determination of Ground-State 7329
Magnetization Process of Helical 7031
Configurations in the Cubic Spinel, Classical Theory of 7636
Coupling in:
Crystals with Two Paramagnetic Species 6173
Ruby 8342
Degeneracy Dependent Statistics, Acceptor State 7914
Echo Experiments in Ce and Er Doped CaW 7668
Excitation and Relaxation in Nuclear Quadrupole Resonance 7354
Flip:
Mechanism,
Cross Relaxation by 7965
Diamond 7965
Maser Pumping by 7965
Narrowing of Paramagnetic Resonance Lines 6162
Flopping in MnF by High Magnetic Fields 7050
Hamiltonian:
of Co^{2+} 7654
Spin: Hamiltonian: (Cont'd)
Constants in YIG, Calculation of Uniaxial 7637
Inversion in Masers 8468
Paramagnetism 9210
Populations by Simultaneous Passage, Inversion of 8468
Relaxation of F-Center Electrons 7664
Resonance in:
CdTe 8771
Ge 7663, 9220
Graphite 8772
InSb 6124
Rutile 6165
Si 6164, 8770, 9220
Systems, Theory of Entropy and Cross-Relaxation in 7950
Wave:
in a Co Alloy, Dispersion Relation for 7332
Dispersion Relations 7331, 9322
Interactions in Ferro- and Antiferromagnetism, Theory of 6136
Resonance in Ni Films 8327
Spectrum of YIG 7333
Theory of Ferromagnetism 7952
Waves, Propagation and Generation of 7330
Waves in Ferromagnets 8781
Spin-Lattice:
Interaction for Donor Electrons in Ge and Si 6168
Relaxation,
Measurement of 8834
Nuclear 9382
Relaxation in:
Alkali Halides 7967
Cr^{3+} Doped Corundum 8343
Free Radicals 6172
Ge 9304, 9305
Neodymium Ethyl Sulfate 7968
Paramagnetic Salts 8833
Ruby 6169, 7969, 7970
Semiconducting Rutile 6170
Si 6171, 9304, 9305
Relaxation via Quadrupole Coupling, Nuclear 6175
Spin-Orbit:
Coupling in Inorganic Complexes 7006
Splitting on the Fermi Surfaces of the Hexagonal Close-Packed Metals, Effect of 7591
Spin-Phonon Interaction in:
MgO 9377
Paramagnetic Crystals 8340
Ruby 8341
YIG 6147
Spin-Spin Relaxation, Theory of 7658-7660
Spinel Structure,
Dislocations, Stacking Fauls and Twins in the 6932
Exchange Interaction of Fe^{3+} and Mn^{2+} in 7966
Spinels,
Crystal Distortion and Phase Transformations in Mn^{3+} 8590
Cubic-to-Tetragonal Phase Transformations in Transition Metal 9151
Distribution of Cations in 9153
Magnetic Anisotropy in Ferrimagnetic 8319
Spiral:
Growth Layers on $BaTiO_3$ Crystals 7876
Walls in Thin Magnetic Films 7038
Spirals on GaAs (111) Surfaces 8207
Spraying, Properties of Ferrite Thin Films Prepared by 6976
Spreading Resistance in Cylindrical Devices 7696
Sputtering, Atom Ejection Patterns in Single Crystal 7279
Sputtering:
of Semiconductors by Low Energy Argon Ions 6052
Techniques for Applying Contacts to CdS 6667
Squaring Unit, Varistor 7513
Squelch Circuits 6858
Stability:
of Inorganic Complexes, Geometrical 7006
Limits of Binary Semiconductor Compounds, Composition 8168
of Tuned Transistor Amplifiers 7132
Stabilization of:
Junction:
Surfaces 7420
Transistors 9012
Time Delay Multivibrators 6838
Transistor:
Circuits, Use of Si Resistor for 7126
Trigger Circuits 7152
Stabilization Networks for Functional Electronic Blocks, Optimum 7121
Stabilizer, Zener Diode Voltage 6736
Stabilizer for:
an Electromagnet, Transistor Current 6293
Transistor Power Supplies 6541
Stacking:
Fault, Antiferromagnetic Ordering in 7963
Fault Energy in Graphite 6938
Faults in the Spinel Structure 6932
Stark Splitting Observation by Means of Tunneling Transitions 8278
Static:
Switching, Theory of 7175
Switching System, Elliott Sheffer Stroke 7176
Statistical Theory of Kinetic Phenomena 6396
Statistics:
in Dilute Electron Gases 7296
of Electrons in Semiconductors 6390
in Ge 7295
Steady State, Fluctuation from the Nonequilibrium 6125
Steering:
Circuits, Magnetic 8137
Circuits for Controlling Reversible Counters 6281
Stereo Preamplifier and Tone Control for Magnetic Cartridges 6275
Stereophonic High-Fidelity System, Amplifier for a 7755
Stoichiometric Deviations in Oxide Monocrystals, Modified Bunsen Method for Determination of 6642
Stoichiometry, Solid Solutions of Semiconductors with Deviations from 7401
Stoichiometry:
in Compound Semiconductors 7254
of $PbNb_2O_6$-Type Compounds, Non- 6676
Stomach Pressure of Animals, Telemetering System for 8529
Storage,
Survey of Digital 8540
Thin Film Ferromagnetic 6655
Storage:
- See also Memory
Devices, Coherer Information 6584
Elements, Low Temperature 6289
Light Intensifier Display Panel 7718, 7719
Matrix Using Ferromagnetic Thin Films 7190
Reading Circuitry 8544
Time in Junction Transistors 6253, 6258
Transfer Circuits 8546
Units 8540
Units,
Capacitor 8128
Cryotron 6808, 7192
Delay Line 7804
Ferroelectric: 6592, 6593
Capacitor 8545
Low Flux Density Materials for High-Speed 6804
Magnetic: 8544
Core 6587, 7188, 7806, 7809, 8121, 8134, 8135
Disc 6287
Drum 6285, 6286, 8541, 8542
Film 6288, 6801, 7190
Tape 8116, 8130-8133

Storage: Units, (Cont'd)
Nondestructive-Readout 6587-6589, 6593
Superconductive 6591
Tunnel Diode 6583, 7805
Strain:
Aging in Si Crystals Containing Oxygen and Carbon 7573
Enhanced Diffusion 7859
Transducers,
Piezoresistive 6534
Semiconductor 6814
Strains, Calculation of Magnetostriction 8302
Strength of:
Crystalline Materials 8602
NaCl Whiskers, Effect of Dislocations on the 6009
Stress in Very Thin Electrodeposits, Measurement of 7078
Striations in Ge, Detection of 8191
Strip-Line Circulators, Y-Junction 6794
Stroboscope, Fractional Millimicrosecond 6907
Strontium in KaCl, Measurement of Concentration of 8244
Strontium-Bismuth Titanate, Dielectric Permeability of 9232
Strontium Sulfide, Paramagnetic Resonance Studies of Eu and Sm Activators in 8879
Strontium Titanate,
Hamiltonian for the Paramagnetic Spectrum of Iron in 6712
Paramagnetic Resonance of Transition Metal in 8847
Strontium Titanate Single Crystals, Commercial Availability of 7833
Structure,
Nuclear Magnetic Resonance Analysis of Crystal 8588
Slow Neutron Interaction Analysis of 8666
Structure of:
Ag-Sb-Te 6954
Bi at Low Temperatures 8171
BiPt 8288
Clean InSb Surfaces 8638
Co and Co-Ni Alloys, Effect of Plating Parameters on the 6994
$CoCl_2$-$6H_2O$ 8172
Crystals 8587
Crystals, Method of Determining the Mosaic 7245
Etched Ge Surfaces 6644
Grain Boundaries 8610
$LiH_3(SeO_3)_2$ 8173
Magnetic Films, Effects of Heat Treatment on 7873
Mn^{3+} Spinels 8590
SiC Surfaces 6048
Solid Solutions 8583
Solution-Grown Polyoxymethylene Single Crystals 9188
a System Having Ferroelectric and Ferromagnetic Properties 6082
Thin Ferrite Films 6974, 6976
ZnO 8612
ZnSb 8589
Structure in Vacuum Evaporated Thin Ge Films 7257
Suhl Instability in Ferrite Devices 6241
Sulfide Phosphors,
Edge Emission in 9406
X-Ray Photoconductivity of 6191
Sulfur, Photoconductivity in Rhombic 6113
Sulfur:
from As, Separation of 6946
Diffusion in GaAs 7865
as an Impurity in InAs 6339
Superconducting:
Al 6693
Al,
Absorption in 6695
Critical Field of 8283
Energy Gap of 6695, 6696
Superconducting: Al, (Cont'd)
Nuclear Spin Relaxation in 8843
Penetration Depth in 6696
Alloys,
Critical Temperature Theory of 8745
Thermodynamic Treatment of Dilute 6114
Antiferromagnetic Metals 8290
Be Thin Films 8757
Ce Phosphate Glass, Intermediate State in 8287
Contacts 6812, 9291
Crowe Cells 6289
CuS, X-Ray Spectra of 8371
Device Utilizing Tunneling 7842
Devices, Study of Persistent-Current 7728
Films,
Critical Fields of Thin 7626
Far-Infrared Transmission through 8853
Magnetic:
Field Penetration in 8754
Phase Transition of 6409
Measurement of Magnetic-Field Attenuation by 6408
Properties of 6809
Ga, Nuclear Quadrupole Resonance in 7030
Ground States 8280
Hg 6693
Hg, Critical Field of 8284, 8748
In, Critical Field of 7312, 8748
In-Hg 6119, 6411
La, Transition Temperature of 8744
Memory Element, Persistor 6813
Mn Binaries 8758
Nb, Lattice Specific Heat of 8399
Nb_3Sn, Critical Field of 7946
Pb 6693
Pb,
Isotope Effect in 8756
Resistivity Limit of 8755
Transition Hysteresis in 9292
Pb-In Alloys, Time Delays in Transition of 6697
Ring, Flux Trapping in a 9294
Sn,
Critical Field of 7312, 8748
Specific Heat of 7405
Transition Temperature of 9166
Sn: 6693
Films,
Critical:
Currents in 8285, 8286
Field of 6118, 8285, 8747
Low Residual Resistivity of 6410
Transition in 8281
Ta, Critical Fields of 7312
Transition, Time Delays in the 6697
Transition:
of Nb_3Sn, Isotope Effect on the 7313
in Purified Ta 7623
Temperature Produced by Electrostatic Charging, Changes in 8282
Zn, Effect of Pressure on the Critical Field of 8283
Superconductive:
Coaxial Line, Characteristics of a 7116
Device for Detecting Small Voltages 6602
Devices - See Cryotrons, Crowe Cells
Gating Circuits 8094
Transition, Thermal and Electrodynamic Properties of 7945
Transition in Thin Wires and Films 7945
Wires, Fabrication of Multiple-Characteristic 8476
Superconductivity,
Analog Solution for the Static London Equations of 7622
BCS Theory of 8737
Coulomb Effects in the Theory of 8740
Critical Field in 8741
Gauge Invariant Formulation of the Bardeen-Cooper-Schrieffer Theory of 6691
Superconductivity, (Cont'd)
Law of Corresponding States in 6693
Meissner Effect in the Quasi-Chemical Equilibrium Theory of 7624
Quasi-Particles and Gauge Invariance in the Theory of 6406
Strong-Coupling Limit in 8739
Transitions in 8742, 8743
Superconductivity:
of Contacts with Interposed Barriers 6407
of Dilute In-Hg Alloys 6119, 6411
and Ferromagnetism, Coexistence of 6138
Superconductors,
Adiabatic Magnetization Cooling of 9295
Critical:
Currents in 9293
Temperature of 8746
Electron Tunneling between 7627
Energy:
Gap in 8749
Level Density of 8746
Ferromagnetic 7625, 8738
Hall Effect in 7314
Intermediate State in Cylindrical 6117
Measurement of Magnetic Fields in 6116
Spin Alignment in 6694
Surface Impedance of 8750-8753
Transport Properties of 6115
Very Low Transition Temperature of 6692
Superconductors in:
the Intermediate State, Thermal Conductivity of 8404
a Magnetic Field, Surface Impedance of 8279
Superexchange Interaction:
in Substituted Ferrimagnetic Rare Earth Iron Garnets, Statistics of 7340
and Weak Ferromagnetism, Anisotropic 7341
Supermalloy, Gyromagnetic Ratio of 7343
Superparamagnetism of Ferromagnetic Particles 9370
Suppressor, Feedback Quadrature 6600
Surface:
Alloying with Al-Containing Solder 8975
Barrier:
Counters 6301-6303, 6908, 6911
Rectifying Contacts 8976
Transistors,
Effects of Surface Recombination on the Current Amplification Factor of 6764
Fabrication of 9014, 9015
Whisker Mounting on 9016
Channels on Si p-n Junctions, Anomalous 6741
Characteristics of III-V Intermetallic Compounds 6340, 6983
Charge, Influence of Ambient Atmosphere on 6391
Concentration of:
Diffused Layers, Calculation of 6635
In in Ge from Gaseous Diffusion 6331
Currents, Multiplication in 6421
Currents in Inversion Layers of Semiconductors 7080
Density, Determination of 7300
Effects Due to the Interaction of MgO and Gases 9190
Energies of Crystals, Measurement of 6999
Energy States, Carrier Trapping by 7267
Irregularities on Single Crystal Ferromagnetic Resonance Parameters, Effect of 6436
Layers of LiF, Effects of Temperature on Dislocations in 6643
Levels 8239
Levels,
Adsorption Effects on 9211
Ge 9213
Si 9212
Noise in CdS, Measurement of 7951
Passivation of Micro-Components 7706
Photovoltaic Effect in Si 9426

Surface: (Cont'd)
Properties, Radiation Effects on 7582
Recombination-Surface Potential Relationship 9258
Spin Waves 9323
States: 8239
on Crystals 8660-8662
in PbS Photoconductors, Role of 6467
States of:
Diamond and Graphite 7004
Ge: 6129, 6670, 8664
Transistors, Effect of H_2O on 9012
Ionic and Valence Crystals 8238
a One-Dimensional Crystal 6381, 7588
Si 8663, 8664
ZnO 8240
Structure, Effect of Etching on 6644
Structure:
Determination by Electron Microscope 8205
SiC 6952
Studies, New Tools for 8633
Tension of Ge, Temperature Dependence of the 8160
Treatment of Si Devices 6771
Treatments for Ge 8299
Surfaces,
Adsorption of:
Gases on:
Bi_2Te_3 6659
Ge 6368
Oxygen on:
InSb 8638
Si 8230
Breakdown of Ge 7632
Carrier Density in Diffused Layers at 7300
Catalysis at 6980, 8232
Cleaning of Ge 6422
Conductivity of Ge 7321, 8299, 9281
Damage in:
GaAs 6660
InSb 6660
Si 6330
Damaged Layers and Crystalline Perfection in III-V Compounds 8234
Dendrite Growth on Ge 6349
Dielectric Breakdown in LiF 7255, 7256
Displacement Processes on Ge 8231
Electron Microscope Studies of Cleaved KCl 6981
Etching and Inhibition of III-V Compounds 8640
Field Effect on Cleaned Ge 6129
Gas Etching and its Effect on Semiconductor 8643
Heterogeneity in Irradiated Solid 7582
Impedance of: 8298
Superconductor 8750-8753
Impurities on 8613
Infrared Techniques for Measuring Properties of 9310
InSb 6021
Magnetic Resonance Studies of 9193
Magnetoresistance Effect on Ge 7947
Magnetostatic Modes at 9323
Mobility at 6421, 7267, 7300, 8264
Oxidation:
of Clean Ge 8637
Mechanisms for Steam and Oxygen at Si 8227
Properties of:
Ge 8233, 9311, 9312
Semiconductor 6421, 8774
Si 7283, 8233, 9320
SiC 6048
Protective Treatment for Device 8019
Recombination in:
CdS 9261
Ge 9283
Si 6391, 8703, 9259
Si-Electrolyte 9260
Refractive Index of Si 6723
Relaxation in Ge 9319

Surfaces, (Cont'd)
Semiconductor 7276
Space Charge Calculations for Semiconductor 7322
Spirals on GaAs (111) 8207
Transport at 8710
Trapping in Organic Solid 7029
Surge Protector for Si Power Rectifiers 6919
Susceptibility:
- See also Permeability
at Moderate Magnetic Fields 7962
Susceptibility of:
CdS, Dielectric 9231
$CoBr_2 \cdot 6H_2O$ 8314
$Co(C_2H_3O_2)_2 \cdot 4H_2O$ 8819
an Electron Gas in Alkali Metals, Paramagnetic 7356
Ferrimagnetic Garnets 8791
Ga, Anisotropy of the Magnetic 7326
Ge 7324, 7325, 8823, 8848
Graphite, Diamagnetic 9215
Iron-Yttrium and Iron-Rare Earth Paramagnetic Ferrites 8338
Mg 8849
Mixed Paramagnetic Crystals 8337
$Mn(C_2H_3O_2)_2 \cdot 4H_2O$ 8819
$Ni(C_2H_3O_2)_2 \cdot 4H_2O$ 8819
Ni-Cd Ferrites 8825
Permalloy Films 6426
Radical-Anion Salts 7621
Si 8823, 8848
Si-Fe, Photo-Measurement of 8789
Si-Ge 8824
Small Ferrite Spheres 7954
Three and Four Level Systems, Saturation Effect of 8829
$TiCl_3$ 8305
Sweep:
Circuits, Linear 8085
Generators, Linear 7494
Switchboard, Telephone 9116
Switches,
Broadband:
Microwave Absorption 6528
Reflective Ferrite 9043
Carrier Injection Variable Resistance 7485
Cryotron 7446
Electro-Optical 7221
Faraday-Rotation 6529
Four-Layer Tunnel 6759
Frequency Selective 7766
Ge-Filled Waveguide 9253
High Current 7154
High Speed Magnetic 8119
High Voltage 6758
Isolating 6841
Limit 7523
Micro-Energy 7484
Microwave: 6216
Transverse Ferrite 9035
Multidiode 7762
Open Circuit Impedance for 7483
Optimum Noiseless Load-Sharing Matrix 7767
p-n-p-n Sandwich 6760
Si Controlled 7537
Speech-Path 8092
Television Master 6271
Tetrahedral Junction 6525
Switching,
Diode for Microwave 6265
Ferroelectric 6592
Ferromagnetic 8465
Theory of Static 7175
Switching:
in $BaTiO_3$, Factors Effecting 8251
Behavior of Alloyed Junction Transistors 6765
Characteristics, Positive Temperature Coefficient Thermistors with 6920
Characteristics of:
Junction Transistors 6229

Switching: Characteristics of: (Cont'd)
p-n-p-n Diodes 6733
Transistors 7428-7430
Circuit Design, Charge Control Parameters in 8091
Circuits 6226, 6507, 6556, 6839-6841, 7177, 7761, 7770, 7797, 7798, 7812, 7823, 8507, 8534
Circuits,
Binary 8508
Bistable 9083
Broadband UHF 9081
Charge Control Parameters of 8091
Cryotron 6810, 7192, 7447
Ferreed 6246
Flip-Flop 9101
Four-Layer Diode 7823
Gate 9084, 9085
High Speed Magnetic 8119
Magnetic 6841, 8538
Parametric 7769
Power 8509, 9086
Stabilization of 9080
Three-State 9087
Thyratron 8506
Transistor Magnetic Core 6841
Trigger 9082
Tunnel Diode 6557, 6571, 6572, 6870, 6882, 8009, 8010, 8054
Circulators, Microwave Ferrite 6793
with Computer Diodes, Microwave 6265
by Domain Walls in Ferrites, Fast 6796
of Ferrite Cores, Partial 6577, 6587, 6588
Functions, Synthesis of Minimal Stroke and Dagger 6869
in Guanidine Aluminum Sulfate Hexahydrate 7598
Mechanism in Ferroelectric Colemanite Crystals 6087
Networks, Statistical Analysis of Transistor-Resistor 6876
Properties of:
Ferrites 9350
Toroidal Square Loop Magnetic Materials 8039
Rate in Ferrites, Effect of Previous History on 6795
Systems,
Design of 9115
Elliott Sheffer Stroke Static 7176
Magnetic Thin Film 6578
in Thin Magnetic Films, Nanosecond 6579
Transistor Parameters, Measurement of 6818
Transistors 6511, 7422, 7424, 7427, 7707-7709, 7839, 7840
SYMMAG, High Speed Magnetic Switch 8119
Symmetry of:
the Low Temperature Phase of BaTi, Crystal 6084
Metal Chelate Salt Crystals, Crystal 6367
Synthesis, Network 6819, 6820, 7120, 8480-8483
Synthesis of:
Aluminum Nitride Crystals 6038
Diamond 7898, 7899
SiI_4 6325
ZnS with Zincblende 7874
Synthetic Quartz, Effect of Impurities on Growth of 7884

T

Tachometers 7832
Talc, Dislocations in 8598
Tamm Surface States 8239
Tantalum,
Critical Field of Superconducting 7312
Field Dependence of Photoelectric Emission from 6193
Intermediate Superconducting State in 8287
Knight Shift in 7973
Nuclear Magnetic Resonance in 7352

Tantalum, (Cont'd)
Superconducting Transition in Purified 7623
Thermal Properties of 9441
Tantalum:
Electrodes, Metalizing of 8982
in Ge,
Diffusion of 7569
Solubility of 7569
Tape:
Cartridges 9120
Readers, Photoelectric 8126
Recorders,
Magnetic 8115, 8130-8133
Miniature 8115
Motor Speed Control for Satellite 6898
Recording, FM Systems for 9119
Recording Heads 8117
Storage:
Capacity and Properties, Magnetic 8116, 8130, 8131
Units, Magnetic 8132, 8133
Tape-Wound Cores, Magnetization in 7442
Target Miss Indicators 8105
Tecnetrons,
Equivalent Circuits and Characteristics of 8032
Theory and Design of 8031
Teflon, Polymorphic Phase Transitions in 9152
Telemetering:
Systems, Multiplex 8530
Systems for Stomac Pressure of Animals 8529
Telemetry,
Data Conversion Circuits for Earth Satellite 6274
Filters for Multiplexed 6269
Heartbeat 7500
Microwave Projectile 7164
Systems, Light Modulated 9117
Telephone:
Amplifiers, Audio- and Carrier-Frequency Transistor 7756
Cable Pairs by Pulse Code Modulation, Video Transmission over 7786
Circuits, Negative Impedance Repeater 7167
Dial Tone Gating Circuits 7787
Message Circuit Noise, Measuring Set for 6865
Negative Impedance Repeaters 7788
Repeaters 7409, 7505
Ringing Generators 6272
Set 9114
Switchboard 9116
Switching Systems, Design of 9115
Systems,
Channel Converter for Carrier Frequency 7506
Diode Limiter for 7499
Transmission by Infrared Radiation 6927
Teletype Actuaters, Magnetic Core 8519
Television:
Cameras 6863, 7504, 7821
Circuits 7165, 7166
Deflection Circuits 6861, 6864, 8109, 8527, 9113
High Voltage Generators 7166
Horizontal Sweep Circuits 7166
Magnetic Deflection, Vertical Scan System for 6861
Master Switchers 6271
Receivers,
Design Considerations for 6859
Limiters for 6862
Power Supplies for 7783, 8526
Video Processing Circuits for Transistor 6860
Screens, Polychromatic Electroluminescent 6567
Transmitters 8110
Tuners 6314, 7784
Video Amplifiers 7785, 8106-8108
Tellurium,
Absorption in 6178
Chemical Analysis of 8615
Energy Band Structure of 6178
Optical Activity in 7680
Tellurium, (Cont'd)
Recombination:
through Dislocations in 6096, 6936
and Trapping in 6394
Tellurium:
from As, Separation of 6946
in Ge,
Diffusion of 7569
Solubility of 7569
in InSb, Distribution Coefficient of 6320, 7847
and Selenium, Solid Solutions of 7552
by Zone Melting, Purification of 7565
Tellurium-Cadmium, Phase Diagram for 6317
Tellurium-Selenium System, Lattice Constants of Solid Solutions in the 7552
Temperature:
Compensated Amplifiers 8492, 8493
Dependence of Current Amplification Factor of Thin Film Cryotrons 8477
Terbium,
Electrical Resistivity of Polycrystalline 7016
Saturation Magnetization and Ferromagnetic Interaction in 9335
Terbium-Doped YIG, Ferrimagnetic Resonance Field of 7647
Ternary Semiconductor Alloys 7229
Tetragonal Solids, Debye Temperature of 8913
Tetrahedral Junction 6525
Tetramethylammonium-Trichloro-Mercurate, Ferroelectric Properties of 8253
Tetrode Junction Transistors, Fabrication of 8433
Texture of NiFe Thin Films 9183
Thallium, Solubility of Ge in 6001
Thallium in Pb, Determination of 8192
Thallium Bromide, Ultraviolet Absorption in 8368
Thallium Chloride, Ultraviolet Absorption in 8368
Thallium Halides,
Polymorphism of 7549
Preparation of Thin Layers of 7549
Thallium Telluride in Bi_2Te_3 and Sb_2Te_3, Solid Solubility of 6003
Thallous Halides, Optical Absorption in 6197
Theater Lighting Control Systems 6296
Thermal:
Activation Energies:
from Glow Curves, Evaluation of 6208
in NaCl and KCl Crystals 6209
Conductivity,
Detection of α-γ Fe Phase Transformation by 7848
Effect of Point Imperfections on Lattice 7074
Peltier Effect Measurement of 7072
Theory of 6396
Conductivity: 7686, 8408, 9430, 9431
Tensor of Dielectrics 7999
Conductivity of:
Ag-Sb-Te 7020
Alloys 8916
Bi_2Te_3 8001, 8919
Ceramic Oxides 8405
Ceramics 9436
Ferroelectric Ceramics 7289
Fused Quartz 7682
Ga in the Normal and Superconducting States 8917
Ge 6202, 7071, 7398, 7683, 9432
Halide Crystals 9433
InAs 6202, 7685
InSb 8001
KCl-KBr Solid Solutions 9270
LiF 6201, 6725
Metals and Alloys 8000
Mo 8000
NaCl 7684
the PbS Group 7399
PbS and PbSe 8918
PbTe 8001
Semiconductors, Theory of 6396
Si 6202, 8402
Silica 9435
Thermal: Conductivity of: (Cont'd)
Superconductors in the Intermediate State 8404
Synthetic Sapphire 7073
Detection Elements, $BaTiO_3$ Thin Film 6042
Diffusivity of:
Armco Iron 6726
Ge 6726
Semiconductors 7688
Solids 6726
Drift in Junction Transistors 8055
EMF in:
Cu_2O at High Temperatures 6204
Semiconductors 6396
Etching of Ag to Detect Dislocations 8180
Excitation Induced Polarization Decay in Diamond 7995
Expansion of:
Bi 9440
BiPt 8288
GaP 8852
Gd, Magnetostriction Contribution to 8777
Organic Crystals 9155
Si 6207, 8934
Triglycine Sulfate 8692
Oxidation, Impurity Redistribution and Junction Formation in Si by 6751
Power in Ti_2O_3, Temperature Dependence of the 7309
Properties, Measurement of Diode and Transistor 6925
Properties of:
(Ga, In) As 8932
Graphite 9441
PbTe 6238
Mixed Valence Compounds 6524
Mo 9441
Ta 9441
Resistance Due to Isotopes and Other Point Defects 9434
Resistivity:
- See Thermal Conductivity of Metals and Alloys 8403
of Point Defects, Low Temperature 6200
Spreading Resistance in Mesa Diodes 7696
Test Set 6925
Thermal-Optical Conversion, Thermodynamics of 9412
Thermally:
Induced Conductivity in CdS 7310
Stimulated:
Conductivity in Semiconductors 7935
Currents in Photoconductors 6190
Thermionic:
Behavior of p-n Junctions 6218
Emission of:
Si 8664
UC, ZrC, and ZrC-UC 9313
Thermistor:
AGC Circuits 8524
Bolometers 7722
Choppers, dc Amplifiers Using 6295
Converters 6295
Noise Figure Meter 8145
Pirani Gauges 8566
Thermal Conductivity Detectors for Gas Chromatographs 7530
Thermistors,
Fabrication and Properties of Semiconducting Diamond 8457
Flake 7721
Measurement of Change of State and Motion of a Medium by 8148
Properties of 8036
Thermistors:
with Switching Characteristics, Positive Temperature Coefficient 6920
for Temperature Compensation of Transistor Circuits, Use of 7738

Thermocouple:
Bonding into Samples, Alloys for 6668
Furnace for SiC Device Fabrication 7093
Thermocouples,
Alloys for Bonding 6668
Stationary and Transient Behavior of Refrigerating 6523
Thermodynamic Data for Group III-V Compounds 6626
Thermodynamics of:
a Nonlinear RC System 7021
Thermal-Optical Conversion 9412
Thermoelectric:
Air Conditioning Systems for Totally Enclosed Environments 8578
Behavior of Junctions 6218
Cooling of Diodes 7075
Devices, Efficiency of 6239
Effects in Cu-Au Alloys 6205
Efficiency of Semiconductors 8002
Elements, Semiconductor 8458
Energy Converters 6310, 7722
Figure of Merit 7400, 8408
Generators, Analysis of Radiation-Powered 7440
Heat Pump 9034
Materials 9034
Power Generators, Semiconductors for 8459
Power of:
Bi_2Te_3 8919, 8925, 8926
CoSi 8931
CoSi-FeSi 8931
CoSi-NiSi 8931
CrSi 8931
Cu- and Ag-Alloys 8407
Ge, Effect of Impurities on 7398
Ionic Crystals 8921
Mg Binary and Ternary Alloys 8930
MnSi 8931
PbS and PbSe 8918
Radical-Anion Salts 7621
Semiconducting Oxide Glasses 7311
Si-Co Compounds 7620
Sn 6120
Wustite and Magnetite 8733
Properties, Effects of
Radiation on 7402, 7403
Random Inhomogeneities on 7019
Properties of:
AgSe 7077
Bi_2Te_3 8927, 8929
Bi_2Te_3 and Related Materials 7687
$Bi_2Te_{3-x}Se_x$ 7919
Cd-Sn-As 6108
Junctions 6218
Metal Alloys 8920
the p-Phenylenediamine-Chloranil Complex 8735
PbSe 6059
PbTe 8927
Sb_2Te_3-Bi_2Te_3 Alloys 7401
Refrigerating System for Submarines 8576
Refrigeration, Applications of 8577
Refrigerators 6615
Thermoelectricity of the PbS Group 7399
Thermoelements Using Mixed Valence Compounds 6524
Thermo-Junctions of PbTe and Bi_2Te_3 8928
Thermoluminescence,
Defect Measurements in Quartz by 7853
Thermodynamics of 9412
Thermoluminescence of:
Alumina Ceramics 7553
NaCl 7388, 8378, 8885
Potassium Azide 7389
ZnS 6187, 8379
Thermoluminescent Dosimeters 7502
Thermomagnetic:
Behavior of Pure Ni Ferrite 6156
Effect in:
Crystals 7905
InSb 8933
Sn 6210
Generator 9439
Properties of Zn 9296
Thin:
Circuit Microelectronics 7122
Film:
Circuit Techniques 6821
Computer:
Memories and Switching Circuits 6578
Storage Matrix, Ferromagnetic 7190
Cryotrons,
Fabrication of 7192
Temperature Dependence of Current Amplification Factor of 8477
Deposition, Analysis of Residual Gases in High-Vacuum Evaporators for 6345
Dielectric, Silicon Nitride 6366
Memory, Vacuum Evaporated Random Access 6888
Resistance for Microsystems Electronics, Ti 7107
Semiconductors, Electrical Properties of 6384
Films,
Analogies between Twistors and 6797
Crystal Orientation Effects in Sn-Te 6953
Magnetic Phase Transition of Evaporated 6409
Reflectivity and Transmissivity of Metallic 8394
Films:
of Ge by the Disproportionation of Ge Di-iodide, Formation of 6032
by Impact Evaporation, Preparation of Magnetic 6975
Layers of:
InSb, Preparation and Properties of 6654
the Thallium Halides, Preparation of 7549
Magnetic:
Films,
Nanosecond Switching in 6579
Spiral Walls in 7038
Films Electrodeposited in a Magnetic Field, Influence of Substrates on 7039
Thomson Effect in Semiconductors 8923, 8924
Thorium Oxide, Paramagnetic Resonance of Gd^{3+} in 8847
Threshold:
Sensitivity of Radiation Receivers 8565
Transducers, Functional Unit 6776
Thulium, Electrical Resistivity of Polycrystalline 7016
Thyratron:
Control Circuit 9144
Transistor Circuit, High Power Bistable 8506
Time:
to Amplitude Converters 8575
Delay Circuits 6268, 6846, 6847, 8522
Timing:
Device 9149
Meter for Missile Control Values 8150
Tin,
Adiabatic Magnetization Cooling of Superconducting 9295
Critical:
Currents in Superconducting 9293
Field of Superconducting 7312
Domain Distribution in Superconducting 6117
Effective Mass in Gray 7298
Elastic Constants of β 7405
Intermediate Superconducting State in 8287
Neutron Irradiation of Gray 7280
Phase Transformations and Properties of Gray 8586
Quenched-In Defects in 9166
Solubility of:
Ge in 6001
Si in 6001
Specific Heat of β 7405
Superconducting 8748
Superconductivity in 6693
Superconductivity of Contacts with Interposed Barriers in 6407
Thermomagnetic Effect in 6210
Time Delays in the Superconducting Transition of 6697
Transformation of Gray 6930
Tin:
Films,
Critical:
Currents in Superconducting 8286
Fields of Thin Superconducting 6118
Magnetic Fields and Currents for the Destruction of Superconductivity in 8285
Magnetic Phase Transition of Evaporated Superconducting 6409
Superconducting 6410, 8747
Superconducting-Normal Transition in 8281
in Se,
Diffusion Coefficient of 7547
Distribution Coefficient of 7547
in Sn-In Alloys, Diffusion of 9182
Whiskers, Tensile Strength of 7895
Tin Selenide,
Electrical and Optical Properties of 6132
Preparation of 6132
Tin Sulfide,
Absorption Properties of 7273
Conductivity in 7273
Effective Mass in 7273
Energy Gap Width of 7273
Hall Coefficient of 7273
Preparation of 7273
Tin Telluride, Solid Solutions of InTe and CdTe in 7231
Tin Telluride Films, Crystallographic Orientation of Evaporated 6953
Titanate System, Piezoelectric Properties of a Mixed 6088
Titania, Paramagnetic Resonance of V^{4+} in 7975
Titania Maser, Operation of a Cr-Doped 8474
Titanium, Zone Refining of 8194
Titanium Thin Film Resistance for Microsystems Electronics 7107
Titanium^{3+} in Al_2O_3, Paramagnetic Resonance of 8355
Titanium Chloride, Magnetic Transition and Susceptibility of 8305
Titanium Dioxide,
Elastic Moduli and Acoustic Attenuation in 8410
Electron-Spin Resonance in 6170
Growth of 6044
Paramagnetic:
Properties of Cr^{3+} in 6806
Resonance:
of Fe^{3+} in 6165
Spectrum of Fe^{3+} in 8349
Piezoresistivity of 6402, 6404
Stability and Aging of 7901
Titanium Dioxide-Zinc Oxide System, Phase Equilibria in 8580
Titanium Iron, Magnetization Curves for 6152
Titanium Sesquioxide,
Effective Mass in 7309
Resistivity, Hall Coefficient, and Thermal Power of 7309
Tone Generators 8112
Torque Measurements on Doped YIG 7640
Tourmaline Piezoelectric Force Gage 7729
Transceivers, Application of dc Converters to 8525
Transducer Properties of $PbTiZrO_2$ Ceramics 6532
Transducers,
Piezoresistive Strain 6534
Radiation Tracking 7529
Semiconductor Strain 6814
Solid State 6311

Transducers for Ultrasonic Delay Lines, Thickness-Shear Mode $BaTiO_3$ 6533
Transfer:
  Circuits, Magnetic 8093
  Function Synthesis of Active RC Networks 6819
  Graphs of a Linear System 7452
Transfluxors to Electromechanical Control Systems, Applications of 7522
Transformations in Gray Sn 6930, 8586
Transformers for Partially Filled Transmission Lines, Stepped 6790
Transient:
  Behavior of Junction:
    Diodes 6223, 6224
    Transistors 6765
  Effect in Junction Diodes, Increased Speed of 6496
  Junction Temperatures in Power Transistors 6230
  Operation of Transistors with Inductive Loads 6756
  Processes in Junctions at Arbitrary Injection Levels 7418
  Response of:
    Junction Transistors 6253
    Variable Capacitance Diodes 6735
  Sweep-Out on the Decay Rate of Excess Carriers, Effects of 6094
Transistor:
  Bias:
    Methods 6266
    Networks 7465
  Cascode Configuration, Analysis of 6260
  Circuits,
    Complementary 6822
    Stabilization of 7126
    Temperature Compensation of 7738
  Curve Tracer, High Current Adapter for 6924
  Graph Plotter 8152
  Magnetic Film Recording Channel 7170
  Matching Impedances 6256
  Modules, Microminiaturization of 6257
  Mounting Washers 6313
  Operation beyond Cutoff Frequency 7710
  Parameters,
    Design of Systems to Tolerate Variable 7461
    Measurement of: 6258, 7463
      Switching 6818
  Power Dissipation 7466
  Properties, Automatic Instrument for Measurement of 8428
  Ratings and Reliability 8020
  Reliability, Evaluation of 6730
  Scaling Theory 6762
Transistors,
  Admittance Parameters of 7731
  Analog 6753
  Autopsy Techniques for 7432
  Avalanche:
    Breakdown in 8025, 8439
    Mode Operation of 8436
  Base:
    Connection for 6233
    Containing a Dispersed Colloidal Phase in 6515
    Layer Design for 7423
  Binistor 6613, 7709
  Carrier Lifetime in 7707
  Characteristic Frequencies of 6536
  Characteristics of: 7427, 8022
    Base and Emitter in 8995
    Imperfect Emitter 8026
  Characterization of 7462
  Charge:
    Carriers in the Base Region of 7148
    Control Parameters of 7094
  Collector:
    Spreading Resistance 7696
    Voltage Stability Criteria for 6509
  Compound Junction 8513
  Cooling of 7697, 9011
Transistors, (Cont'd)
  Current:
    Amplification Factor in 6231
    Build-Up in 7425
    Drift Calculation of 8055
    Gain in 6508, 6763, 7096, 7097, 8021
  Distortion in 7095
  Double:
    Diffusion Process for Ge 8028
    Tetrode 8023
  Drift 6102, 6503, 6761
  Electrode Connection to 6770
  Electroplating of 9017
  Encapsulating 6772
  Equivalent:
    Circuits for 6254, 6761, 7463, 7464
    Hybrid-π Circuit for 8027
  Evaporation of Several Electrodes for 6769
  Fabrication of 8028, 8029
  Failure Mechanism with Inductive Loads of 6756
  Field-Effect:
    Effect of Electron-Hole Pair Generation on the Characteristics of Photoconductive 7070
    Method of Fabricating 8029
  Field-Effect in 6504
  Frequency:
    Cut-Off of 7426
    Response of 7732, 7843
  GaAs 7431
  Gettering in 7713
  Heat:
    Dissipation in 7102
    Dissipators for 8447
    Sinks for 8446
  High Current:
    Measurement of Characteristics of 6924
    Operation of 7099
  High Frequency: 6514, 6917, 7423, 7712, 8431, 9004
    Behavior of 6255
  High Voltage 6758
  Junction:
    Alloyed 6510, 6511, 6513, 8431, 9001
    Diffused 6327, 6511-6513, 6749, 6757, 6767, 6917, 6949, 7100, 7422, 7423, 7839, 8017, 8028, 8438, 8441, 9001, 9005
    Epitaxial 7219, 7268
    Fabrication of 8998, 8999
    Fabrication by:
      the Oxide Masking Technique of 6514
      Silicon Dioxide Diffusion Masks of 6327
      Thermal Oxidation of 6751
    Gettering in 8441
    Production of Stable n- or p-Type Layers on 6771
    Regrown-Diffused 6768
    Vapor Grown 6750, 9007
  Large-Signal Parameters of 8440
  Lead Attachment to 7228
  Logarithmic Characteristic of 7415
  Low-Melting Glasses for Sealing 6773
  Microwave 6513
  Minority Carrier:
    Decay Time in 6507
    Injection in 8024
    Recombination in 6503
  Mixer 6505
  Nanosecond Range Behavior of 6605
  Neutron Radiation Damage in 6767
  Noise in 6231, 6232, 6766
  Packaging of 9013
  Parallel Operation of Power 7737
  p-n-p-n 6227, 6506, 6511, 6757, 6758, 6760, 7424, 7537, 7708, 7840
  Point Contact:
    Fabrication and Properties of 8429
    Preparation of Point Contact Assemblies for 8994
Transistors, (Cont'd)
  Power: 6230, 6510, 6917, 7536, 7712, 8430, 9008
    Capacity of 6762, 8442
  Protective Resin Surface Treatment for Ge and Si 8019
  Pulse Testing of 6605
  Radiation Effects on 6508, 6755
  Saturation:
    Condition in 6229
    Operation of 7099
  Shot Noise in 6232
  SiC 7101, 7433
  Small Signal Parameters of 7095
  Space-Charge Layer Widening in 8437
  Spacistor 8434, 8435
  Stable 9012
  Storage Time in 6253
  Surface Barrier: 6764, 9014, 9015
    Whisker Mounting on 9016
  Switching: 6227, 6511, 6758, 6818, 7422, 7424, 7537, 7707-7709, 7839, 7840
    Characteristics of 6605, 6765, 7099, 7427
  Tetrode 8433
  Thermal Test Set for 6925
  Transconductance of Alloyed and Drift 7098
  Transient:
    Characteristics of 7428-7430
    Switching Behavior of 6765
    Temperatures of 6230
  Transport:
    Efficiency of 6503
    Factors 6228
  Tunnel 6759
  Unipolar 7101, 7433
Transistors-Transductors Systems 7144
Transition:
  Metal Content in Alloys, Sensitive Determination of 8156
  Metals, Crystal-Chemical Characteristics of Semiconducting Compounds of 7584
  Metals in:
    Si, Spin Resonance of 6164
    Single Crystal Oxides, Paramagnetic Resonance of 8847
  Temperature of BiPt 8288
  Temperatures, Superconductors with Very Low 6692
Transmission:
  Equations, Fresnel 8909
  Line Amplifiers, Theory of Negative Resistance 8467
  Lines,
    Correction of Delay and Frequency Distortion in 7789
    Parametric Amplification along Nonlinear 6546
    Stepped Transformers for Partially Filled 6790
  through Normal and Superconducting Films, Far-Infrared 8853
  of X-Rays in Ge, Effect of Elastic Strain on the 7371
Transmissivity Properties of Metallic Films 8394
Transmitters,
  Broadband Nonreciprocal 8041
  Transistorized TV 8110
Transponder, Solid State Radar 7223
Transport:
  in CdS, Neutral 6192
  Coefficients in Alkali Metals 7299
  Factors of Junction Transistors 6228
  Processes in Solids 6395, 8707
  Properties of Superconductors 6115
Trap States in Tunnel Diodes, Tunneling from 7411
Trapped Radicals in Organic Deposits 7367
Trapping,
  Carrier Concentration Fluctuations Due to 9252
  Current Noise in CdS Due to Multiple Re- 6095

Trapping:
Kinetics of Additively Colored KBr 7993
Noise in CdS 7319
Trapping in:
Organic Solids, Surface 7029
Photoconductors 9256
Semiconductors 9256
Te 6394
ZnS, Paramagnetic Resonance Studies of 8893
Traps,
Absorption and Emission Spectra of Electron in One-Dimensional Deep 7930
Method of Determining Ionization Energy of 6190
Traps in:
CdS 6095, 6419, 7022, 7951, 8702
PbS 6467
Semiconductors 8261
Si 6097, 8237
ZnO 7022
Traveling Wave:
Harmonic Generators 9097
Magnetic Devices 6528
Parametric Amplifiers 6545, 7474, 8066
Triangular Moment Arrangements in Manganese Spinels 7037
Triboluminescence in Diamond 7987
Trigger:
Circuit Stabilization 7152
Circuits 9082
Circuits,
Binistor 7709
Cascode 7153
Controlled Rectifier 6840
Cryotron 6810
Indicator Lights for 7764
Magnetic Core 7771
Magnetoresistive 6842
Parametric 7768, 7769
Solid State 6774
Stabilization of 7152
Switching:
Levels in 7482
and Memory Criteria in 7763
Tunnel Diode 6870, 7179
Triglycine Selenate, Ferroelectric Properties of 6083
Triglycine Sulfate,
Effect of Hydrostatic Pressure on the Ferroelectric Properties of 6083
Elastic Constants of 6043
Ferroelectric:
Properties of 6083, 8691
Transition in 8692
Polarization Reversal in 9239
Preparation and Properties of 6043
Spontaneous Polarization of 8246
Thermal Expansion in 8692
Trigonal Solids, Debye Temperature of 8913
Trinistor Controlled Rectifiers 7837
Tungsten, Irradiation Damage in 7902
Tungsten Trioxide, Solid Solutions of Metals and 6998
Tunnel:
Currents, Magnetic Field Effects on 6701
Currents in InSb, Effect of Landau Levels on 7633
Diode:
Adder-Subtracter Circuits 6882
Characteristics, Measurement of 6312, 6535, 6617
Circuits 8151
Circuits, Noise in 7459
Converters 7156
Counters 6557
Crystal Calibrator 8151
Curve Tracers 6312, 6617, 6817
Decade Scaler 7224
Down Converters: 7492
with Conversion Gain, Low-Noise 6561
Frequency Divider 6488
Generator Supplies 7544
Tunnel: Diode: (Cont'd)
Inverters 9139
Locked Pairs 7180
Logic Circuits 6572, 6872, 6873, 7178, 7179, 7796
as a Logic Element 6571
Oscillators 6550, 7150
Oscillators,
Millimeter Wave 8090
Voltage Tuning in 8089
Pulse Power Supply 7544
Scalers 6879
Shift Register 6870
Storage 7805
Switching Circuits 6557, 6572, 6870
Trigger Circuits 7179
Diodes,
Characteristics and Fabrication of 8955
Design of 7082
Effects of Magnetic Fields on 7412
Emission Spectrum of 6181
Equivalent Circuit of: 6487
and Frequency Characteristics of 8012
Excess and Hump Current in 7410
Forward and Reverse Tunneling Currents in 6489
GaAs 7150, 7431, 8956
Low Resistivity Ge for Fabricating 8200
Maximum and Minimum Currents in 6737
Neutron Bombardment of 7083
Noise Performance of 7700, 7701
Pressure Dependence of:
the Characteristics of 6220
Reverse Characteristic of Ge 8011
Properties of 6485-6487
Shot Noise in 6740
Temperature Dependence of Current in 6738
Theory and Fabrication of 6484
Tunneling in 8418
Tunneling from Trap States in 7411
Diodes: 6219, 7838
as Circuit Elements 6487, 6488
as Storage Elements 6583
Effect in Semiconductors, Theory of the 6416
Junction Transistors 6759
Tunneling, Electron-Electron Scattering in n-p 6700
Tunneling in:
Ge 8418
InSb 6701, 8278
Sb-As-Doped Ge Junctions 8958
Semiconductors, Zener 6131
Superconductors 7627, 7842
Tunneling Current, Temperature Dependence of 8957
Tunneltron 7842
Twin:
Boundaries, Techniques for Revealing 8188
Faults in fcc Metals 9177
Formation in Evaporated Ag Films 9178
Generation in Dendritic Growth 6351
Structure of InSb Dendrites, Internal 6348
Twins in the Spinel Structure 6932
Twist in SiC Whiskers, Determination of 6022
Twistor:
Memory 7510
Shift Register 9053
Twistors Represented by Confocal Hollow Prolate Spheroids, Magnetic Fields of 6797

U

Ultra High Frequency:
Broadband Switching Circuits 9081
Harmonic Generators 8099
Ultrasonic:
Absorption and Dispersion in YIG 9451
Attenuation:
in Alkali Halides, Measurement of 6480
in CdS, Photosensitive 8942
Ultrasonic: Attenuation: (Cont'd)
and Dispersion in Metals at Low Temperatures 6211
in Metals 8413
in Semimetals, Magnetic Field Dependence of 6728
Delay Lines, Thickness-Shear Mode BaTi Ceramic Transducers for 6533
Drilling of Semiconductor Slices 7900
Frequency Power Generators Using Transistors 6294
Measurement of Magnetization in Mn Ferrites 8787
Velocity, Measurement of 7531
Waves in Quartz, Excitation and Attenuation of 8941
Ultraviolet Absorption in:
Irradiated LiF Crystals 8367
Thallous Halides 8368
Unipolar Transistors, SiC 7433
Uranium, Stimulated Infrared Emission from Trivalent 7669
Uranium Glass, Decay Rate of the Phosphorescence of 7068
Uranium Carbide, Thermionic Emission of 9313

V

Vacancies in:
$Co_xFe_{3-x}O_4$ 8317
Ge 6627
NaCl 6628
Pt 9167
Vacancy:
Annealing in Impure Metals, Theory of 7240
Association with $CaCl_2$ Impurity in KCl Crystals 7868
Condensation during Cooling of Solids 8595
Diffusion, Nonequilibrium 8594
Interaction in Si, Electron Spin Resonance Determination of 8176
in Si, Electron Capture by a Lattice 6097
Vacuum Evaporation, Masking Technique for 6769
Valence:
Band:
in Ge under Shear, Change of the 7586
Parameters in Si, Cyclotron Resonance Measurement of 8706
Structure of:
Alakli Iodides 7320
Ge in External Magnetic Field 7909
Compounds, Preparation of Mixed 6524
Crystals, Surface States of 8238
Electrons, Wave Functions for 9203
Valencies in Mg-Mn Ferrites, Ion 8584
Valley-Orbit Splitting of Sb in Ge 7003
Vanadium, Zone Refining of 8194
Vanadium in:
α-Al_2O_3, Electron Spin Resonance of 8351
TiO_2, Paramagnetic Resonance of 7975
Vanadium-Activated Zn and Cd Sulfide and Selenide Phosphors 6461
Vanadium^{2+} in ZnF_2, Paramagnetic Resonance of 8352
Vanadium^{3+} in Al_2O_3, Large Zero Field Splitting of 7359
Vanadium^{4+} Concentration on Conductivity of High V Phosphate Glass, Effect of 7944
Vanadium Phosphate Glass, Conductivity of High 7944
Vanadium Sapphire, Electron Spin Resonance of V in 8351
Vapor:
Decomposition, Formation of Ge Single Crystal Films by 7887
Deposition of Si, Epitaxial 6650
Grown:
Ge,
Chemical Purity of 6651

Vapor: Grown: Ge, (Cont'd)
Concentration of Iodine in 6640
Dislocations in 6651
Incorporation of As into 6641
Ge Junctions, Electrical Properties of 6750
Si and Ge Single Crystal Films 6649
Variable Capacitance Diode 6734
Growth of Ge, Closed-Cycle Process for the 6651
Phase Diffusion of P in Si, Effect of Oxide Layers on 7862
Pressures of III-V Compounds 6626
Vapor-Zone Refining 8616
Varactor:
Diode:
Nonreciprocal Phase Shifter 7735
Package for Microwave Frequencies 7698
Parametric Amplifier 8069
Phase Shifters 8051
Radio Receivers 7780, 7781
Diodes,
Design of 7081
Figure of Merit for 7081
GaAs 6226, 6308, 7836
Impedance of 7124
Noise Properties of 7115
Si 7124, 7835
SiC 7087
Transient Response of 6735
Vapor Grown 6734
Diodes for Phase-Locked Oscillators 7698
Harmonic Generator for Space-Vehicle Applications 6843
Varactors,
Design and Properties of 8417
Figures of Merit of 8960
Varactors Using Space Charge Layers 6251
Variable:
Capacitance Diodes, Design and Properties of 8417
Reactance Converters 6543
Varistor Squaring Unit for Analog Computers 7513
Varistors 9021
Varistors, Dynamic Current-Voltage Characteristics of SiC 7108
Velocity Meter, Water 7830
Veterinary Applications: Telemetering System for Stomach Pressure of Animals 8529
Vibration Spectra, Center Law of Lattice 7917
Vibrations, Modes of Lattice 8241
Video:
Amplifiers 6258, 7130, 8107, 8108
Current Amplifiers 7165
Detectors, Microwave 6267
Processor with Pulse-for-Pulse AGC 7743
Transmission over Telephone Cable Pairs by Pulse Code Modulation 7786
Vitreous Materials, Hall Effect in and Other Properties of 7949
Vocoder, Correlator for a 6903
Voight Effect in Semiconductors 7679
Voltage:
Generators, Television 7166
Measurements, Superconductive Device for Low 6602
Reference Diodes, Characteristics and Applications of 6736
Regulators,
Analysis of Magnetoresistive 8143
Corbino Disk 7106
Direct Current 9134
Overload Protection for 7520
Regulators: 6894, 7196, 7198, 9132
- See also Power Supplies
Supplies, Stabilized 7197
Voltage-to-Frequency Converter 8510
Voltmeters,
dc Milli- 8559
Electrometer 8560
Volume Changes in Ni_3Mn on Ordering 8167
Vycor, Moisture Gettering with Porous 7713

W

W-Type Memory Element 8129
Wafer Slicer, Crystal 6306
Walker Modes in Large Ferrite Samples 6792
Wall:
Effect in Ferrimagnetic Resonance 8810
Motion in Ferromagnetic Thin Films 9349
Orientation in Ferroelectric Domain Growth of $BaTiO_3$ 7923
Walls in Thin Magnetic Films, Spiral 7038
Warm Electrons in Nonpolar Crystals, Variational Treatment of 7924
Washers, Transistor Mounting 6313
Water Velocity Meter 7830
Wattmeters,
Hall Effect 9019
Thermistor 8145
Wave:
Analyzers 7204, 9145
Functions, Strain-Induced Changes of Donor State 7614
Functions:
of Activators, Atomic 7925
for Bloch Electrons in an Electric Field 6091
for Valence Electrons 9203
Guides with Gyromagnetic Media, Characteristics of 8466
Representation Energy Band Calculation for Alkalis 7906
Waveform Generators 7153, 7493, 7494, 9101
Waveguide Junction, Tetrahedral Ferrite-Loaded 6525
Whisker Mounting on Diodes and Transistors 9016
Whiskers,
BeO Flagpole 6045
Fe 9176, 9191
Growth of: 6034, 7895
Cu 6970
Impedance Matching of 8950
In-Ge Plated 8949
NaCl 6009
SiC 6022
Whiskers:
for Al Bonded Diodes 8951
on Cleavage Steps in Crystals 8206
under High Fields, Observation of Domains in Iron 7034
Wideband Amplifiers, Modulation-Demodulation 6570
Work-Hardening in fcc Crystals, Orientation Dependence of 8600
Wurtzite:
Structure, Synthesis of ZnS with 7874
Structure Crystals, Infrared Absorption in 8365
Structures, Bond Structure of 8654
Wurtzite-Type Binary Compounds, Double Refraction in 6194
Wustite, Conductivity and Thermoelectric Power of 8733

X

X-Ray:
Attenuation Coefficients for Ge 6684
in Cubic Powders, Scattering of 9158
Diffraction:
Microscopy, Determination of Crystal Perfection by 6945
Studies of Pyrographite 7851
Study of GaSb-Ge Alloys 6622
Excited Carriers in Semiconductors, Measurement of Decay Times of 6684
Induced Surface Hardening in NaCl, Annealing of 8650
Measurement of Lattice Parameters 9154
Method for Film Thickness Measurement 9156
Photoconductivity of Sulfide Phosphors 6191
X-Ray: (Cont'd)
Reflection Studies of Annealing and Oxidation in Thin Solid Films 7871
Reflectivity of Quartz 9160
Scattering:
from Cu and Al under Cyclic Stress 9164
in Cubic Solid Solutions 9162
from Fatigued Metals 9163
from Neutron Irradiated Cu, Small-Angle 9157
by Plastically Deformed Mg Single Crystals, Small-Angle 9165
Spectra of Superconducting CuS 8371
X-Rays, Production of Color Centers in Alkaline Earth Fluorides by 7059, 7060
X-Rays in Ge, Effect of Elastic Strain on the Anomalous Transmission of 7371

Y

Y-Junction Strip-Line Circulator 6794
Yield:
Instability in Fe, Low Temperature 8939
Strength of Crystals, Effect of Screw Dislocations on the 7694
Stress of NaCl, Temperature Dependence of 8938
Young's Modulus:
in Ferromagnetics, Temperature Dependence of 8943
of Germania 9449
of Silica 9449
Ytterbium, Resistivity of 8274
Ytterbium in:
Al and Ga Garnets, Paramagnetic Resonance of 6446
CaF_2, Paramagnetic and Optical Spectra of 7976
Yttrium, Elastic Constants of 8411
Yttrium Gadolinium Garnets, Ferromagnetic Resonance Absorption in 6145
Yttrium-Gadolinium-Iron Garnets, Initial Permeability Characteristics of Mixed 6444
Yttrium Gallium Garnet,
Absorption Spectrum of 7978
Crystalline Field for Ni^{2+} and Co^{2+} in Single Crystals of 7379
Growth of 6364
Paramagnetic Resonance of Cr^{3+} in 8350
Yttrium Garnets, Device Applications of 7054
Yttrium Indium Garnets, Permeability and Preparation of 8330
Yttrium Iron Garnet,
Adiabatic Demagnetization and Specific Heat in 7952
Calculation of Uniaxial Spin Hamiltonian Constants in 7637
Dielectric Properties of 9227
Domain Structure in 7646
Elastic Constants of 7691
Electron Spin Resonance in 8328
Ferrimagnetic:
Resonance in: 8810
Rare Earth Doped 7347
a Single Crystal Disc of 7052
Resonance Field of Tb Doped 7647
Ferromagnetic:
Resonance in 6705
Resonance Parameters in 6436
Generation of Microwave Electromagnetic Radiation in 7169
Infrared Faraday Effect in 8396
Line Width:
Maximum in 7051
Narrowing in Ga Substituted 6143
Magnetostriction of 8304
Microwave:
Power Absorption in 8038
Properties of 9364, 9368
Nonlinear Response of 7055

Yttrium Iron Garnet, (Cont'd)
Saturation Effects in Ferrimagnetic Resonance of 6439
Spin-Phonon Interaction in 6147
Spin-Wave Spectrum of 7333
Subsidiary Resonance in the Coincidence Region in 7348
Substitution of Sm in 6443
Torque Measurements on Doped 7640
Ultrasonic Absorption and Dispersion in 9451
Yttrium Iron Garnet:
Circulators 6243, 8463
Crystals, Infrared Method for Detecting Flaws in 6322
Doped with Rare Earth, Temperature Dependence of Ferrimagnetic Resonance Line Width in 7053
by the Flame Fusion Process, Growth of 6040
at Low Temperatures, Specific Heat of 6476
Resonance Isolators 7115
Resonators 6791
Spheres, Technique for Polishing Single Crystal 7277
Yttrium Iron Garnets,
Ferrimagnetic Resonance in Impurity Doped 6440
Growth of 6364
Incorporation of Nd in 6977
Yttrium-Ytterbium Garnet System, Magnetic Properties of 8817

Z

Z Bands in NaCl:Sr and KCl:Sr, Dichroism of 9397
Zeeman:
Effect of the Purely Cubic Field Fluorescence Line of $MgO:Cr^{3+}$ Crystals 7360
Modulation Microwave Spectrometer 6603
Zener:
Diode:
Bridge Gating Circuits 7480
Logic Circuits 7765
Stabilized Power Supply 6736
Voltage:
and Current Regulators 7816
References, Long-Term Stability of 7817
Diodes,
Characteristics and Applications of 6736
Temperature-Compensated 7535
Diodes as Voltage Breakdown Gating Elements 7765
Effect in Semiconductors 8705
Tunneling in Semiconductors 6131
Zeolite Powder Compacts, Electrical Properties of 9289
Zero Field Splittings of V^{3+} in Al_2O_3, Pulsed Field Measurements of Large 7359
Zinc,
Effect of Pressure on the Critical Field of Superconducting 8283
Ettingshausen-Nernst Effect in 9438
Galvanomagnetic Properties of 9296
Solubility of:
Ge in 6001
Si in 6001
Surface Energy of 6999
Thermomagnetic Properties of 9296
Zinc:
as a Differential Charge Compensator in GaP-Si Alloys 6621
Doped Ge, Magnetic Susceptibility of 6425
Vapor into Cu, Grain Boundary and Lattice Diffusion of 9180
Zinc in:
Cu_2O, Diffusion of 7567
GaAs,
Diffusion of 7228, 7566, 7572
Distribution Coefficient of 8166
Ge, Solid Solubility of 6002
InSb, Diffusion of 7252
Zinc Antimonide,
Anisotropy of Electrical Properties of Single Crystals of 7286
Cyclotron Resonance Absorption in 8768
Preparation of 7286
Preparation and Properties of 6363
Radiation Effects in 7402, 7403
Structure of 8589
Zinc Arsenide, Electrical Properties of 7027
Zinc-CdS-Mn Phosphors, Field Amplification of 7982
Zinc Fluoride, Paramagnetic Resonance of Ni^{2+}, V^{2+} and Cr^{3+} in 8352
Zinc Fluoride:Mn, Moving Crucible Growth of 8217
Zinc Fluorosilicate, Paramagnetic Resonance Spectrum of Mn^{2+} in 7365
Zinc-Mercury Phosphors, Photo- and Electroluminescence in 7988
(Zinc, Mercury) Sulfide, Solid Solutions of 7677
Zinc-Nickel Ferrites, Deposition of Thin Films of 7886
Zinc Oxide,
Absorption in 8366
Absorption Edge in 9398
Crystalline Field for Ni^{2+} and Co^{2+} in Single Crystals of 7379
Diffusion of Li in 7227
Edge Emission in 9407
Effect of Pressure on the Resistivity o 6403
Electron Scattering Due to Acoustic Modes in 6403
Growth of 8218
Lattice Structure and Properties of 8612
Li as a Donor and an Acceptor in 7227
Luminescence in 8880
Luminescence of Se Activated 8382
Optical Properties of 8361
Piezoelectric Scattering in 8693
Precipitation of Li on Dislocations in 7227
Preparation of Junctions by the Decomposition of 7419
Reactions of Oxidized Li with 7227
Relation of Traps to Noise in 7022
Resistivity of 6403
Sintering of 8626
Surface States of 8240
Zinc Oxide Surfaces, Conductivity of 9284
Zinc Oxide-Titanium Dioxide System, Phase Equilibria in 8580
Zinc Selenide,
Fluorescence of 9416
Optical and Photoelectric Properties of 7397
Zinc Sulfide,
Absorption Edge in 9398
Conductivity Pulses in Irradiated 6688
Crystalline Field for Ni^{2+} and Co^{2+} in 7379
Defects in 7561
Edge Emission in 9406, 9407
Electroluminescence of 6183, 6458, 7062, 8881, 8883, 9411
Energy Levels of:
Ag Luminescent Centers in 9418
Donor-Acceptor Pairs in 6380
Fluorescence of 6456, 9414-9416
Forbidden Zone Width of 8658
Growth of 6354, 8213, 8214
Zinc Sulfide, (Cont'd)
Heat Treatment of 6354
Ionic Properties of 6080
Luminescence in 6455
Maintenance of 7063
Paramagnetic Resonance Absorption in 9386
Phase Transitions in 8585
Phosphorescence of Mn-Activated 7068
Photoconductive Trapping in 8893
Photoelectronic Properties of 8902
Piezo-Optic and Electro-Optic Constants of 7369
Properties of 6039
Solid Solubility of AlP in 8161
Synthesis of 7874
Thermoluminescence in 6187, 8379
Thin Luminescent Films of 7894
Zinc Sulfide:
in Crystal Counters, Properties of 6967
Films, Evaporation of 6968
Preparation, Particle Growth during 6969
and Selenide Phosphors, Vanadium Activated 6461
Zinc Sulfide:Ag, Effect of CdS Addition in 6460
Zinc Sulfide-Cadmium Sulfide, Preparation of Solid Solutions of 6030
Zinc Sulfide:Cu,
Effect of CdS Addition in 6460
Electroluminescence in 8377
Infrared Emission in 8871
Light Stimulation of 7986
Zinc Sulfide:Cu, Fe, Photo-Dielectric Effect in 8890
Zinc Sulfide:In,
Effect of CdS Addition in 6460
Optical Properties of Luminescent 7991
Zinc Telluride, Optical and Photoelectric Properties of 7397
Zinc Telluride Layers,
Electrical Conductivity of 7392
Photoelectric Properties of 7392
Zinc Telluride-Cadmium Telluride Alloys, Solid Solution in 6624
Zincblende Structure, Surface Characteristics of III-V Intermetallic Compounds Having a 6340
Zirconium into Ni, Diffusion of 9181
Zirconium Carbide, Thermionic Emission of 9313
Zone:
Casting, Preparation of AlSb-GaSb Alloys by 6623
Equalization, Concentration Distribution in a Billet during 7866
Growth of Crystals Using an Arc Image Furnace, Floating 7265, 7266
Melting, Growth of GaAs 6342, 7431
Purification of:
SiI_4 6016, 6035
Te 7565
Recrystallization, Preparation of Ferroelectric Monocrystals by 6041
Refiner, Electron Beam 6305
Refining,
Continuous 7857
Growth of Peritectic Compounds Using 6015
Modified:
Boat for 8617
RF Coil to Facilitate 7264
Purification Factor Characterization of 7564
Vapor- 8616
Refining:
of GaAs 7576
of Metals 8194
Processes, Efficiency of 7248
of Si 8193

ANNUAL CUMULATIVE AUTHOR INDEX

Abarenkov, I.V. 8362
Abboud, F.L. 6861
Abdiukhanov, M.A. 7426
Abe, R. 8685
Abel, Jr. G.J. 8155
Abel, J.L. 9239
Abeles, B. 6726
Abraham, C. 7342
Abraham, G. 7485
Abraham, R.P. 6255
Abrahams, E. 7015
Abrahams, M.S. 7244, 7559, 8932
Abrahams, S.C. 6321
Abrams, H.J. 7515, 9133
Abrikosov, A. 8753
Achter, M.R. 9180
Adams, D.K. 7155
Adams, E.N. 6190, 7412
Adawi, I. 7304, 7924
Adcock, W.A. 8996
Addamiano, A. 6359, 6039, 8161
Adelson, E. 7337
Adirovich, E.I. 6224
Adlington, R.E. 6025
Adrian, F.J. 8593
Aerts, A.E. 6381, 8238, 8264, 8660, 8661, 8662
Agaev, Ya. 7938
Agakhanian, T.M. 8440
Aharoni, A. 6703, 6842, 7342, 9338
Ahearn, A.J. 8613
Ahlburg, H. 6184, 6459
Aisenberg, S. 6712
Aitchison, R.E. 8488
Akimchencko, I.P. 8199
Albers, Jr., W.A. 7267, 7947
Albert, W. 7273
Albin, J. 8093
Alder, B.J. 7378
Aldrich, R.W. 7103
Aleksandrov, K.S. 6043
Alekseevskii, N.E. 8286, 8289
Aléonard, R. 8338
Alexander, W. 9105
Alford, Jr., C.H. 6873
Alfrey, G.F. 6688, 8882, 8883
Alger, R.S. 8179
Allard, J.G. 6628
Allegretti, J.E. 7736
Allen, D.E. 6529, 7529
Allen, F. 7196
Allen, F.G. 8663
Allen, G. 9199
Allen, J.W. 6389, 7566, 8585
Allen, L.C. 8668
Allen, R.B. 7862
Allen, R.L. 7501
Allerton, G.L. 7615
Allgaier, R.S. 6413, 7849, 9298
Allington, R.W. 8529
Allison, H.W. 9181
Allred, W.P. 6319, 6362, 7419
Amar, H. 9328
Ambegaokar, V. 6074
Ambrosio, B.F. 8542
Amelinckx, S. 6631, 6937, 6938, 8598, 8603, 8610, 8650
Amirkhanova, D.Kh. 8933
Anderson, E.E. 6443, 6444, 8330, 9227
Anderson, G. 6480, 7249
Anderson, J.L. 6896
Anderson, J.R. 8545
Anderson, M.E. 7792
Anderson, P.W. 6694
Anderson, R.L. 6734, 6750, 8421
Anderson, T.N. 8462
Andrä, W. 8797
Andresen, H.G. 7364
Andreyev, V.S. 8098
Andrievskii, A.I. 6951
Andronik, I.K. 7285
Ansel, G. 7208
Ansley, W.G. 6758
Antell, G.R. 7882, 8203
Antoncik, E. 8392
Antonowicz, K. 7368
Aoki, Y. 8074
Aoyagi, K. 7390
Apfel, J.H. 9423
Apker, L. 7320
Apple, E.F. 6460, 8871, 9406
Arai, Y. 8048
Arajs, S. 7057, 9375
Arams, F.R. 8044, 9048
Arase, E.M. 8915
Arata, H. 9282
Arbell, H. 6187
Arbogast, C.L. 6210
Ard, Jr., W.B. 6166
Arend, H.T. 8691, 8854
Arkad'eva, E.N. 7391
Armstrong, D.B. 6800
Armstrong, L.D. 7091, 8975
Armstrong, M.E. 9111
Armstrong, R.A. 7970
Armstrong, R.W. 6954
Arnold, E. 6107
Arnold, Jr., G.W. 6376, 7853
Arnoldt, P. 7153
Arnott, R.J. 7575
Aronson, A.I. 9071
Arrott, A. 7036, 9336
Arsenault, W.R. 8542
Artamonov, O.M. 7678
Artman, J.O. 6163, 8831
Artman, R.A. 8926
Asada, T. 6056
Asano, S. 8385
Asanuma, M. 9340
Ascarelli, G. 7297
Aschner, J.F. 7422
Ashbel', N.I. 8500
Aspinall, D. 7186
Astrov, D.N. 8334, 8820
Atalla, M.M. 6751, 7276
Atkins, K.R. 7943
Atkinson, H.H. 9157
Atlas, L.M. 7553
Attic, F.H. 7502
Atwater, H.A. 9255
Auer, Jr., J.H. 9107
Auerbach, I.L. 8124, 8534, 8535
Augustine, F. 8190
Auld, B.A. 6792
Austin, A.E. 7337
Austin, I.G. 8271, 8397, 8912
Austin, W.E. 8146
Authier, A. 6630
Avakian, P. 6966, 7239
Aven, M. 6039
Averbach, B.L. 9162, 9198
Avinor, M. 6461, 8891, 9416
Avivi, P. 7353
Avramenko, V.P. 8815
Axelby, G.S. 9054
Axelrod, J.M. 7228
Axon, P.E. 8130
Ayres, W.P. 8100
Azároff, L.V. 7005, 7245

Baasch, T.L. 7721
Baba, H. 7562
Babbitt, R.W. 7275
Babuska, I. 9223
Bacchella, G.L. 9167
Bachmann, L. 8205
Bacon, R. 6633
Bady, I. 7045, 8812
Bagno, S. 7215, 8104
Bailey, Jr., C.M. 8554
Bailyn, M. 7299, 8266
Baird, J.R. 6547
Bakanowski, A.E. 6225
Baker, A.N. 6758
Baker, D.J. 7269
Baker, J. 6447, 8345
Baker, L.R. 8035
Baker, N. 9428
Baker, R.P. 7817
Baker, W.E. 6640, 6641, 8622
Balain, K.S. 6120, 9438
Balchan, A.S. 9394
Baldcock, G.S. 8114
Baldwin, Jr., J.A. 9038
Balicki, M. 7402
Balkanski, M. 6398
Ballard, S.S. 9433
Ballato, A.D. 6815
Ballentyne, D.W.G. 7062
Balluffi, R.W. 7241, 8594
Baltensperger, W. 8778
Baltzer, P.K. 6174, 9325
Banbury, P.C. 9319
Bancie-Grillot, M. 8888, 9413
Banewicz, J.J. 6427
Banks, E. 6974
Baranov, L.I. 8962
Baranskii, P.I. 8003, 8924
Barker, R.C. 7442
Barker, R.S. 8648
Barker, W.A. 8833
Barlow, H.E.N. 6601
Barlow, H.M. 6100, 8714
Barnard, R.D. 6079
Barnes, C.R. 6366
Barnes, J.F. 8713
Barnes, W.J. 7563
Barney, H.L. 8449
Barrack, C.M. 8033
Barrett, C.S. 8171
Barry, J.N. 7427
Barson, F. 6511, 8441
Barsukov, Yu.K. 8013
Bartels, B.E. 9025, 9026
Barter, L.D. 7810
Bartholomew, D.D. 7113
Bartlett, B.E. 8897
Barton, L.E. 6826, 8429
Baruch, P. 7208
Basinski, Z.S. 8412
Basov, N.G. 8452, 8470
Bassani, F. 7281
Batdorf, R.L. 6745
Bate, G. 6654
Bate, R.T. 6414, 6941, 7072, 9300
Bates, L.F. 6156, 9361
Batifol, E. 7568
Bauer, C.L. 9175
Bauminger, R. 7353
Baxter, P. 8254
Baynham, A.C. 8673
Bazhan, A.N. 8501
Beal, J.C. 6601
Beal, M.T. 8272
Beale, J.R.A. 8029
Bean, C.P. 7955, 9275, 9370
Beard, G.B. 9420
Beardsley, L.P. 6394
Beattie, A.R. 8697, 9254
Beauchamp, E.K. 8189
Beauchamp, K.G. 6834
Beaufoy, R. 8091
Beauzee, C. 7858
Becherer, H.K. 6510
Bechmann, R. 6815, 6816, 7369, 7730, 9443
Becker, J.A. 8633
Bedo, D.E. 7269
Beecroft, R.I. 9152
Beer, A.C. 8509, 9300
Beers, D.S. 6726
Behrndt, M.E. 6409
Bekey, G.A. 8547
Bell, H.V. 9105
Bell, J.S. 7197
Bell, N.W. 6295, 7483
Bell, R.L. 7690
Bell, R.O. 9363
Bello, P. 7455
Belov, K.P. 6428, 7960, 8303, 8763, 8943
Belov, V.F. 7960
Bemski, G. 6124, 8358
Benanti, M. 6778, 6779, 7109
Benbow, T.G. 7185
Bender, B.G. 6374, 6375
Benedek, G.B. 8808
Benjamin, R. 6778, 7109
Bennett, A.I. 6349, 7891, 7892
Bennett, L.H. 7352, 7973
Bennion, D.R. 6799
Benson, K.E. 7262
Bengtivegna, M.J. 8975
Benz, W. 6254
Ben-Zvi, A. 6209
Bereskin, A.B. 6275
Berestovskü, G.N. 7428
Berger, H. 8143
Bergeron, C.J. 9296
Bergman, R.H. 7178
Bergman, R.S. 7055
Berkowitz, A.E. 9327
Berlincourt, D.A. 6532, 8258
Berman, I. 7090
Berman, L.S. 8140
Berman, R. 7073
Bernard, M. 6007
Bernard, W. 7021
Bernheim, R.A. 7974
Bernstein, H. 7862
Bernstein, L. 6374, 6375
Berreman, D.W. 9160
Berry, C.R. 8631
Berss, R.R. 8934
Bertolone, N.P. 6034
Bertolotti, M. 9262
Berz, F. 6420, 8773
Bessen, L.V. 7781
Bessey, W.H. 9246
Betts, D.D. 6004
Bhatia, A.B. 6211
Bhide, V.G. 8689, 8690
Bickart, T.A. 6604
Bickford, Jr., L.R. 9353
Bickley, J. 6536
Bierstedt, P.E. 7621
Bikker, P. 6856
Bilaniuk, O.M. 8574
Billings, A.R. 6903
Billings, T.E. 9127
Billington, C. 7065, 7066, 7067, 7068
Biondi, M.A. 6695, 6696
Biorci, G. 9362
Bir, G.L. 7912
Birkhol, U. 8002
Birks, L.S. 9180
Birman, J.L. 6456
Birnbaum, M. 6906
Birss, R.R. 8775, 8776
Bissell, H.M. 7748
Biswas, A.B. 8590
Bither, T.A. 7033
Bittmann, C.A. 6513, 7422
Bjorkstam, J.L. 9234, 9235
Blackmore, R.W. 8154
Blair, R.R. 6881, 7083
Blaise, J. 8105
Blakemore, J.S. 6096, 6178, 6392, 6394, 6936
Blakeslee, A.E. 6332
Blanc, J. 6105
Blancheville, P. 8110
Blank, J.M. 7122
Blankenship, J.L. 6301, 6302, 6911
Blatt, F.J. 8407
Blatt, J.M. 7624
Blaugher, R.D. 8758
Blecher, F.H. 6820
Bleckner, E. 6845
Blet, G. 7716
Blewitt, T.H. 8651
Blickensderfer, J.A. 8541
Blinc, R. 9233
Bloembergen, N. 7350, 7720, 7972
Blok, J. 6468, 8453, 9022, 9256
Bloom, M. 6265
Blue, M.D. 6205
Blum, S. 6956
Blumberg, R.H. 6118, 6409
Blumberg, W.E. 7298, 7664, 7666, 7967, 8347, 9382
Bobeck, A.H. 9053
Bobisch, P. 7752
Bockemuehl, R.R. 7070
Bode, K. 7506
Bodó, Z. 6093, 8696, 8700
Boelger, B. 7662
Boesch, F.T. 8053
Boff, A.F. 6496
Bogachev, I.N. 8167
Bogdanov, S.V. 7599
Bogle, A.G. 6256
Bogusch, R. 7191
Bohrer, J.J. 6821
Bohun, A. 8378, 8885
Boiko, I.I. 7935, 9266
Bok, J. 6388
Bolef, D.I. 8004, 9148, 9447
Bölger, B. 6247, 6448
Bolling, G.F. 6957, 8632
Boltaks, B.I. 6069
Bömmel, H.E. 6147, 6212, 7382, 8941, 9451
Bonnanno, J.L. 8992
Bonch-Bruevich, V.L. 6092, 6379, 9264
Bond, W.L. 7246, 8170
Bondar, V.V. 8289
Bonfield, W. 7690
Bonfiglioli, G. 6644
Bonn, T.H. 7747, 8536
Bonner, A.L. 7167
Booker, Jr., C.A. 6847
Booker, G.R. 6963
Boorse, H.A. 8399
Booy, H.C. 8453
Bopp, C.C. 9104
Borkowski, C.J. 6302, 6911
Borovskii, I.B. 8371
Bose, M. 6690, 8735
Bossard, B.B. 8069
Bourke, R.C. 6363
Bousquet, L. 8112
Bouwknegt, A. 8420
Bowers, K.D. 8353
Bowers, R. 7324, 7400
Bowlden, H.J. 7909
Bowyer, C.S. 6088
Boyd, C.R. 7473, 7489
Boyd, D.R. 6667, 6780
Boyd, E.L. 6430, 7956
Boyet, H. 8041
Boyle, A.J.F. 7643
Boyle, W.S. 7372
Bozorth, R.M. 7625, 7946, 8163, 9372
Bradley, A. 9230
Bradley, E.M. 6887, 7190, 8795
Bradley, W.E. 8976, 9014
Bradmiller, R.W. 9089
Bradshaw, S.E. 6027
Brady, L.E. 9421, 9422
Bragg, R.H. 7245
Braginski, A. 8634
Brailsford, A.D. 7372, 9287

ANNUAL CUMULATIVE AUTHOR INDEX

Brand, Jr., F.A. 6778, 6779, 7109, 8260, 9428
Brandt, N.B. 7910
Braner, A.A. 6208, 6209
Brankoff, K. 7826
Brannon, P. 6234
Branwood, A. 8682
Brard, P. 8465
Braun, J.H. 6958
Braun, P.G. 7651
Braunstein, R. 8932
Bray, P.J. 6417, 8836, 9170
Brazda, J. 9149
Brebrick, R.F. 7849, 8168
Bregman, F. 7213
Bremer, J.W. 6808, 7448
Brenet, J. 6687
Brennan, D. 9192
Brennemann, A.E. 6410, 8477
Bresler, A.D. 6249
Bretemps, F.R. 7525
Brezina, B. 8691, 9240
Brice, J.C. 9273
Briggs, G.R. 6244
Bright, R.L. 8522
Brini, D. 7801, 8022
Brissot, J.J. 7846, 8431
Broadbent, K.D. 6594, 6888, 6891
Broadley, Jr., H.R. 9044
Brochocki, A. 8208
Brock, E.G. 6167
Brock, G.E. 7371
Brockhouse, B.N. 7332, 9217
Brockus, C.G. 6675
Broersma, S. 7395
Brog, K.C. 6597, 7200
Bron, W.E. 7555, 8859, 9395
Brooks, E.J. 9180
Brooks, H. 6075, 7010, 8672
Broom, R.F. 6591, 6697
Brophy, J.E. 6434
Brophy, J.J. 6095, 6192, 6418, 6419, 7022, 7319, 7951, 8702, 9261, 9309
Brophy, V.A. 7874
Bross, H. 7905
Brotzman, J. 8575
Broudy, R.M. 6347, 7914
Brouillette, J.W. 7103
Brout, R. 8782, 8785
Brown, A.E. 8410
Brown, A.L. 7301
Brown, C.S. 7884, 8944
Brown, D.R. 8540
Brown, E. 7852
Brown, F.C. 6106, 7610
Brown, J. 6100, 8714
Brown, J.S. 7127
Brown, L. 7954
Brown, P.J. 8156
Brown, S.C. 7297
Brown, T.H. 9138
Brown, T.M. 6996
Brown, Jr., W.F. 9186
Brown, W.L. 6913
Brownlow, J.M. 6801
Brownson, J.W. 6947
Broz, J. 8584
Brubaker, J.F. 7515, 9133
Bruce, G.D. 8128
Bruck, G. 8145
Bruin, F. 7827
Brunner, J. 6698
Bruns, R.A. 8491
Bruynooghe, W.M. 6477
Bube, R.H. 6721, 7069, 8591, 8900, 9257
Buchman, W.W. 6727
Buck, D.A. 6592
Budnick, J.I. 7352, 7623, 7973, 8743
Budylin, B.V. 7235
Buehler, E. 6322
Buehler, G.V. 7723
Buelow, F.K. 6575, 7177
Buffler, C.R. 6436
Bullough, R. 7573, 8202
Bunbury, D.St.P. 7643
Bura, P. 7475
Burdukov, Yu.M. 8419
Burgess, R.E. 6731
Burke, Jr., J.R. 6413
Burke, R.L. 6818
Burley, D.M. 8307
Burnham, D.C. 7610
Burns, F.P. 8449
Burnysheva, A.N. 8809
Burrus, C.A. 7150, 8090
Burton, L.W. 8991
Busch, G. 7619, 8586, 8653, 8824
Buschert, R.C. 7707
Busen, K. 6331
Bussard, E.J.H. 9077
Bussey, H.E. 8298
Butcher, P.N. 8043
Butler, K.H. 7925
Butler, S.A. 6572, 7179
Butler, Jr., T.W. 7726
Button, K.J. 6065
Bylander, E.G. 6786
Byrnes, J.J. 8194

Cable, J.W. 8821
Cagle, W.B. 7797
Cahn, J.W. 7875, 8802
Caille, L. 8428
Caldwell, P.N. 8988
Cali, J.P. 6942, 6943
Callaway, J. 7001, 7074, 9207
Callen, E.R. 7644
Callen, H.B. 7021, 7644, 7650
Calvin, M. 6719, 7992
Cambornac, M. 8557
Campos, F.P. 6153
Camras, M. 9120
Cannon, W.D. 7789
Cape, J. 8857
Capone, B.R. 7277
Caravel, A. 7816
Carbonel, M. 6229
Carbrey, R.L. 7786
Cardona, M. 6075, 7010, 7913, 8672
Carey, R. 8324, 9361
Carley, D.R. 6757
Carlin, H.J. 7740, 8050
Carlsen, R.A. 7798
Carlson, A. 6962
Carlson, A.I. 6474
Carlson, A.W. 7084
Carlson, R.D. 6281
Carlson, R.O. 7863
Carman, Jr., J.N. 8952, 8998
Carr, Jr., W.J. 6135
Carreon, D.G. 6863
Carroll, J.E. 8485
Carroll, P. 6948
Carruthers, P. 6200
Carson, D.N. 6274
Carson, J.W. 6446
Carstedt, V.E. 7818
Carter, D.L. 6165, 6713, 8349
Carter, I.P.V. 6590, 6885, 7809
Carter, J.L. 7724
Carter, Jr., P.S. 6791
Carter. W.S. 7963
Caspari, M.E. 6998
Caspers, W.J. 7658, 7659, 7660
Cassignol, E. 7452
Castle, Jr., J.G. 8344, 8468
Castro, P.S. 7123, 7131, 7722
Castro, R.L. 7618
Caswell, D. 9035
Caswell, H.L. 6345, 8747
Catalano, S.B. 7885
Catlin, A. 7079
Catton, W.T. 6850
Cave, E.F. 9440
Caywood, Jr., W.P. 7445
Celli, V. 7281
Cense, A. 6856
Cerofolini, G.F. 7788
Chaldyshev, V.A. 8656
Chalmers, B. 6323
Chambre, P.L. 9431
Champion, F.C. 6113
Champlin, K.S. 6126, 6699, 7629
Champness, C.H. 9297
Chandler, J.A. 6736
Chandrasekhar, B.S. 7405
Chang, H. 6797, 6804
Chang, H.C. 6037, 7101, 7433
Chang, K.K.N. 6261, 6561, 6831, 8061, 8467
Chang, T.T. 9160
Chang, W.S.C. 8473
Chang, Y.F. 8014
Chapman, R. 9065
Charap, S.H. 7645
Chardack, W.W. 6849
Charters, M.L. 6084
Chasmar, R.P. 8760
Chaudhuri, A.R. 8187
Chechernikov, V.I. 8825
Chen, W.H. 7797
Chen, Z.-R. 8817
Chennette, E.R. 6231
Cherepanov, V.I. 6176
Chernaya, N.S. 6128, 9318
Chernikova, L.A. 9288
Cherry, L.V. 7259, 7349
Cherry, W.H. 7945
Chesson, F.W. 6846
Chester, P.F. 6170, 8344, 8468
Chetkin, M.V. 8396
Chevillot, J.-P. 6687
Chevychelov, A.D. 6483
Chick, B. 6480
Chien, R.T. 7120, 7767
Chih-ch'ao, L. 7937
Childs, C.B. 7557
Chipman, D.R. 9158
Chirgwin, K.M. 7519
Chirkin, L.K. 7108
Chirlian, P.M. 7739
Chisholm, H. 8561
Chizhikov, D.M. 7547
Cholet, P.H. 6782
Chougnet, P. 8153
Chow, W.F. 6557, 6870, 7796, 9060
Chow, Y. 7452
Choyke, W.J. 6453
Chrenko, R.M. 6050
Christensen, H. 7268
Chynoweth, A.G. 6593, 6701, 6738, 6745, 6746, 6747, 7291, 7633, 7676, 8246, 8278, 9239
Cibelius, Jr., C.A. 8556
Circuit, M.P. 6285
Claassen, R.S. 7410
Clarebrough, L.M. 8600
Clark, C.B. 7432
Clark, J.J. 9342
Clark, O.M. 7416
Claussen, W.F. 7848
Claytor, R.N. 6724
Cleek, G.W. 9449
Cleiren, A.P. 9414, 9415
Cleland, J.W. 7929
Clemens, P.L. 6844
Clemer, P.J. 7439
Clevenger, Jr., T.R. 6155
Cloot, P.L. 6278
Cloud, W.H. 7033, 7337
Clow, H. 6156
Cluley, H.J. 7687
Cluwen, J.M. 9103
Cmolik, C. 8258
Coale, F.S. 6530
Coates, C.L. 6568
Cobbold, R.S.C. 6507
Cocca, U. 9023
Cochran, J.F. 6116
Cochran, W.T. 6865, 9217
Cody, G.D. 6726
Coghill, H.D. 6968
Cohen, E. 7105, 8760
Cohen, J. 7595
Cohen, M.H. 7591, 7606, 8413
Cohen, M.L. 6811, 7446
Cohen, M.S. 6973, 8796, 9355
Cohen, S.G. 7353
Colburn, J. 6512
Coleman, D.R. 6497
Coleman, P.D. 7921
Coleman, R.V. 9191
Coles, B.R. 7036
Colin, R. 8112
Collins, D.A. 7007
Collins, D.J. 6541
Collins, T. 8812
Coltman, R.R. 8651
Colvin, R.V. 7016
Colwell, J.F. 8236
Combs, C.M. 8631
Comley, W. 7513
Compton, D.M.J. 6640, 6641, 8622
Compton, W.D. 6376
Comstock, R.L. 7112
Conger, R.L. 9349
Conn, J.B. 7077
Connell, L.J.C. 8424
Connolly, T.J. 9435
Conrad, G. 8061
Conrad, II, G.P. 9185
Conwell, E.M. 6109, 7301
Cook, Jr., C.R. 7802
Cook, J.S. 6015, 8244
Cooke, I. 8883
Cooper, B.R. 7047
Cooper, H.W. 6326
Cooper, J.N. 6813
Cooper, R. 7594
Cooper, R.W. 7640
Coopersmith, M. 8785
Coovert, R.E. 8293
Coppen, P.J. 6752
Corbett, J.W. 6050, 6051
Corbyn, D.B. 6540
Corciovei, A. 9329
Corelli, J.C. 8927
Coren, R.L. 7044, 8322
Corenzwit, E. 7313, 8744
Corliss, L.M. 9366
Cornelison, B. 9011
Corner, W.D. 8777
Cornish, A.J. 7012
Correlli, J.C. 7402, 7403
Cosenza, F. 8104
Cossee, P. 8337
Cottini, C. 7928
Cottrell, A.H. 7903
Coufova, P. 8854
Covert, P.W. 9140
Cowan, J.A. 8838
Cowles, L.E.J. 7688
Cox, D.L. 9009
Cox, E.L. 7794
Cox, L.G. 8151
Crane, H.D. 7775
Craven, J.H. 6267
Crawford, Jr., J.H. 9403
Crawford, Jr., J.N. 8177
Crecraft, H.E. 7495
Critchlow, D.L. 6572, 7179
Crittenden, Jr., E.C. 6813
Crocker, A.J. 8641
Croft, W.J. 6141, 6976, 9184
Croll, I.M. 6994
Cromack, J. 8473
Crone, R.L. 8949
Crooks, R.K. 8143
Crosby, D.R. 7180
Cross, L.G. 9047
Crouch, W.M. 7203
Crow, R.P. 9091
Crowley, T.H. 6800
Crownover, J.W. 9143
Crump, B. 7437
Cruz, Jr., J.B. 8481
Csavinszky, P. 7613
Cuccia, C.L. 6831
Cuevas, M. 9285
Culligan, G. 7210
Cunnell, F.A. 6356, 7572, 7576, 8623
Cunningham, J.A. 7173
Cunningham, Jr., J.R. 6443, 6444, 8330
Currie, M.R. 7138
Curry, M.A. 8274
Curtain, C.C. 8147
Curtis, Jr., O.L. 7929
Cushman, N. 7441
Cutler, I.B. 8636
Cutler, M. 6218
Cuypers, R. 8650
Czerlinsky, E.R. 6645, 8329
Czyzak, S.J. 6011, 6967, 7880

Dabbs, J.W.T. 6303, 6908
Dacey, G.C. 6486, 6745
Dahlin, R.K. 9076
Dahlke, V.W. 8498
Dally, L. 7477
Dalven, R. 8865
Damask, A.C. 7240
Damle, R.V. 8689, 8690
Damon, D.H. 7325
Damon, R.W. 6245, 9323
Daniel-Szabó, J. 8316
Daniels, J.J. 7968
Daniels, J.M. 6162
Daniels, R.E. 7774
Daniels, W.B. 9444
Danielson, G.C. 6199, 7932
Danilov, V.N. 8180
Darlington, S. 8492
Das, M.B. 6761
D'Asaro, L.A. 6328
Dash, W.C. 7242, 7243, 7558, 8211
Daskam, S.W. 6757
Date, M. 8357
Dauenbaugh, C.E. 9312
Davey, J.E. 7257
Davidson, Jr., W.F. 7718
Davies, D.M. 7501
Davies, I.F. 6598, 7820
Davies, L.W. 7248
Davis, D.D. 7625, 7946, 8163
Davis, H.L. 7032
Davis, Jr., L. 6243, 6794
Davis, P.W. 8870
Davis, R.E. 6513, 7703
Davisson, J.W. 7255, 7256
Daw, A.N. 6228
Dayal, B. 8665
Dean, P.J. 6113
Dearborn, E.F. 8218
DeBitetto, D.J. 8812
DeBlois, R.W. 9275
DeBolt, H.E. 6300, 7202
Debye, P.P. 6064
Deetscreek, V.D. 6972

ANNUAL CUMULATIVE AUTHOR INDEX

DeGennes, P.G. 6705, 8332
deGraaf, A.M. 8778
DeGrasse, R.W. 9109
Degtyarev, I.F. 8805
de Hoog, F.J. 8453
de Jager, J.T. 8070
Dejardin, G. 6191
Dekeyser, W. 8610
Dekker, A.T. 9315
DeLano, Jr., R.B. 6410
de La Rue, R.E. 6044
Delavignette, P. 6938, 8598, 8603
Della Torre, E. 6250
DeLoach, B.C. 8071
De Maria, G. 6929
Demars, G.A. 6421, 8774, 8845
DeMars, R.D. 6993
Dement'yev, Ye.P. 9063
Denton, R.L. 9148
Denton, R.T. 7476, 8072
Denz, A.R. 7499
Dermatis, S.N. 6964
de Ronde, F.C. 8006
Desai, U.D. 7211
DeSautels, A.N. 8493
Deschamps, R. 8028
Desoer, C.A. 7457
Desorbo, W. 8287, 9166
Desvignes, F. 6451, 8431
Detwiler, D.P. 6081
Deutsch, S. 7135
Deutschbein, O. 6007
Devlin, G.E. 7313
Devor, D. 7725
Devyatkova, E.D. 7682, 7683
Dewald, J.F. 8240
De Wijn, H.W. 7490
DeWolf, N. 7709
Dexter, D.L. 6473, 9389
Dexter, R.N. 8769
Dhawan, S.K. 6274
Diamond, H. 6076, 6077, 7593
Diehl, M.H. 7504
Diemer, G. 6518, 6236, 7145
Dienes, G.J. 7240, 7861
Diesel, T.J. 6402, 6404, 7316, 8256
Dietrich, A.F. 6907, 8516
Dietrich, W. 6579
Dietz, R.E. 7383, 9337
Dikhoff, J.A.M. 6648
Dill, H.G. 6817
Dillon, Jr., J.A. 6048, 6049, 6440, 7053, 7347
Dirnbach, P.H. 6866
Dismukes, J.P. 8459
Ditzenberger, J.A. 6946, 7233, 8762
Diven, L. 7791
Dobrovol'skii, V.N. 9268
Docherty, I.S. 8488
Dodd, D.M. 8364
Dodson, G.A. 6730
Dolce, A. 8259
Dolecek, R.L. 7628
Doleiden, F.H. 9278
Dolejsi, J. 8378
Domenicali, C.A. 8920
Domenico, R.J. 6576
Dominick, F.J. 8045
Donahoe, F.J. 8408
Donahue, D.J. 6327
Donovan, P.F. 6913, 8572
Donovan, R. 7943
Dooley, J.A. 6508
Dorain, P.B. 7058
Dorda, G. 7321
Doronkin, E.F. 8084
Dorosheski, G. 9274
Dorsi, D. 8194
Doucette, E.I. 6326, 8417
Doucette, H.W. 6326
Douglass, R.L. 7333
Doviak, R.J. 7699
Downey, E.J. 8051
Downs, R. 7117
Doyle, E.J. 7505
Doyle, W.T. 8904
Drabble, J.R. 6478, 9437
Dransfeld, K. 6147, 6212, 7382, 8941, 9451
Dresselhaus, G. 7314, 8279, 8751, 8752
Dresselhaus, M.S. 7314, 8279, 8751, 8752
Drewes, G.W.J. 7652
Drickamer, H.G. 6457, 7854, 7915, 8858, 9393, 9394
Driol, A. 8022
Drobchenko, L.D. 8788
Drougard, M.E. 8251, 9246
Drowart, J. 6929
Dryden, J.S. 8244
D'Stefan, D.J. 6665
Dubinin, V.G. 8878, 8879
Dubrovskii, G.B. 7717
Dudkin, L.D. 7584
Duffek, E.F. 7432
Duffin, M.V. 6866
Duga, J.J. 6632, 8765
Duinker, S. 7171, 8040
Dulin, F.H. 8580
Dumaire, M. 8119
Dumke, W.P. 8716
Dunlap, Jr., W.C. 7887
Dunn, C.G. 9334
Dunne, T.G. 7292
Dunnet, W.J. 6876
Dunthorne, D. 6598
du Pré, F.K. 8812
Dupuis, M. 8398
Duraffourg, G. 7568
Dusek, J. 9277
Dutton, D. 6197
Duwez, P. 6622
Dvir, M. 7667
Dwight, K. 9357
Dwork, L.E. 9093
Dyett, M.J. 8441
Dymanus, A. 7046, 8420
Dzyaloshinskii, I.E. 8333

Eagles, D.M. 7377, 8585
Eannarino, G. 8984
Earle, J. 6869
Early, J.M. 6569
Easley, J.W. 6508, 7083
Ebhardt, R. 7080
Eck, T.G. 8849
Eckert, Jr., J.P. 7747
Eckhardt, W. 6570
Eckhart, G. 6008
Economos, G. 6155
Edel'shtein, V.M. 7547
Edens, G.E. 8567
Edington, J.M. 7830
Edmond, J.T. 8726
Edmund, J.T. 6356, 6669
Edwards, C. 7643
Edwards, D.B.G. 7186, 7189
Edwards, D.F. 6198, 7370
Edwards, H.H. 6808, 7448
Edwards, P.L. 6045, 6157
Edwards, W.D. 6647
Effer, D. 7882
Efremov, N. 6316
Eggers, F.G. 7169
Ehrenreich, H. 7282
Eichbaum, B.R. 9351
Eichbaum, R. 6803
Einspruch, N.G. 7691
Eisinger, J. 7298, 8347, 9427
Eisler, H. 8515
Ekiss, J.A. 6263
Ekstrom, L. 7244, 7559
Elco, R. 8096
Elleman, D.D. 8755
Elliott, J.F. 8551, 9439
Elliott, N. 9366
Elliott, R.J. 7384, 7634, 8265, 8306
Ellis, Jr., R.C. 6326, 6990
Ellsworth, R. 6839, 8561
Elmgren, J.A. 7995
Emes, H.R. 7738
Emile, Jr., P. 7825
Emms, E.T. 7759
Enck, F.D. 8937
Endo, I. 8092
Englebart, D.C. 6539
English, A.C. 8191
Ensley, D. 6290
Enz, U. 7031
Eppler, R.A. 7854, 8858, 9393
Epstein, A. 6424
Epstein, M. 9018, 9146
Erb, T. 9073
Erdman, D.C. 9088
Eriksen, B.K. 7195
Eriksen, W.T. 6459, 6184
Erlbach, E. 6061, 6408
Ernsberger, G.W. 9130
Erokhina, N.A. 6520
Ertel, A. 7092
Esaki, L. 6484, 6485, 8955
Eshbach, J.R. 6245, 9323
Esseling, L.A.L. 8526
Esveldt, C.J. 6585
Etzel, H.W. 6628, 9169
Euler, F. 6645
Evans, J.A. 7323
Evans, J.F. 6558
Evans, R. 8561
Ewald, A.W. 6930
Ezhik, I.I. 8380, 8886

Fabri, G. 7928
Fagen, E.A. 6689
Falicov, L.M. 7591
Falk, D.S. 8243
Falk, R.B. 9332
Fan, H.Y. 8862, 8863, 9400
Fang, P.H. 6082, 6086, 6160
Fara, H. 8594
Farach, H.A. 6162
Faria, S. 6969
Farnell, G.W. 9222
Farnsworth, H.E. 7870
Farr, J.D. 9313
Farrell, L.B. 6931
Fatehally, R.A. 9206
Fathauer, G.H. 7821
Fatuzzo, E. 7598, 8253, 9242
Faulkner, A.H. 9078
Faust, Jr., J.W. 6348, 6351, 6352, 6954, 6964, 6989, 7888, 7889, 7890, 7893, 8188, 8639
Favre, R. 7764
Favro, L.D. 8972
Feber, G. 8359
Fedorov, V.B. 8339
Fedorus, B.A. 7310
Feher, G. 6062, 8706
Fein, H. 6851
Feiner, A. 6246
Feinstein, S. 7808
Feist, W.M. 7760
Feldman, G. 6042, 6053
Feldman, M. 7532
Feldmann, W.L. 7291
Felker, J.H. 8492
Feller, A. 6560
Felmly, R.A. 6537
Feltin'sh, I.A. 7942
Ferro, A. 6644, 9362
Feuerstein, W.J. 6748
Feuillade, G. 6636
Fiedler, H.C. 9344
Field, W.G. 8329
Figielski, T. 6073
Filberich, L. 9131
Filimonov, A.A. 6089
Finch, C.B. 8158
Fine, M.E. 6930
Finegold, L. 8011
Finkel, L. 7480
Finkelstein, M.B. 8527
Finlayson, D.M. 7980
Finn, M.C. 6339
Finnemore, D.K. 8284, 8748
Firestone, R.F. 7553
Fisch, E.A. 6568, 7191
Fischer, G. 8759
Fischer, R.F. 9053
Fischer, T.L. 6852
Fischler, A.S. 6121, 7027
Fishbein, W. 8069
Fisher, J.C. 8280
Fisher, S.T. 6832, 8102
Fitch, C.J. 6584
Fitzgerald, P.M. 6843
Flairty, C.W. 7773
Flaschen, S.S. 6773, 8985
Fleck, Jr., P.L. 6270
Fletcher, P.C. 7330, 9363
Fletcher, R.C. 8328
Flicker, H. 7272
Flinn, P.A. 7406
Flint, P.S. 6495
Flippen, R.B. 8819
Florio, J.V. 8678
Floyd, Jr., A.L. 9029
Fochs, P.D. 6961
Fock, M.V. 7986
Fok, M.N. 8881
Folberth, O.G. 8654, 8658
Folen, V.J. 6140
Follett, W.H. 7832
Fomin, N.V. 7374
Foner, S. 7359, 9049
Foreman, Jr., M.B. 8572
Forgacs, R.L. 7531
Forman, R. 6422
Forrest, M.L.N. 8439
Forst, J.J. 6534, 6814
Forstat, H. 6158, 6708, 8401
Forster, J.H. 6225
Foster, E.L. 7073
Foster, L.M. 6928
Fotland, R.A. 6978, 7193, 8387
Fousek, J. 9240
Fowler, Jr., C.A. 7034
Fox, A.G. 8042, 8475
Foy, P.W. 6745
Francis, A.B. 6474
Francois, M. 6343
Frank, C. 8478
Frank, F.C. 6984
Frank, R.C. 7250, 8210
Frankel, D.R. 7322, 8295, 8710
Franklin, D.P. 6283
Franks, A. 9163
Franks, L.E. 6563
Frauenfelder, H. 6116
Fray, S.J. 7673
Frazer, B.C. 6704
Fredericks, W.J. 7985
Frederikse, H.P.R. 7309, 8766
Freedman, G. 6770
Freedman, J.F. 6430
Freeman, A.J. 7638, 7926
Freeman, H. 8518
Frei, A.H. 8297
Frei, E.H. 6842, 7904, 9338
Freitas, L.G. 7897
Fridrikhov, S.A. 8300
Friedberg, S.A. 6148, 8819
Friedland, S.S. 6607, 6910, 8569, 8570, 8571
Friedman, A.N. 6383, 8727
Friedman, E. 7365, 8832
Friedman, H.D. 9194
Fritsche, H. 9285
Fritts, R.W. 6238, 9034
Fritz, J.F. 9342
Fritzsche, H. 7003, 7614
Froggatt, R.J. 8135
Frolov, V.N. 7147
Frood, D.G.H. 8721
Frosch, G.J. 6358
Frost, E. 8069
Frost, R.T. 7402, 7403, 8927
Frost, W.T. 7793
Fryberger, D. 9146
Fryer, E.M. 7034
Fu-Chouh, Pu. 8780
Fujimoto, F. 7824
Fujimura, Y. 6836
Fujita, I. 8868
Fukui, H. 8012
Fuller, C.S. 6338, 9006, 9278
Fuller, H.W. 7038, 7345
Fuller, W.D. 7131
Fullwood, R. 7207
Fumi, F.G. 6382
Furdyna, J.K. 7395
Furuichi, J. 8684
Furukawa, Y. 8386, 8418, 8957, 8958
Furuoya, T. 6010, 6012
Fuschillo, N. 9155
Fuselier, C.R. 7423

Gaddy, O.L. 7496
Gaertner, W.W. 6479, 8009
Gage, A.A. 6849
Gage, D.S. 8460
Galavanov, V.V. 6520
Galejs, J. 7762
Galindo, F.A. 7487
Galkin, G.N. 6521, 9263
Galkina, O.S. 9288
Galt, J.K. 7952
Galvin, T.J. 7482
Gaman, V.I. 8966
Ganesan, S. 8692
Garber, M. 6158, 8314, 8407
Garber, R.I. 8602
Gardner, L.B. 6880
Garfunkel, M.P. 6695, 6696
Garland, C.W. 9446
Garlick, G.F.J. 9206
Garrett, C.G.B. 6251, 6980
Garrison, J.L. 7167
Garstens, M.A. 9046
Garver, R.V. 6216, 6217
Garwin, R.L. 6061, 6408
Gashurov, G. 6030
Gassmann, G.G. 8514
Gatehouse, R.N.B. 6867
Gatos, H.C. 6026, 6340, 6369, 6371, 6660, 6983, 8209, 8234, 8640

Gatti, E. 7928
Gauvin, M. 8558
Gayek, H.W. 7517
Gazza, G.E. 6663
Gebbie, H.A. 8271
Gee, A. 8884
Geesner, C.R. 6366
Geil, Jr., P.H. 9188
Geist, D. 6425, 8848
Geiszler, T.D. 6527
Gel', E.P. 8178
Geller, S. 6159, 6646, 7340, 8163
Gelles, I.L. 7965
Gemperle, R. 7957
Genco, J.I. 6360
Gennon, S. 8059
Genser, M. 7419
Georgobiani, A.N. 8881
Gerber, E.A. 8047
Gere, E.A. 8359
Gergely, Gy. 8730
Gerlach, L. 6330
Germagnoli, E. 7928, 9167
Gerritsen, A.N. 7325
Gerritsen, H.J. 6806, 7975, 8474
Gersdorf, R. 8302
Gershenzon, M. 6358, 6500
Gerson, R. 6085, 7603, 8414, 9228
Gerthsen, P. 7206
Geschwind, S. 8350
Geusic, J.E. 8342
Geyling, F.T. 6534
Ghausi, M.S. 7742
Giacalone, J.J. 8929
Giacoletto, L.J. 6490, 6505
Giaever, I. 7627, 8749
Gianino, P.D. 7277, 8045
Giannelli, G. 7415
Gianola, U.F. 6800
Gibbons, J.F. 8437
Gibbons, P.E. 7528
Gibbs, D.F. 6358
Gibbs, P. 8183
Gibbs, W.E.K. 8560
Gibson, A.F. 8673
Gibson, J.B. 6997
Giedd, G.R. 6409
Gilbert, C.P. 6596
Gill, J.C. 7971
Gilleo, M.A. 6159, 8791
Gillett, C.M. 7323, 8725
Gilman, J.J. 6999, 7694, 7856, 8185, 8186, 9173
Gilmartin, M.J. 6279
Gilsing, J.A.A. 7206
Gilson, P.R. 7810
Gindin, I.A. 8602
Ginsberg, D.M. 8853
Ginther, R.J. 7502
Ginzburg, N.I. 8285
Giordmaine, J.A. 7655
Gippius, A.A. 8373
Giraudier, L. 7577
Girifalco, L.A. 7859
Githens, J.A. 6279
Gittinger, N.C. 7140
Gittleman, J.I. 7945
Givens, M.P. 9388
Gjevre, J.A. 8411
Glackin, R.N. 9101
Glaister, R.M. 7548, 8677
Glang, R. 8201, 8444
Glassbrenner, C. 7071
Gleason, F.R. 6149
Glendinning, W.B. 7434
Glicksman, M. 7934
Gliki, N.V. 7876
Glover, A.C. 6287
Glover, III, R.E. 8282
Glucharoff, T. 6596
Gluck, S.E. 8519
Gobeli, G.W. 8663, 9400
Goering, H.L. 6361, 6623, 6965
Goetzberger, A. 6754, 7089
Goff, J.F. 7398
Goggin, P.R. 7583
Goland, A.N. 6997, 7280, 8926
Gold, L. 7564
Gold, R.D. 7698
Goldman, A. 6858
Goldman, M.V. 6301
Goldring, G. 6977
Goldsborough, J.P. 6172, 6901
Goldsmith, G.J. 6531
Goldstein, B. 7252, 7253, 7865
Goldstein, I. 8060, 8075
Goldstein, Y. 9213
Goldstick, G.H. 7761
Gomi, Y. 8803
Gooch, C.H. 7572, 8623
Gooch, G.M. 7116
Good, Jr., R.H. 7932
Goodall, W.M. 6907, 8516
Goodman, A.M. 6535, 7025
Goodman, B.B. 6692
Goodman, C.H.L. 6768, 8169
Goodman, G. 8252
Goodrich, H.C. 8527
Goodwin, D.W. 8698
Goodwin, F.E. 6273
Goorissen, J. 6024, 7261, 8193
Gorban', I.S. 8369, 8370
Gordeev, G.V. 7315
Gordon, B.M. 8549
Gordon, G.E. 6915
Gordon, J.P. 6449
Gordon, R.B. 9175
Gordon, W.L. 8849
Gor'kov, L.P. 8741, 8745, 8753
Gorshkov, M.M. 8373
Gorsuch, P.D. 9176
Gorter, C.J. 7962
Gorter, E.W. 6585
Gorton, H.C. 6499, 8016, 8624, 8872
Gosar, P. 9426
Goss, A.J. 6025
Gossard, A.C. 6146
Gossick, B.R. 6214, 6515
Goto, E. 6872, 8122
Goto, M. 8321
Gottlieb, P. 6548, 7049
Gould, R.W. 7138
Goulding, F.S. 6835, 6905
Gourary, B.S. 7930, 8263, 8593
Gow, J. 6511
Grabner, L. 6415
Grabowski, K.P. 7139
Graham, Jr., C.D. 7041
Graham, J. 7850
Grainger, R.J. 8569, 8571
Gran, B.E. 7043
Granata, S. 9167
Granath, J.A. 7792
Grannemann, W.W. 6230, 6290, 8103
Granville, J.W. 8673
Gray, C.R. 6860, 6862
Gray, P.E. 7440
Gray, R.L. 7510
Greatbatch, W. 6849
Greebe, C.A.A.J. 6501
Green, A. 7688
Green, H.S. 8779
Green, J.J. 6144
Green, M. 6099, 8230, 8231, 8233
Green, R.W. 6151
Greenaway, D.L. 7587
Greene, J.C. 7134
Greene, R.F. 8710
Greenstein, L.J. 9018, 9146
Gregg, D.W. 6457
Gregory, L.A. 9141
Gregory, M.B. 9074
Greifer, A.P. 7056, 9184
Greig, D. 7399, 8918
Greig, W.J. 7249
Greiner, J.H. 6149
Greiner, R.A. 7482
Greive, T. 8490
Gremmelmaier, R. 7163
Grenier, C.G. 6120, 9296, 9438
Grewe, T. 9075
Griefer, A.P. 6141
Grika, V.M. 8948
Grillot, E. 9413
Grimes, Jr., E.S. 7113
Grimley, T.B. 9211
Grimmeiss, H.G. 7589, 7990
Grimmond, R. 8544
Grimsdale, R.D. 7188
Grinberg, A.A. 7307, 7430
Grinich, V.H. 6889
Gritton, G.V. 7681
Griunier, A. 8583
Groom, H.H.G. 8125
Groschwitz, E. 7080
Gross, B. 9230
Gross, D. 8283
Gross, E.F. 8866, 8888, 9236, 9249, 9413
Grosskreutz, J.C. 9164
Grossman, J.J. 6988
Grossweiner, L.I. 7236
Grosvalet, J. 6498
Grover, G.M. 9313
Grover, N.B. 9213
Groves, J.R. 8564
Groves, R.D. 6478, 9437
Gruenberg, H. 8073
Gualtieri, J.G. 8643
Gubanov, A.I. 6058, 9203
Gudmundsen, R.A. 8973, 8999
Guemene, M. 8428
Guentert, O.J. 7851
Guggi, W.B. 7486, 9113
Guinier, A. 9161
Guiraud, J.P. 6398
Gullemin, E.A. 8483
Gummel, H.K. 7676
Gumnick, J.L. 6193
Gurevich, L.E. 7373, 8395
Gurevich, V.M. 7596
Gutin, S.S. 8948
Gutmann, P.F. 6304
Gutorov, Yu.A. 6069
Gutowsky, H.S. 7974
Guttman, L. 7639
Gutwin, O.A. 6588, 6801
Guyon, E. 9161
Guyton, J.H. 8503
Gyorgy, E.M. 8798, 9347, 9348

Haak, F.A. 7018
Haas, C. 7273, 7570
Haas, I. 6580, 7508
Haas, W. 6807
Haayman, P.W. 9010
Haberecht, R. 6330
Haebler, D.V. 9131
Haering, R.R. 6190, 7412
Haga, E. 8921
Hagedorn, F.B. 9348
Hagstrum, D. 7631
Hagstrum, H.D. 9314
Hahn, E.L. 7354, 7967
Haisty, R.W. 7518
Hajko, V. 8316
Haken, H. 8782
Hakimi, S.L. 8481, 9057
Hakki, B.W. 7921
Halbert, M.L. 6301
Halden, F.A. 6044
Hale, A.P. 6653
Hale, D.R. 8190
Hale, M.E. 7345
Hall, H.T. 7898
Hall, Jr., J.F. 6723
Hall, J.J. 7586
Hall, L.L. 7794
Hall, P.M. 8736
Hall, R.C. 9352
Hall, R.N. 6219, 6233, 8970
Hall, T.C. 7706
Hallett, J.E. 6543
Halloran, M. 8769
Halperin, A. 6187, 6208, 6209, 9417
Halpern, J. 8964
Halsted, R.E. 6133, 9406
Ham, F.S. 6384, 7606, 7654, 9174
Hamada, S. 8764
Hamada, T. 6442
Hamasaki, J. 6259
Hambleton, K.G. 8956
Hamburger, T. 6291, 9124
Hamilton, D.J. 7425, 8968
Hamilton, D.R. 6022, 6350, 6453, 6656, 7888, 7890
Hamilton, J.F. 9421, 9422
Hammerslag, J.G. 7780
Hamming, R.W. 8588
Hammond, R.H. 7030
Handler, P. 8664
Haneman, D. 6021, 6659, 8389, 8638
Hanlet, J.M.N. 8212
Hanlon, J.E. 6639
Hanna, D.A. 7601
Hanna, S.S. 8311
Hannemann, L. 8115
Hansen, E.B. 6400
Hanson, R.C. 6106
Hanzel, A.L. 9349
Happ, W.W. 7123, 7722
Happel, Jr., R.J. 6045
Harada, R.H. 7878, 8197
Harbourt, C.O. 7408
Hardenbergh, G.A. 8120
Hardies, C.E. 6262
Hardin, R.H. 8051
Harding, W.R. 6356, 8573
Hardtke, F.C. 6717
Hardy, J.R. 8175
Hardy, L.H. 7738
Hare, W.F.J. 7422
Hargreaves, M.E. 8600
Harkless, E.T. 6559
Harman, C.G. 6057, 6668
Harman, T.C. 6339, 6931, 7247
Harnden, Jr., J.D. 7773
Harnik, E. 9213
Harnischmacher, E. 7790
Harper, W.R. 6673
Harrick, N.J. 6634, 9267, 9310
Harris, A.B. 6476
Harris, P.E. 6838
Harrison, D.E. 6318
Harrison, D.N. 6600
Harrison, M.J. 6728, 8413
Harrison, S.E. 6806
Harrison, W.A. 9208, 9209
Harrity, J.W. 8649
Harte, K.J. 6431
Harten, G.A. 7161, 7500
Harten, H.U. 6391, 8703, 9259, 9260
Hartman, T.E. 7691
Harvey, A.F. 8528
Harvey, R.L. 6365
Harvey, W.W. 6369, 9283
Hasegawa, H. 9304
Hass, M. 6472, 6671
Hastings, J.M. 9366
Haszko, S.E. 7020
Hatcher, R.D. 8915
Hattori, M. 9269
Haudler, P. 9281
Haugen, G.L. 9079
Haun, Jr., R.D. 8067
Hausen, D.K. 8116
Hauser, W. 7954
Havens, Jr., W.W. 7585
Havinga, E.E. 9225
Hawker, P.D.T. 6875, 8118, 9121
Hawkins, J.K. 8129
Hawkins, T.D.H. 8894
Hayes, W. 8839
Haynes, M.K. 7511
Hayter, S.G. 7523
Hayward, D.O. 9192
Heal, H.G. 7234
Heap, B.R. 8306
Heaps, J.D. 6394
Heasell, E.L. 6104, 8715
Heberle, J. 8311
Hedderly, D.L. 9097
Heer, R. 8644
Heffner, H. 8065
Hegyi, I.J. 6621
Heidelberg, R.F. 6427
Heidenreich, R.D. 9343
Heijligers, H.J.M. 9414
Heikes, R.R. 6239, 6524, 8220
Heiland, G. 8612, 9281, 9284
Heilmeier, G.H. 6561, 8088
Heinchon, J. 7782
Heister, W. 9189
Heller, G.S. 6123, 6242
Heller, W.R. 7555
Hellicar, N.J. 8254
Helms, H.D. 7769
Helsdon, P.B. 7165
Hempstead, C.F. 8353
Hendershot, J.H. 9081
Henisch, H.K. 6280, 8450
Henkels, H.W. 6227, 6516, 8702, 7104
Henle, R.A. 6576
Henoch, B.T. 8066
Henry, J.J. 6916
Henry, W.E. 6150, 9335
Henschke, R.A. 6527
Hensel, J.C. 8359, 8706
Hensler, D. 8769
Hensley, E.B. 6252
Hepburn, W.D. 8221
Herbst, J.A. 8426
Hergenrother, K.M. 6960, 8018
Herick, D.J. 7166
Herkart, P.G. 7271, 7272
Herlet, A. 8442
Herman, F. 6067, 6122
Herndon, M. 6732
Herrick, C.S. 6324
Herring, C. 7019
Hersh, H.N. 6005
Hertz, C.H. 7163
Hesler, J. 6582
Hetherington, F.E. 6553
Heuer, A. 6798
Hibberd, R.C. 8432
Higgin, R.M. 7594
Hilbiber, D. 6889
Hilbinger, A.R. 8033
Hildebrandt, A.F. 8755
Hilibrand, J. 7081
Hill, D. 8732
Hill, R.L. 7173
Hill, R.M. 7055
Hilsum, C. 6297, 8573, 8726

ANNUAL CUMULATIVE AUTHOR INDEX

Himes, R.C. 6360, 6361, 6623, 6959, 6965
Hinckfuss, I.C. 7172
Hines, M.E. 6550
Hinsdale, J.G. 9092
Hirai, M. 9168
Hirakawa, K. 8276
Hirota, E. 8335
Hirschmann, E. 8021
Hirshfeld, A.T. 8399
Hittle, C.E. 7170
Hlavacek, A.R. 6756
Ho, Y.-C. 6876
Hochgraf, L. 7505
Hockings, E.F. 8459
Hodara, H. 7130
Hodges, A.J. 6786
Hoff, Jr., M.E. 9107
Hoffman, G.R. 6288, 8374
Hoffmann, A. 9286
Hofheimer, R.W. 7803
Hofmann, H.R. 7787
Hofmeister, E. 7080
Hogg, D.C. 9109
Hoh, S.R. 7727
Holford, K. 6837, 8559
Holländer, E.F. 8597
Hollander, Jr., L.E. 6402, 6404, 7618, 8256, 8410, 8935
Hollar, E. 8769
Holliday, J.E. 9200
Hollitscher, H. 7527, 8562
Holmen, J.O. 7043
Holmes, J.R. 9330
Holmes, P.J. 6664
Holonyak, Jr., N. 6739, 7103
Holroyd, L.V. 9440
Holt, D.B. 7000
Holtzman, A.H. 9185
Holub, A.J. 6828, 7754, 9069
Hon, J.F. 9170
Honey, R.C. 7753
Honor, H.I. 6733
Hook, H.O. 7718
Hooper, G.D. 9332
Hooton, I.N. 8133
Hopfield, J.J. 8850, 9250, 9398, 9399, 9407
Hopkins, D.C. 7312, 8756
Hopper, A.L. 7128
Horiuchi, S. 8621
Horiye, H. 8649
Hormats, E.I. 6167
Horn, F.H. 6971
Horne, R.J. 8934
Hornig, A. 6171
Hornstra, J. 6932, 8611, 9276
Horowitz, I.M. 7498
Hoskins, R. 7725
Hosler, W.R. 8766
Hough, J.M. 9206
Houska, C.R. 9162, 9198
Housley, R.M. 8346, 8844
Houston, B.B. 7877, 8642
Houston, M.D. 7258
Howald, B.W. 6272
Howard, B.T. 6730
Howard, N.R. 6013
Howard, R.E. 7556
Howard, W. 6403
Howiski, J.R. 8144
Howland, F.L. 8983
Hrivnák, L. 8711
Hrostowski, H.J. 6179, 7378
Hsu, H. 6545
Hu, H. 9358
Hu, K.C. 6244
Hu, M.-K. 6902
Huang, C. 8083, 9083, 9093
Huber, F. 6807, 7017
Hubner, K. 8922, 9221
Hudelson, G.D. 8578
Hudson, D.E. 7995
Huelsman, L.P. 8480, 9055
Huettner, O.A. 7804
Huffman, D.R. 6475
Hughes, F.L. 8217
Hughes, R. 8061
Huibregtse, E.J. 9246
Hulliger, F. 8653
Hulm, J.K. 8758
Hulme, K.F. 7847
Humphrey, F.B. 9347
Hunt, J.M. 7514
Huntington, H.B. 9442
Hupp, A.C. 7517
Hurst, C.A. 8779
Husimi, K. 8249, 8787, 9237
Hutcheon, I.C. 6600, 6824
Hutchison, F. 8777
Hutson, A.R. 6403, 8693
Hyde, J.S. 8830, 8835
Ian'-Shen, S. 8037
Ibuki, S. 8376, 8388
Ichimiya, T. 7562
Ida, I. 8048
Iglitsynz, M.I. 7418
Ignatkov, V.D. 7569
Iida, S. 8317
Iizima, S. 8899, 9410
Iles, P.A. 6752
Imenkov, A.N. 8419
Ingham, Jr., H.S. 8215, 8729
Inoue, M. 6934
Inoue, T. 8317
Ioffe, V.A. 7311, 7939
Ipatova, I.P. 8395
Irani, K.S. 8590
Irons, H.R. 7184
Irving, B.A. 6047
Ishibashi, Y. 6872
Ishida, H. 6872
Ishiguro, M. 9397
Ishii, Z. 6012
Ishikawa, Y. 9051
Ishmukhametov, B.Kh. 8783
Isupov, V.A. 6680
Itskevich, E.S. 8914
Ittner, III, W.B. 6118, 7447, 7626
Ivankina, J.S. 7554
Ivanov, K.P. 8792
Ivanov, Yu.L. 7307
Ivanov-Omskii, V.I. 8262
Iwasaki, H. 9244
Iziumova, T.G. 8906
Jaccard, C. 7363
Jaccarino, V. 6449, 8347
Jackson, B. 7417
Jackson, G.E. 6278
Jackson, J.M. 9132
Jackson, R.B. 8082
Jackson, R.W. 6912
Jacobs, G. 8857
Jacobs, H. 7109, 8260
Jacobs, I.S. 7050, 7955, 8319, 9324
Jacobs, J.E. 9031, 9429
Jacobsen, E.H. 8694
Jaentsch, O. 8015
Jaeschke, R.L. 9106
Jaffe, B. 6532
Jaffe, H. 6532, 8258
Jaffe, M. 8223
James, B.D. 6495, 6653
James, J.R. 6260
Janin, J. 6191
Janousek, V. 8671
Janovec, V. 8691
Jarrett, H.S. 7337
Jarvis, D.B. 6574, 6874
Jasinski, W. 7474
Jelley, J.V. 6789
Jenkins, W.N. 8142
Jennings, V.J. 6014
Jenny, D.A. 8980
Jensen, H.A. 6759
Jensen, R.V. 6357
Jochems, P.J.W. 8425, 8994, 9000, 9008, 9135
Johannessen, P.R. 7160
John, H.F. 6351, 6352, 7888, 7889, 7890, 7893, 8019, 8188
Johnson, Jr., C.E. 9186
Johnson, C.M. 7723, 9043
Johnson, F.A. 7673
Johnson, K.M. 7157
Johnson, L.F. 6196, 8864
Johnson, L.R. 8617
Johnson, R.A. 7408
Johnson, R.B. 8986
Johnson, R.E. 7076
Johnson, V. 7564
Johnston, R.C. 6818
Johnston, T.L. 7695
Johnston, W.D. 6524, 8220
Johnston, W.G. 7856, 8185
Johnstone, B.M. 7477
Jona, F. 6083, 6679
Jones, A.R. 7212
Jones, D.V. 6840
Jones, E.M.T. 7753, 8141, 9072
Jones, Jr., J.P. 9068
Jones, L.W. 9032
Jones, M.E. 8996
Jones, R.C. 7714, 7715
Jones, R.D. 6290
Jones, Jr., R.E. 6114
Jones, R.H. 7673
Jones, R.V. 8807
Jonker, G.H. 9214
Jonscher, A.K. 6494, 8963
Jordan, A.G. 7436, 8096
Jordan, E.L. 6327
Jordan, R.D. 8179
Jorgensen, P.J. 8636
Joseph, A.S. 8849
Joseph, L. 6528
Josephs, J.J. 6892
Joshi, M.V. 8525
Joshi, S.K. 8400, 8667, 8913
Jovanovic, D.T. 6304
Judge, D.L. 7526
Juenker, D.W. 6193
Jung, P. 7815
Juretschke, H.J. 7044, 8326
Kaczér, J. 7957, 8325
Kadanoff, L.P. 6115
Kaenel, R.A. 6882
Kagan, S. 9112
Kagan, Yu. 8296
Kahan, G.J. 6410
Kaifu, Y. 9419
Kaiser, H.R. 8139
Kaiser, W. 6179, 6338, 7226, 7246
Kalish, I.H. 7711
Kallestinov, G.V. 8966
Kallmann, H. 6470, 7578
Kalnins, I.L. 8985
Kamal, A.K. 6828, 7458, 7491, 7735, 7754
Kambouris, G.N. 8021
Kamimura, H. 9373
Kaminow, I.P. 6441, 7046, 8807
Kaminsky, G. 7086
Kammer, E.W. 8930
Kampe, T.W. 6868
Kamysheva, L.N. 7920
Kanai, Y. 7933, 8292
Kandaurova, G.S. 8800
Kane, B. 6798
Kane, E.O. 6131, 6700, 9220
Kaneko, T. 7334
Kanter, H. 6055
Kanzaki, H. 8618
Känzig, W. 8647, 8837
Kapitsa, M.L. 8300
Kaplan, R. 6417, 8836
Kaplan, T.A. 7329, 7636
Kaptsov, L.N. 8501, 8502, 8505
Karan, C. 8441
Karew, J.J. 7182
Karo, A.M. 9218
Karpenko, B.V. 8290
Karrer, S. 9034
Karstensen, F. 6024
Kataev, G.I. 8943
Kathan, L.S. 8666
Kato, R. 8367, 8393
Kattner, L. 6774
Katz, E. 7597
Katz, J.M. 9368
Katz, M.J. 8643
Katzman, M. 7724
Kaufman, M.M. 7805
Kaufman, W.M. 6776
Kaupp, H.R. 7180
Kawaji, S. 6129, 9282
Kawamura, T. 8438
Kay, E. 6975
Kay, H.F. 7548
Kear, F.W. 7745
Kearns, D.R. 6719, 7992
Kebler, R.W. 6040
Keffer, F. 6194, 6429, 7048
Keith, R.J. 7172
Keith, W.W. 6282
Keizer, E.O. 7768
Keldysh, L.V. 8717
Keller, J.B. 7328
Keller, S.P. 7396
Kellett, P. 7176
Kelley, C.M. 6796
Kelley, R.H. 9408
Kelly, E. 7277
Kelly, W.H. 9420
Kembadjian, H. 8059
Kemp, W.R.G. 8916
Kenan, R.P. 8331
Kendall, H.W. 7719
Kendrick, W.M. 7164
Kennedy, D.P. 6102, 6503, 7696
Kepler, R.G. 7621, 8262
Kern, R. 8586
Kerr, D. 8127
Keshler, Jr., C.P. 9127
Kesperis, J.S. 6949
Kevane, C.J. 6221
Keyes, R.W. 6068, 7663, 8724, 9299
Keywell, F. 6329, 9274
Khaikin, A.S. 8907
Khalatnikov, I.M. 8753
Khan, I.H. 7549
Kharlamova, T.E. 7087
Khazanov, B.I. 7469
Kylystov, A.S. 7896, 8813, 8816
Kholuyanov, G.F. 7087, 7108
Khomenko, L.A. 7569
Khromov, B.P. 8789
Khutsishvili, G.R. 8320
Khvostenko, G.I. 7939
Kibler, L.U. 8504
Kido, K. 8618
Kiel, A. 6173, 7366
Kieselbach, R. 7530
Kihn, H. 8113
Kikuchi, C. 6447, 8351, 8356, 8471, 8771, 9050
Kikuchi, M. 6742, 8445, 8899, 9410
Kikuchi, R. 8195, 8801, 8802, 9326
Kikuchi, T.T. 7657
Kilburn, T. 6288, 7186, 7188, 7189
Kilkson, R. 7883
Kim, C.S. 7156
Kim, Y.W. 6417, 8836
Kinariwala, B.K. 7454, 8482
King, B.R. 8401
King, J.C. 8364, 9450
King, J.H. 8271
King, P.D. 7524
King, R.E. 6566, 8897
Kingery, W.D. 8405
Kingston, D.L. 7881
Kippenhan, B.W. 8201, 8628
Kirenskii, L.V. 8323, 8805
Kirk, E.S. 8268
Kirkpatrick, R.J. 6513
Kirsch, J. 6652
Kirvalidze, I.D. 7617
Kischio, W. 7589
Kiseda, J.R. 8039
Kiselev, A.A. 8362
Kiss, M.J. 8101
Kissner, R.L. 8150
Kita, S. 8007
Kitamura, S. 7393, 8384
Kittel, C. 6437, 6705, 7330, 7336
Klaassen, F.M. 6468, 8453
Klabunde, C.E. 8651
Klasens, H.A. 6236
Klassen, F.M. 9022, 9256
Klecak, G.L. 8614
Kleimack, J.J. 7422
Klein, C.A. 6064, 7948
Klein, D.L. 6665
Klein, M. 7424
Klein, M.V. 7684
Kleinman, D.A. 7106, 8852, 8855
Kleinman, L. 6066, 9216
Klemens, P.G. 7686, 8916, 9430, 9434
Klement, F.D. 7989
Klement, Jr., W. 6622
Klensch, R.J. 8113
Klick, C.C. 6933, 8241, 9418
Klier, J. 7125
Klimowski, J. 8686
Klinger, M.I. 6396
Klokholm, E. 9182
Kloss, A. 7407
Knechtli, R.C. 6827
Knight, L. 6285
Knight, R.D. 6772, 7900
Knight, W.D. 7030
Knippenberg, W.F. 6501
Knowles, J.E. 9360
Knox, K. 7358, 9384
Knox, R.S. 7610
Ko, W.H. 6223
Kobagashi, T. 7521
Kobayashi, A. 9282
Kobelev, V.V. 6142
Kobuke, Y. 6188, 6463
Kobus, A. 8208
Koc, S. 9258
Koch, R.C. 9110
Koehler, W.C. 8822
Koelmans, H. 7990, 7991
Koenig, S.H. 6383, 6405, 7586, 8720, 8727
Koerts, W. 7652
Kohane, T. 7616
Kohn, J.A. 8831
Kohn, W. 6074, 9381
Kohra, K. 6012, 7872, 8174
Koide, S. 9373
Kokes, R.J. 8232
Kokin, A.A. 8841
Kokosh, G.V. 7401
Kolk, A.J. 7078
Koll, A.J. 6845
Kollar, F. 7814
Koller, L.R. 6968, 7894
Kolm, C. 8929

ANNUAL CUMULATIVE AUTHOR INDEX

Kolomiets, B.T. 7674, 7949, 8262, 9224
Koloskova, N.G. 8827
Komatsubara, K. 6506
Komienko, L.S. 8355
Komiya, H. 8376, 8388
Kondo, J. 9306
Kondorskii, E.I. 8786, 9288
Konigsberg, R.L. 7194
Konitzer, J.D. 8856
Konopleva, R.F. 7605
Konorov, P.P. 7392
Konstantinova, V.P. 6043
Kontorovich, M.I. 7147
Kontsevoi, Iu. A. 7418
Kooi, C.F. 9187, 9368
Kopelman, B. 8990
Kopp, H. 7506
Kopp, W.J. 7167
Kopvillem, U.Kh. 8827
Kopylovskii, B.D. 8373
Korkowski, V.J. 9039
Kornfel'd, M.I. 7941
Koroncai, A.K. 7161, 7500
Korringa, J. 8331
Korsunskii, M.I. 8198
Kosenko, V.E. 7569
Kosfeld, R. 6900
Kosler, S. 7263
Kostelich, J.F. 6272
Koster, G.F. 8845
Kostin, V.N. 8905
Kostyshyn, B. 6434
Kosyakov, V.I. 6680
Kot, M.V. 7285, 7286
Kotiukov, Iu.N. 8809, 8811
Kotlarski, J.R. 6562
Kotzebue, K.L. 8068
Koutecky, J. 7004, 8239, 9205
Kouvel, J.S. 6432, 7338, 7339
Kovach, L.D. 7513
Kowalchik, M. 6001
Kozlovskaya, V.M. 6046
Kraemer, L.M. 7580
Krainik, N.N. 7293
Krajewski, I. 6877
Kramarov, O.P. 6041
Kramer, B. 6470
Kramer, M. 9140
Kramer, N.H. 6841
Kramer, R.A. 6928
Kremheller, A. 6032, 6182, 6354, 6969
Kretsu, I.V. 7286
Krieble, J.G. 6324
Krikorian, N.H. 9313
Krinchik, G.S. 8396, 8851
Kringlebotn, M. 7749
Kristianpoller, N. 6209
Kristofel, N.N. 8874
Kritikos, H. 7699
Kroemer, H. 6416
Kroger, H. 7381
Krohn, A. 6996
Krokhin, O.N. 8452
Kropschot, R.H. 8407
Kroupa, F. 8184, 9223
Krueger, H.H.A. 6532
Krumme, J.B. 7987
Krupicka, S. 7642, 7964
Ku, W.H. 7740
Kubat, M. 7407
Kubota, B. 8335, 8630
Kudriautsev, O.M. 9021
Kudriavtsev, I.P. 8799
Kudzin, A.Iu. 8815
Kuh, E.S. 6819
Kuhlmann-Wilsdorf, D. 6939
Kuhrt, F. 6298, 9020
Kulp, B.A. 9408
Kulwicki, B.M. 6317
Kunckel, H. 9114
Kunin, V.Ia. 7901
Kunzler, J.E. 7952
Kurata, T. 6506
Kurilo, P.M. 8003
Kurokawa, K. 6259
Kurosawa, T. 8718, 9272
Kurtz, A.D. 6637, 7862
Kushida, T. 8808
Kuwabara, G. 7390
Kuwahara, K. 8321
Kuz'min, V.A. 7148, 7149
Kuznetzoff, P. 7091
Kwestroo, W. 7651
Labes, M.M. 6690, 8735
Labutin, V.K. 7464
Lacey, J.W. 8513
Lacy, R.D. 8126
Ladany, I. 6492, 7414
Lade, R.W. 7409, 8086
Laegreid, N. 6052
LaFontaine, J.F. 8549
Laherrere, J.P. 7028
Lainé, D.C. 8046
Lakshmanan, T.K. 8422
Lam, Jr., D.G. 8936
Lambe, J. 6447, 8345, 8351, 8356, 8471, 8771, 9047, 9050
Lamont, K. 7756
Lamorte, M.F. 6635
Lampert, M.A. 6098
Lamy, R.C. 7771
Landauer, R. 6546
Lander, J.J. 7227
Landsberg, P.T. 6390, 8659, 8697, 9254
Langer, J.S. 7014
Langfelder, R. 7823
Langlais, D.G. 6502
Lanigan, M.J. 7189
Lapluye, G. 8687, 8688
Laponsky, A.B. 7023
Larach, S. 6235, 6567
Larisch, R.W. 8136
LaRosa, R. 7701
Larrabee, R.D. 6452, 6777, 9265
Larsh, A.E. 6915
LaRue, J.J. 7119
Lasher, G.J. 7965
Lassiter, E.M. 7160
Last, J. 6580, 6774
Latorre, R.J. 7776
Laughlin, R.D. 8989
Laukonis, J.V. 9191
Laurance, N. 7251
Lauriente, M. 7039
Lavine, J.M. 6491
Lavine, M.C. 6026, 6340, 6371, 6660, 6983, 8209, 8228, 8234, 8640
Law, J.T. 9320
Lawrence, P.E. 8319
Lawson, T.C. 6862, 7782
Lawson, W.D. 6465, 8867
Lax, B. 6065, 6130
Lax, M. 6125, 8704, 9252
Layburn, R.L. 8524
Lazarev, B.G. 8757
Lazarev, V.B. 8160
Lazazzera, V.J. 7370
Lean, J.B. 8939
Lebedev, V.V. 8000, 8078
le Can, C. 6765
Leck, J.H. 8146
LeCraw, R.C. 6143, 7051, 9364
Lederhandler, S. 6008
Ledford, R.L. 6844
Lee, C.A. 6489, 7086
Lee, D.W. 8405
Lee, E.W. 8775, 8776
Lee, F. 7494
Lee, M.A. 8165
Lee, T.H. 6843
Lee, V.J. 8626
Leef, G.R. 7727
Leenov, D. 8099
LeGraw, R.C. 8328
Legvold, S. 6151, 7016, 8274, 8736
Lehmann, W. 6183, 6522, 8377
Lehovec, K.I. 6333
Leinfelder, B.A. 8972
Leivo, W.J. 7987
LeLoup, T.E. 8951
Lemaire, H.P. 6976
LeMay, C.Z. 7101
Lempicki, A. 6455
Lentz, J.J. 8094
Leon, B.J. 7453
Lescroel, Y. 8313
Lesk, I.A. 6739, 6749, 6759, 7103, 7122
Lessoff, H. 7056
Leupold, H. 8399
Lever, R.C. 9044
Lever, R.F. 7270
Levesque, P. 9194
Levey, L. 6793
Levin, E.R. 9226
Levine, A.K. 6030
Levinger, B. 8295
Levinger, J.S. 7404
Levinstein, H. 8864, 9308
Levitin, R.Z. 8303, 8943
Levy, I.E. 9013
Levy, M. 6504
Levy, R.A. 8925
Lewin, M.H. 6571
Lewinski, D.A. 6865
Lewinter, S.W. 7493
Lewis, H.R. 6116, 6806, 7975, 8474
Lewis, N. 9417
Li, C.H. 7695
Li, G.-D. 8817, 9041
Li, J.C.M. 8606
Li, K. 6583
Li, T. 8475
Libovicky, S. 8599
Lidow, E. 8987
Lieb, D.P. 7417
Liebman, F. 8104
Liehr, A.D. 7006
Ligenza, J.R. 7581, 8227
Liid'ya, G.G. 8375
Lilienstein, M. 7819
Lim, M. 8057
Lin, H.C. 6756, 9064
Linares, Jr., R.C. 7379, 8224
Lind, E.L. 8900
Lindaman, R. 7174
Lindemann, W.W. 6788
Linden, D.A. 8437
Lindley, D.H. 9319
Lindsay, J.E. 8080, 9102
Lindsay, R. 6427
Link, G.L. 7958
Lipaeva, G.L. 9232
Lipkin, H.J. 8889
Lipman, N.H. 7210
Litovchenko, V.G. 7283
Little, W.A. 9004
Little, W.J. 8207
Liu, S.H. 7932
Livingston, J.D. 9370
Lloyd, A.G. 7520
Lloyd, D.J. 6903
Lo, A.W. 6571, 6583
Lob, W.H. 7772
Loebner, E.E. 6621
Loferski, J.J. 8008
Logan, R.A. 6103, 6701, 6738, 6747, 7633, 8278
Loken, M.K. 7162
Lombardini, P.P. 7699
Lommasson, T. 6290, 8103
Lommel, J.M. 7041
Long, D. 7302, 7303
Long, M.W. 7205
Longerot, C.D. 6290
Longini, R.L. 6349, 7891, 9001, 9002
Longo, T.A. 6737
Looney, D.H. 9037
Loos, J. 7649
Lord, H. 8269
LoSasso, L.A. 8063
Loscoe, C. 6479
Lothe, J. 8605
Lotsch, H. 7741
Loudon, R. 7384, 8265, 8695
Lougher, E.H. 6363, 7072
Love, T.A. 7209
Love, W.F. 7316
Lovell, C.A. 6246
Low, H. 6566
Low, J.J. 8956
Low, W. 6161, 6714, 7359, 7365, 7667, 7976, 7977, 7979, 8832, 8847, 9376, 9386
Lowe, L.F. 6943
Lowell, R. 8101
Lowen, J. 6226
Lowry, Jr., L.R. 9130
Lowry, T.N. 6246
Lucas, M.S.P. 7728
Lucovsky, G. 6782, 6784
Ludwig, G.W. 6164, 7654, 8176, 8770
Luethi, B. 7611
Luettgenau, G. 6866
Luke, C.L. 8192
Luke, W.G. 7729
Lukes, F. 6716, 7994
Lumpkin, O. 7158
Lundsten, R.H. 9341
Lur'e, M.S. 7922
Lurio, A. 6674
Lushchik, C.B. 8375, 8875
Lushchik, N.E. 8875
Luttinger, J.M. 9210
Lyashenko, V.I. 6128, 9318
Lynch, D.W. 8245
Lynch, J.T. 7182
Lynn, D.K. 7763
Lyons, D.H. 6935, 7329
Lyons, V.J. 8582
Lytal, K.E. 7458
Lyubin, V.M. 9224
Maaz, K. 6412
Macaulay, I.J. 7172
Macdonald, J.R. 6423, 8679
MacDonald, R.W. 6771
Machlin, E.S. 9201
Machlup, S. 6718
Mackintosh, I.M. 6334, 6913
Macklem, F.S. 6296
Macpherson, A.C. 6732
MacPherson, M.R. 6817
MacRae, A.U. 9308
Mader, C.L. 7681
Maeda, H. 7984, 8294, 8761
Magee, V. 7435
Mahendroo, P.P. 8842
Maiman, T.H. 6248, 7725
Maissel, L.I. 6207, 7097, 8974, 8981
Makhov, G. 8471, 9047, 9050
Makow, D.M. 6565
Male, J.C. 8372
Malinofsky, W.W. 7275
Mallery, P. 8137
Mallory, M.L. 9420
Malovetskaya, V.M. 6521
Maly, V. 7497
Managan, W.W. 7831
Mandel, M. 6172, 6901
Mandelkorn, J. 8699
Manenkov, A.A. 8339, 8343
Manganne, R. 8105
Mangiaracina, R. 7367
Manley, O.P. 8196
Mann, H. 7152, 7831
Manning, W.H. 8552
Mano, K. 8081, 8109
Many, A. 6401, 9213
Mapother, D.E. 6116, 7312, 8284, 8748, 8756, 9292
Maradudin, A.A. 7918, 7930, 8263
Marcel, P. 7879
Marcus, P.M. 7906
Marcus, S.M. 7509
Marette, S. 6636
Margoninski, Y. 6670
Marinace, J.C. 6651, 6750, 7887, 9023
Maringer, R.E. 6632
Marinov, A. 7353
Mark, A. 8216
Markham, J.J. 6005, 7665, 8856
Markouskii, L.Ya. 8382
Markov, M.N. 8907
Marks, G.S. 7601
Marsden, B. 6271
Marsh, B.B. 8574
Marsh, J. 7870
Marshall, B.J. 6724
Marshall, S.A. 6445, 7362, 7657, 8846
Marshall, T.C. 9228
Marshall, W. 7335, 7998
Martin, A.V.J. 8031, 8032
Martin, Jr., D.C. 6950
Martin, M.B. 8117
Martin, P.C. 6115
Martin, Jr., T.L. 7463
Marvin, J.F. 7162
Marzolf, J.M. 9139
Mascarenhas, S. 7237, 7238, 7897
Maserjian, J. 8999
Masher, D.P. 6871
Mashkevich, V.S. 9219
Maslennikova, F.V. 8800
Mason, D.R. 6015, 6317, 7274
Mason, W.P. 6814
Massman, A. 6859
Masters, J.I. 7277
Masuda, I. 6188, 6463, 8843
Masumi, T. 8767, 9231
Masuno, K. 9244
Mataré, H.F. 6071, 6072, 8708, 8896
Matarrese, L.M. 8217
Mathers, H.W. 6841
Matlow, S.L. 6991, 7002
Matoshin, V.M. 8948
Matsui, A. 8393
Matsumura, K. 8621
Matsumura, T. 6038
Matsuoka, Y. 6872
Mattei, J.I. 8105
Matthias, B.T. 6138, 8347, 8744
Mattingly, L. 6859
Mattis, D.C. 6384, 7296
Mattuck, R.D. 8340
Matz, A.W. 6763
Maurer, R. 8498, 8646
Maurushat, Jr., J. 8510
Maxwell, K.H. 8230, 8231
May, Jr., J.E. 6533
Mayburg, S. 7009
Mayer, J.W. 6607, 6910, 8569, 8571
Mayer, L. 7873, 9331
Mayer, S.E. 6960, 8931
Mazo, R. 8398
Mazurov, M.E. 8098
McAdam, J.C. 8447
McAleer, W.J. 7578
McAlister, A.J. 7257
McCaldin, J.O. 6018, 7228, 8162, 8197
McCall, D.W. 8588
McCall, Jr., G.S. 7045
McCarthy, K.A. 8207, 9433
McCarthy, W.A. 8436
McClelland, J.D. 9441

ANNUAL CUMULATIVE AUTHOR INDEX

McClung, Jr., F.J. 6594, 9330
McClure, D.S. 6067, 9390, 9391
McClure, J.W. 6715, 7914
McCollum, R.L. 9199
McCombie, C.W. 9396
McConkey, E.A.G. 8648
McDade, P.J. 8215
McDonald, R.S. 6051
McDuffie, Jr., G.E. 6444
McElroy, M.R. 9128
McGahan, T.E. 6370
McGee, J.D. 9380
McGregor, R.R. 8149
McIlvaine, O.T. 9030
McInnes, I.G. 8106
McIntyre, R.J. 6743
McKay, R.W. 6795, 9040
McKenney, H.F. 8496
McKenzie, J.M. 6914, 9150
McKinney, J.E. 6088
McLean, T.P. 7612, 8695
McLeod, M.G. 7526
McMahon, H.O. 8476
McMahon, R.E. 6577
McManus, G.M. 7406
McMillan, M. 7656
McMullen, C.W. 7141
McNally, F.X. 7039
McNaught, R.A. 6905
McNulty, J. 6658
McVey, E.S. 9085, 9100
Mead, C.A. 7099
Meechan, C.J. 7864
Meeks, E. 6331
Mefferd, W.L. 6362
Mehl, W. 7278
Mehnert, R.A. 6326
Mehrtens, D.H. 7126
Meier, D.A. 9042
Meijer, G. 6461, 8891
Meindl, J.D. 6778, 6779, 7109, 7121, 8487
Meissner, H. 6407
Melamed, N.T. 8004
Melcher, J.L. 8100
Melik-Gaikazyan, I.Ya. 7554
Mel'nikov, A.I. 7630
Mel'nikova, V.I. 8167
Meltzer, B. 6482, 8961
Melvin, D.K. 9115
Memelink, O.W. 8006
Mendelsohn, L.I. 9045
Mendlowitz, H. 6177
Menes, M. 8004, 9447, 9448
Mengert, P. 9252
Menyuk, N. 9357
Mergerian, D. 7362
Merrifield, R.E. 7621
Merritt, P.E. 7461
Merz, K.M. 6139
Merz, W.J. 8901, 8902
Mesnard, G. 8259
Messenger, G.C. 8010
Messner, D. 7060
Methfessel, S. 6435
Mette, H. 6479, 9428
Metzger, S. 8530
Meuer, G. 9416
Meyer, E.W. 7776
Meyer, H. 6476
Meyer, H.J.G. 8006
Meyer, J.W. 8472
Meyer, M.A. 9122
Meyer, N.I. 7095
Meyer, R.L. 9028
Meyerhofer, D. 6357
Meyerhoff, A.J. 8537
Meyers, N.H. 7622, 8754
Meyers, S.T. 6890
Miasek, M. 7908
Michel, R.E. 9303
Middelhoek, S. 6435
Midgley, D. 8451
Mieher, R.L. 6175
Mieklejohn, W.H. 9294
Mii, N. 6836
Mikhailova, T.G. 8675
Mikheeva, M.N. 8286
Mikoshiba, N. 9251
Miksch, E.S. 6432
Mikulyak, R.M. 6500
Milano, U. 6243, 6794
Milenbach, H. 9142
Miles, T.J. 6767
Milevskii, L.S. 8608
Milford, F.J. 6597
Milgram, M. 6997
Miller, A. 7015, 9153
Miller, C.E. 6159, 6646, 8163
Miller, D.P. 6953
Miller, D.S. 9375
Miller, E.C. 6276, 6551
Miller, G.L. 6913, 8572
Miller, G.T. 8226
Miller, H.A. 8515
Miller, H.H. 9108
Miller, J.C. 6583
Miller, J.F. 6361, 6623, 6959, 6965
Miller, L.E. 7100
Miller, P.B. 8750
Miller, R.C. 6386, 6677, 7400, 8250, 8683
Miller, R.H. 6904
Miller, S.L. 6220, 7707, 8011
Miller, W.D. 7162
Mills, J.R. 8267
Mills, R.L. 8331
Milnes, A.G. 6797, 7436
Mims, W.B. 7668, 9380
Minamoto, M.T. 7093
Minkowski, J.M. 7661
Minnaja, N. 7670
Minner, W. 7098
Minomura, S. 7915
Mirlin, D.N. 7940, 7941
Misarova, A. 7288
Miselyuk, E.G. 7569
Mishin, D.D. 8788
Mitchell, D.L. 6132
Mitchell, E.N. 6586, 6886
Mitchell, E.W.J. 8389
Mitchell, P.V. 6006
Mitra, S.S. 8400, 8667, 8913
Mitsek, A.I. 8794
Mitskevich, V.V. 8910
Miura, T. 8109
Miyadai, T. 7346
Miyahara, S. 8312
Miyahara, Y. 6484
Miyake, K. 6070
Miyatani, S. 8734
Miyazawa, H. 8294, 8761
Mizuno, H. 6934
Mizuno, J. 8172
Mizuta, H. 8317
Mlavsky, A.I. 6960, 8931
Moates, G.H. 6016
Mochan, I.V. 6206
Mock, J.B. 8352
Mockus, E.S. 9013
Mogen, D.C. 7737
Mohanty, G.P. 7005
Mohr, R.J. 7118
Moizhes, B.Ya. 6471, 7682
Mojoni, A. 6644
Mokrytzki, B. 6292
Moll, J. 6496, 7545
Mollwo, E. 8612
Molyneux, L. 6850, 7830, 8152
Momo, L.R. 9049
Monaghan, R. 7829
Moncaster, M.E. 8573
Montalenti, G. 9362
Montgomery, D.J. 7375
Montgomery, H.C. 6489
Moody, P.L. 6026, 6344, 8209
Moon, R.M. 9359
Mooney, R.W. 6189, 6464
Moore, A.C. 6655
Moore, B.W. 7811
Moore, D.L. 7702
Moore, R.A. 6211, 6512
Moore, W. 7927
Morehead, Jr., F.F. 6458
Morelock, C.R. 6970
Morgan, D.J. 8306
Morgan, H.L. 7758
Morgan, J.V. 7011
Morgan, L.P. 6574, 6874, 9138
Morgan, R.E. 8555
Morgan, S.P. 7085
Morgan, T.N. 9280
Morinet, G. 8687, 8688
Morita, A. 6097
Moriya, T. 6433, 7341
Morosov, A.V. 7630
Morozov, A.I. 7632
Morrison, G.H. 6940, 8614
Morrison, S.K. 7697
Morrison, S.R. 9311, 9312
Mortenson, K.E. 6549, 6830
Moruzzi, V.L. 7037, 8157
Moskalenko, S.A. 8360
Moss, R. 6348, 6657, 9187
Moss, T.S. 8894, 8911
Moto-Oka, T. 6872
Moulton, G.C. 6166
Moulton, W.G. 6166
Mount, T.E. 8486
Movshovich, M.E. 8062
Moy, M.S. 6843
Mrozowski, S. 7029, 7367
Mudar, J. 6186
Mueller, C.W. 7698, 8997
Mueller, H.J. 7389
Mueller, R.K. 6788, 9179
Muldawer, L. 7551
Mullen, J.B. 6320
Mulligan, Jr., J.H. 8494
Mullin, J.B. 7847
Munakata, M. 7944
Munushian, J. 8051
Muramori, K. 8312
Murata, K. 6872
Murphy, E.J. 7936
Murphy, J.C. 6163, 8831
Murray, A.M. 9396
Murray, G.T. 9201
Murray, Jr., R. 7766
Murray, R.B. 7209
Murray, R.P. 8054
Musatov, I.K. 8892
Muss, D.R. 7902
Mutabzija, R. 8965
Mutter, W.E. 8441
Myer, J.H. 8978, 8979
Myers, J. 7302
Myers, O.E. 9379
Myers, R.A. 9049
Naborowski, J.G. 7466, 7776
Nachtrieb, N. 7860
Nadashkevich, I.I. 6142
Naess, E. 8108
Nagamori, K. 7800
Nagasawa, A. 9178
Nagorsen, H. 9131
Nagy, Jr., J. 7817
Nahman, N.S. 7116
Naiderov, V.Z. 8550
Nakada, Y. 7056
Nakagawa, K. 6872
Nakamura, A. 8304
Nakamura, E. 8684
Nakamura, K. 8367, 8393
Nakamura, T. 7923
Nakashima, S. 8367
Nakau, T. 8275
Nakazawa, K. 6872
Nall, J. 6774
Nambu, Y. 6406
Nanavati, R.P. 6253, 6268, 7429
Narayanan, M.A. 8525
Narud, J.A. 6555
Nash, F. 6165, 8349
Nash, W.B. 8810
Nasledov, D.N. 7937, 7938, 7942, 8419
Nassau, K. 7259, 7349, 7668, 8222
Nathan, M.I. 6220, 8011
Navon, D. 7708
Nazarova, T.F. 7949
Nechaev, A.M. 8539
Nechtow, M. 6329
Néel, L. 9356
Neff, G.W. 6572, 7179
Negishi, K. 8248
Neitzert, C. 8568
Nekrasov, M.M. 8416, 8676
Nelson, C.M. 9403
Nenno, S. 9171
Nergaard, L.S. 7467
Nesbitt, E.A. 9343
Nesbitt, L.B. 9275
Neugebauer, T. 8669
Neville, Jr., E.J. 7451
Nevitt, M.V. 6152
Newey, C.W.A. 8938
Newhall, E.E. 6800
Newhouse, V.L. 6808, 7448, 8138
Newman, R.C. 6032, 7573, 8202, 9424
Nicholson, H.C. 6348, 6657
Nicholson, R.W. 6835
Nicoll, F.H. 7110
Nicols, G.M. 8839
Nielsen, E.G. 7459, 7700
Nielsen, J.W. 6364, 6440, 7347, 8218, 8350
Nielson, S. 8867
Nieveen van Dykum, A. 6856
Nii, R. 8001, 8292
Nikanorov, S.P. 8409
Nikitin, E.N. 7620
Nikitine, S. 7671
Nine, H.D. 8942
Ninomiya, T. 7868
Nishiguchi, K. 8787
Nishimura, J. 8182, 8213
Nishina, Y. 7932
Nishiyama, Z. 9171
Nishizawa, J. 6493
Nitsche, R. 8253, 8901
Nixon, J.D. 6718
Noakes, J.E. 9336
Noble, G.A. 7665, 8840
Noble, R. 8131
Noble, V.E. 7267
Nolle, A.W. 8842
Nolta, J.P. 7018
Nomura, K.C. 6096, 6178, 6392, 6394, 6936
Nomura, R.C. 7680
Norder, W.A. 9339
Norman, R. 6580
Norman, R.S. 9045
Norr, M.K. 8642
Northover, W.R. 6773
Northrip, J.W. 7290
Northrop, D.C. 7528, 8573
Norwood, M.H. 6475, 8940
Nose, H. 8327
Nosov, Iu.R. 7469
Novey, T.B. 8644
Novikov, S.R. 7307
Novikova, S.I. 8820
Novotny, B. 7460
Nowalk, T.P. 7104
Nowick, A.S. 9395
Nozaki, T. 7562
Nran'yan, A.A. 6058
Nudelman, S. 6186
Nuralieva, R.D. 8851
Oakes, F. 6822
Obelbermann, E.J. 7495
Oda, Z. 9282
Odani, Y. 8803
O'Dwyer, J.J. 9229
Ofer, S. 7353
Offenbacher, E.L. 9226
Offner, F. 7744
Offner, F.F. 9147
Ogawa, S. 8305, 8336, 9178, 9387
Ogino, Y. 8621
Ogletree, W.A. 9067
Oguchi, T. 6136, 6429
Oguey, H.J. 6578, 6702, 7953
O'Hara, S. 7892
Ohkura, H. 7993
Ohlsen, G.T. 7175
Ohm, E.A. 9109
Oi, I. 6434
Oka, M. 6056
Okada, K. 8247
O'Kane, D.F. 6198, 7274
Okaya, A. 6165, 6713, 8173, 8349
Okazaki, S. 8701
Oki, H. 8701
Okkerse, B. 6024, 7260, 8193
Oku, T. 6056
Okumura, K. 6252
Okwit, S. 7118, 8044, 9048
Oliphant, T.A. 6691
Oliver, D.J. 8281
Oliver, J.W. 8571
Ollom, J.F. 7641
Olsen, J.L. 8283, 8746
Olsen, K.H. 8121
Olsson, J.K.A. 8134
Oman, R.M. 6048, 6049
Omura, K. 6056
Onaka, R. 8868
O'Neil, J.P. 7811
Onsager, L. 8398
Onstad, R.C. 6269
Onuki, M. 7993
O-Ohata, K. 9204
Opechowski, W. 7656
Orloff, W. 7732
Orlov, I.N. 8456
Orlova, M.P. 8820
Oroshnik, J. 6401
O'Rourke, M.J. 6734, 6750
Orr, W.H. 8205
Orshanskaya, N.S. 8382
Osada, K. 8379
Ostroff, E.D. 8123, 9122
Overhauser, A.W. 7961, 9287
Overn, W.M. 9039
Ovsyannikova, I.A. 8371
Owen, H.A. 7728
Owen, W.E. 7470
Owens, E.B. 6339

ANNUAL CUMULATIVE AUTHOR INDEX

Pace, J.H. 6169, 7969
Pacey, D.J. 6299
Padwick, G.C. 8543
Page, J.G. 8133
Page, R.K. 7507
Pagel, B.R. 6781
Paige, E.G.S. 7609, 7612, 8722
Pajgrt, M. 8495
Pake, G.E. 6172, 8828
Pakswer, S. 9024
Paladino, A.E. 8581
Palik, E.D. 7679
Palistrant, M.E. 8860
Palla, P. 8687, 8688
Pallett, J.E. 6482
Palma, M.U. 7652
Palma-Vittorelli, M.B. 7652
Palmer, D.R. 9312
Palmer, W. 7344
Pan, P.M. 6160
Pankey, Jr., T. 7326
Pankove, J.I. 6181, 6812, 9003, 9432
Pappalardo, R. 7379, 7383, 7978
Pappert, R.A. 9248
Paranjape, B.V. 6090, 7404
Pardue, T.E. 9005
Parent, R.J. 9108
Pargas, P. 7522
Paritskii, L.G. 7391
Park, D. 7441
Parker, C.A. 7563
Parker, H.W. 9007
Parker, R.A. 7287
Parkes, D.A. 6790
Parkinson, D.H. 7450
Parmenter, R.H. 9290, 9291
Parratt, L.G. 7871, 9156
Parravano, G. 8626
Parris, S.R. 6848
Parrott, J.E. 6523
Partovi, F. 8784
Partridge, G.R. 7168
Paskell, E. 6510, 8443
Paskin, A. 9158
Pasnak, M. 9341
Pass, H.W. 7458
Passau, P. 6481
Passow, E.B. 9118
Pasternak, J. 7255, 7256
Pastrynak, I. 9236
Pasynkov, V.V. 7108
Patek, K. 9411
Patel, J.R. 8187
Paton, F. 6104, 8715
Patrick, L. 6453, 6454
Patrina, I.B. 7311
Patterson, D.A. 9404
Paul, D.I. 6134
Paul, W. 6075, 6403, 7010, 7913, 8672
Paull, S. 9099
Pavlov, B.V. 7674
Pawling, J.F. 6854
Payne, H. 6967
Paynter, D.A. 6864
Peacock, R.N. 6116
Pearce, J.R. 6541
Pearlman, N. 7398
Pearson, A.D. 6773, 8985
Pearson, J.D. 6543
Pearson, J.J. 7637
Pearson, R.F. 7640
Pedersen, B.O. 7488
Pedersen, L. 7505
Pederson, D.O. 7142, 7479, 7742, 7763
Pedko, A.V. 6428
Pedrotti, L.S. 7385, 8887
Peet, C.S. 8624, 8872
Peil, W. 6582
Pell, E.M. 6019, 6337, 6638, 6753, 7571, 7574, 7867, 8625
Pellikan, S.G. 7147
Pellin, R.A. 6958
Pelzl, H. 7166
Pemrov, A.V. 7682
Pendergast, R.J. 8833
Penfield, Jr., P. 6823
Pepinsky, R. 6387, 8173
Pepper, R.S. 7142, 7479
Peria, W. 9289
Perkal'skaia, V.A. 8966
Perkins, G.D. 6944
Perl, M.L. 9032
Perlin, Yu. E. 8860
Perlow, G.I. 8311
Perry, G.H. 6587
Pershan, P.S. 7720
Peter, M. 6449, 7357, 8352
Peters, A.J. 6103
Peters, L.A. 7164
Peterson, J.D. 7705
Peterson, W.C. 7119
Petrak, J.R. 7204, 9145
Petrakovskii, G.A. 8813
Petritz, R.L. 6467
Petrolo, J. 8220
Pettit, G.D. 7396
Pfann, W.G. 6029, 6251, 7857
Pfyffer, H. 8489
Phariseau, P. 7588, 8657
Philipp, H.R. 7320, 7394
Philips, Jr., W.L. 7692, 7693
Phillips, J.C. 6066, 6180, 9216
Pickart, S.J. 6154, 9365
Pickering, B.A. 8154
Pickover, M.B. 6898
Pidd, R.W. 9313
Pietrzak, J. 8686
Pihl, C. 6333
Piksis, A. 7386
Pikus, G.E. 7912
Pinckaers, B.H. 6895
Pincus, P. 8781
Pinkerton, A.P. 9230
Piper, W.W. 6133, 9409
Pippin, J.E. 6564
Pisa, G. 7420
Pistol'kovs, A.A. 8037
Pittelli, E. 7650
Pitzalis, O. 7121, 8487
Plath, R.H. 9054
Plendl, J.N. 7917
Ploos van Amstel, J.J.A. 9012
Plotkin, S. 7158
Plus, L. 6857
Plyavin, I.K. 7983
Poberovskaya, I.S. 7311
Pohl, H.A. 7008, 7028
Pohl, R.O. 6201, 6725
Pohm, A.V. 6586, 6802, 6878, 6886, 8497, 9070
Pokrovskii, V.N. 8656
Pollak, M. 6068, 8724
Pollak, P.I. 7578
Polonskii, Iu, A. 7901
Poltinnikov, S.A. 7300
Polukarov, Yu. M. 8289
Pomerantz, M.A. 7024
Pope, A. 6290
Poplavskaya, O.I. 8502
Poplawsky, R.P. 7266
Popov, Yu. M. 8470
Popova, A.A. 7960
Porbansky, E.M. 8200
Porfir'eva, N.N. 9271
Porreca, G. 7211
Porsche, H. 7790
Porter, C.S. 9364
Porter, J.H. 6853
Porter, J.L. 6955
Portis, A.M. 6146, 6705, 6709, 7284, 7666, 9423
Post, D. 9445
Potakhova, G.I. 8674
Potekhina, N.D. 7307
Potter, F.J. 8058
Potter, N.L. 6540
Poulis, N.J. 7653
Powell, R.C. 7592
Power, M. 9399
Powers, E.J. 6843
Powers, J.K. 7270
Prager, H.J. 6561
Pratt, Jr., G.W. 6059, 8655
Pratt, P.L. 8938
Prener, J.S. 8871, 9406
Presnov, V.A. 8299
Pressman, W. 7328
Preston, R.S. 8311
Pretzel, F.E. 7681
Prewitt, C.T. 7851
Price, Jr., C.H. 7154
Price, P.J. 7411, 7663, 8723, 9307
Price, R.J. 9086
Priebe, Jr., H.F. 6883, 7806
Primak, W. 9445
Pringle, D.H. 8114, 8221
Pringle, J.P.S. 7234
Prior, A.C. 6101, 8709
Prior, J.R. 8372
Prise, W.J. 8448
Proebster, W.E. 6578, 6579
Proffitt, P.M.C. 7687
Prokhorov, A.M. 8343, 8355
Prosen, R.J. 7043
Prosser, V. 7997, 8908
Prudnikov, I.N. 8098
Prugh, T.A. 6257
Prussin, S.A. 6650
Prutton, M. 8795
Pruzhinina, V.I. 9021
Pry, R.H. 6432, 9344
Pucel, R.A. 6487
Pugachevich, P.P. 8160
Pugh, E.W. 6430
Pugsley, I.D. 7477
Pulfer, J.K. 8089
Pultorak, J. 8977
Pulvari, C.F. 7294
Pustynskii, I.N. 8107
Putkovich, R.P. 9134
Putley, E.H. 8731
Putzer, E.J. 9379
Queisser, H.J. 6785
Quilliet, A. 9426
Quinn, D. J. 8743
Quinn, H.F. 6994
Quirk, E.J.M. 6377, 8127
Raal, F.A. 8457
Rabenau, A. 7589
Radcliffe, Jr., A.J. 7265, 7499
Rado, G.T. 6140
Raff, S.J. 7828
Raffel, J.I. 8540, 9126
Rafuse, R.P. 6544
Raillard, H. 8200, 6556
Raisbeck, G. 9271, 8993
Rama Char, T.L. 7211, 6995
Ramazanov, P.E. 7790, 8890
Ramdas, A.K. 8862, 8863
Ramsa, A.P. 6853, 8260
Ramsay, D.A. 6955, 7144
Ramsey, J.B. 8627
Ranby, P.W. 7439, 9423
Rand, M.J. 9445, 7713
Raney, W.P. 8674, 6212
Ransom, P. 7307, 6028
Rappaport, P. 8058, 6519
Rase, D.E. 6540, 8580
Rashba, E.I. 7318, 7653, 7935
Raskin, J.S. 7592, 7181
Rasmussen, A.L. 9399, 7592
Rasmussen, R.A. 6843, 8036
Rasor, N.S. 7270, 9441
Ratner, A.M. 8876, 6561, 8877
Ratner, E.S. 6059, 8565
Ratner, M. 6080
Rauch, C.J. 8938, 6123
Rauscher, D. 7423
Rautenberg, T.H. 8299, 9429
Ravich, L.E. 7328, 8214
Ray, B. 6624, 7230, 8311, 7546
Ray, C.E. 7681, 7112
Raybold, R.L. 7851, 6666
Raymo, C.T. 7154, 8570
Rayne, J.A. 7405, 7663, 7406
Rayner, M.J. 8281
Razbash, R. Ya. 9086, 7599
Razbirin, B.S. 6883, 8888
Razmadze, A.K. 7310
Read, A.A. 6802, 6878, 8497, 9070
Read, P.L. 7597
Read, Jr., W.T. 8954
Reade, R.F. 8372, 6950
Redfield, A. 8448, 8843
Rediker, R.H. 6578, 6226, 8964
Redmond, K. 7199, 7465, 7731
Reeber, M.D. 8343, 6119, 6411
Reed, B. 6072, 8896
Reed, H.J. 7043, 7196
Reed, J.F. 8908, 8615
Rees, D. 8098, 9052
Reese, J.D. 6257, 6230
Reese, W.E. 6650, 7027, 8861
Reggia, F. 8795, 6528, 8461
Reich, B. 9021, 7732
Reid, F.J. 9344, 6499
Reiffel, L. 6487, 7387
Reinberg, A.R. 8160, 7236, 7657
Reingold, I. 6430, 7724
Reiss, H. 7477, 7226
Reiss, R. 8089, 7671
Renius, O. 8977, 9052
Renner, T. 7294, 6626
Rettinger, M. 8107, 7170
Reukauf, D.C. 9134, 7792
Reuschel, K. 8731, 9286
Reuther, J.F. 9379, 8579, 9095
Revuz, J. 8430, 8431
Reynolds, D.C. 6785, 6011, 7385, 7880, 7881, 8873, 8887, 9405
Reynolds, J.M. 6120, 9296, 9438
Reynolds, W.N. 7583
Rez, I.S. 6089, 7596
Reznik, M.V. 8198
Rhoderick, E.H. 6289, 6697
Rhoderick, E.N. 8281
Rhodin, T.N. 8205
Rhys-Roberts, C. 8681
Riabinkin, Iu.S. 8995
Richards, J.C.S. 6293
Richards, J.L. 6342, 7270, 8641
Richards, R.K. 8506
Richardson, D.A. 8648
Richardson, J.M. 6395, 8707
Ridinger, P.G. 6246
Ridler, D.S. 8544
Ridley, B.K. 6094
Rieckhoff, K.E. 7968
Riederman, N.H. 6974
Riggs, R.H. 7750
Rimai, L. 7972, 8845
Rimmer, M.P. 6473
Ridner, W. 6769
Roach, W.E. 6264, 6762
Robbins, H. 6373, 6985, 6986, 8139
Robbins, P.B. 6203
Robbrecht, G.G. 6477
Roberts, D.H. 8898, 9279
Roberts, J.A. 6786
Roberts, L.D. 6303, 6908
Robertson, I.S. 7980
Robertson, W.J. 7492
Robin, J. 8270
Robinette, S.L. 6595
Robinson, B.J. 6247, 6448, 8070
Robinson, C.F. 6944
Robinson, L.E. 9065
Robinson, N.D. 8135
Robinson, N.O. 8097
Robinson, R.J. 6095, 6192, 6419, 8702, 9309
Robinson, S.A. 9016
Robinson, W.A. 6237
Robinson, W.H. 9165
Robinson, W.K. 6148
Rocard, Y.A. 9025
Rodgers, G.B. 8457
Rodrigue, G.P. 7054
Rodrigues de Miranda, H. A. 8517
Roehling, D.H. 9313
Rogers, J.L. 8464, 9038
Rogers, J.N. 8315
Rogers, S.C. 9094
Rogh, R.S. 6086
Rogoff, M. 8148
Rohrer, H. 8746
Rollin, B.V. 8267
Rollins, F.R. 9164
Romanenko, V.N. 7866
Romankevich, V.N. 8728
Rongen, J. 6856
Rood, J.W. 8099, 9096
Root, C.D. 7413, 7417
Roovers, W.A. 8953
Ropp, R.C. 6189
Rosado, J.A. 6216, 6217
Rose, A. 6783
Rose, F.W.G. 6104, 8715
Rosenbaum, J. 8446
Rosenberg, A.J. 6003, 6108, 6979, 7231, 8228, 8229, 8635
Rosenberger, G.B. 7449
Rosenblum, R. 9303
Rosenstock, H.B. 8241, 9401
Rosenthal, L.A. 7159
Roshon, Jr., D.D. 6434
Rosi, F.D. 6357, 7271, 8459, 8616, 8932
Rösner, O. 8619
Rossol, F.C. 7348
Roth, L.M. 6168, 9305
Roth, R.S. 6082, 6160
Roth, W.L. 7035, 7561, 8204
Rothstein, J. 6755
Rothwarf, F. 8277
Rowen, J.H. 7169
Rowland, T.J. 9383
Rowley, L.H. 9142
Royce, B.S.H. 6113
Rubin, B. 6035
Rubin, L.G. 8187
Rubin, R.J. 7590
Rubin, W.L. 9059
Rubinstein, H. 7038
Rudenberg, H.G. 8960
Rudness, R.G. 6040
Rufer, R.P. 8553
Runyan, W.R. 7102
Rupert, G.N. 7681
Rupp, R.L. 6940, 8614
Ruppel, W. 9290
Rupprecht, G. 6064, 7996, 9212
Rupprecht, H. 9286
Rush, J.J. 7585
Rushbrooke, G.S. 8306
Rushing, C.C. 7681
Russel, J.P. 8267
Russell, D.J. 7822
Russell, G. 6649
Russell, R.D. 7814
Rustgi, O.P. 8394
Ruth, R.P. 7885, 7887
Rutter, J.W. 8971
Ryan, W.D. 6553
Rywak, J. 9144
Ryvkin, S.M. 7307, 7391, 7605

Saada, G. 8601, 8607
Saari, V.R. 6513
Saburi, O. 8255
Saburi, T. 9171
Sachs, H.M. 9018
Sachs, M. 7361
Sachse, H.B. 6642
Sagar, A. 6060, 6068, 6111, 6378, 8639
Sager, G. 8058
Saha, A.R. 7151
St. Johnson, A. 6284
Saintesprit, R. 6335
Saito, H. 6056
Saito, S. 7525
Sakiotis, N.G. 6529
Sakrison, D.J. 7463
Sakudo, T. 8225
Salkovitz, E.I. 8793, 8930
Salmi, E.W. 9313
Salter, F. 7187
Samelson, H. 7874, 9181
Sampson, D.F. 6169, 7969
Samusenko, A.G. 6571
Sandberg, I.W. 7734
Sandler, N.P. 6650
Sandlin, B.T. 8402
Sandulova, A.V. 6951, 7567

ANNUAL CUMULATIVE AUTHOR INDEX

Sangster, R.C. 6341
Santilli, R.A. 6857, 7778, 7779
Santini, M. 8834
Saphir, R. 6947
Sarachik, M.P. 6061, 6408
Sard, E.W. 6552, 7134, 8079
Sasaki, Y. 6010, 6012, 6442, 9051
Sato, H. 9215, 9326
Sato, I. 9051
Sauer, H.A. 8235
Sauer, J.A. 9155
Saunders, J. 6145, 6243, 6794
Saunders, N.H. 6682
Saunders, N.N. 8406
Saunders, W.K. 6215
Sauzade, M. 7813
Savage, A. 6677, 8250
Savage, H. 6662
Savchenko, M.K. 8805
Savintsev, P.A. 8164
Sawaguchi, E. 6084
Scanlon, W.W. 7254
Scarbrough, A.D. 9084
Scarr, R.W.A. 7111
Schaefer, G. 8363
Schaeve, D.K. 8511
Schaffner, G. 6833
Schauer, R.F. 6802, 6878
Schawlow, A.L. 7106, 7360, 7386
Schellekens, A.M.H. 8526
Scherer, P.M. 7931
Scheuplein, R. 8183
Schieber, M. 6977, 7904
Schieve, W.C. 6377, 7024
Schlimpf, L.G. 6855
Schindler, A.I. 8793
Schlaeppi, H.P. 6590, 6885
Schlax, T.R. 8086
Schlereth, F.H. 7195
Schleuning, H.W. 6974
Schloemann, E. 6144, 6145, 6526, 6706, 6710, 7959
Schlosser, H. 7906
Schmeltzer, R.A. 6509
Schmidlin, F.W. 6813
Schmidt, J.D. 7195
Schmidt, P.F. 7017
Schmitt, E.J. 8546
Schnable, G.L. 9017
Schneider, B. 6766
Schneider, E.E. 8152
Schneidmesser, B. 7073
Schofer, H.S. 6086
Schossberger, F.V. 7886
Schreiber, W.F. 8507
Schubert, J. 8498
Schuele, W.J. 6972, 9327
Schulman, J.H. 7502
Schultz, J.B. 6551, 8523
Schultz, J.M. 6643
Schultz, J.W. 6936
Schultz, T.D. 9247
Schulz, D.P. 6735, 8548
Schulz, R.B. 9146
Schupp, L.J. 9190
Schüppel, W. 8797
Schwartz, B. 6373, 6504, 6985, 6986
Schwartz, C.M. 6203
Schwarz, R.F. 7017
Schweinler, H.C. 8823
Schwuttke, G.H. 6336, 6945
Scott, A.B. 6717
Scott, B. 8407
Scott, D.C. 7113
Scott, G.G. 7343, 9333
Scott, N.J. 9156
Scott, R.G. 9188
Scouler, W.J. 7059
Scovil, H.E.D. 9109
Sears, G.W. 6970, 7579
Sebek, S. 7420
Secunde, R.R. 7533
Seeger, C.L. 8070
Seeger, K. 9253
Seelbach, W.C. 8039
Segal, R.E. 7743
Sehr, R. 6690, 8735
Seiden, P.E. 6241, 6439, 9368
Seidensticker, R.G. 6350, 6656, 7888, 7890
Seifert, J.R. 7615
Sekiyama, H. 9373
Selig, T.R. 7082
Selikson, B. 6685
Selwood, P.W. 9337
Semenenko, E.E. 8757
Senatorov, K. Ya. 8502
Serbulenko, M.G. 8948
Serova, F.G. 8923
Sestak, B. 8599
Sette, D. 9262
Setterington, R.A. 7111
Shafer, M.W. 8157
Shafer, W.L. 6883
Shain, J. 6470
Shal'nikov, A.I. 8285
Shanavi, G.I. 9232
Shapiro, D.N. 8062
Sharpe, C.B. 6675, 8670
Sharpe, G.E. 7456
Shashkov, Yu. M. 8199
Shatas, R.A. 6377, 7024
Shavlo, S.T. 8380, 8886
Shaw, D. 7437
Shaw, H.J. 6241, 6439
Shaw, R.W. 7312, 8284, 8748, 8756, 9292
Sheard, F.W. 7685
Sheff, S. 6346
Sheleg, A.U. 8242
Shen, R. 6496
Shenker, H. 6112
Shepherd, A.A. 7435
Sherin, R.J. 6599
Sherman, B. 6239
Sherrill, M.D. 8282
Sherwell, R.J. 8956
Sherwood, J.N. 8219
Shevchenko, I.B. 7392
Shevel, Jr., W.L. 6588, 6801, 6804, 9350
Shibata, A. 8166
Shiffman, C.A. 6117
Shiklosh, T. 8780
Shilliday, T.S. 8870
Shimizu, M. 7356
Shiozawa, L.R. 6962
Shirane, G. 6083, 6676, 6679, 6704
Shiren, N.S. 9377
Shirer, D.L. 8563
Shirkov, D.V. 8740
Shockley, W. 6744, 6754, 6785, 7545, 8017, 8922, 9080, 9221
Shombert, D.J. 6941, 7736
Shortes, S.H. 6953
Shotov, A.P. 6399, 8967
Shrader, R.E. 6235
Shtivel'man, K. Ya. 7911
Shtrikman, S.S. 7904, 8804, 9338
Shul'man, A.R. 7630, 8178, 8300
Shulman, R.G. 7358, 9384, 9385
Shur, Ya. S. 8800
Shvarts, K.K. 8875
Shvartsenau, N.F. 7565
Shveikin, V.I. 8024
Sickert, R.G. 8576
Sidhu, S.S. 6153
Sidiakin, V.G. 8728
Sidles, P.H. 6199
Sie, J.J. 8077
Siegel, B.M. 8205
Siegman, A.E. 7950, 8473
Sievers, III, A.J. 7048
Sigorskii, V.P. 8052
Sihvonen, Y.T. 6667, 6780
Sikkeland, T. 6915
Silber, L.M. 6793, 6974
Silliman, S.D. 9095
Sils, V. 8982
Silver, M. 6658, 7927
Silverman, J. 9446
Silverman, S.J. 7264
Silverstein, S. 7711
Silvestri, V.J. 8159, 8582
Sil'vestrova, I.M. 6043
Simmons, C.D. 6860, 7484
Simmons, R.O. 7241
Simon, A.H. 8113
Simon, R.E. 6363, 6722, 6981, 7072, 8390
Simonov, Iu. L. 7132
Simons, S. 7999
Simpson, O. 6591, 8573
Sims, A.R. 7526
Sims, G.D. 7733
Sinani, S.S. 7401
Sinclair, R.N. 7332
Sines, G. 7895
Singer, K. 7170
Singh, S.P. 8665
Singwi, K.S. 8666
Sinha, A.P.B. 8590
Sinyakov, E.V. 8815, 9245
Sirgo, H.V. 7270
Sirota, N.N. 8181, 8242
Sirvetz, M.H. 6145
Sivo, L. 6393
Skinner, P. 8132
Skrotskii, G.V. 8906
Slack, G.A. 6707, 7071
Slade, A.E. 6810, 7512
Sladek, R.J. 7305, 7306, 7317, 9299
Slavikovskii, G.F. 8180
Slifer, L.W. 7729
Slifkin, L. 7557
Sloan, S.C. 7113
Slobodzinski, E.J. 8508
Slonczewski, J.C. 7327
Sluss, Jr., J.A. 6767
Smagin, A.G. 8049
Smakula, A. 6966, 7059, 7060, 7239
Smallman, C.R. 6554, 6809, 7512
Smallman, R.E. 9157, 9197
Smart, J.S. 7635
Smethurst, J.O. 7505
Smilen, L.I. 7143
Smiltens, J. 6625
Smirnov, I.A. 7682, 7683
Smirnova, T.V. 6206
Smirous, K. 7919
Smith, A.C. 6220
Smith, A.D. 6290
Smith, A.W. 7052, 7646, 8566
Smith, D.N. 8374
Smith, D.O. 7042, 8796, 9355
Smith, F.A. 6465
Smith, G.W. 8346, 8844
Smith, J.F. 6210, 8411
Smith, J.G. 9048
Smith, K.C. 6795, 9317
Smith, M.J. 8268
Smith, N.R. 9143
Smith, P.H. 6221
Smith, P.L. 8271
Smith, R.C. 6353
Smith, S.D. 8911
Smith, T. 7980
Smith, W.A. 7594
Smith, W.J. 6349, 7891
Smith, W.L. 7478
Smits, F.M. 7085
Smokotin, E.M. 7896, 8811
Smoluchowski, R. 6006, 7237, 7238, 7556, 8729, 9165
Smorodina, T.P. 7552
Smulkowski, O. 7208
Smyth, R.R. 7201
Snitko, O.V. 7283
Snowden, D.P. 7284
Sobolev, V.V. 8866
Sobolevskaya, R.B. 7630
Soden, R.R. 8381
Sofar, L. 7421
Soloman, A.H. 8087
Solomon, A.L. 6531
Solomon, R. 6741
Soltoff, B.M. 7783
Soma, T. 6872
Somlyody, A. 6266
Sommer, R.D. 9129
Sonder, E. 8237, 8645, 8823
Sondhauss, C. 7752
Sonin, A.S. 6089
Soohoo, R.F. 6426, 7331, 9322
Sorenson, A.A. 7198
Sorger, G.U. 7828
Sorokin, P.P. 7669, 7965
Sorrows, H.E. 6467
Sosniak, J. 9302
Sosnowski, L. 6073
Southgate, P.D. 6213, 8945, 8946, 8947
Spacek, L. 8005
Spain, B. 7456
Sparkes, J.J. 7094
Sparks, J.E. 7156
Sparnaay, M.J. 6368
Spear, W.E. 7607
Spector, C.J. 6370, 8417
Spedding, F.H. 6151, 7016, 8274, 8736
Spence, R.D. 6158, 6708
Spencer, C.W. 8268
Spencer, E.G. 6143, 7051, 8328, 9364
Spencer, H.E. 6469, 7011
Spencer, R.H. 7160
Speros, D.M. 9190
Spicer, W.E. 6222, 6722, 8390
Spiegel, P. 6879
Spiess, P. 7420
Spinner, S. 9449
Spitzer, W.G. 8227, 8855
Spokas, J.J. 7013
Sprague, R. 6633
Spratt, J.P. 7097
Spriggs, S. 7886
Sproull, R.L. 6981
Spruch, G.M. 6470
Spry, W.J. 7931, 8291
Spyut, A.B. 9013
Sree, V. 6995
Srivastava, K.G. 6629, 9317
Srygley, O.C. 6845
Staar, D.A. 6848
Stachiewicz, B.R. 8524
Stafeev, V.I. 7075
Stafiichuk, E.A. 9245
Stambaugh, E.P. 6360
Stanchi, L. 7415
Standley, K.J. 8810
Staniforth, A. 6267
Stankevich, K.S. 8829
Stankowska, J. 9241
Statz, H. 6421, 6712, 8774, 8845
Stauss, H.E. 9367
Stavik, O. 6514
Steele, D.R. 6277
Steele, E.L. 7471
Steele, M.C. 6777, 7934
Steenis, O.L.V. 8953
Steiger, W. 7755, 8010
Steimle, W. 7468
Stein, F.S. 6227
Stein, H.J. 6672
Steinberg, R. 6608
Stemme, O. 8797
Stemple, N.R. 7292
Stepanov, A.V. 8409
Stepanova, A.A. 8288
Stephenson, I.M. 7733
Stephenson, W.L. 6897, 9138
Stern, D.R. 6355
Stern, E. 6674, 7114, 9036
Sternglass, E.J. 6054, 9200
Sterzer, F. 6570, 8087
Stevens, K.W.H. 8469
Stevenson, A. 6650, 7916
Stevenson, I.R. 8020
Stevenson, M.J. 7669, 8768
Stevenson, R. 9371
Stevenson, R.W.H. 7980
Stewart, J.L. 7096
Stewart, Jr., R.M. 6802, 6878
Stewart, W.C. 7728
Stickler, J.J. 6123
Stinchfield, R.P. 8936
Stineman, J.W. 9016
Stinson, D.C. 9187
Stitch, M.L. 8097
Stocker, C.F. 7081
Stockmann, F. 8612
Stoddard, A.E. 7388
Stokes, R.J. 7695
Stone, B. 8732
Storms, E.K. 7681
Stoudenheimer, R.G. 9033
Stourac, L. 7919
Stout, J.W. 9385
Strakhov, L.P. 7678
Straley, R. 6798
Strandberg, M.W.P. 6805, 7355, 8340
Stratton, L.J. 7519
Stratton, R. 6397, 8712
Straumanis, M.E. 9154
Strauss, A.J. 6003, 6108, 6339, 6344, 6931, 7247, 7878
Stride, A.A. 9273
Strong, H.M. 7899
Strull, G. 9117
Strumane, G. 6631, 6937
Struthers, J.D. 6946, 7233, 8762
Strutt, M.J.O. 6766, 7129, 8297, 9019
Struzhinskii, V.A. 7712
Stuart, R.A. 6292
Stuckes, A.D. 6202
Studders, R.J. 9332
Steutzer, O.M. 6542
Stupp, E. 6171
Su, K.L. 9058
Subashchiev, V.K. 7300
Subbarao, E.C. 6676, 6678, 6679, 7600
Subramanian, M. 7491
Suchet, J.P. 7907, 9202
Sudovtsev, A.I. 8757
Suemitsu, D. 7521
Sugano, S. 7357, 7358, 7360, 7386, 9373
Sugano, T. 6764
Sugarman, R.M. 6605
Suge, Y. 8767
Sugihara, M. 9345
Sugioka, E. 9397
Sugiura, Y. 7966, 8304, 9354
Sugiyama, K. 8007, 9282
Suhl, H. 6138, 6195, 6240, 6694, 8744, 8806
Sullivan, D.J. 6790, 7038
Summers, D. 6824
Summers, T. 6290
Suomi, V.E. 9108
Suran, J.J. 7122
Suss, J.T. 6714
Sussman, A. 7110
Suzuki, N. 8276
Suzuki, T. 8787
Svirina, E.P. 8763
Swalin, R.A. 8620
Swanson, J.A. 6581
Swartz, J.M. 8872
Swenson, C.A. 9152
Swenson, Jr., G.W. 9111
Swift, W.B. 7482, 9108
Swihart, J.C. 6693, 8754
Swoboda, C. 7774
Swoboda, T.J. 7033
Sydnor, R.L. 9111
Sylvan, T.P. 8533
Symons, N.K.J. 9188
Synorov, V.F. 8299
Szabo, A. 7970
Szaynok, A. 6078, 6385
Szegho, C.S. 9024
Szekely, M.E. 7509
Szerlip, A. 7777
Szigeti, B. 7672
Szymanski, B. 8358

Tabellini, L. 7801
Taborko, N.I. 8456
Tachikawa, K. 6742
Taft, E.A. 7320, 7394
Tagaya, M. 9171

ANNUAL CUMULATIVE AUTHOR INDEX

Tagoshima, I. 8095
Takagi, S. 7824
Takagi, T. 8081
Takei, W.J. 6704
Takeuchi, N. 9397
Tallan, N.M. 6081
Talley, T.J. 7505
Tamai, Y. 9195
Tamiya, J. 8076
Tanabe, Y. 6038, 8213
Tanaka, S. 8257, 8767
Tanaka, T. 8257, 8365, 8366, 9244
Tancrell, R.H. 6577, 7183
Tanenbaum, M. 6322, 6620
Tanis, A.P. 8526
Tannenbaum, E. 6751, 8629
Tannhauser, D.S. 8733
Tansal, S. 8754
Tanttila, W.H. 9378
Tarpinian, A. 6663
Tatsumoto, E. 8321
Tauc, J. 8392
Taylor, G.O. 6708, 8401
Taylor, K.N.R. 6654, 6688, 8883
Taylor, N.H. 8532
Taylor, R.C. 7077
Taylor, T.C. 7026
Taylor, T.I. 7585
Teaney, D. 6709, 7666
Tebble, R.S. 8406
Tefft, W.E. 8936
Teitler, S. 7295, 7679
Temko, K.V. 7418
Templeton, I.M. 6602
Templeton, L.C. 8237, 8645
Tenzer, R.K. 9346
Terhune, R.W. 6447, 8471, 9047, 9050
Terman, L.M. 7438
Tewordt, L. 8737
Thanos, H. 7778
Thaxter, J.B. 6242
Theuerer, H.C. 6017, 7268
Theus, R. 7506
Thien Chi, N. 8458
Thies, A.W. 8111
Thomas, D.E. 6701, 8278
Thomas, D.G. 7604, 8361, 8850, 9250, 9399
Thomas, H. 6435
Thomas, Jr., J.E. 7250, 7265, 7266, 7947, 8210
Thomas, K. 9163
Thomas, L.A. 7884
Thomas, L.C. 7746
Thomas, N. 8869
Thomas, R.C. 7082
Thompson, C. 6822
Thompson, F.C. 6825
Thompson, G.J. 9134
Thompson, H.D. 6943
Thompson, J.E. 6286, 9452
Thomson, A.F.H. 8038
Thomson, R. 8604
Thomson, S.J. 8219
Thorensen, R. 8542
Thorington, L. 8455
Thornton, W.A. 7063
Thorp, J.S. 6169, 7969
Thouless, D.J. 8739
Thun, R. 8627
Thurell, Jr., J.R. 8991
Thurmond, C.D. 6001, 6179, 6338, 7232
Thurston, M.O. 7133
Tiablikov, S.V. 8780
Tiemann, J.J. 6488, 6740
Tiisler, E.S. 8375
Tiley, J.W. 9015
Tiller, H.D. 7389
Tiller, W.A. 6954, 6957, 8632, 8971
Tillman, R.M. 6884, 6589, 9090
Tilton, R.S. 7781
Timofeev, V.B. 8369
Timofeeva, V.A. 7876
Tink, E.M. 8531
Tinkham, M. 7048, 8853
Tippett, J.T. 7795
Tipple, P.M. 8427
Tirmizi, S.M.A. 7073
Title, R.S. 8383, 8893
Tkach, G. 6798
Tobocman, W. 6691
Todd, C.E. 8010
Tollin, G. 6719, 7992
Toman, K. 8589
Tomásek, M. 7004, 8239, 9205
Tomboulian, D.H. 7269, 7381
Tomik, J. 8671
Tomita, T. 6023
Tomono, M. 7704, 8026
Tompkins, H.E. 9125
Tompkins, J.E. 6528
Tomura, M. 9419
Tonoyan, A.A. 8181
Tornillo, L.M. 6814
Tosi, M.P. 6382
Toth, J.R. 7519
Toth, R.S. 7883
Townes, W.D. 8831
Towns, G. 7076
Townsend, J.R. 7902
Toy, W.N. 6883, 9098
Toyoda, H. 8609
Traite, M. 7117
Trambarulo, R.F. 7472
Trapeznikova, Z.A. 8878, 8879
Trapnell, B.M.W. 9192
Tredgold, R.H. 8681, 8682, 8713
Trenholme, W.M. 7214
Treuting, R.G. 6367, 6646
Treves, D. 7034, 8804
Triebwasser, S. 8680
Trivich, D. 7883
Trofimenko, A.P. 7310, 7935
Troinar, E. 9293
Trokhimenko, Ia.K. 8056
Troup, G.J. 7443
Trousdale, R.B. 9082
Truell, R. 6480
Truesdell, R.M. 7146
Trumbore, F.A. 6002, 6686, 8200
Tsarenkov, B.V. 8419
Tsekvava, B.E. 8909
Tsepelevich, E.E. 6089
Tsikin, A.N. 7901
Tsubokawa, I. 8818
Tsui, R.T.C. 6410
Tsuzuku, T. 9172
Tubota, H. 8276
Tucker, E.B. 8341
Tulp, T.J. 8517
Tummers, L.J. 8994
Turchinskaya, M.I. 8318
Turnbull, A.R.T. 7462
Turner, D.R. 6372, 6661, 6982, 6987, 8235
Turner, E.F. 6216
Turner, E.H. 7051
Turner, J.A. 6288
Turner, K.I. 6286
Turner, W.J. 7027, 8861
Turobinski, T.J. 8223
Turov, E.A. 8794, 9321
Tutihasi, S. 8368
Tyler, W.W. 9424
Tyson, C.B. 7783
Ubbink, J. 6247
Uchaikina, R.F. 8825
Uchida, Y. 8367, 8393
Uehara, Y. 6188, 6463
Uehling, E.A. 9234, 9235
Uenohara, M. 6829
Ufimtsev, B.F. 8164
Uher, E. 7263
Uhlir, A. 8959
Unterleitner, F.C. 6167
Ure, Jr., R.W. 6239, 7400
Uritskii, Z.I. 7373
Vacek, K. 7981
Vaddiparty, Y.P. 7751
Vager, Z. 6977
Vail, C.R. 7728
Van Allen, R.L. 6262, 7211
Van Arkel, A.E. 8337
van Berkum, P.A. 7166
van Biljon, L. 8025
Van Bosse, J.G. 9116
Vance, A.W. 7481
van Dam, J.F. 8526
van Damme, K.J. 8070
van den Broek, J. 7962
van der Does de Bye, J.A.W. 6684
van der Heide, H. 8538
van der Lugt, W. 7653
van der Maesen, F. 6683, 7273
van der Pauw, L.J. 7308, 9276
Van der Velde, J.C. 6606
van der Ziel, A. 6232, 8076
van Dijkum, A.N. 6856
van Gool, W. 9414, 9415
Van Houten, S. 8719
van Lieshout, L.J.A. 6846
van Ligten, R.H. 7708
van Lint, V.A.J. 8649
Van Ommen, B. 8040
van Oosterhout, G.W. 7550
Van Ostenburg, D.O. 6445
van Overbeek, A.J.W.M. 8512, 9061
Van Putten, Jr., J.D. 6606
Van Roosbroeck, W. 8261
van Santen, J.G. 6518, 7145
Van Sciver, W.J. 7064
Van Soest, P.C. 7827
Van Styvendael, M. 6481
van Tol, M. 7206, 7213
Van Uitert, L.G.G. 6367, 7061, 8222, 8381
Van Vleck, J.H. 9369, 9372
Van Vliet, K.M. 9256
Varsanyi, F. 7360
Vartanian, Jr., P.H. 8100
Vaughan, W.H. 7256
Vavilov, V.S. 6521, 8373
Veach, C.W. 8949
Vedam, K. 6387, 8173
Veigele, W.J. 9378
Veloric, H.S. 7249, 7423
Venables, J.D. 6347, 8206
Vendlerova, V. 7420
Verber, C.M. 9378
Verderber, R.R. 9183
Vereshchagin, I.K. 8880
Vergnolle, J. 8458
Verhaeghe, J.L. 6477
Verma, A.R. 6952
Vermandé, J. 8415
Veter, V.V. 8323
Vick, G.L. 6402, 6404, 8410, 8935
Vickery, J.C. 7820
Vierhout, R.R. 6899
Vincent, D.H. 8311
Vincent, J. 7716
Vincent, R. 6559
Vineyard, G.H. 6997
Vinogradoso, B.N. 7148
Vinokurov, L.A. 7986
Vinokurov, V.M. 8348
Vinopal, J. 7420
Visvanathan, S. 7376, 7380
Vitasek, E. 9223
Vitol, I.K. 7983
Vladimirov, V.I. 8595
Vlasov, K.B. 8301, 8783
Vodicka, V.W. 7137, 7710
Vodop'ianov, K.A. 8674, 8675
Vogel, J.S. 7129
Vogt, K.S. 8503
Vogt, O. 7619, 8824
Volger, J. 8652
Volkenshtein, N.V. 8318
von Aulock, W.H. 7641
von Baeyer, H.C. 7074
Vonsovsky, S.V. 9321
Vorob'ev, A.A. 7235, 8164
Vorozhtsov, B.I. 8674, 8675
Vosko, S.H. 9381
Vul, B.M. 8470
Wachtel, A. 6462, 7677, 7988
Wachtman, Jr., J.B. 8936
Wada, E. 6872
Waddas, R. 8814
Wade, G. 8065
Wadsworth, M.E. 8636
Wagner, Jr., J.B. 8158
Wagner, M. 8895
Wagner, P.E. 8344, 8468
Wagner, R.S. 6033, 6323
Wagoner, G. 8772
Wahl, F. 8596
Wainfan, N. 7871, 9156
Wainwright, H.W. 9127
Wajda, E.S. 8628
Wakefield, J. 6032, 7573, 8202
Waku, S. 9244
Waldner, M. 6393
Waldron, R.A. 8466
Walker, L.R. 6449, 7647, 7952
Walker, P.A. 8919
Walker, W.P. 7079
Wallace, D.C. 6199
Wallace, L.F. 7101, 7433
Wallace, W.E. 7259, 7349, 9374
Waller, E.E. 7130
Wallis, R.F. 7295, 7909, 7918
Wallmark, J.T. 6347, 6538, 6775, 7509
Walmsley, R.H. 7943
Walter, F.J. 6303, 6908
Walter, J.L. 9334
Walters, G.K. 9193
West, E.J. 6992
West, F. 8950
West, J.W. 8983
Westmacott, K.H. 9041, 9157, 9197
Westwood, A.R.C. 7648
Wentzel, G. 7689
Wernick, J.H. 7020, 7229, 8194
Wertwijn, G. 8742
Wessel, G.K. 6760
West, G.K. 7444
Wheatley, C.F. 7779
Wheatley, C.J. 8064
Whelan, J.M. 6946, 7233, 8762
Whetten, N.R. 7023, 9316
White, B.H. 6756
White, D.L. 6681
White, F.A. 8927
White, G.K. 8403
White, H.G. 6063
White, R.L. 6446
White, W.H. 6750, 8628
Whitlock, W.S. 6297
Whitmore, D.H. 9436
Wickham, R. 7576
Widdows, S.J. 6587
Widmer, H. 6652
Wieber, R.H. 8624
Wiechec, W. 6796
Wieder, H.H. 6087, 7007, 9238, 9243
Wiegand, D.A. 6006, 7237, 7238, 7556
Wiencek, Z. 7785
Wiener, G. 9358
Wiese, J.R. 7551
Wigen, P.E. 8838
Wiggins, C.S. 8882
Wiggins, J.S. 6607, 6910, 8569, 8570, 8571
Wikner, E.G. 8649
Wilcher, J.H. 8491
Wilcox, C.S. 9107
Wilcox, D.D. 9119
Wilcox, L.R. 7720
Wildi, B.S. 6424
Wilhelmsen, C.R. 7701
Wilkinson, M.K. 8821, 8822
Wilkner, E.G. 7967
Willardson, R.K. 6319, 6362, 6944, 8509, 8765, 9300
Willens, R.H. 6622
Willett, R.M. 8085
Williams, A.J. 7625, 7946
Williams, C.W. 7807
Williams, F.C. 9123
Williams, F.E. 6185, 6380, 9409, 9429
Williams, G.W. 7646
Williams, R. 6450
Williams, R.A. 9015
Williams, R.C. 6122, 9301
Williams, R.L. 6466, 6517, 6720, 6721, 6909, 6912, 9027
Williams, W.S. 9270
Willis, D.W. 8132
Willis, J.B. 7573, 8202
Weiss, M.T. 6438
Weissfloch, C. 9371
Welkowitz, W. 7117
Wellford, A.L. 7516
Wells, A.F. 8587
Wells, F.H. 8133
Welsh, J.P. 7697
Wendel, G. 7982
Wentore, Jr., R.H. 9196
Weiss, G.P. 7042, 8796, 9355
Weiss, H. 8034
Weiss, J.A. 6525
Weber, H.J. 7808
Weber, M.J. 7354, 8845
Webster, R.R. 8513, 9066
Weertman, J. 7560
Weger, M. 6711, 9376, 9386
Weglein, R.D. 6827, 7136, 7139
Wehner, G.K. 6052, 7279
Wei, Y.M. 6294
Weichman, F.L. 8903, 9425
Weil, F. 8423
Weiman, I. 7529
Weinberg, D.L. 7350, 7351
Weiner, J.R. 6942
Weingarten, L.R. 6941
Weinreich, G. 6063, 6386
Weinreich, O. 6072, 8896
Weinstein, M.A. 9412
Weisbaum, S. 8041
Weisberg, L.R. 6105, 7253, 7271, 8616
Weiser, K. 6020, 6956, 7869
Webb, G.N. 9101
Webb, H.D. 9111
Webb, P.P. 6912
Webb, W.W. 6009, 6034, 6631
Watkins, H. 7078
Watkins, J. 8315
Watkins, T.B. 8969
Watson, R.E. 7638, 7926
Waugh, J.B. 6835, 6914
Weaver, J.A. 6574, 6874
Wasilik, J.H. 7287
Watanabe, A. 7052
Watanabe, H. 8826
Watanabe, N. 8292
Watanabe, Y. 6493
Waters, W.P. 8979
Watkins, G.D. 6050, 6051, 7654

Wilson, B.F. 7829
Wilson, B.L.H. 9279
Wilson, D.K. 6062
Wilson, E. 6894
Wilson, E.S. 8520
Wilson, W.B. 6203
Wiltse, J.C. 9043
Winder, C.F. 8141, 9072
Winkel, J.T. 9136
Winslow, J. 7529
Wintermute, J.T. 7523
Witt, F.J. 6563
Witte, R.S. 6658
Wittels, M.C. 6627
Witteman, W.G. 9313
Wittig, K. 7784
Wittry, D.B. 7228
Wohlers, M.R. 8053
Wojtowicz, P.J. 9151, 9325
Wold, A. 7575
Wolf, A.A. 6564, 8484
Wolf, E.L. 9087
Wolf, H.C. 9392
Wolf, I. 7040
Wolf, M. 6787
Wolf, P. 6579
Wolfe, P.N. 7602
Wolfe, R. 7020
Wolfendale, E. 9137
Wolff, E.A. 9011
Wolff, G. 6573
Wolff, G.A. 8643
Wolff, P.A. 7633, 7675
Wolfson, R.G. 6930
Wolfstirn, K.B. 7608, 9278
Woll, H.J. 8521
Wollam, J.S. 9374
Wollan, E.O. 6137, 8822
Wolsky, S.P. 8637
Wonson, R.C. 8436
Wood, D.L. 7379, 7978, 8364, 9402
Wood, R.H. 7818
Woodbury, H.H. 6164, 7654, 8176, 8770
Woodley, R.E. 6717
Woods, A.D.B. 9217
Woods, J. 7855
Woodward, A.E. 9155
Woodward, J.G. 6250
Woolley, J.C. 6624, 7230, 7323, 7546, 8725
Worrell, E.A. 9056
Wray, K.L. 9435
Wright, D.A. 8928
Wright, G.B. 6130
Wright, M.J. 7812
Wright, P.G. 7197
Wright, W.L. 8577
Wul, B.M. 6399, 8967
Wyder, P. 7611
Wysocki, J.J. 6519, 8008, 8273

Xiao, F.-K. 9041
Xin, H.-W. 8817

Yaek, I.V. 8375
Yafaev, N.R. 8348
Yafet, Y. 7324
Yaffe, T.H. 7503
Yahia, J. 7309
Yamaguchi, J. 8621
Yamaguchi, S. 8308, 8309, 8310
Yamartino, E.J. 9044
Yamashita, H. 8376, 8388
Yamashita, J. 8718
Yanai, H. 6764
Yando, S. 8454
Yaqub, M. 9295
Yaroshetskii, I.D. 7605
Yasufuku, M. 8438
Yatsko, R.S. 6949
Yavin, A.I. 6609
Yeadon, R.E. 8648
Yee, R. 6637
Yefsky, S.A. 7130
Yetter, G.R. 7825
Yetter, L.R. 6149
Yin, H.B. 6551
Yochelson, S.B. 7799
Yokozawa, Y. 8354
Yonemitsu, H. 8294
Yoshida, I. 7289
Yoshida, S. 8092, 8463
Yoshimatsu, M. 7872, 8174
Yoshizawa, M. 8376
Yost, H.J. 9056
Youla, D.C. 7143, 8050
Young, A.P. 6203
Young, A.S. 6465, 8867
Young, D.A. 7582
Young, D.R. 7192, 8754
Young, Jr., F.W. 8177
Young, T. 8391
Younger, J.J. 6843
Yourke, H.S. 7770, 8508
Yueh-ch'ing, C. 7567
Yunovich, A.E. 6127
Yurkevich, M.I. 6951

Zabara, M.I. 8905
Zakharchenia, B.P. 9413
Zakharov, A.L. 8434, 8435, 8499
Zakrzewski, J.T. 7126
Zallen, R. 6184, 6459
Zaripov, M.M. 8348
Zarkhi, L.D. 8027
Zarouni, A. 7748
Zauberis, D.D. 6153
Zavadovskaya, E.K. 7554
Zavaritskii, N.V. 8404, 8917
Zdanuk, E.J. 8637
Zeender, R.J. 7959
Zeiger, H.J. 6123
Zelenka, J. 8479
Zelený, M. 8325
Zelinka, R.J. 7737, 8023, 8433, 9062
Zemel, J. 8710
Zetterstrom, R.B. 6403
Zharkov, G.F. 8738
Zhiliakov, S.M. 8816
Zholkevich, G.A. 7397
Zhukov, V.F. 7617
Zhuravlev, N.N. 8288
Zigenlaub, R. 6110
Zil'berman, G.E. 8876
Zimmer, C.R. 6258
Zimmerer, R.W. 6603
Zimmerman, E. 7431
Zimmerman, III, W. 8617
Zimmerman, W.B. 7375
Zlai, C.-Y. 8817
Zorzy, J. 8060
Zuev, A.F. 8815
Zuev, K.P. 6204
Zuleeg, R. 7137, 7710
Zwerdling, S. 6065, 6346
Zyrianov, P.S. 8906
Zyuzin, N.I. 8288

Pre-publication Announcement

A BOOK
OF CLASSIFIED
ABSTRACTS
ON

ORGANIC SEMICONDUCTORS

FEATURING

- Over 1000 Abstracts
- Subject Index
- Material Index
- Author Index

You save money by ordering now at the pre-publication price of $20.00

Payment will not be due until the book is issued in the Fall of 1962.

SEND YOUR ORDER TODAY TO

CAMBRIDGE COMMUNICATIONS CORPORATION
238 Main St., Cambridge 42, Mass.

Please enter our Pre-publication Order for ORGANIC SEMICONDUCTORS to be published in the Fall of 1962, at the special price of $20.00.

Name .....
Position .....
Company .....
Division, if any .....
Address .....
City ..... Zone ..... State .....

in'for·ma'tion re·triev'al, *n.* **1.** rapid location of technical information on specific topics.

information retrieval system for the solid state:

SOLID STATE ABSTRACTS ON CARDS

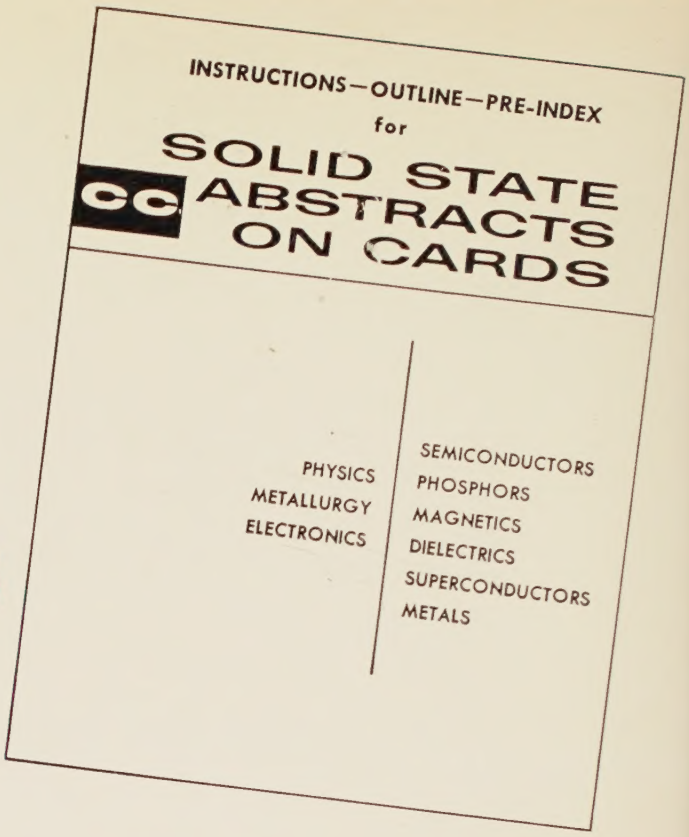

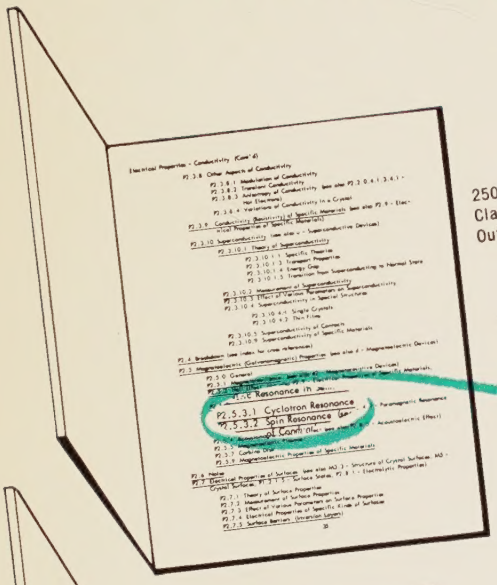

2500-Topic Classification Outline

Send for your free copy of our new 120 page book describing this unique system which is now being used in more than 300 solid state laboratories throughout the world.

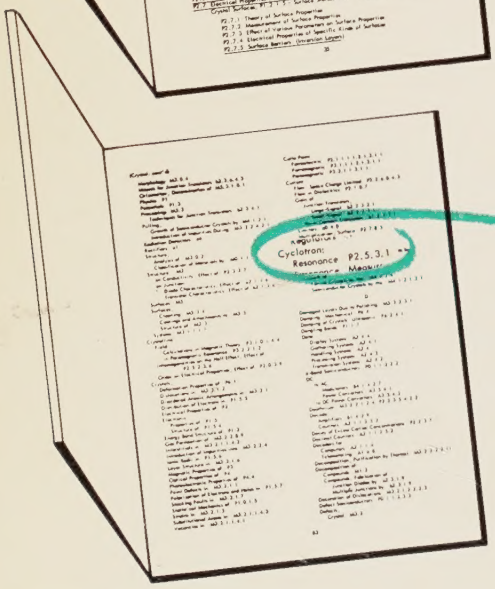

4000-Entry Alphabetical Pre-Index

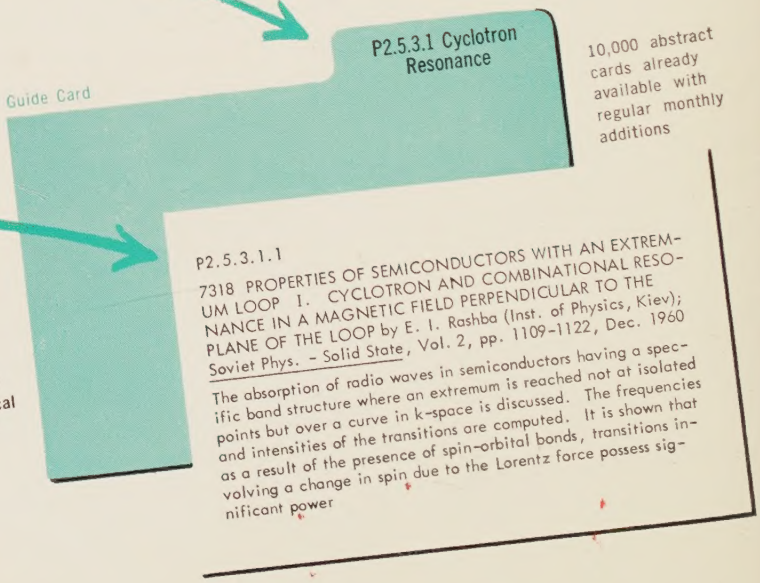
P2.5.3.1 Cyclotron Resonance
Guide Card
P2.5.3.1.1
7318 PROPERTIES OF SEMICONDUCTORS WITH AN EXTREMUM LOOP I. CYCLOTRON AND COMBINATIONAL RESONANCE IN A MAGNETIC FIELD PERPENDICULAR TO THE PLANE OF THE LOOP by E. I. Rashba (Inst. of Physics, Kiev); Soviet Phys. - Solid State, Vol. 2, pp. 1109-1122, Dec. 1960
The absorption of radio waves in semiconductors having a specific band structure where an extremum is reached not at isolated points but over a curve in k-space is discussed. The frequencies and intensities of the transitions are computed. It is shown that as a result of the presence of spin-orbital bonds, transitions involving a change in spin due to the Lorentz force possess significant power

10,000 abstract cards already available with regular monthly additions

CAMBRIDGE COMMUNICATIONS CORPORATION

236 MAIN STREET • CAMBRIDGE 42, MASSACHUSETTS • Tel. 491-0710